Modeling Diffusion as Random Walks in Random Environments

by

Jacob Hass

A dissertation accepted and approved in partial fulfillment of the

requirements for the degree of

Doctor of Philosophy

in Physics

Dissertation Committee:

Raguveer Parthasarathy, Chair

Eric Corwin, Advisor

Jayson Paulose, Core Member

Hank Childs, Institutional Representative

University of Oregon

Fall 2025

DISSERTATION ABSTRACT

Jacob Hass

Doctor of Philosophy in Physics

Title: Modeling Diffusion as Random Walks in Random Environments

This dissertation explores the physics of the *Random Walks in Random Environments* (RWRE) model for diffusion which, until now, has only been of mathematical interest. I show how the statistics of extreme particles, those that move the furthest the fastest, in a large systems of diffusing particles, differ in the RWRE model compared to the classical model for diffusion. This is done by characterizing the distribution of the extreme particles for the RWRE model mathematically and verifying the accuracy these predictions using high precision numerics.

The classical theory for diffusion assumes that the motion of particles in a large system is independent. However, this assumption is fraught because particles diffuse in a common underlying environment which causes correlations in the motion of nearby particles. The RWRE model for diffusion models this common environment as a space-time random forcing field.

Although fluctuations of the typical particle are the same for the RWRE model and classical diffusion, the fluctuations of the extremes are quite different. The fluctuations of the extremes have previously been shown to be surprisingly linked to the Kardar-Parisi-Zhang (KPZ) equation which is typically used to describe growth processes [1]. In this dissertation, I use these results to characterize the extreme location, the particle that has moved the furthest at a given time, and the extreme first passage time, the first time a particle passes a location. I then

consider a more general class of RWRE models and show how they are connected to KPZ equation. Finally, I provide some initial results for the RWRE model in dimension $d = 2$.

This paper contains previously published and coauthored material.

CURRICULUM VITAE

NAME OF AUTHOR: Jacob Hass

GRADUATE AND UNDERGRADUATE SCHOOLS ATTENDED:

University of Oregon, Eugene, OR, USA
California Polytechnic State University, San Luis Obispo, CA, USA

DEGREES AWARDED:

Doctor of Philosophy, Physics, 2025, University of Oregon
Bachelor of Science, Physics, 2018, California Polytechnic State University (magna cum laude)

AREAS OF SPECIAL INTEREST:

Random Walks, Stochastic Processes, Kardar-Parisi-Zhang Universality Class

PROFESSIONAL EXPERIENCE:

Graduate Research Assistant, Physics, University of Oregon, 2020-2025
Graduate Teaching Assistant, Physics, University of Oregon, 2020-2021
Electronics Engineer, Department of Defense, 2018-2020

GRANTS, AWARDS AND HONORS:

Emerging Soft Matter Excellence Award Finalist, APS, 2024
Lokey Graduate Science Award, University of Oregon, 2020
First Year Academic Award, University of Oregon, 2020
College of Science and Mathematics Academic Excellence and Physics Academic Excellence, California Polytechnic State University, 2018
JW Van Dyke Memorial Scholarship for Scholastic Achievement, California Polytechnic State University, 2015

PUBLICATIONS:

Hass, J. B., Carroll-Godfrey, A. N., Corwin, I., & Corwin, E. I. (2023, February). Anomalous fluctuations of extremes in many-particle diffusion. Physical Review E , 107 (2), L022101. doi: 10.1103/PhysRevE.107.L022101

Hass, J. B., Corwin, I., & Corwin, E. I. (2024, May). First-passage time for many-particle diffusion in space-time random environments. Physical Review E , 109 (5), 054101. doi: 10.1103/PhysRevE.109.054101

Hass, J. B., Drillick, H., Corwin, I., & Corwin, E. I. (2024, December). Extreme Diffusion Measures Statistical Fluctuations of the Environment. Physical Review Letters, 133 (26), 267102. doi: 10.1103/PhysRevLett.133.267102

Hass, J., Drillick, H., Corwin, I., & Corwin, E. (2025, March). Universal KPZ Fluctuations for Moderate Deviations of Random Walks in Random Environments (No. arXiv:2504.00266). arXiv. doi:10.48550/arXiv.2504.00266

Hass, J. (2025, May). Super-Universal Behavior of Outliers Diffusing in a Space-Time Random Environment (No. arXiv:2505.01533). arXiv. doi:10.48550/arXiv.2505.01533

Ark, F., Hass, J. B., & Corwin, E. I. (2025, August). Universal Fluctuations in the Tail Probability for d=2 Random Walks in Space-Time Random Environments (No. arXiv:2508.15999). arXiv. doi:10.48550/arXiv.2508.15999

ACKNOWLEDGEMENTS

There are many people that have helped me on my academic journey thus far. I'm sure if I included everyone that has supported me the list would be longer than my thesis so please forgive me if I've missed you.

– I would first like to thank my family for being so supportive. Spending time together and talking on the phone always helped me relax. I don't think I could have done without your support.

– My partner Lily for continuing to encourange me to pursue my dreams. You always helped me through the rough patches and kept me going. Thanks for taking the leap to travel to Oregon with me five years ago.

– My advisor, Eric, for always pushing me to do better and try things I didn't think I could accomplish. You helped me stop underestimating myself as much. I really relied on your advice to help me develop research ideas I couldn't quite formulate yet. I wouldn't have been as successful without your advise.

– Ivan who taught me the basics of formal mathematics which greatly shaped how I think about physics.

– My lab mates Aileen, Eddie, Franscesca and Viola for the fun banter every day over lunch.

– Cam, Francesco and Peter for for their wonderful advice about graduate school and academia. Conferences were always more fun with you there.

TABLE OF CONTENTS

Chapter Page

Chapter Page

LIST OF FIGURES

Figure Page

LIST OF TABLES

CHAPTER I

INTRODUCTION

Diffusion is the physical process by which particles move from areas with a high concentration of particles to lower concentration. I study how particles diffuse and attempt to model their motion. The motion of these particles is modeled as a random process as particles bump into each other and are influenced by the environment they are submerged in. Since the motion is so chaotic, one must study the statistics of the motion instead of the trajectories. One statistic of particular interest is the distance a particle travels in a given time frame averaged over many different experiments.

To study diffusing particles mathematically, we approximate the movement of a particle as a random walk on a lattice. The motion of this random walk is defined as follows. Start with a walk at position $x = 0$. Then flip a coin and if heads move up to $x = 1$, and if tails move down to $x = -1$. For each time step, repeat this process of flipping a coin and moving up or down. Although quite simple, this model for diffusion, the classical model, has been used to successfully model the random motion of pollen[2, 3], viruses[4] and even stock prices [5].

However, this model ignores the common environment which particles diffuse in. I study a model for diffusion, the *Random Walks in Random Environments* (RWRE) model, which accounts for this environment by introducing a (space-time) random forcing field. The random field is introduced by weighting the coin that is flipped to determine if a particle moves up or down. Note, a weighted coin is simply a coin which is more likely to land on heads than tails or vice-versa. Since the field is random in space and time, the weighting of the coin is different at each location and time. For example, any walks at site $x = 1$ at time $t = 1$ will flip one weighted coin and any walks at site $x = -1$ and $t = 1$ will flip a *different* weighted coin. Since walks at the same location and time flip the same weighted coin, the motion of particles at the same location and time is correlated. Physically, this makes sense because the common environment in which particles diffuse in causes the motion of nearby particles to be correlated.

The statistics of a typical particle predicted by the RWRE model matches the statistics predicted by the classical model. In this thesis, I show that for a large system of diffusing particles, the statistics of the *extreme* particle, that which moves the fastest the furthest, differs between the RWRE and classical model. Specifically, I study the extreme location, the position of the particle that has moved the furthest at a given time, and the extreme first passage time, the first time a particle passes a given position. By measuring these extreme statistics, previously hidden information can be measured about the chaotic environment that particles diffuse in. For example, I show that the effective stickiness of particles can be measured using extreme statistics. Measuring the stickiness of particles is quite difficult as it requires using microrheology to track the trajectory of two nearby particles. Characterizing the statistics of extremes provides a more accessible means to measure the stickiness of particles.

The remaining chapters of my thesis are papers published in Physical Review E, Physical Review Letters, or in submission. The outline of the remaining chapters are as follows.

Chapter II is the first paper I published as a graduate student where we study the simplest form of the RWRE model in which particles can only move with a step size of one. We derive mathematical predictions, using previous results from the mathematics literature [6, 7], for the statistics of the extreme location and compare these the predictions from classical theory. We could only derive these predictions in the limit that the number of particles in the system goes to infinity. Since a system of an infinite number of particles is unrealizable, our first question was "How big does the system need to be for our predictions to be accurate?" To answer this question, we simulated our model numerically. We decided to start with a system as reasonably large as we could make on most computers. This required quadruple precision floating point numbers which let us simulate systems of nearly 10^{4500} particles (note, an estimate for the number of atoms in the universe is 10^{80}). Of course, this large a system is absurd, but our predictions were confirmed because they perfectly matched the numerics. We then checked if our predictions could be used to characterize the behavior of smaller, more realistic system sizes. We found that our predictions were accurate even for systems of 100 particles.

In Chapter III, we use the same RWRE model but study the extreme first passage time. As compared to the extreme location, the extreme first passage time is relevant to more physical systems. For example, the extreme first passage time sets the time scale for neuron activation since the first ion to reach a neuron receptor triggers the activation [8]. As with the first paper, we derive predictions for the extreme first passage time and verify these predictions numerically.

Chapter IV extends the results of the previous two papers to a more general class of RWRE models where walks can take steps of any size. This means that walks are not constrained to taking steps of size 1, but could take steps of size 0, 1, 2, etc. The more general framework allowed us to better understand how the underlying environment effects the extreme location and extreme first passage time. For example, if the weighted coins are more likely to be heavily weighted in one direction or the other (i.e. falls on heads with probability 0.99 or vise versa), the effect of the environment on the extreme statistics is more dramatic than if the weighted coins are more likely to be fairly weighted. Thus, we predicted that by measuring the extreme statistics experimentally, information about the weighting of the coins is also measured. Understanding the weighting of the coins is important because it pertains to how "sticky" two walks are. The scenario where the coins are weighted more in one direction or the other corresponds to particles which tend to stick to each other; whereas a fair coin corresponds to particles which move independently of each other.

Chapter V contains all the mathematics required to derive the results presented in Chapter IV including novel methods to the Physics literature. This paper formalizes the mathematical framework of the results in Chapter IV and derives these results pedagogically.

Chapter VI is my first single author paper and extends the results in Chapter IV and V to *any* RWRE model. This chapter provides predictions for the extreme location and extreme first passage time for any RWRE model which I verify numerically for a diverse selection of models. I show that there is a remarkably simple relationship between the statistics of the underlying environment and the extreme statistics which is called a hyperuniversality class.

Chapter VII explores computational results for RWRE models in two dimensions. The trouble with higher dimensions is that there is much less mathematical literature to build on compared to one dimension. Many of the techniques used to analyze RWRE models in one dimension break down in two or higher dimensions. This paper provides insight into two dimensional RWRE models using computational simulations and conjectures some theoretical results by naively extending our results from one dimensional RWRE models.

CHAPTER II

ANOMALOUS FLUCTUATIONS OF EXTREMES IN MANY-PARTICLE DIFFUSION

This chapter is published as: Hass, J. B., Carroll-Godfrey, A. N., Corwin, I., & Corwin, E. I. (2023, February). Anomalous fluctuations of extremes in many-particle diffusion. Physical Review E , 107 (2), L022101. doi: 10.1103/PhysRevE.107.L022101. My contribution to the paper was developing and running the code to generate the numerics. I also helped derive the theoretical results alongside Ivan Corwin.

2.1 Abstract

In many-particle diffusions, particles that move the furthest and fastest can play an outsized role in physical phenomena. A theoretical understanding of the behavior of such extreme particles is nascent. A classical model, in the spirit of Einstein's treatment of single-particle diffusion, has each particle taking independent homogeneous random walks. This, however, neglects the fact that all particles diffuse in a common and often inhomogeneous environment that can affect their motion. A more sophisticated model treats this common environment as a space-time random biasing field which influences each particle's independent motion. While the bulk (or typical particle) behavior of these two models has been found to match to high degree, recent theoretical work of Barraquand, Corwin and Le Doussal on a one-dimensional exactly solvable version of this random environment model suggests that the extreme behavior is quite different between the two models. We transform these asymptotic (in system size and time) results into physically applicable predictions. Using high precision numerical simulations we reconcile different asymptotic phases in a manner that matches numerics down

to realistic system sizes, amenable to experimental confirmation. We characterize the behavior of extreme diffusion in the random environment model by the presence of a new phase with anomalous fluctuations related to the Kardar-Parisi-Zhang universality class and equation.

2.2 Introduction

Our world is fueled by outliers. Information in signals is carried by the leading edge [9, 10, 11, 12, 13, 14, 15, 16]. A viral or bacterial infection is spread by the first few pathogens to enter a host and the first host to enter a new region [17, 4]. A species is evolved by the fittest mutations [18, 19, 20]. Scientific revolution is sparked by the first new idea. In all of these contexts the precipitating action is driven by the extremes among a great number of agents (varying from $N \sim 10^2$ to $N \sim 10^{60}$ depending on the context) evolving in a complex but shared environment. How does the nature of the shared environment affect these outlier behaviors? Conversely, can we infer the nature of the shared environment from the behavior of these outliers? Despite their obvious importance, these overarching questions are still unanswered.

The classical model for many-particle diffusion as independent homogeneous random walks provides an easily calculable solution, but entirely neglects the effects of the shared and likely inhomogeneous environment. This model is the basis for diffusion coefficients [21, 22, 23], which succinctly describe the behavior of typical particles in a many-particle diffusion. A more sophisticated model treats the shared environment as a space-time random biasing field with short-range space-time correlations. Each particle thus articulates independent random walks subject to forcing by the common biasing field. While this refined model does not affect typical particle diffusion behavior [24], it drastically impacts the behavior of extreme particles. In this work, we provide predictions for the behavior of extreme particles moving in a random and inhomogenous environment. We find that the variance in the position of the extreme particle is a robust and sensitive measurement of the nature of the environment and show how this variance can be understood as the sum of two contributions: the randomness present in the environment, and the sampling of random walks in that environment. We show that by subtracting out the variance due to sampling we can produce direct measurements of the environment, inaccessible from measurements of the motion of a typical particle or of the bulk. This residual environmental variance is characterized by a novel power law that we demonstrate holds even when the number of particles is as small as a few hundred.

2.3 Background

Building on observations by Brown [2, 3] from 1827, Einstein [21, 22, 23] (along with Langevin [25], Sutherland [26, 27] and Smoluchowski [28, 29]) proposed a theory of diffusion based on modeling particles by independent random walks with variance controlled by a diffusion coefficient intrinsic to the particle/environment pair. Soon after, Perrin experimentally verified Einstein's statistical predictions [30, 31].

Probing the effectiveness and limitations of Einstein's diffusion model has remained a challenge. On short time scales, particle motion is ballistic, dominated by inertia [32, 33, 34, 35, 36, 37]. Many physically relevant situations require the addition of new concepts to accurately model them. Certain diffusive processes are better modeled by Levy flights [38] or other types of anomalous diffusions [39, 40] instead of simple random walks. Other work has focused on active particles which inject energy into their environment [41, 42]. Further, in environments which

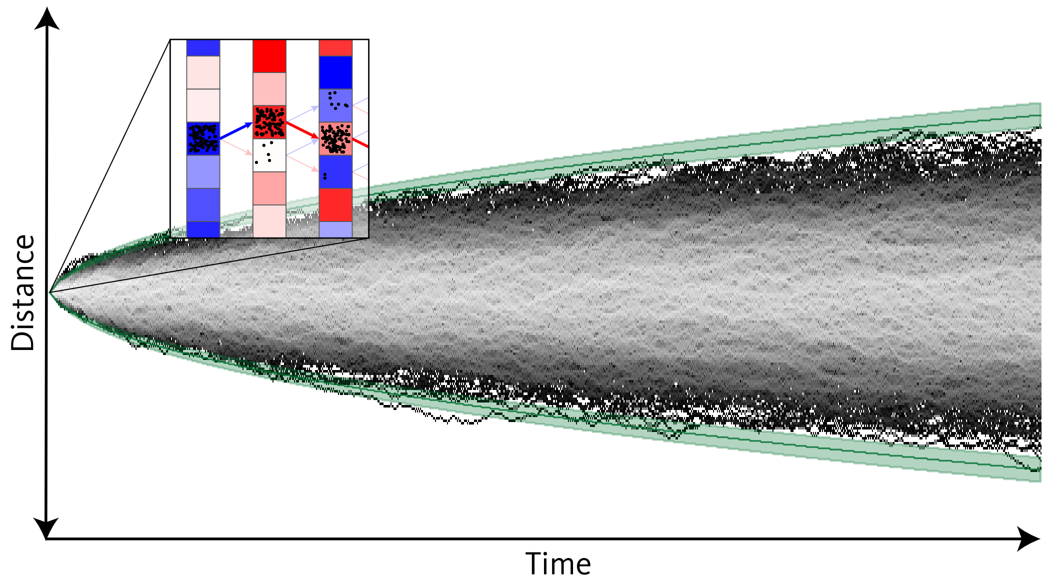

Figure 1. A system of $N = 10^5$ particles evolving in a given random environment. The heat map records the site occupancy density. We also plot in green the asymptotic theory mean location for the maximum particle location. Around this is a shaded region with a width of two standard deviations based on the asymptotic theory variance. This region generally contains the extreme-most particle over time. The zoomed-in inset shows the spatial locations of $N = 10^2$ particles over time. Color indicates the bias (red is biased down and blue is biased up) and is chosen independently at each space-time box. The location of particles within each box is chosen for ease of visualization.

are slowly mixing, Einstein's theory may also break down due to the presence of quenched disorder [43, 38]. Unlike the above deviations from the classical model, our approach is intended to describe generic many-particle diffusions.

The random walk in random environment (RWRE) model goes back to [44, 45] (see also [46, 47, 48, 49, 50]) and comes in two types – long-range [51, 52, 53, 39, 54, 55] and short-range [56, 57, 58, 59, 60, 61, 62] temporally correlated environments. We focus here on the latter. In this context, typical RWRE particles behave like Brownian motion, matching the behavior from Einstein's model [63, 64]. The motion of atypical particles is controlled by large deviations of the RWRE's transition probability as first studied in [65].

Barraquand and Corwin [6] discovered the exactly solvable Beta RWRE discussed extensively below and uncovered a remarkable connection between its large deviations for times of order $\log(N)$ and the statistics of the Kardar-Parisi-Zhang (KPZ) universality class [66, 67], namely the Gaussian Unitary Ensemble (GUE) Tracy-Widom distribution [68]. Soon after [69] recognized that a phase transition should occur in the $(\log(N))^2$ time frame while [7] discovered that in this frame the GUE Tracy-Widom distribution is replaced by the KPZ equation one-point distribution [1, 70, 71, 72, 73]. See [74, 75, 76, 77, 78, 79, 80] for further developments. The recursion relation (2.3) for RWRE transition probabilities solves a discrete version of the multiplicative noise stochastic heat equation (mSHE)

$$\partial_t Z(x,t) = \frac{1}{2}\partial_x^2 Z(x,t) + \xi(x,t)Z(x,t) \tag{2.1}$$

with ξ space-time white noise. The logarithm of the mSHE $h(x,t) = \log Z(x,t)$ solves the KPZ equation

$$\partial_t h(x,t) = \frac{1}{2}\partial_x^2 h(x,t) + \frac{1}{2}(\partial_x h(x,t))^2 + \xi(x,t). \tag{2.2}$$

Hence, large deviations for RWREs, in particular beyond the solvable model and even in experimental settings, may relate to the KPZ equation and its universality class – especially in light of the rich canon of work on KPZ universality in various contexts using theoretical [81, 66], numerical [82, 83], and experimental [84] methods. The KPZ connection is quite useful since its statistics and power-laws are well studied.

2.4 Models for diffusion

Although physical diffusion is continuous in time and (typically) occurs in three-dimensional space, here we work with discrete models in one spatial dimension. The principal reason for this choice is that it is the setting for the exactly solvable Beta RWRE [6] (a continuous *sticky Brownian motion* limit of this model exists [76]) that will enable us to compare numerical results to exact theoretical predictions. Beyond that, discretization is common for numerical simulations and higher dimensions are more challenging numerically due to anisotropy issues arising from the choice of lattice and due to the lack of exactly solvable models, c.f. [69]. In real diffusion in a common environment, there will be length and time scales on which the environment decorrelates. Our discrete model can be thought of as coarse-graining the environment in space and time onto a lattice and thus we do not expect discrete and continuous models to differ greatly for long-times and large-scales. Our model ignores any higher order interactions as we expect them to be less present in the behavior of extreme particles, for which the local density is necessarily low. Additionally, there are physical settings where particles take discrete states [85, 86] or evolve in quasi-one-dimensional spaces [87, 88].

We study the *Beta RWRE* introduced in [6] (see Fig. 1). We model the environment by a collection $\mathbf{B} = \left\{B(x,t) : x \in \mathbb{Z}, t \in \mathbb{Z}_{\geq 0}\right\}$ of independent identically distributed random variables all drawn from the uniform distribution on $[0,1]$. At time $t = 0$ we start with N particles all at site 0. Given an instance of the environment $\mathbf{B}$ the particles proceed as follows. Each particle at x and t independently flips the same weighted coin which has probability $B(x,t)$ of heads (moving the particle to site $x+1$ at time $t+1$) and $1 - B(x,t)$ of tails (moving to $x-1$ instead). Thus, while particles do not interact with each other, those at the same place and time are all influenced by the common environment.

This model is exactly solvable when $B(x,t)$ are distributed according to the Beta distribution, $Beta(\alpha, \beta)$ [6]. For simplicity, we focus on the special case $\alpha =$

$\beta = 1$ corresponding to the uniform distribution. The classical simple symmetric random walk (SSRW) model arises in the limit $\alpha = \beta \to \infty$ where all $B(x,t) \equiv 1/2$ and the environment is deterministic.

We focus on the behavior of the right-most particle at time t. We denote this by Max_t^N, with N the number of particles in the system. Two types of randomness affect Max_t^N: that of the environment and that of sampling the random walks in that environment. The effect of the environment is via the transition probability $p_{\mathbf{B}}(x,t)$, the probability that a single random walker initially at 0 will end up at x at time t for a given environment $\mathbf{B}$. This satisfies the recursion relationship,

$$\begin{aligned} p_{\mathbf{B}}(x,t) =& p_{\mathbf{B}}(x-1,t-1)B(x-1,t-1)+ \\ & p_{\mathbf{B}}(x+1,t-1)\big(1-B(x+1,t-1)\big) \end{aligned} \tag{2.3}$$

with initial condition $p_{\mathbf{B}}(0,0) = 1$ and $p_{\mathbf{B}}(x \neq 0,0) = 0$. Since each random walker is independent, conditional on the environment, the distribution of the ensemble of N walks is determined by $p_{\mathbf{B}}(x,t)$. Given the environment $\mathbf{B}$, the probability that a single random walker is at or above x at time t is given by the tail probability, $P_{\mathbf{B}}(x,t) = \sum_{y \geq x} p_{\mathbf{B}}(y,t)$. This and the independence of random walkers, conditional on the environment, imply

$$\mathrm{Prob}_{\mathbf{B}}(\mathrm{Max}_t^N \leq x) = \big(1 - P_{\mathbf{B}}(x,t)\big)^N, \tag{2.4}$$

where the left-hand side is the probability, given the environment $\mathbf{B}$, that $\mathrm{Max}_t^N \leq x$.

We study how Max_t^N varies upon sampling a new environment and random walkers therein. Eq. (2.4) suggests that a good proxy for Max_t^N is the location Env_t^N of the $1/N$-quantile of $P_{\mathbf{B}}(x,t)$, i.e., Env_t^N equals the maximal x such that $P_{\mathbf{B}}(x,t) > 1/N$. Notice that Env_t^N only accounts for the variation due to the environment. The variation due to sampling in that environment is denoted Sam_t^N and defined by $\mathrm{Max}_t^N = \mathrm{Env}_t^N + \mathrm{Sam}_t^N$. We use the notation $\mathrm{Mean}\,(\bullet)$ and $\mathrm{Var}\,(\bullet)$ for the mean and variance of a quantity $\bullet$ (e.g. $\mathrm{Max}_t^N, \mathrm{Env}_t^N, \mathrm{Sam}_t^N$) averaged over both the environment and the sampling of random walkers in that environment.

Numerical Methods We numerically simulate our models for system sizes varying from $N = 10^2$ to $N = 10^{300}$. We consider such large and physically unrealistic system sizes like 10^{300} in order to see how asymptotic theory applies for as wide a range as possible of finite system sizes. We evolve the system for times from $t = 0$ to $t = 5000 \log(N)$. As explained below, $\log(N)$ and $(\log(N))^2$ set key timescales and our range of times ensure that for all choices of N, we encompass these scales. We simulate such large systems by tracking occupation variables instead of individual particle trajectories. In particular, if there are $N(x,t)$ particles at site x at time t, then the number that move to site $x+1$ is binomially distributed with $N(x,t)$ samples and success probability $B(x,t)$ (the remainder move to site $x-1$). We sample these binomial distributions utilizing quadruple-precision floating point numbers and making approximations to the binomial distribution when dealing with sizes beyond our precision limits, as described in [89]. The rightmost particle location (identified by the maximal x with $N(x,t) \geq 1$) at each time represents a sample of Max_t^N. By repeatedly sampling new environments along with random walk occupation variables $N(x,t)$ therein we numerically measure $\mathrm{Var}\left(\mathrm{Max}_t^N\right)$. To distinguish from the true value we denote this numerically measured variance by $\mathrm{Var}^{\mathrm{num}}\left(\mathrm{Max}_t^N\right)$ and plot it in Fig. 2. In like fashion, we measure $\mathrm{Var}^{\mathrm{num}}\left(\mathrm{Env}_t^N\right)$ for each sampled environment by using Eq. 2.3 to compute $p_{\mathbf{B}}(x,t)$. Fig. 3 shows $\mathrm{Var}^{\mathrm{num}}\left(\mathrm{Env}_t^N\right)$ as a function of time (see [89] for $\mathrm{Mean}^{\mathrm{num}}\left(\mathrm{Max}_t^N\right)$ and $\mathrm{Mean}^{\mathrm{num}}\left(\mathrm{Env}_t^N\right)$). The data presented in Fig. 2 and 3 took approximately three weeks to run in parallel on 500 cores of the University of Oregon high performance computing cluster, Talapas.

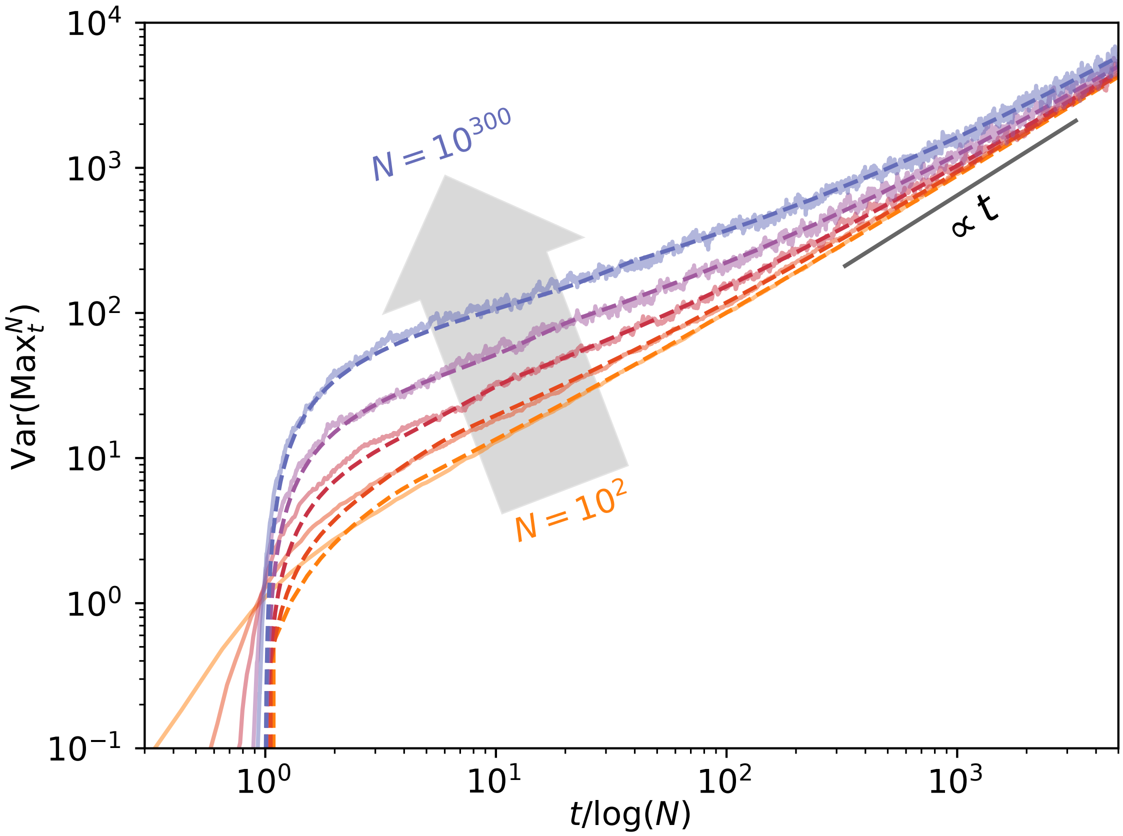

Figure 2. Plots of $\mathrm{Var}^{\mathrm{num}}\left(\mathrm{Max}_t^N\right)$ (solid) computed over 10000, 5000, 1000, 500 and 500 environments (respectively) and $\mathrm{Var}^{\mathrm{asy}}\left(\mathrm{Max}_t^N\right)$ (dashed) for $N = 10^2, 10^7, 10^{24}, 10^{85}, 10^{300}$

2.5 Asymptotic Theory Results

We describe asymptotic results on the behavior of Max_t^N, Env_t^N and Sam_t^N as both N and t tend to infinity in different limits. Given a fixed relationship between t and $\log(N)$ such as $t/\log(N) = \hat{t}$ or $t/\log(N)^2 = \hat{\hat{t}}$ for $\hat{t}$ or $\hat{\hat{t}}$ fixed, we write $f(N,t) \gg g(N,t)$ if $f(N,t)/g(N,t)$ tends to infinity as N and t do subject to their relationship. We use the notation $\mathrm{Var}^{\mathrm{asy}}(\bullet)$ to denote the asymptotic theory formula for the variance of $\bullet$, interpolated back to finite N and t. SSRW theory

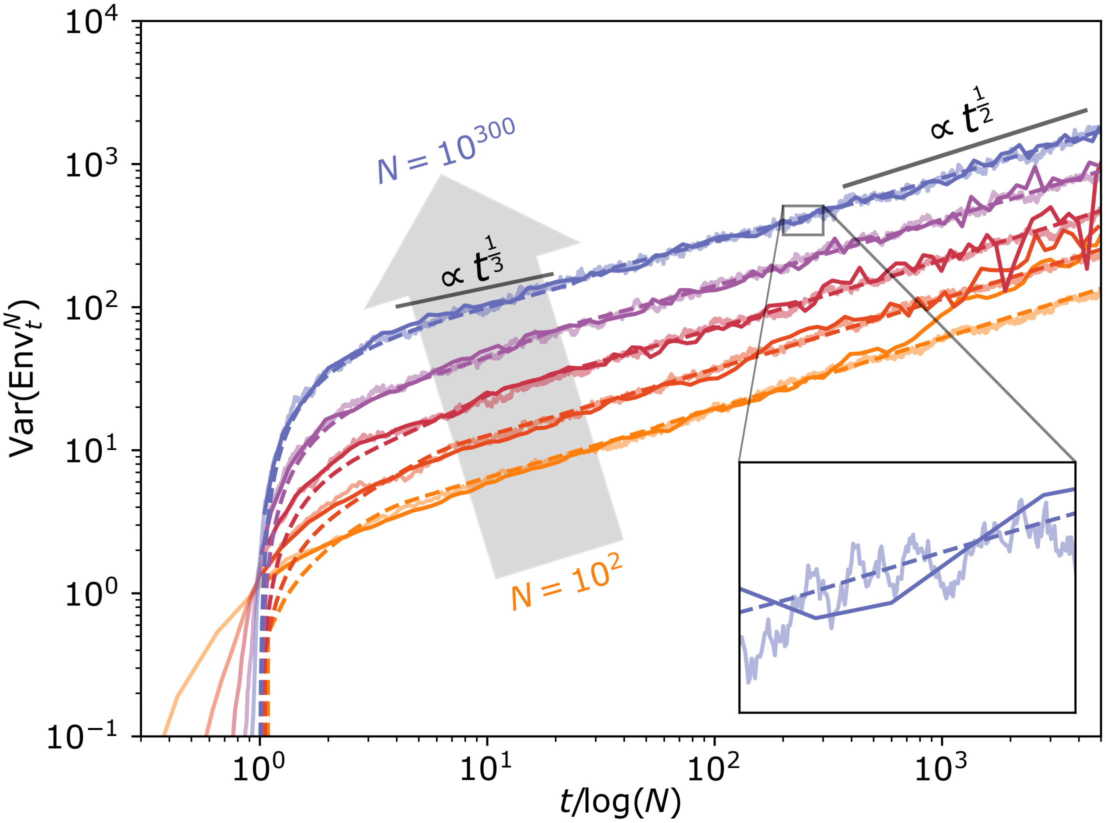

Figure 3. Plots of $\mathrm{Var}^{\mathrm{num}}\left(\mathrm{Env}_t^N\right)$ (transparent solid) computed over 500 environments, $\mathrm{Var}^{\mathrm{asy}}\left(\mathrm{Env}_t^N\right)$ (dashed), and $\mathrm{Var}^{\mathrm{num}}\left(\mathrm{Max}_t^N\right) - \mathrm{Var}^{\mathrm{asy}}\left(\mathrm{Sam}_t^N\right)$ (dark solid) smoothed in each $1/25^{th}$ of a decade for $N = 10^2, 10^7, 10^{24}, 10^{85}, 10^{300}$. The three curves agree as shown in the zoomed-in inset.

follows from Stirling's formula while asymptotic results for the RWRE rely on tools from quantum integrable systems [6, 7, 80] and are derived first for Env_t^N and then for Max_t^N and Sam_t^N.

SSRW Max_t^N**:** For $t/\log(N) = \hat{t}$ with fixed $\hat{t} < (\log 2)^{-1}$, we have $N \gg 2^t$ and hence with very high probability every reachable site in the lattice at time t is occupied, hence $\mathrm{Var}\left(\mathrm{Max}_t^N\right) \approx 0$. When $\hat{t} > (\log 2)^{-1}$, we show in [89] that Max_t^N is asymptotically a Gumbel random variable. For $\hat{t}$ large, $\mathrm{Var}^{\mathrm{asy}}\left(\mathrm{Max}_t^N\right) \approx \frac{\pi^2}{12}\frac{t}{\log(N)}$.

RWRE Env_t^N**:** For $t/\log(N) = \hat{t}$ with fixed $\hat{t} < 1$, $\mathrm{Var}\left(\mathrm{Env}_t^N\right) \approx 0$. To see this, note that $P_{\mathbf{B}}(t,t) = B_{0,0} \cdots B_{t-1,t-1}$. Taking logs and applying the central limit theorem shows that $\log\big(P_{\mathbf{B}}(t,t)\big) \approx -t + t^{1/2}G$ for G a standard Gaussian. This implies that $P_{\mathbf{B}}(t,t) \approx e^{-t} \gg 1/N$. Thus the RWRE stops saturating the lattice when $t = \log(N)$ plus a order $(\log(N))^{1/2}$ Gaussian fluctuation. For the SSRW this happens at time $\log_2(N)$ plus order one fluctuations.

$\mathrm{Var}\left(\mathrm{Env}_t^N\right)$ displays two asymptotic regimes. For fixed $t/\log(N) = \hat{t} > 1$, $\mathrm{Var}\left(\mathrm{Env}_t^N\right)$ takes asymptotic form,

$$V_1(N,t) := \Big(\frac{\log(N)}{t}\Big)^{2/3}\sigma_\chi^2 \frac{2^{2/3}\big(1-\frac{\log(N)}{t}\big)^{4/3}}{1-\big(1-\frac{\log(N)}{t}\big)^2}, \tag{2.5}$$

where $\sigma_\chi^2 \approx 0.813$ is the variance of the GUE Tracy-Widom distribution [90, 68]. As shown in [89], this follows from the result of [6]: For $v \in (0,1)$, $\log P_{\mathbf{B}}(vt,t) = -tI(v) + t^{1/3}\sigma(v)\chi_t$ where $I(v) = 1-\sqrt{1-v^2}$, $\sigma(v) = (2I(v)^2/(1-I(v)))^{1/3}$ and χ_t is random converging to the GUE Tracy-Widom distribution as t goes to infinity.

For $t/(\log(N))^2 = \hat{\hat{t}}$, $\mathrm{Var}\left(\mathrm{Env}_t^N\right)$ takes asymptotic form

$$V_2(N,t) := \frac{t}{2\log(N)} \cdot \mathrm{Var}\left(h\Big(0, \frac{4(\log(N))^2}{t}\Big)\right), \tag{2.6}$$

where $h(0,s)$ is the height at 0 and time s of the *narrow wedge* solution to the KPZ equation (2.2). As shown in [89], this follows from [7]: For $v \in (0,\infty)$, $\log P_{\mathbf{B}}(vt^{3/4},t) \approx -\frac{v^2t^{1/2}}{2} - \log(t)/4 + \log(v) - v^4/12 + h(0,v^4)$.

Interpolating between these regimes, and extrapolating past $(\log(N))^2$ (see also [80]) we find two power-laws,

$$\mathrm{Var}^{\mathrm{asy}}\big(\mathrm{Env}_t^N\big) \approx \begin{cases} \sigma_\chi^2\big(\frac{\log(N)}{2}\big)^{\frac{1}{3}}t^{\frac{1}{3}} & 1 \ll \frac{t}{\log(N)} \ll \log(N), \\ \frac{1}{2}\pi^{\frac{1}{2}}t^{\frac{1}{2}} & \frac{t}{\log(N)} \gg \log(N). \end{cases} \tag{2.7}$$

For finite N and t these regimes have a gentle crossover that we capture by setting $\mathrm{Var}^{\mathrm{asy}}\big(\mathrm{Env}_t^N\big) := I(N,t)V_1(N,t) + \big(1 - I(N,t)\big)V_2(N,t)$ where $I(N,t) := \frac{1}{2}\cdot\left(1-\mathrm{erf}\left(\frac{t-(\log(N))^{3/2}}{(\log(N))^{4/3}}\right)\right)$ (with $\mathrm{erf}(x) = 2/\sqrt{\pi}\int_0^x e^{-t^2}dt$ the error function) interpolates from 1 to 0 over an interval of width $(\log(N))^{4/3}$ around $(\log(N))^{3/2}$.

2.6 RWRE Sam_t^N and Max_t^N

We identify the additional contribution from sampling the many-particle diffusion given an environment. Using Eq. (2.4) and Taylor expansion of the results of [6] and [7] quoted above, [89] shows that for $t/\log(N) = \hat{t} > 1$ the sample fluctuation Sam_t^N is of Gumbel type with variance

$$\mathrm{Var}^{\mathrm{asy}}\left(\mathrm{Sam}_t^N\right) = \frac{\pi^2}{6}\frac{\left(\frac{t}{\log(N)}-1\right)^2}{2\frac{t}{\log(N)}-1} \approx \frac{\pi^2}{12}\frac{t}{\log(N)} \tag{2.8}$$

as $\hat{t}$ grows. This limit matches the behavior of the SSRW model. In [89] we also show that Sam_t^N is asymptotically independent of Env_t^N, thus

$$\mathrm{Var}\left(\mathrm{Max}_t^N\right) \approx \mathrm{Var}\left(\mathrm{Env}_t^N\right) + \mathrm{Var}\left(\mathrm{Sam}_t^N\right). \tag{2.9}$$

2.7 Comparison of Numerical and Theoretical Results

Fig. 2 and 3 show that the asymptotic theoretical predictions for $\mathrm{Var}\left(\mathrm{Max}_t^N\right)$ and $\mathrm{Var}\left(\mathrm{Env}_t^N\right)$ are in excellent agreement with the numerical measurements. Fig. 3 further shows that we reliably recover $\mathrm{Var}\left(\mathrm{Env}_t^N\right)$ using $\mathrm{Var}^{\mathrm{num}}\left(\mathrm{Max}_t^N\right) - \mathrm{Var}^{\mathrm{asy}}\left(\mathrm{Sam}_t^N\right)$, as expected from Eq. 2.9. Notably, while these results were derived for asymptotically large $\log(N)$ and t, they hold nearly perfectly down to $N = 10^2$. Fig. 3 reveals that while we readily see the long-time $t^{1/2}$ power-law for $\mathrm{Var}\left(\mathrm{Env}_t^N\right)$ from Eq. 2.7, the $t^{1/3}$ power-law is elusive. Although the full characterization of the short-time regime is in excellent agreement with the numerical results, the $t^{1/3}$ power-law is difficult to capture since the transitional window of $\log(N)$ to $(\log(N))^2$ is too narrow for realistic sizes of N, even up to $N = 10^{300}$. By measuring the long-time $t^{1/2}$ power law, we measure the short-time scaling behavior of the KPZ equation up to a prefactor using Eq. 2.6. Fig. 4 shows the tight matching of the asymptotic theory curves and numerically measured values for the variance of $\mathrm{Max}_t^N, \mathrm{Env}_t^N$ and Sam_t^N for a given value of $N = 10^7$.

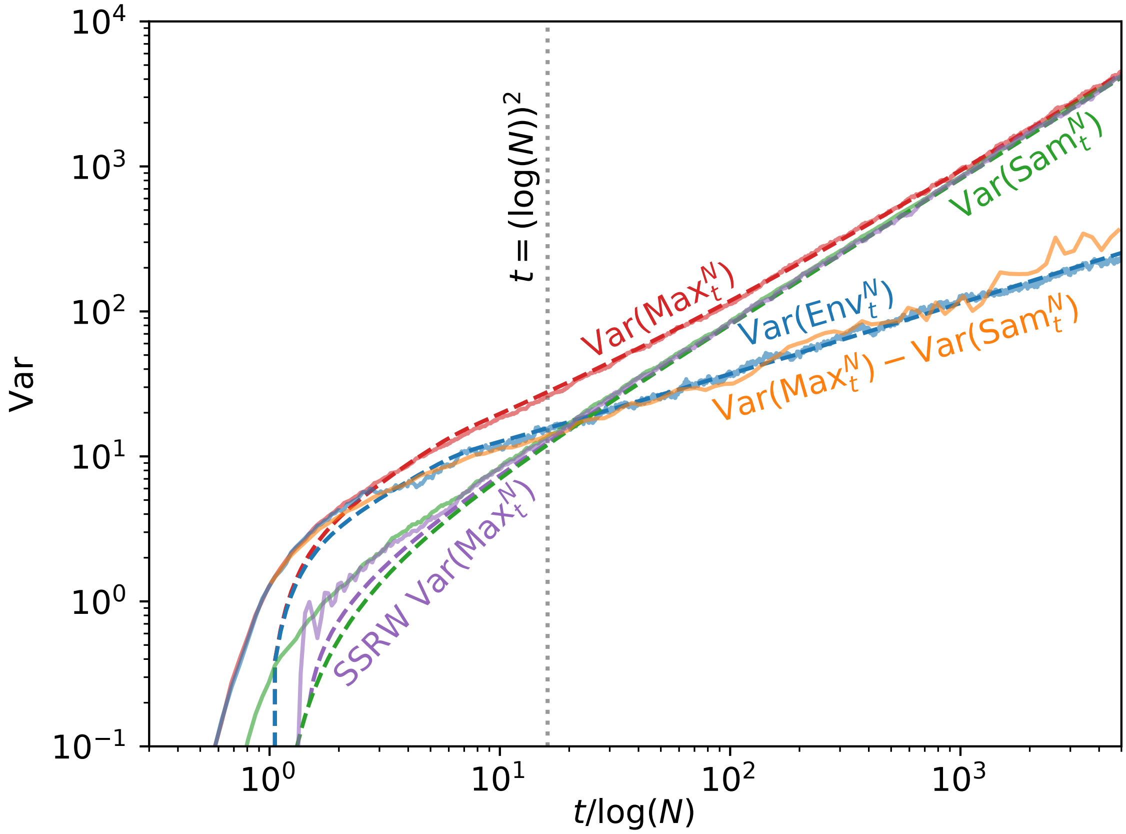

Figure 4. Variance of the maximal particle $\mathrm{Var}\left(\mathrm{Max}_t^N\right)$ (red), environment $\mathrm{Var}\left(\mathrm{Env}_t^N\right)$ (blue), and sampling $\mathrm{Var}\left(\mathrm{Sam}_t^N\right)$ (green) for RWRE, and variance of the maximal particle $\mathrm{Var}\left(\mathrm{Max}_t^N\right)$ (purple) for SSRW, all for $N = 10^7$. Dashed lines are $\mathrm{Var}^{\mathrm{asy}}(\bullet)$, while solid lines are $\mathrm{Var}^{\mathrm{num}}(\bullet)$. $\mathrm{Var}^{\mathrm{num}}\left(\mathrm{Max}_t^N\right) - \mathrm{Var}^{\mathrm{asy}}\left(\mathrm{Sam}_t^N\right)$ (orange; smoothed as in Fig. 3) closely matches the environment curve (blue).

Notice that for $t \approx \log(N)$ the asymptotic theory and numerical values for the variance of Sam_t^N do not fit as well as for large t. This is likely a result of finite-size effects and quickly goes away at larger values of t or when N increases. The fit for $N = 10^{300}$ in Fig. 2 and 3 remains tight over the entire range of t.

2.8 Conclusion

The link between RWREs and KPZ universality with its wealth of theoretical, numerical and experimental evidence strongly suggests that aspects of the picture presented here will persist beyond discrete and solvable models, even to experiments. When t is of order $\log(N)$, variances should be non-universal, depending in a difficult to determine way on the nature of the environment. By contrast, when $t \gg \log(N)$, we anticipate that the scaling exponents and functional forms we have identified for the variances of $\mathrm{Env}_t^N, \mathrm{Sam}_t^N$ and Max_t^N will be universal, as will the relation (2.9). The leading coefficients in Eq. (2.7) should be non-universal and hold within them all of the accessible information about the correlation structure of the environment – we call these *extreme diffusion coefficients*. Further theoretical study, such as for the general α, β Beta RWRE model, should provide a natural first test of this universal picture and an understanding of how the extreme diffusion coefficients relate to the microscopic environment. A continuum model that should provide an even wider testing-ground amenable to numerics involves particles $x_i(t)$ for $i = 1, 2, \ldots$ satisfying $dx_i(t) = F(x_i(t), t)dt + D(x_i(t), t)dB_i(t)$ where $F(x, t)$ and $D(x, t)$ are random forcing (as in [69]) and diffusivity (generalizing diffusing diffusivity, c.f. [91]) fields common to all particles while B_i are Brownian motions independent between different i. Changing the correlation structures of F and D will probe the transition between temporally mixing versus quenched environments, which should have very different behavior (c.f. [92, 93]) and warrants further study. Considering higher dimensions as in [69] may lead to further theory that better model real physical systems. A study of higher order cumulants may reveal other ways to probe the hidden environment, although they may be harder to observe numerically or experimentally.

In physical systems it is impossible to directly measure the environmental variance. However, an indirect measurement can be performed via the approach presented here by using $\mathrm{Var}\left(\mathrm{Env}_t^N\right) \approx \mathrm{Var}\left(\mathrm{Max}_t^N\right) - \mathrm{Var}\left(\mathrm{Sam}_t^N\right)$. The sample variance $\mathrm{Var}\left(\mathrm{Sam}_t^N\right)$ is now computed using $\mathrm{Var}\left(\mathrm{Sam}_t^N\right) = \frac{\pi^2 D}{6} \frac{t}{\log(N)}$ where D

is the diffusion coefficient. One could repeatedly track the motion of the leading edge of diffusing particles in a system of colloids confined to a quasi-1D channel thereby directly measuring $\mathrm{Var}\left(\mathrm{Max}_t^N\right)$ for system sizes ranging from N 10^2 to N 10^{10}. Further, one can also perform complementary measurements on the time of first passage of diffusing objects, which opens the door to experiments done on all manner of diffusing objects, including light or sound diffusing through a scattering medium, dye molecules in a fluid, or any other object whose first passage can be measured. By measuring the environmental variance and extreme diffusion coefficient we will gain a new microscope through which to probe the hidden nature of the underlying environment in which the diffusion occurs. Our work should serve as a guide in the development and analysis of novel experimental measurements of the extreme behavior of many-particle diffusion.

2.9 Acknowledgements

We thank G. Barraquand and P. Le Doussal for discussions and S. Prolhac for providing numerics for $\mathrm{Var}\left(h(0,s)\right)$. This work was funded under the W.M. Keck Foundation Science and Engineering grant on "Extreme Diffusion". I.C. also wishes to acknowledge ongoing support from the NSF through DMS:1811143 and DMS:1937254, the Simon Foundation through a Simons Fellowship in Mathematics (Grant No. 817655), and the Packard Foundation Fellowship for Science and Engineering. Much of this work was performed while I.C. held a Miller Visiting Professorship from the Miller Institute for Basic Research in Science, and while in residence at the Mathematical Sciences Research Institute in Berkeley, California (NSF Grant No. 1440140). E.I.C. wishes to acknowledge ongoing support from the Simons Foundation for the collaboration Cracking the Glass Problem via award 454939. This work benefited from access to the University of Oregon high performance computing cluster, Talapas.

2.10 Supplementary Material

2.10.1 Numerical Methods. We expand upon our description of the numerical methods used in our simulations. We consider varying system sizes from $N = 10^2$ to $N = 10^{300}$ with time varying from $t = 0$ to $t = 5000\log(N)$. We simulate such large systems by utilizing the full range of quadruple-precision floating point numbers and making approximations to the binomial distribution when dealing with sizes beyond our precision limits. These approximations are necessary given the limitations of our precision and do not seem to affect the behavior of the system in any significant manner. In particular, for a site x at time t where the number of particles, $N(x,t)$, is below 2^{31} we use the C++ Boost integer implementation of a binomial distributed random number generator to choose the number of particles that will move right versus left. Above 2^{31} the integer implementation overflows and we instead approximate the binomial distribution by a Gaussian distribution of mean $N(x,t)B(x,t)$ and variance $N(x,t)B(x,t)(1 - B(x,t))$, as dictated by the central limit theorem. For sufficiently large $N(x,t)$, the variance itself will fall outside of the precision of a quadruple floating point number. This occurs when $N(x,t) > 10^{64}$, above which we approximate the binomial simply by its mean. The number of particles that move right is then $N(x,t)B(x,t)$. Psuodo-code of the simulation is given:

1. Start N particles at $x = 0$

2. For each site:

    draw $B(x,t)$ from $\mathcal{U}_{[0,1]}$

if $(N(x,t) > 10^{64})$

$N(x+1,t+1) = N(x,t)B(x,t)$

$N(x-1,t+1) = (1-B(x,t))N(x,t)$

else if $(2^{31} < N(x,t) < 10^{64})$

$\mu = N(x,t)B(x,t)$

$\sigma^2 = N(x,t)B(x,t)(1-B(x,t))$

$N(x+1,t+1)$ is drawn from $\mathcal{N}(\mu,\sigma^2)$

$N(x-1,t+1) = N(x,t) - N(x+1,t+1)$

else if $(N(x,t) < 2^{31})$

$N(x+1,t+1)$ is drawn from $\mathrm{Bin}(N(x,t),B(x,t))$

$N(x-1,t+1) = N(x,t) - N(x+1,t+1)$

where $\mathcal{U}_{[0,1]}$ is the random uniform distribution on the range $[0,1]$, $\mathcal{N}(\mu,\sigma^2)$ is the Gaussian distribution with mean μ and variance σ^2, and $\mathrm{Bin}(n,p)$ is the Binomial distribution with number of trials n and probability p. Note that our simulation differs from Monte Carlo, or agent based, simulations because we can group all the particles at a site together and iterate over each site. Our code is available at `https://github.com/CorwinLab/RWRE-Simulations`.

When estimating the statistics (e.g. mean and variance) for $\mathrm{Max}_t^N, \mathrm{Env}_t^N$ and Sam_t^N, the optimal manner would be that for each N and t we simulate a large number of environments and then build up histograms for the behavior of these quantities with one data point corresponding to one environment. Of course, in numerically computing the quantities for time t, we naturally compute them for all times smaller than t too, but for the same environment. Moreover, Env_t^N can be computed simultaneously for all N and t relative to the same environment, providing even further computational savings. We employ this computationally efficient approach to couple together the estimation for different values of N and t to the same pool of environments. There is a cost, however, to doing this. For example, the statistics that we numerically compute for Max_t^N for time t and time t' will themselves be correlated since they are derived from studying the same collection of environments. This correlation seems to be short-lived in time though, and is only evident upon zooming into the numerical measurements, for instances as in the inset in Fig. 3 of the main text.

2.10.2 Asymptotic Theory Results.

2.10.2.1 SSRW Max_t^N**.** For the SSRW where $B(x,t) \equiv 1/2$, we use the same notation $p(x,t)$ and $P(x,t)$, dropping the $\mathbf{B}$ subscript. Now assume that the ratio $\hat{t} = t/\log(N)$ tends to some finite value. As explained in the main article, if $\hat{t} < (\log(2))^{-1}$ then $N \gg 2^t$. In that case, $p(t,t) = 2^{-t} \gg 1/N$ which means that it is highly likely that there are many particles occupying the right-most site at $x = t$. This implies that $\mathrm{Mean}\left(\mathrm{Max}_t^N\right) \approx t$ and $\mathrm{Var}\left(\mathrm{Max}_t^N\right) \approx 0$.

When $\hat{t} > (\log(2))^{-1}$, the maximal random walk at time t will likely occur significantly below t and have non-trivial fluctuations which we now describe. For the SSRW, observe that $p(2k-t,t) = 2^{-t}\binom{t}{k}$ for $k = 0,\dots,t$. Thus, using Stirling's formula for binomial coefficients (or more generally using Cramer's theorem from the large deviation theory for sums of independent identically distributed random variables) we arrive at the asymptotic for $v \in (0,1)$ that

$$P(vt,t) \approx e^{-tI_{\mathrm{SSRW}}(v)} \quad \text{where} \quad I_{\mathrm{SSRW}}(v) = \frac{1}{2}\big((1+v)\log(1+v) + (1-v)\log(1-v)\big). \tag{S10}$$

$I_{\mathrm{SSRW}}(v)$ is known of as the large deviation rate function for the SSRW.

We may now combine this with Eq. (2.4) of the main text to show that Max_t^N is approximately distributed as a Gumbel random variable with location $\mu \approx t\hat{v}$ and shape $\beta = 1/I'_{\mathrm{SSRW}}(\hat{v})$, where $\hat{v} = I^{-1}_{\mathrm{SSRW}}(1/\hat{t})$ (here f^{-1} means the inverse function and not the reciprocal). A Gumbel random variable with location μ and shape β has

$$\text{cumulative distribution function } e^{-e^{(-x-\mu)/\beta}}, \quad \text{mean } \mu + \beta\gamma, \quad \text{and variance } \frac{\pi^2}{6}\beta^2, \tag{S11}$$

where $\gamma \sim .57721$ is the Euler-Mascheroni constant.

To see the above limit, observe that

$$\mathrm{Prob}\big(\mathrm{Max}_t^N \leq t\hat{v} + x\big) = \big(1 - P_{\mathbf{B}}(t\hat{v}+x,t)\big)^N \approx \big(1 - e^{-tI_{\mathrm{SSRW}}(\hat{v}+x/t)}\big)^N$$
$$\approx \big(1 - e^{-tI_{\mathrm{SSRW}}(\hat{v}) - I'_{\mathrm{SSRW}}(\hat{v})x}\big)^N = \big(1 - N^{-1}e^{-I'_{\mathrm{SSRW}}(\hat{v})x}\big)^N \approx e^{-e^{-I'_{\mathrm{SSRW}}(\hat{v})x}}.$$

The first equality follows from Eq. (2.4) of the main text, the second approximation uses (S10), the third uses Taylor expansion, the fourth follows from the definition of $\hat{v} = I^{-1}_{\mathrm{SSRW}}(1/\hat{t})$, while the final one uses the approximation $(1 - x/N)^N \approx e^{-x}$. Notice that in Taylor expanding we have assumed that lower order terms do not cause issues. This can be easily justified by going to further orders in the Stirling formula expansion.

Based on the above Gumbel asymptotics, we can now record the asymptotic form of the mean and variance of Max_t^N for the SSRW. Writing $\hat{v}(\hat{t})$ to make this dependence explicit and recalling that $\hat{t} = t/\log(N)$ we see that

$$\mathrm{Mean}\left(\mathrm{Max}_t^N\right) \approx t\hat{v}\big(\tfrac{t}{\log(N)}\big) + \frac{\gamma}{I'_{\mathrm{SSRW}}\Big(\hat{v}\big(\tfrac{t}{\log(N)}\big)\Big)}, \quad \mathrm{Var}\left(\mathrm{Max}_t^N\right) \approx \frac{\pi^2}{6\Big(I'_{\mathrm{SSRW}}\Big(\hat{v}\big(\tfrac{t}{\log(N)}\big)\Big)\Big)^2}. \tag{S12}$$

Inverting I_{SSRW} to find $\hat{v}(\hat{t})$ is non-trivial though can be done numerically or in certain limits. For instance, noting that for v near zero, $I_{\mathrm{SSRW}} \approx v^2/2$ we see that for $\hat{t}$ near infinity, $\hat{v}(\hat{t}) \approx \sqrt{2/\hat{t}}$ and hence $I'_{\mathrm{SSRW}}\big(\hat{v}(\hat{t})\big) \approx \sqrt{2/\hat{t}}$. From this and (S12) it follows that for $\hat{t} \gg (\log(2))^{-1}$, asymptotically

$$\mathrm{Mean}\left(\mathrm{Max}_t^N\right) \approx \Big(\sqrt{2\log(N)} + \frac{\gamma}{\sqrt{2\log(N)}}\Big)t^{1/2}, \qquad \mathrm{Var}\left(\mathrm{Max}_t^N\right) \approx \frac{\pi^2}{12}\frac{t}{\log(N)}.$$

On the other hand, (S12) also shows that as $\hat{t}$ tends to $(\log(2))^{-1}$ from above, the mean goes to t and the variance goes to zero.

2.10.2.2 RWRE $\boldsymbol{Env_t^N}$***.*** Assume that the ratio $\hat{t} = t/\log(N)$ tends to some finite value exceeding 1. The key theoretic result we use here is due to [6]. They show that for $v \in (0,1)$,

$$\log\big(P_{\mathbf{B}}(vt,t)\big) = -tI(v) + t^{1/3}\sigma(v)\chi_t \quad \text{where} \quad I(v) = 1-\sqrt{1-v^2}, \quad \sigma(v) = \left(\frac{2I(v)^2}{1-I(v)}\right)^{1/3}. \tag{S13}$$

Here $I(v)$ is the large deviation rate function and $\sigma(v)t^{1/3}$ is the scalings of the random environment-dependent fluctuations χ_t around that rate function. [6] showed that as $t \to \infty$, the distribution of χ_t converges to a Tracy-Widom GUE distribution χ. For reference below, let us note that [90]

$$\mu_\chi := \mathrm{Mean}\,(\chi) \approx -1.771, \qquad \sigma_\chi^2 := \mathrm{Var}\,(\chi) \approx .813.$$

As in the case of the SSRW, we now solve for $\hat{v} = \hat{v}(\hat{t})$ such that $P_{\mathbf{B}}(\hat{v}t,t) = 1/N$. Note that $\hat{v}t$ will then equal the $1/N$-quantile Env_t^N. From (S13), $\hat{v}$ must satisfy

$$tI(\hat{v}) - t^{1/3}\sigma(\hat{v})\chi_t = \log(N) = t/\hat{t}. \tag{S14}$$

Canceling t and dropping the $t^{1/3}$ term momentarily yields to first order that $\hat{v}$ is given by

$$\hat{v}_0 = I^{-1}(1/\hat{t}) = \sqrt{1-(1-1/\hat{t})^2}.$$

We can now Taylor expand $I(\hat{v})$ and $\sigma(\hat{v})$ in (S14) around $\hat{v} = \hat{v}_0$ and solve for $\hat{v}$ to the next order. Doing so we find that

$$\hat{v} = \hat{v}_0 + t^{-2/3}\frac{\sigma(\hat{v}_0)}{I'(\hat{v}_0)}\chi_t + O(t^{-4/3}).$$

Recalling that $\hat{v}t$ is supposed to yield the $1/N$-quantile, we conclude that

$$\mathrm{Env}_t^N = \hat{v}_0 t + t^{1/3}\frac{\sigma(\hat{v}_0)}{I'(\hat{v}_0)}\chi_t + O(t^{-1/3}). \tag{S15}$$

From this we can extract the asymptotic mean and variance of Env_t^N. Written explicitly (i.e., plugging in I and $\hat{v}_0$) this yields the following asymptotic formulas

$$\begin{aligned}\mathrm{Mean}\left(\mathrm{Env}_t^N\right) \approx M_1(N,t) :=& \left(1-\left(1-\tfrac{\log(N)}{t}\right)^2\right)^{1/2} t \\ &+ (\log(N))^{2/3} t^{-1/3}\frac{2^{1/3}\left(1-\tfrac{\log(N)}{t}\right)^{2/3}}{\sqrt{1-\left(1-\tfrac{\log(N)}{t}\right)^2}}\mu_\chi \\ \mathrm{Var}\left(\mathrm{Env}_t^N\right) \approx V_1(N,t) :=& \left(\frac{(\log(N))^{4/3}}{t^{2/3}}\right)\frac{2^{2/3}\left(1-\tfrac{\log(N)}{t}\right)^{4/3}}{1-\left(1-\tfrac{\log(N)}{t}\right)^2}\sigma_\chi^2,\end{aligned}$$

where above we have used that

$$\frac{\sigma(\hat{v}_0)}{I'(\hat{v}_0)} = \frac{2^{1/3}\hat{t}^{-2/3}(1-1/\hat{t})^{2/3}}{\sqrt{1-(1-1/\hat{t})^2}}.$$

For $\hat{t} = t/\log(N)$ large, it follows from the above expressions that

$$\mathrm{Var}\left(\mathrm{Env}_t^N\right) \approx \sigma_\chi^2\left(\tfrac{\log(N)}{2}\right)^{\frac{1}{3}} t^{\frac{1}{3}}. \tag{S16}$$

It is important to understand the order of the limits here. First we should fix $\hat{t} = t/\log(N)$ and take N and t to infinity. Then we take $\hat{t}$ large and find the above 1/3 power-law. That said, with some additional work using the methods of [6] it is possible to show that for the entire range $1 \ll t/\log(N) \ll \log(N)$, this 1/3 power-law persists. We will not provide the details for that here. However, below we will consider when t is of order $(\log(N))^2$. In that case, for small t in that range, we will find a perfect fit to the 1/3 power-law, thus agreeing with the assertion that this power-law persists over the full range $1 \ll t/\log(N) \ll \log(N)$.

Now assume that the ratio $\hat{\hat{t}} = t/\log(N)^2$ remains strictly positive and finite as N and t tend to infinity. While [6] probes $P_{\mathbf{B}}(x,t)$ for x linearly growing with t, [7] probes the regime where x grows like $t^{3/4}$. They show that for $v \in (0,\infty)$,

$$\log\left(P_{\mathbf{B}}(vt^{3/4},t)\right) \approx -\frac{v^2t^{1/2}}{2} - \frac{\log(t)}{4} + \log(v) - \frac{v^4}{12} + h(0,v^4) \tag{S17}$$

where $h(y,s)$ denotes the (random) height at spatial position y and time s of the *narrow wedge solution to the Kardar-Parisi-Zhang (KPZ) equation*

$$\partial_s h(y,s) = \tfrac{1}{2}\partial_y^2 h(y,s) + \tfrac{1}{2}\big(\partial_y h(y,s)\big)^2 + \xi(y,s)$$

driven by space-time white noise ξ, see [1, 66]. Using this result, we will be able to prove this other $(\log(N))^2$ time scale.

We may solve (S17) perturbatively (as in the $\log(N)$ case) for $\hat{\hat{v}}$ such that $P_{\mathbf{B}}(\hat{\hat{v}}t^{3/4},t) = 1/N$. The $1/N$-quantile $\mathrm{Env}_t^N = \hat{\hat{v}}t^{3/4}$ is then given by

$$\mathrm{Env}_t^N \approx \hat{\hat{v}}_0 t^{3/4} + \frac{t^{1/4}}{\hat{\hat{v}}_0}\left(h(0,\hat{\hat{v}}^4) - \frac{\hat{\hat{v}}_0^4}{12} - \log(\hat{\hat{v}}_0)\right) + O(t^{-1/4}) \quad \text{where} \quad \hat{\hat{v}}_0 = 2^{1/2}\hat{\hat{t}}^{-1/4}.$$

From this we can explicitly compute the asymptotics of the mean and variance as

$$\begin{aligned}
\mathrm{Mean}\left(\mathrm{Env}_t^N\right) &\approx M_2(N,t) := \big(2t\log(N)\big)^{1/2} + \sqrt{\tfrac{t}{2\log(N)}}\mathrm{Mean}\left(h\Big(0,\tfrac{4(\log(N))^2}{t}\Big)\right)\\
\mathrm{Var}\left(\mathrm{Env}_t^N\right) &\approx V_2(N,t) := \tfrac{t}{2\log(N)}\cdot\mathrm{Var}\left(h\Big(0,\tfrac{4(\log(N))^2}{t}\Big)\right).
\end{aligned} \tag{S18}$$

Notice that in the mean we have dropped the lower order contributions from the terms $\frac{\hat{\hat{v}}_0^4}{12}$ and $\log(\hat{\hat{v}}_0)$. The values of $\mathrm{Mean}\,(h(0,s))$ and $\mathrm{Var}\,(h(0,s))$ for varying $s > 0$ can be computed numerically through evaluation of the Fredholm determinant formula from [70, 71, 72, 73]. The result of this computation is recorded as Fig. 3 of [83]. In particular, the horizontal axis (labeled t in [83]) corresponds to our s variable, and the red circles record the value of $\mathrm{Mean}\left(\frac{h(0,s)+\frac{s}{24}}{(s/2)^{1/3}}\right)$ while the blue triangles record the values of $\mathrm{Var}\left(\frac{h(0,s)+\frac{s}{24}}{(s/2)^{1/3}}\right)$ (note that the $s/24$ shift here does not change the variance as it is deterministic). For $s > .33$ we approximate the mean and variances by interpolating between the numerically evaluated values in [83] (S. Prolhac kindly provided the data set used to create Fig. 3 in that paper). For $s < .33$ we use the short-time behavior of the KPZ equation explained below for our values of the mean and variance.

There are two key asymptotics for $h(0,s)$ derived in [70, 71, 72, 73]: $\frac{h(0,s)+\frac{s}{24}}{(s/2)^{1/3}} \approx \chi$ as $s \to \infty$ where χ is a Tracy-Widom GUE distributed, and $h(0,s) \approx -\frac{1}{2}\log(2\pi s) + s^{1/4}\pi^{1/4}2^{-1/2}G$ as $s \to 0$ where G is standard Gaussian distributed. These imply corresponding asymptotics for the mean and variance. In particular, as $\hat{\hat{t}} \to 0$,

$$\mathrm{Var}\left(\mathrm{Env}_t^N\right) \approx \sigma_\chi^2 2^{-1/3}\log(N)\hat{\hat{t}}^{1/3} = \sigma_\chi^2\left(\tfrac{\log(N)}{2}\right)^{\frac{1}{3}} t^{\frac{1}{3}}$$

which agrees perfectly with (S16). This shows that the long-time behavior in the $t = O(\log(N))$ scaling regime and the short time behavior in the $t = O(\log(N)^2)$ scaling regime match even up to the pre-factor. This strongly suggests the 1/3 power-law in Eq. 2.7 of the main text for the entire regime $1 \ll t/\log(N) \ll \log(N)$.

On the other hand, from the short-time KPZ asymptotic we find that as $\hat{\hat{t}} \to \infty$,

$$\mathrm{Var}\left(\mathrm{Env}_t^N\right) \approx \frac{1}{2}\pi^{1/2}t^{1/2}$$

thereby recovering Eq. (2.7) for the regime $t \gg (\log(N))^2$ in the main text. This indicates that for finite N and t it is necessary to stitch together the two regimes to get a reasonable formula for $\mathrm{Var}\left(\mathrm{Env}_t^N\right)$. We have found that an error function centered at $t = (\log(N))^{3/2}$ with a width of $(\log(N))^{4/3}$ produces a smooth transition between the two regimes. Thus, our final expression for the asymptotic mean and variance is given by

$$\mathrm{Var}^{\mathrm{asy}}\left(\mathrm{Env}_t^N\right) = \frac{1 - \mathrm{erf}\left(\frac{t-(\log(N))^{3/2}}{(\log(N))^{4/3}}\right)}{2} V_1(N,t) + \frac{1 + \mathrm{erf}\left(\frac{t-(\log(N))^{3/2}}{(\log(N))^{4/3}}\right)}{2} V_2(N,t), \quad \text{(S19)}$$

provided that $t \geq \log(N)$ and 0 for $t < \log(N)$. Here $\mathrm{erf}(x) = 2/\sqrt{\pi}\int_0^x e^{-t^2}dt$ is the error function. This construction is shown in Fig. S6. On the other hand, such stitching is unnecessary when it comes to the mean since the large t behavior of $M_1(N,t)$ matches the behavior of $M_2(N,t)$ all the way as $t \to \infty$. This can be seen through direct asymptotics of the formulas and is illustrated in Fig. S5. On this account, we simply take

$$\mathrm{Mean}^{\mathrm{asy}}\left(\mathrm{Env}_t^N\right) = M_1(N,t). \quad \text{(S20)}$$

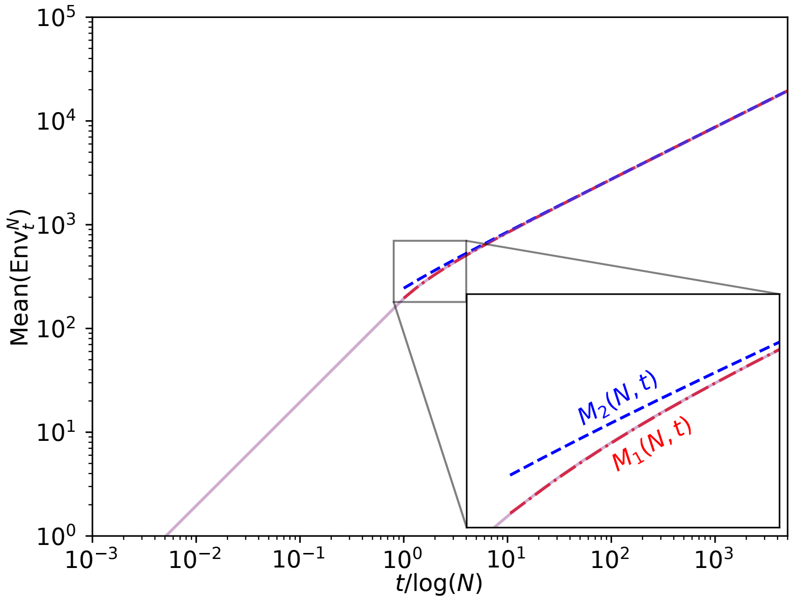

Figure S5. The asymptotic mean functions $M_1(N,t)$ and $M_2(N,t)$ are plotted for $N = 10^{85}$ in red and blue dashed lines, respectively. They agree closely for the full range of $t > \log(N)$ and also match the numerically measured values $\mathrm{Mean}^{\mathrm{num}}\left(\mathrm{Max}_t^N\right)$ given by the purple curve (which is linear, as expected, until roughly time $t = \log(N)$).

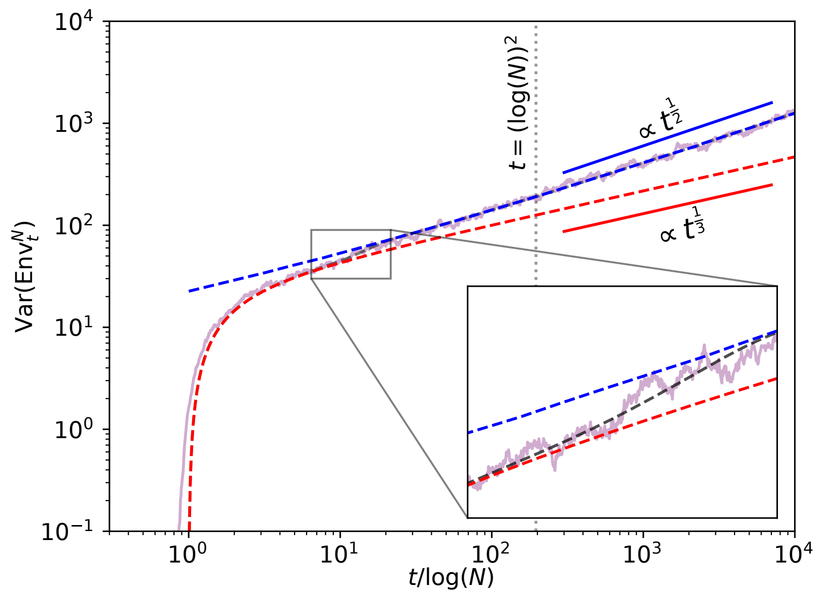

Figure S6. The asymptotic variance functions $V_1(N,t)$ and $V_2(N,t)$ are plotted for $N = 10^{85}$ in red and blue dashed lines, and the stitched together formula for $\mathrm{Var}^{\mathrm{asy}}\big(\mathrm{Env}_t^N\big)$ from (S19) is plotted as the black dashed line. The purple curve is the numerically measured curve $\mathrm{Var}^{\mathrm{num}}\big(\mathrm{Env}_t^N\big)$. The inset shows how the stitching captures the transition between the two asymptotic curves V_1 and V_2, and the solid lines show the asymptotic power-laws that V_1 and V_2 demonstrate as $t \to \infty$. The vertical dotted line indicates the regime crossover at $t = (\log(N))^2$.

2.10.2.3 RWRE Sam_t^N ***and*** Max_t^N***.*** Assume for the moment that $t = \hat{t}\log(N)$ for $\hat{t} > 1$. Then (S13) implies that

$$P_{\mathbf{B}}(\mathrm{Env}_t^N + x, t) = \exp\Big(-tI\big(\tfrac{\mathrm{Env}_t^N}{t} + \tfrac{x}{t}\big) + t^{1/3}\sigma\big(\tfrac{\mathrm{Env}_t^N}{t} + \tfrac{x}{t}\big)\chi_t\Big) \qquad \text{and} \qquad P_{\mathbf{B}}(\mathrm{Env}_t^N, t) = \frac{1}{N}.$$

If we Taylor expand to the next order in the exponential we find

$$\begin{aligned} P_{\mathbf{B}}(\mathrm{Env}_t^N + x, t) &\approx \exp\Big(- tI\big(\tfrac{\mathrm{Env}_t^N}{t}\big) - I'\big(\tfrac{\mathrm{Env}_t^N}{t}\big)x + t^{1/3}\sigma\big(\tfrac{\mathrm{Env}_t^N}{t}\big)\chi_t\Big) \\ &= \frac{1}{N}e^{-I'\big(\frac{\mathrm{Env}_t^N}{t}\big)x} \approx \frac{1}{N}e^{-I'(\hat{v}(\hat{t}))x}. \end{aligned}$$

The Taylor expansion requires a bit of explanation. We expand $I\big(\frac{\mathrm{Env}_t^N}{t} + \frac{x}{t}\big) \approx I\big(\frac{\mathrm{Env}_t^N}{t}\big) + I'\big(\frac{\mathrm{Env}_t^N}{t}\big)\frac{x}{t}$ to first order. The similar expansion of σ would produce a lower order term. However, there is a subtlety that we should point out. The χ_t

random variable implicitly depends on x as well. Namely, if we look at the random transition probability as we vary around Env_t^N, the fluctuations of this quantity will vary with x. However, we assume here that this fluctuation does not contribute to leading order. This assumption would be true if, for instance, χ_t looked locally like a random walk with independent and identically distributed intervals. This property is believed to be universal to models in the KPZ class and thus it is reasonable to assume that the same holds here. We do not attempt to justify this theoretically beyond this heuristic, though note that it yields very good agreement with our numerical simulations. The final approximation in the above string of equations involves replacing $I'\big(\frac{\mathrm{Env}_t^N}{t}\big)x$ by $I'(\hat{v}(\hat{t}))x$ which relies on the fact that $\frac{\mathrm{Env}_t^N}{t} \approx \hat{v}_0$ to highest order.

Combining the above deduction with (2.4) in the main text and $(1-x)^N \approx e^{-xN}$ (for x small) yields

$$\mathrm{Prob}(\mathrm{Max}_t^N \leq \mathrm{Env}_t^N + x) \approx \left(1 - \frac{1}{N} e^{-I'(\hat{v}(\hat{t}))x}\right)^N \approx e^{-e^{-I'(\hat{v}(\hat{t}))x}}. \tag{S21}$$

If we define Sam_t^N by the equality $\mathrm{Max}_t^N = \mathrm{Env}_t^N + \mathrm{Sam}_t^N$ then the above calculation shows that Sam_t^N is asymptotically independent of Env_t^N and asymptotically is Gumbel distributed with location and shape parameters

$$\mu(t) = 0, \qquad \beta(t) = 1/I'(\hat{v}(\hat{t})) = (\hat{t}-1)(2\hat{t}-1)^{-1/2} \approx (\hat{t}/2)^{1/2}$$

where the approximation is for $\hat{t} \gg 1$. This justifies the addition law for variances (Eq. (2.9) in the main text)

$$\mathrm{Var}\left(\mathrm{Max}_t^N\right) \approx \mathrm{Var}\left(\mathrm{Env}_t^N\right) + \mathrm{Var}\left(\mathrm{Sam}_t^N\right) \tag{S22}$$

and (using the Gumbel variance formula in (S11)) this also justifies Eq. (2.8) of the main text which provides the asymptotic formula for the variance (we also record that the asymptotic mean is 0)

$$\mathrm{Mean}^{\mathrm{asy}}\big(\mathrm{Sam}_t^N\big) = 0, \qquad \mathrm{Var}^{\mathrm{asy}}\big(\mathrm{Sam}_t^N\big) = \frac{\pi^2}{6}\frac{\left(\frac{t}{\log(N)} - 1\right)^2}{2\frac{t}{\log(N)} - 1} \approx \frac{\pi^2}{12}\frac{t}{\log(N)}, \tag{S23}$$

where the approximation is for $\hat{t} \gg 1$.

Putting together (S19), (S20), (S22) and (S23) we conclude that

$$\begin{aligned}\mathrm{Mean}^{\mathrm{asy}}\big(\mathrm{Max}_t^N\big) &= M_1(N,t),\\ \mathrm{Var}^{\mathrm{asy}}\big(\mathrm{Max}_t^N\big) &= \frac{1 - \mathrm{erf}\left(\frac{t-(\log(N))^{3/2}}{(\log(N))^{4/3}}\right)}{2}V_1(N,t) + \frac{1 + \mathrm{erf}\left(\frac{t-(\log(N))^{3/2}}{(\log(N))^{4/3}}\right)}{2}V_2(N,t)\\ &\quad + \frac{\pi^2}{6}\frac{\left(\frac{t}{\log(N)} - 1\right)^2}{2\frac{t}{\log(N)} - 1}.\end{aligned} \tag{S24}$$

The above calculation assumed $\hat{t} = t/\log(N)$ converges to a finite value. However, in a similar manner based on (S17) we can probe the behavior when $\hat{\hat{t}} = t/(\log(N))^2$ converges to a finite value. This behavior agrees perfectly with the large $\hat{t}$ limiting behavior above. Thus, we conclude that the formula for $\mathrm{Var}^{\mathrm{asy}}\big(\mathrm{Sam}_t^N\big)$ should hold for all $t \gg \log(N)$.

Fig. S7 show our asymptotic theory formulas for the mean of the maximal particle fit closely with our numerical simulations.

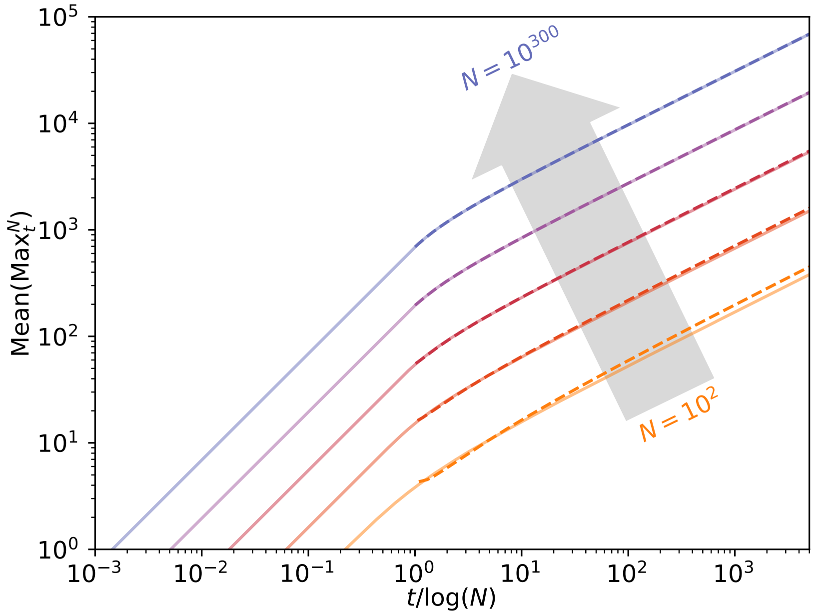

Figure S7. The mean position of the maximal particle location (solid line) for $N = 10^2, 10^7, 10^{24}, 10^{85}$ and 10^{300} for 10000, 5000, 1000, 500 and 500 instantiations of the environment, respectively. The theoretical prediction (dashed line) given in Eq. (S24) is also shown. We find the theoretical predictions for the mean position of the maximum particle, $\mathrm{Mean}\left(\mathrm{Max}_t^N\right)$, are in agreement with the data.

CHAPTER III

FIRST PASSAGE TIME FOR MANY PARTICLE DIFFUSION IN SPACE-TIME RANDOM ENVIRONMENTS

This chapter is published as: Hass, J. B., Corwin, I., & Corwin, E. I. (2024, May). First-passage time for many-particle diffusion in space-time random environments. Physical Review E , 109 (5), 054101. doi: 10.1103/PhysRevE.109.054101. My contribution to the paper was developing and running the code to generate the numerics as well as deriving the theoretical results.

3.1 Abstract

The first passage time for a single diffusing particle has been studied extensively, but the first passage time of a system of many diffusing particles, as is often the case in physical systems, has received little attention until recently. We consider two models for many particle diffusion – one treats each particle as independent simple random walkers while the other treats them as coupled to a common space-time random forcing field that biases particles nearby in space and time in similar ways. The first passage time of a single diffusing particle under both of these models show the same statistics and scaling behavior. However, for many particle diffusions, the first passage time among all particles (the ‘extreme first passage time’) is very different between the two models, effected in the latter case by the randomness of the common forcing field. We develop an asymptotic (in the number of particles and location where first passage is being probed) theoretical framework to separate the impact of the random environment with that of sampling trajectories within it. We identify a new power-law describing the impact of the environment on the variance of the extreme first passage time.

Through numerical simulations we verify that the predictions from this asymptotic theory hold even for systems with widely varying numbers of particles, all the way down to 100 particles. This shows that measurements of the extreme first passage time for many-particle diffusions provide an indirect measurement of the underlying environment in which the diffusion is occurring.

3.2 Introduction

The *extreme* (or fastest) first passage time beyond a barrier among many particles diffusing in a common environment determines the function of a variety of system such as oocyte fertilization [94, 95, 96], neuronal activation [8] and information flow in networks [97, 98]. When particles are modeled as independent simple symmetric random walks (SSRW) or Brownian motions [22, 21, 23], there has been extensive study of the first passage behavior for a single particle [99], or recently for many particles [94, 100, 95, 101, 102, 103, 104, 105, 106].

We probe the behavior of extreme first passage time for a model of many particle diffusion where particles are modeled as random walks in a common environment of space-time inhomogeneous biases which are, themselves, modeled by a random field with short-range correlations in space and time. We focus on this (time-dependent) random walk in random environment (RWRE) model in one spatial dimension as would be relevant to diffusion in long and thin capillaries. Self-averaging of the environment implies that the statistical behavior of a single (or typical) particle in the RWRE model remains unchanged compared to the SSRW model [63, 64, 24]. However, the extreme behavior of particles in the RWRE model has recently been shown to be quite different to that of the SSRW, with statistics and power-laws related to the Kardar-Parisi-Zhang (KPZ) universality class and equation [6, 7, 107] (see also [108, 109, 69, 76, 110, 77, 111, 78, 112, 113, 80]).

Those works focus on the statistical behavior of the locations of the particles that move the furthest from a common starting position as a function of time and the number of particles, N. The location of the furthest particle is a complementary measurement to the extreme first passage time which measures time as a function of the location of a boundary.

Here we leverage the theoretical and asymptotic (in $N \to \infty$) results on extreme particle locations in the RWRE model [6, 7] to make precise finite N predictions about extreme first passage time statistics as a function of the location, L, of first passage and the number of particles, N. We show that the effect of the randomness of the environment and of sampling N random walks in that environment are approximately independent. This means that by probing the extreme first passage time we are able to gain access to certain measurements of the hidden environment in which the diffusion occurs. Using numerical simulations, we show that these predictions remain valid down to quite small systems of $N = 100$.

3.3 Background

Classical modeling of diffusion [22, 21, 23] has served as a basis for the development of more complex models such as Lévy flights in biological systems [38], anomalous diffusion where the mean squared distance is not linear [40, 39], and active materials where particles have internal stores of energy [41, 42]. The aforementioned models modify the existing framework of classical diffusion to better model specific phenomenon, whereas we study a model that aims to better capture the behavior of classical diffusion in generality.

We consider a particular type of random walk in random environment (RWRE) models. RWRE models have been studied extensively and come in various forms, including those with short range correlated forces [56, 57, 58, 59, 60], long range correlated forces [39, 51, 52, 53, 54] and only spatially varying random forces [44, 45, 51, 50, 49]. We consider a short range, spatially and temporally varying random field.

Extreme first passage time statistics for classical models of many particle diffusion (e.g. N independent SSRWs) have been studied extensively [94, 100, 95, 101, 102, 103, 104, 105, 106]. For RWRE models with a temporally constant environment, [93, 106, 92] studied the aspects of first passage times for one and many particle diffusions. In our setting of a temporally varying environment, [69] (see the supplementary materials in [69]) initiated the study of extreme first passage time upon which we will expand.

3.4 Summary of Results

We summarize our main results and outline the remainder of the paper. We study the mean and variance of, Min_L^N, the extreme first passage time. An illustration of our model and the extreme first passage time can be found in Figure 8. We find that the effects of the environment are negligible for the mean of Min_L^N as compared to a homogenous environment, but introduce significant additional variance. Therefore, we focus on characterizing the variance of Min_L^N.

We show that Min_L^N can be decomposed into two sources of randomness: randomness due to the random environment, which we denote Env_L^N, and the randomness due to sampling random walks within that environment, which we denote Sam_L^N. The main result of our paper is presented in Figure 9 which shows a comparison of the numerical measurements and derived predictions for the variance of Min_L^N, Env_L^N and Sam_L^N.

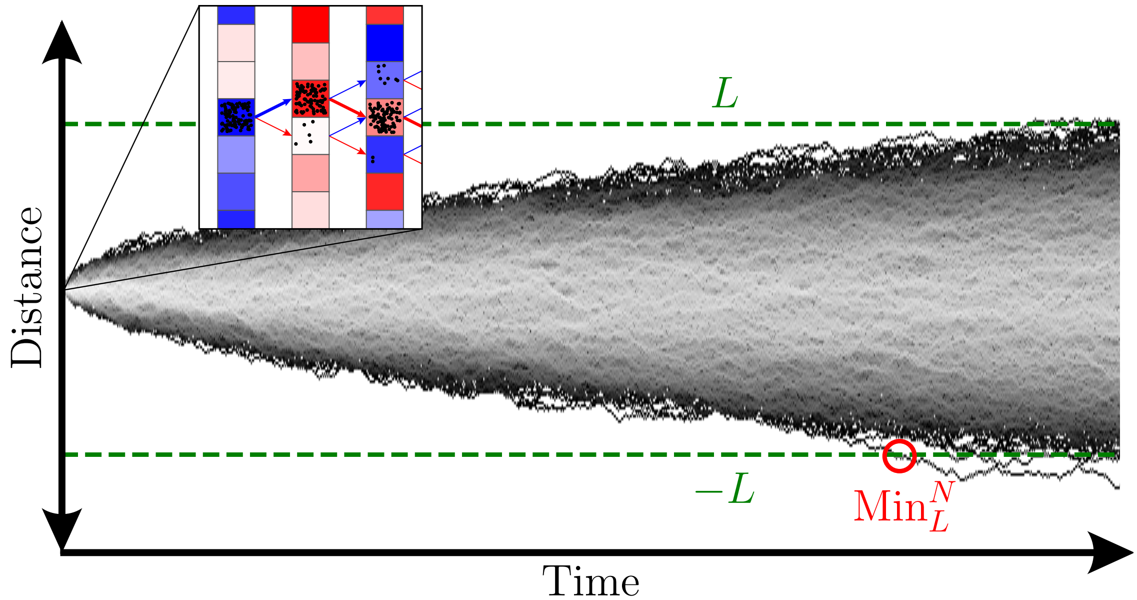

Figure 8. A system of $N = 10^5$ particles evolving according to our RWRE model. The green dashed lines denote a barrier at $-L$ and L. The extreme first passage time, Min_L^N, is identified by the red circle and is the first time when one of these N walkers crosses this barrier. The inset illustrates the dynamics of particles in the first three time steps (not all 10^5 particles are shown to avoid cluttering). The color of each box in the inset corresponds to the bias of the location (blue means upward bias and red means downward bias).

To distinguish our numerical measurements from the true value, we will introduce a superscript so that $\mathbb{E}^{\text{Num}}[\bullet]$ and $\text{Var}^{\text{Num}}(\bullet)$ represent the numerically measured mean and variances of $\bullet$. Similarly, we use the notation $\mathbb{E}^{\text{Asy}}[\bullet]$ and $\text{Var}^{\text{Asy}}(\bullet)$ to represent our formulas derived in the asymptotic limit that L and N tend to infinity.

As in many extreme value statistics problems, the characteristic scale for the system is set by $\ln(N)$. We find three distinct scaling regimes, in the limit that L and N tend to infinity, but dependent on the relation between L and $\ln(N)$.

For short distances, when $L < \ln(N)$, the extreme particle moves ballistically. The extreme first passage time is approximately $\mathrm{Min}_L^N \approx L$ so

$$\mathrm{Var}\left(\mathrm{Env}_L^N\right) \approx 0 \tag{3.1}$$

for $L < \ln(N)$. The nature and location of this crossover is derived in Section 3.7.1.

The medium and large distance regimes prove more complicated than the short distance regime. We provide the characteristic power laws here, but more precise formulas for $\mathrm{Var}\left(\mathrm{Env}_L^N\right)$ in the medium and large distance regime are derived in Section 3.7.2 and 3.7.3, respectively.

We define the medium distance regime to be distances for which $\ln(N) < L < \ln(N)^{3/2}$. In this regime we find that the variance in the randomness due to the environment scales like

$$\mathrm{Var}\left(\mathrm{Env}_L^N\right) \approx c_1 \frac{L^{8/3}}{(\ln(N))^2} \tag{3.2}$$

where $c_1 = \mathrm{Var}\left(\max(\chi, \chi')\right)/2^{1/3}$ and χ and χ' are independent Gaussian Unitary Ensemble (GUE) Tracy-Widom (TW) random variables.

We define the large distance regime as $L > \ln(N)^{3/2}$. We find

$$\mathrm{Var}\left(\mathrm{Env}_L^N\right) \approx c_2 \frac{L^3}{(\ln(N))^{5/2}} \tag{3.3}$$

where $c_2 = \pi^{1/2}/2^{5/2}$.

Although the scalings in Eq. 3.2 and 3.3 differ, we show in Section 3.7.3 that the medium and large distance regimes are consistent. Specifically, we show our equation for $\mathrm{Var}\left(\mathrm{Env}_L^N\right)$ derived in the large distance regime, but in the limit $L \ll (\ln(N))^{3/2}$, recovers the power law in Eq. 3.2. This indicates there is a smooth crossover from the medium to large distance regime. We produce a continuous curve for $\mathrm{Var}\left(\mathrm{Env}_L^N\right)$ by stitching together the medium and large distance via smooth interpolation as discussed in Section 3.7.4.

We show that the randomness introduced by sampling is independent from that due to the environment as $L \to \infty$. Thus,

$$\mathrm{Var}\left(\mathrm{Min}_L^N\right) \approx \mathrm{Var}\left(\mathrm{Env}_L^N\right) + \mathrm{Var}\left(\mathrm{Sam}_L^N\right). \tag{3.4}$$

Using this fact we derive $\mathrm{Var}\left(\mathrm{Sam}_L^N\right)$ in Section 3.7.5 and find

$$\mathrm{Var}\left(\mathrm{Sam}_L^N\right) \approx \frac{\pi^2}{24}\frac{L^4}{(\ln(N))^4}. \tag{3.5}$$

We note that this is the same result as one finds in the absence of any environmental randomness.

As seen in Figure 9, our theory for $\mathrm{Var}\left(\mathrm{Env}_L^N\right)$ and $\mathrm{Var}\left(\mathrm{Sam}_L^N\right)$ closely match the numerical results except for when L is very close to $\ln(N)$ where finite size effects dominate. We recover $\mathrm{Var}\left(\mathrm{Min}_L^N\right)$ using Eq. 3.4 and this approximation closely matches the data. We see $\mathrm{Var}\left(\widetilde{\mathrm{Min}_L^N}\right)$ closely matches $\mathrm{Var}\left(\mathrm{Sam}_L^N\right)$ since $\mathrm{Var}\left(\widetilde{\mathrm{Min}_L^N}\right)$ does not contain any randomness due to the environment, and is only composed of randomness due to sampling random walks in the same environment.

We can recover the variance due to the environment by rearranging Eq. 3.4 as $\mathrm{Var}\left(\mathrm{Env}_L^N\right) \approx \mathrm{Var}\left(\mathrm{Min}_L^N\right) - \mathrm{Var}\left(\mathrm{Sam}_L^N\right)$. Figure 10 shows the numerically measured $\mathrm{Var}\left(\mathrm{Min}_L^N\right) - \mathrm{Var}\left(\mathrm{Sam}_L^N\right)$ along with our asymptotic theory for $\mathrm{Var}\left(\mathrm{Env}_L^N\right)$ which match closely for all systems sizes. The ratio of the numerically measured $\mathrm{Var}\left(\mathrm{Min}_L^N\right) - \mathrm{Var}\left(\mathrm{Sam}_L^N\right)$ and our prediction for $\mathrm{Var}\left(\mathrm{Env}_L^N\right)$ is approximately 1 over the full range of L studied, which provides validation of Eq. 3.4. Therefore, the extreme first passage time can be used as a probe to measure the statistics of the underlying diffusive environment.

3.5 Model for Diffusion

We consider independent random walks subject to a common environment which determines the bias at each site. We model the environment as independent and identically distributed (i.i.d.) transition biases $\mathbf{B} = \{B(x,t) : x \in \mathbb{Z}, t \in \mathbb{Z}_{\geq 0}\}$ drawn from a distribution supported on $[0,1]$. In this work we focus on the *Random Walk in Random Environment (RWRE)* model where $B(x,t)$ are drawn from the uniform distribution on $[0,1]$. If instead all $B(x,t) = 1/2$ our model reduces to the *Simple Symmetric Random Walk (SSRW)* model for diffusion. We write $\mathbb{P}(\bullet)$ for the probability of an event $\bullet$, and $\mathbb{E}[\bullet]$ and $\mathrm{Var}(\bullet)$ for the expectation and variance of a random variable $\bullet$ averaged over the random environment $\mathbf{B}$. For a given environment $\mathbf{B}$, we use the notation $\mathbb{P}^{\mathbf{B}}(\bullet)$, $\mathbb{E}^{\mathbf{B}}[\bullet]$ and $\mathrm{Var}^{\mathbf{B}}(\bullet)$ to represent the probability of an event $\bullet$ (in the first case) or random variable $\bullet$ (in the second and third cases) given the environment $\mathbf{B}$. Recall the laws of total probability, expectation and variance

$$\begin{aligned} \mathbb{P}(\bullet) = \mathbb{P}(\mathbb{P}^{\mathbf{B}}(\bullet)), \qquad \mathbb{E}[\bullet] = \mathbb{E}[\mathbb{E}^{\mathbf{B}}[\bullet]], \\ \mathrm{Var}(\bullet) = \mathrm{Var}\left(\mathbb{E}^{\mathbf{B}}[\bullet]\right) + \mathbb{E}[\mathrm{Var}^{\mathbf{B}}(\bullet)]. \end{aligned} \tag{3.6}$$

We now describe the motion of a single particle given the environment $\mathbf{B}$. We denote the position of a single particle at time $t \in \mathbb{Z}_{\geq 0}$ as $X(t) \in \mathbb{Z}$. It evolves as the following Markov chain. We begin at the origin such that $X(0) = 0$. Subsequently for all $t \in \mathbb{Z}_{\geq 0}$ if the particle is at position $X(t) = x$ it flips a weighted coin which has probability of heads $B(x,t)$ and tails $1 - B(x,t)$. If heads, the particle changes position such that $X(t+1) = X(t) + 1$ and if tails then $X(t+1) = X(t) - 1$. We use $p^{\mathbf{B}}(x,t) := \mathbb{P}^{\mathbf{B}}(X(t) = x)$ to denote the probability mass function for $X(t)$ which uniquely solves the Kolmogorov backwards equation

$$\begin{aligned} p^{\mathbf{B}}(x,t) = &p^{\mathbf{B}}(x-1,t-1)B(x-1,t-1) \\ &+ p^{\mathbf{B}}(x+1,t-1)\big(1 - B(x+1,t-1)\big) \end{aligned}$$

for $x \in \mathbb{Z}$ and $t \in \mathbb{Z}_{\geq 0}$ with initial condition $p^{\mathbf{B}}(x,0) = \mathbf{1}_{x=0}$ (with the notation $\mathbf{1}_E$ equals 1 if the event E occurs and 0 otherwise). For $L \in \mathbb{N}$ we define the (random) first passage time, τ_L, for $X(t)$ as

$$\tau_L = \min\bigl(t : X(t) \notin (-L, L)\bigr),$$

i.e., the time when the particle first exits $(-L, L)$.

We consider N particles $X^1(t), \ldots, X^N(t)$ evolving independently in the same environment $\mathbf{B}$. This means that if multiple particles are at the same location and the same time, they use the same biased coins to determine their next move, though the flips of those coins are done independently of each other. For $i \in \{1, \ldots, N\}$ let τ_L^i denote the first passage time for particle $X^i(t)$. Given the environment, the laws of $\tau_L^1, \ldots, \tau_L^N$ are independent and identically distributed. We will study the first time *any* of the N particles leave $(-L, L)$ which we call the *extreme first passage time* and denote by $\mathrm{Min}_L^N = \min(\tau_L^1, ..., \tau_L^N)$. A visualization of our system and the extreme first passage time can be seen in Fig. 8.

The probability distribution of τ_L and consequently that of Min_L^N can be computed by studying $X_L(t) := X(\min(t, \tau_L))$, the random walk $X(t)$ stopped (or absorbed) when it first exits $(-L, L)$. The corresponding probability mass function $p_L^{\mathbf{B}}(x, t) := \mathbb{P}^{\mathbf{B}}(X_L(t) = x)$ uniquely solves the Kolmogorov backwards equation

$$\begin{aligned} p_L^{\mathbf{B}}(x,t) =& p_L^{\mathbf{B}}(x-1,t-1)B(x-1,t-1) \\ &+ p_L^{\mathbf{B}}(x+1,t-1)\bigl(1 - B(x+1,t-1)\bigr) \end{aligned} \tag{3.7}$$

for $x \in [-L+2, L-2] \cap \mathbb{Z}$ and $t \in \mathbb{Z}_{\geq 0}$ subject absorbing boundary conditions whereby

$$\begin{aligned} p_L^{\mathbf{B}}(L,t) &= p_L^{\mathbf{B}}(L,t-1) \\ &\quad + B(L-1,t-1)p_L^{\mathbf{B}}(L-1,t-1), \\ p_L^{\mathbf{B}}(L-1,t) &= p_L^{\mathbf{B}}(L-2,t-1)B(L-2,t-1), \\ p_L^{\mathbf{B}}(-L+1,t) &= p_L^{\mathbf{B}}(-L+2,t-1)\big(1-B(-L+2,t-1)\big), \\ p_L^{\mathbf{B}}(-L,t) &= p_L^{\mathbf{B}}(-L,t-1) \\ &\quad + p_L^{\mathbf{B}}(-L+1,t-1)\big(1-B(-L+1,t-1)\big), \end{aligned} \tag{3.8}$$

and initial condition $p_L^{\mathbf{B}}(x,0) = \mathbf{1}_{x=0}$. The probability of τ_L occurring before time t is the same as the probability of being absorbed before time t which is given by

$$\mathbb{P}^{\mathbf{B}}(\tau_L \leq t) = p_L^{\mathbf{B}}(L,t) + p_L^{\mathbf{B}}(-L,t). \tag{3.9}$$

From this, the probability distribution of the extreme first passage time, Min_L^N, is given by

$$\mathbb{P}^{\mathbf{B}}(\mathrm{Min}_L^N \leq t) = 1 - \big(1 - \mathbb{P}^{\mathbf{B}}(\tau_L \leq t)\big)^N \tag{3.10}$$

since each τ_L^i is independent and identically distributed with probability distribution function $\mathbb{P}^{\mathbf{B}}(\tau_L \leq t)$. Note, for the SSRW model for diffusion we will denote the extreme first passage time as $\widetilde{\mathrm{Min}}_L^N$.

There are two sources of randomness at play in Min_L^N. The first is due to the randomness of the underlying environment, $\mathbf{B}$, and the second due to sampling random walks in said environment. We seek to study the impact of each and their interplay. We define a natural proxy, Env_L^N, for the randomness due to the environment by

$$\mathrm{Env}_L^N \coloneqq \min\left(t : \mathbb{P}^{\mathbf{B}}(\tau_L \leq t) \geq \frac{1}{N}\right). \tag{3.11}$$

Notice that Env_L^N is deterministic given $\mathbf{B}$. Eq. 3.11 is a reasonable choice of Env_L^N as it is approximately the median of the distribution of Min_L^N. This can be shown by substituting $\mathbb{P}^{\mathbf{B}}(\tau_L \leq t) = \frac{1}{N}$ into Eq. 3.10 such that $\mathbb{P}^{\mathbf{B}}(\text{Min}_L^N \leq \text{Env}_L^N) \approx 1 - (1 - 1/N)^N \approx e^{-1}$. The reason the first approximation is not an equality is because $\mathbb{P}^{\mathbf{B}}(\tau_L \leq t) \geq \frac{1}{N}$ in Eq 3.11 and therefore $\mathbb{P}^{\mathbf{B}}(\tau_L \leq t)$ will not strictly be equal to $1/N$ at time Env_L^N. We could also define Env_L^N in Eq. 3.11 by replacing $1/N$ with c/N for $c \in \mathbb{R}_{>0}$, an order 1 constant. However, this would only introduce sub-leading order terms which would not change the power-laws or variance of Env_L^N and Sam_L^N. Thus, we do not include this constant by setting $c = 1$. The difference

$$\text{Sam}_L^N \coloneqq \text{Min}_L^N - \text{Env}_L^N, \tag{3.12}$$

which is still random given $\mathbf{B}$, contains the randomness from sampling $\tau_L^1, \ldots, \tau_L^N$ given the environment $\mathbf{B}$.

While we have chosen to study the extreme first passage time of one or many particles leaving the region $(-L, L)$, we could just as well have studied the analogous time for leaving the region $(-\infty, L)$. The former case (studied mostly here) is the two-sided case while the latter is the one-sided case. The two-sided case benefits from the fact that $\mathbb{E}[\text{Min}_L^N] < \infty$ for all $N \geq 1$ while in the one-sided case, this mean is infinite for small enough N. Owing to this heavy-tailed nature of the one-sided case, it is numerically less efficient to study than in the two-sided case. On the other hand, our theoretical framework and asymptotic predictions provided below can be easily extended to the one-sided case. We will mostly focus on the two-sided case but also record some results for the one-sided case. Thus, in anticipation of that, let us define the first passage time $\tilde{\tau}_L = \min(t : X(t) < L)$ and the stopped random walk $\tilde{X}_L(t) := X(\min(t, \tilde{\tau}_L))$, whose probability mass function $\tilde{p}_L^{\mathbf{B}}(x,t) := \mathbb{P}^{\mathbf{B}}(\tilde{X}_L(t) = x)$ obeys the same equation and initial condition as the double sided case, but without the absorbing boundary at $-L$. Thus $\tilde{p}_L^{\mathbf{B}}(x,t)$ satisfies Eq. 3.7 for $x \in (-\infty, L-1) \cap \mathbb{Z}$ subject to the first two equalities in Eq. 3.8.

3.6 Numerical Methods

In what follows we will study the mean and variance of $\mathrm{Min}_L^N, \mathrm{Env}_L^N$ and Sam_L^N. We will numerically measure the values of these quantities via the methods described here.

Given an environment $\mathbf{B}$, we can exactly sample the motion of N particles in it by following the agent-based definition whereby each particle evolves as a random walk with biases given by $\mathbf{B}$. When N is large it is not feasible to use the agent-based approach. Instead, as in [107], we obtain massive increase in efficiency by noting that if there are $N(x,t)$ particles at site x and time t, they will split into right and left moving populations according to a Binomial distribution. Specifically, the number of particles that move from site x at time t to site $x+1$ at time $t+1$ is drawn from a Binomial distribution with $N(x,t)$ trials and success probability $B(x,t)$. The remaining particles move to site $x-1$ at time $t+1$. We achieve such large values of N by approximating the Binomial distribution as a Gaussian distribution for sufficiently large N as discussed in the supplement of [107]. This occupation variable based approach provides a way to exactly sample the number of particles per site over time which is sufficient to study the first passage times in question here. Furthermore, we use quadruple-precision floating point numbers to realize higher resolutions for large N.

In this work we present results on systems of $N = 10^2$ to $N = 10^{28}$ particles and measure the time of first passage for distances up to $L = 750 \cdot \ln(N)$. We measure the extreme first passage time past multiple distances in the same simulation by recording the time at which a particle first leaves each given boundary. We numerically measure $\mathbb{E}\left[\mathrm{Min}_L^N\right]$ and $\mathrm{Var}\left(\mathrm{Min}_L^N\right)$ by choosing, according to the uniform distribution on each $B(x,t)$, an environment, $\mathbf{B}$, and then sampling Min_L^N as described above. Repeating this for many independently sampled environments allows us to build up the distribution of Min_L^N and thus estimate $\mathbb{E}\left[\mathrm{Min}_L^N\right]$ and $\mathrm{Var}\left(\mathrm{Min}_L^N\right)$. For different values of N we repeat this procedure. However, for a given value of N, we make use of the same environment to study the statistics of Min_L^N for multiple values of L. Although this introduces some correlation in these numerically computed statistics at different distances, these should become negligible for a large sample size (i.e., the number of different instances of $\mathbf{B}$ used).

To study Env_L^N, we compute $p_L^{\mathbf{B}}(x,t)$ for a given environment, $\mathbf{B}$, and distance L by numerically solving Eq. 3.7 with the boundary conditions in Eq. 3.8 and initial condition $p_L^{\mathbf{B}}(x,0) = \mathbf{1}_{x=0}$. From $p_L^{\mathbf{B}}(x,t)$ we calculate $\mathbb{P}^{\mathbf{B}}(\tau_L \leq t)$ using Eq. 3.9. We then measure Env_L^N for a given environment using its definition in Eq. 3.11. By computing $\mathbb{P}^{\mathbf{B}}(\tau_L \leq t)$ for many independent samples of the environment $\mathbf{B}$, we estimate $\mathbb{E}\left[\mathrm{Env}_L^N\right]$ and $\mathrm{Var}\left(\mathrm{Env}_L^N\right)$.

We measure Sam_L^N using the following process. For a given environment $\mathbf{B}$, we calculate the probability distribution of Sam_L^N using Eq. 3.10 and 3.12, i.e.,

$$\mathbb{P}^{\mathbf{B}}(\mathrm{Sam}_L^N \leq t) = 1 - \left(1 - \mathbb{P}^{\mathbf{B}}(\tau_L \leq t + \mathrm{Env}_L^N)\right)^N. \tag{3.13}$$

To exponentiate the probability distribution for large values of N, we utilize arbitrary precision floating point arithmetic. Using $\mathbb{P}^{\mathbf{B}}(\mathrm{Sam}_L^N \leq t)$, we calculate $\mathbb{E}^{\mathbf{B}}[\mathrm{Sam}_L^N]$ and $\mathrm{Var}^{\mathbf{B}}(\mathrm{Sam}_L^N)$ numerically. We are using the notation $\mathbb{E}^{\mathbf{B}}[\bullet]$ and $\mathrm{Var}^{\mathbf{B}}(\bullet)$ introduced in Sec. 3.5. We can then numerically measure $\mathbb{E}[\mathrm{Sam}_L^N]$ and

$\mathrm{Var}(\mathrm{Sam}_L^N)$ by sampling many independent instances of $\mathbf{B}$ and using the laws of total expectation and variance in Eq. 3.6.

We probe four values of N, $N = 10^2, 10^5, 10^{12}$ and 10^{28}. To measure statistics involving Min_L^N we use $20,000, 10,000, 10,000$ and $2,500$ systems for the respective values of N, while to measure statistics involving Env_L^N and Sam_L^N we use $2,000, 2,000, 2,000$ and $1,000$ systems for the respective values of N. Notice that we used fewer systems for Env_L^N and Sam_L^N than for Min_L^N. This is because Min_L^N can be sampling via simulating the motion of N particles as described above while Env_L^N and Sam_L^N require computing the probability distribution by solving the master equation. The former is computationally much less expensive than the latter, hence our reduction in number of systems. For measuring statistics involving Min_L^N for the SSRW model we use $5,000$ systems (in other words, we repeatedly sample N SSRWs and observe Min_L^N for a total of $5,000$ instances).

To compute the data presented in this paper, we used 500 CPUs on a high performance computing cluster for approximately two weeks. Our code is available at `https://github.com/CorwinLab/RWRE-Simulations`.

3.7 Derivation of Asymptotic Predictions

We derive asymptotic predictions for the extreme first passage time for the RWRE model in the limit where both L and N tending towards infinity with certain relationships. We study the mean and variances of $\mathrm{Min}_L^N, \mathrm{Env}_L^N$ and Sam_L^N and develop asymptotic formulas that we subsequently compare to our numerical simulations in Sec. 3.8.

We find that there are three different scaling regimes with smooth transitions between them, consistent with previous results in [107] (which probes for different N the location of the maximum as a function of time, instead of the first passage time as a function of barrier location). The short distance regime is when $L/\ln(N) \to \hat{L} < 1$, in which case we will easily see that with very high probability at least one particle will move ballistically (hence resulting in trivial behaviors for the mean and variances in question). The medium distance regime is when $L/\ln(N) \to \hat{L} \in (1, \infty)$, a finite number greater than 1, in which case we leverage results from [6] to derive our asymptotic formulas related to the Gaussian Unitary Ensemble Tracy-Widom distribution [114]. The large distance regime is when $L/(\ln(N))^{3/2} \to \hat{\hat{L}} \in (0, \infty)$, a finite non-zero number, in which case we leverage results from [7] to derive our asymptotic formulas related to the statistics of the solution to the KPZ equation with narrow wedge initial data [1, 70, 71, 72, 73]. In each of these regimes we derive asymptotic approximations for the mean and variance of Sam_L^N and Env_L^N and argue they are independent when L and N tend towards infinity. Using this independence and these asymptotics for Sam_L^N and Env_L^N, we then likewise provide formulas for the asymptotic mean and variance of the extreme first passage time, Min_L^N, as recorded in Eqs. 3.43 and 3.44.

The study of extreme first passage time for the RWRE model was initiated in [69] (in particular, see the supplemental material in [69]) which focused on the fluctuations of Env_L^N in the medium distance regime. Our work in this section builds upon that analysis, offering some additional justification (based in part on KPZ scaling theory) and refinement as well as expanding to the large distance regime. We also develop the theory describing the sampling fluctuations Sam_L^N. In particular, we describe how the environmental and sampling fluctuations should be independent. Moreover, we propose a finite N formula based on stitching together these two asymptotic regimes. In the subsequent Section 3.8 we verify our theory for a wide range of N through numerical simulations.

3.7.1 Short Distance Regime.

We assume that $L, N \to \infty$ with $L/\ln(N) \to \hat{L} < 1$. In this case, it is very likely that at least one of the N particles will arrive at position $\pm L$ at time $t = L$ in which case we can conclude that $\mathbb{E}^{\text{Asy}}\left[\text{Min}_L^N\right] \approx L$ and $\text{Var}^{\text{Asy}}\big(\text{Min}_L^N\big) \approx 0$. Similarly, we find $\mathbb{E}^{\text{Asy}}\left[\text{Env}_L^N\right] \approx L$ and $\text{Var}^{\text{Asy}}\big(\text{Env}_L^N\big) = \mathbb{E}^{\text{Asy}}\left[\text{Sam}_L^N\right] = \text{Var}^{\text{Asy}}\big(\text{Sam}_L^N\big) \approx 0$. To see this, observe that the probability that a given particle arrives at position $\pm L$ at time $t = L$ is given by

$$p^{\mathbf{B}}(L, L) + p^{\mathbf{B}}(-L, L) = \prod_{x=1}^{L} B(x, x) + \prod_{x=1}^{-L} \big(1 - B(x, -x)\big)$$

where the $B(x, t)$ are i.i.d. uniform random variables. We use the law of large numbers to see that

$$\ln\big(p^{\mathbf{B}}(L, L)\big) = \sum_{x=1}^{L} \ln\big(B(x, x)\big) \approx -L$$

where we have used the fact that $-\ln(B(x, x))$ is an exponential random variable with a mean of 1. The same holds for $p^{\mathbf{B}}(-L, L)$, thus we see that

$$p^{\mathbf{B}}(L, L) + p^{\mathbf{B}}(-L, L) \approx 2e^{-L} \approx 2e^{-\hat{L}\ln(N)} \gg 1/N$$

where we have used that $L/\ln(N) \to \hat{L} < 1$. When $p^{\mathbf{B}}(L, L) + p^{\mathbf{B}}(-L, L) \gg 1/N$ (as above) it is likely that at least one of N independent particles is at $\pm L$. This implies the above claimed results when $\hat{L} < 1$.

One-sided case: In the one-sided barrier case the exact same analysis above goes through except only the $p^{\mathbf{B}}(L, L)$ term should be considered.

3.7.2 Medium Distance Regime Env_L^N Behavior.

The behavior in the medium and large distance regimes is considerably more complex. We first study the random variable Env_L^N in these regimes. Then, based on asymptotics derived for its mean and variance we determine asymptotic predictions for Sam_L^N and Min_L^N.

In the medium and large distance regime our analysis relies on results [6, 7] derived using tools from quantum integrable systems. We will review these results below. In essence they provide precise asymptotic information about the distribution of $\mathbb{P}^{\mathbf{B}}(X(t) \geq L)$ in various limits as t and L grow. This information is not equivalent to the knowledge of the first passage time distribution $\mathbb{P}^{\mathbf{B}}(\tau_L \leq t)$ that we seek to understand here. While the event $\{X(t) \geq L\}$ implies $\{\tau_L \leq t\}$, the opposite is not true. It is possible that a particle will pass the barrier at a time prior to t and then backtrack behind it at time t. However, as L approaches t the events become more and more equivalent since it is harder for a particle to exit $(-L, L)$ and then backtrack when L is large. For instance, when $L = t$ (the maximal possible value) the two events become equivalent. Based on this reasoning we make the following approximation that improves as L grows relative to t:

$$p_L^{\mathbf{B}}(L,t) \approx \mathbb{P}^{\mathbf{B}}(X(t) \geq L), \quad p_L^{\mathbf{B}}(-L,t) \approx \mathbb{P}^{\mathbf{B}}(X(t) \leq -L).$$

Recall that $p_L^{\mathbf{B}}(L,t)$ and $p_L^{\mathbf{B}}(-L,t)$ are the probabilities of absorption at L and $-L$ up to time t and their sum, as in Eq. 3.9, yields $\mathbb{P}^{\mathbf{B}}(\tau_L \leq t)$. Thus, we arrive at the starting approximation for our analysis:

$$\mathbb{P}^{\mathbf{B}}(\tau_L \leq t) \approx \mathbb{P}^{\mathbf{B}}(X(t) \geq L) + \mathbb{P}^{\mathbf{B}}(X(t) \leq -L). \tag{3.14}$$

In the medium distance regime we assume that $L, N \to \infty$ with $L/\ln(N) \to \hat{L} \in (1, \infty)$, a finite number greater than 1. The key input from [6] is as follows. Define the random variable $\chi_{x,t}$ by

$$\ln(\mathbb{P}^{\mathbf{B}}(X(t) \geq x)) = -tI\left(\frac{x}{t}\right) + t^{1/3}\sigma\left(\frac{x}{t}\right)\chi_{x,t} \tag{3.15}$$

where $x \in [0,t] \cap \mathbb{Z}$ and for $v \in (0,1)$

$$I(v) = 1 - \sqrt{1-v^2}, \quad \text{and} \quad \sigma(v)^3 = \frac{2I(v)^2}{1-I(v)}.$$

Then [6] shows that for $v \in (0,1)$, $\chi_{vt,t}$ converges as $t \to \infty$ in distribution to a GUE TW random variable. By symmetry the result of [6] also holds if in Eq. 3.15, $\ln(\mathbb{P}^{\mathbf{B}}(X(t) \geq x))$ is replaced by $\ln(\mathbb{P}^{\mathbf{B}}(X(t) \leq -x))$ and $\chi_{x,t}$ is replaced by $\chi_{-x,t}$. It should be noted that while [6] does not address the joint distribution of $\chi_{x,t}$ for different values of x and t, it is possible to make predictions based on grounds of KPZ universality [66, 67]. In particular, for any $v \in (-1,0) \cup (0,1)$ as $T \to \infty$, the space-time random process $(x,t) \mapsto \chi_{vtT+xT^{2/3},tT}$ should converge to the KPZ fixed point [115], and the limiting processes for distinct v should be independent. Moreover, the local regularity of the KPZ fixed point is known which should translate into estimates on the regularity of $\chi_{x,t}$. Some of this understanding will justify the approximations that follow involving how $\chi_{x,t}$ changes when t varies.

Combining Eq. 3.14 and Eq. 3.15 yields

$$\begin{aligned}&\ln\left(\mathbb{P}^{\mathbf{B}}(\tau_L \leq t)\right) \approx \\ &- tI\left(\tfrac{L}{t}\right) + \ln\left(e^{t^{1/3}\sigma(\frac{L}{t})\chi_{L,t}} + e^{t^{1/3}\sigma(\frac{L}{t})\chi_{-L,t}}\right)\end{aligned} \tag{3.16}$$

We seek to study the random variable Env_L^N which is defined by Eq. 3.11 and essentially is the t such that $\mathbb{P}_{\mathbf{B}}(\tau_L \leq t) = 1/N$ holds. This yields the following implicit equation for Env_L^N

$$\begin{aligned}&- \ln(N) \approx -\mathrm{Env}_L^N \cdot I\left(\frac{L}{\mathrm{Env}_L^N}\right) + \\ &\ln\left(e^{\left(\mathrm{Env}_L^N\right)^{1/3}\sigma(\frac{L}{\mathrm{Env}_L^N})\chi_{L,\mathrm{Env}_L^N}} + e^{\left(\mathrm{Env}_L^N\right)^{1/3}\sigma(\frac{L}{\mathrm{Env}_L^N})\chi_{-L,\mathrm{Env}_L^N}}\right).\end{aligned} \tag{3.17}$$

We will solve this equation perturbatively. The first order solution neglects the second line in Eq. 3.17 and yields

$$\mathrm{Env}_L^N \approx T_0 := \frac{(\ln(N))^2 + L^2}{2\ln(N)} \tag{3.18}$$

i.e., T_0 solves $\ln(N) = T_0 I(\frac{L}{T_0})$. We now assume that $\mathrm{Env}_L^N \approx T_0 + \delta$ with $\delta \ll T_0$ containing the randomness of Env_L^N. Substituting this into Eq. 3.17 we can find δ

approximately by solving

$$\begin{aligned}
-\ln(N) \approx& -(T_0+\delta)\cdot I\left(\tfrac{L}{T_0+\delta}\right)+\\
&\ln\left(e^{T_0^{1/3}\sigma\left(\frac{L}{T_0}\right)\chi_{L,T_0}}+e^{T_0^{1/3}\sigma\left(\frac{L}{T_0}\right)\chi_{-L,T_0}}\right)\\
\approx& -(T_0+\delta)\cdot\left(I\left(\tfrac{L}{T_0}\right)+\delta\partial_t\, I\left(\tfrac{L}{t}\right)\Big|_{t=T_0}\right)+\\
&\ln\left(e^{T_0^{1/3}\sigma\left(\frac{L}{T_0}\right)\chi_{L,T_0}}+e^{T_0^{1/3}\sigma\left(\frac{L}{T_0}\right)\chi_{-L,T_0}}\right).
\end{aligned} \tag{3.19}$$

In the first comparison we neglected the fact that under the perturbation to T_0 we should write $\chi_{L,T_0+\delta}$ and $\chi_{-L,T_0+\delta}$. This, however, is justified by the fact that while T_0 is of order $\ln(N)$, δ (as we will see below) is of order $(\ln(N))^{1/3}$. By the KPZ scaling theory mentioned earlier, this change in the time variable of the χ process should have a small impact which we neglect in our approximation. In the second comparison we utilized the Taylor expansion $I\left(\frac{L}{T_0+\delta}\right)\approx I\left(\frac{L}{T_0}\right)+\delta\partial_t\, I\left(\frac{L}{t}\right)\big|_{t=T_0}$. Since T_0 satisfies $-\ln(N)=-T_0 I(\frac{L}{T_0})$ we can cancel terms and solve for δ in the resulting equation

$$\begin{aligned}
0\approx& -\delta T_0\partial_t\, I\left(\tfrac{L}{t}\right)\Big|_{t=T_0}-\delta I\left(\tfrac{L}{T_0}\right)-\delta^2\partial_t\, I\left(\tfrac{L}{t}\right)\Big|_{t=T_0}+\\
&\ln\left(e^{T_0^{1/3}\sigma\left(\frac{L}{T_0}\right)\chi_{L,T_0}}+e^{T_0^{1/3}\sigma\left(\frac{L}{T_0}\right)\chi_{-L,T_0}}\right).
\end{aligned}$$

Since L and T_0 are both of order $\ln(N)$, it follows from the chain rule that $\partial_t\, I\left(\frac{L}{t}\right)\big|_{t=T_0}$ is of order $(\ln(N))^{-1}$. Since the final term above is of order $(\ln(N))^{1/3}$ the only consistent scaling for δ is that it be of order $(\ln(N))^{1/3}$ as well in which case all terms are of that order except the term with δ^2 which decays like $(\ln(N))^{-1/3}$. Thus, neglecting that term we solve for δ and find

$$\delta\approx\frac{\ln\left(e^{T_0^{1/3}\sigma\left(\frac{L}{T_0}\right)\chi_{L,T_0}}+e^{T_0^{1/3}\sigma\left(\frac{L}{T_0}\right)\chi_{-L,T_0}}\right)}{I\left(\frac{L}{T_0}\right)+T_0\partial_t\, I\left(\frac{L}{t}\right)\big|_{t=T_0}}. \tag{3.20}$$

Therefore, we have shown that

$$\mathrm{Env}_L^N\approx T_0+\frac{\ln\left(e^{T_0^{1/3}\sigma\left(\frac{L}{T_0}\right)\chi_{L,T_0}}+e^{T_0^{1/3}\sigma\left(\frac{L}{T_0}\right)\chi_{-L,T_0}}\right)}{I\left(\frac{L}{T_0}\right)+T_0\partial_t\, I\left(\frac{L}{t}\right)\big|_{t=T_0}}. \tag{3.21}$$

The above conclusion is in agreement with Eq. 89 in [69] (in the one-sided barrier case). In particular, our Env_L^N random variable is essentially the same as $T_{\mathrm{Hit}}(\ell)$ with our L and their ℓ having the same meaning. Our rate function I is the same as their λ, and our $\hat{L}$ is equivalent to $1/\hat{\gamma}$ in their notation.

From Eq. 3.21 we may extract the following conclusion regarding the asymptotic behaviors for the mean and variance of Env_L^N in the medium distance regime:

$$\mathbb{E}^{\mathrm{Asy}}\left[\mathrm{Env}_L^N\right] \approx M_1(L,N) \text{ and } \mathrm{Var}^{\mathrm{Asy}}\big(\mathrm{Env}_L^N\big) \approx V_1(L,N)$$

where M_1 and V_1 are defined as

$$\begin{aligned} M_1(L,N) &:= \frac{(\ln(N))^2 + L^2}{2\ln(N)} \\ V_1(L,N) &:= \frac{\mathrm{Var}\left(\ln\left(e^{T_0^{1/3}\sigma\left(\frac{L}{T_0}\right)\chi_{L,T_0}} + e^{T_0^{1/3}\sigma\left(\frac{L}{T_0}\right)\chi_{-L,T_0}}\right)\right)}{\left(I\left(\frac{L}{T_0}\right) + T_0\partial_t\, I\left(\frac{L}{t}\right)\Big|_{t=T_0}\right)^2}. \end{aligned} \tag{3.22}$$

We have dropped the mean of δ (which is over order $(\ln(N))^{1/3}$) from M_1 and only retrained the first order term T_0. On the other hand, V_1 is precisely the variance of δ (as T_0 is deterministic). $V_1(L,N)$ contains the variance of a non-trivial combination of two random variables χ_{L,T_0} and χ_{-L,T_0}. To estimate this variance we replace both by independent GUE TW random variables χ and χ' (as justified by the above recorded result of [6] and KPZ scaling theory). Under that replacement, the variance in the numerator in V_1 is

$$\begin{aligned} &\int_{\mathbb{R}^2} dxdy\left(\ln\left(e^{T_0^{1/3}\sigma\left(\frac{L}{T_0}\right)x} + e^{T_0^{1/3}\sigma\left(\frac{L}{T_0}\right)y}\right)\right)^2 p(x)p(y) \\ &-\left(\int_{\mathbb{R}^2} dxdy \ln\left(e^{T_0^{1/3}\sigma\left(\frac{L}{T_0}\right)x} + e^{T_0^{1/3}\sigma\left(\frac{L}{T_0}\right)y}\right)p(x)p(y)\right)^2 \end{aligned} \tag{3.23}$$

where $p(x)$ and $p(y)$ are the probability density of the GUE TW distribution. We numerically approximate the double integrals over the xy plane by integrating over the region $x, y \in [-10, 10]$ as is justified by the rapid decay of the density p. In fact, this integral can be approximated in the limit of large N as follows. Observe that $T_0 = \ln(N)\frac{\hat{L}^2+1}{2}$ where we let $L = \hat{L}\ln(N)$. Thus

$$T_0^{1/3}\sigma\left(\tfrac{L}{T_0}\right) = (\ln(N))^{1/3}\left(\tfrac{\hat{L}^2+1}{2}\right)\sigma\left(\tfrac{2\hat{L}}{\hat{L}^2+1}\right).$$

For fixed $\hat{L}$ this implies that the exponent diverges like $(\ln(N))^{1/3}$. Since

$$\ln(e^{rA} + e^{rB}) \approx r\max(A, B) \text{ as } r \to \infty, \tag{3.24}$$

it follows that the numerator in Eq. 3.22 is approximately (as $N \to \infty$) given by

$$\left(T_0^{1/3}\sigma\left(\tfrac{L}{T_0}\right)\right)^2 \operatorname{Var}\left(\max(\chi, \chi')\right) \tag{3.25}$$

where χ and χ' are independent GUE TW random variables. This variance can be computed via numerical integration and this need only be done once (as opposed to for various values of N and L as above).

One-sided case: The same reasoning as in the two-sided case yields expressions for the mean and variance of Env_L^N. Namely, M_1 and V_1 from Eq. 3.22 are replaced now by $\widetilde{M}_1$ and $\widetilde{V}_1$ where $M_1 = \widetilde{M}_1$ and

$$\widetilde{V}_1(L, N) := \left(\frac{T_0^{1/3}\sigma\left(\frac{L}{T_0}\right)}{I\left(\frac{L}{T_0}\right) + T_0\partial_t\, I\left(\frac{L}{t}\right)\big|_{t=T_0}}\right)^2 \operatorname{Var}(\chi)$$

where χ is a GUE TW random variable such that $\operatorname{Var}(\chi) \approx 0.813$. The simplification in $\widetilde{V}_1$ comes from the fact that only the χ_{L,T_0} term is present in the one-sided case – thus rather than dealing with the variance of the ln of a sum of exponentials, the ln and exponential terms cancel and the simpler expression follows.

3.7.3 Large Distance Regime Env_L^N Behavior.

In the large distance regime we assume that $L, N \to \infty$ with $L/(\ln(N))^{3/2} \to \hat{\hat{L}} \in (0, \infty)$, a finite non-zero number. The key input from [7] (see also Eq. (67) in the supplementary material in [69]) is as follows: For $v \in (0, \infty)$ and $x = vt^{3/4}$

$$\ln(\mathbb{P}^{\mathbf{B}}(X(t) \geq x)) \approx -\frac{x^2}{2t} - \frac{x^4}{12t^3} + \ln\left(\frac{x}{t}\right) + h\left(0, \frac{x^4}{t^3}\right) \tag{3.26}$$

where $h(y, s)$ denotes the random height at position y and time s of the narrow wedge solution to the Kardar-Parisi-Zhang (KPZ) equation

$$\partial_s h(y, s) = \frac{1}{2}\partial_y^2 h(y, s) + \frac{1}{2}\left(\partial_y h(y, s)\right)^2 + \eta(y, s) \tag{3.27}$$

where $\eta(y, s)$ is space-time white noise [1, 70, 71, 72, 73]. By symmetry Eq. 3.26 will also hold with $\ln(\mathbb{P}^{\mathbf{B}}(X(t) \leq -x))$ and with an asymptotically independent fluctuation term $h'\left(0, \frac{x^4}{t^3}\right)$ that has the same law as h.

Similar to our analysis in the medium distance regime, combining Eq. 3.14 and Eq. 3.15 yields

$$\begin{aligned} &\ln\left(\mathbb{P}^{\mathbf{B}}(\tau_L \leq t)\right) \approx \\ &-\frac{L^2}{2t} - \frac{L^4}{12t^3} + \ln\left(\frac{L}{t}\right) + \ln\left(e^{h(0, \frac{L^4}{t^3})} + e^{h'(0, \frac{L^4}{t^3})}\right). \end{aligned} \tag{3.28}$$

Env_L^N is essentially the t such that $\mathbb{P}^{\mathbf{B}}(\tau_L \leq t) = 1/N$ which yields the implicit equation for Env_L^N

$$\begin{aligned} -\ln(N) \approx &-\frac{L^2}{2\mathrm{Env}_L^N} - \frac{L^4}{12\left(\mathrm{Env}_L^N\right)^3} + \ln\left(\frac{L}{\mathrm{Env}_L^N}\right) + \\ &\ln\left(e^{h\left(0, \frac{L^4}{(\mathrm{Env}_L^N)^3}\right)} + e^{h'\left(0, \frac{L^4}{(\mathrm{Env}_L^N)^3}\right)}\right) \end{aligned} \tag{3.29}$$

where h and h' are independent as above. The first term on the right-hand side is dominant and solving $\ln(N) = \frac{L^2}{2T_0}$ yields the first order behavior of $\mathrm{Env}_L^N \approx T_0$ with

$$T_0 = \frac{L^2}{2\ln(N)}.$$

Under our scaling of L, this term is of order $(\ln(N))^2$ while the other deterministic terms on the right-hand side of Eq. 3.29 are either order 1 or $\ln(\ln(N))$. Thus, for the sake of the mean of Env_L^N, T_0 will suffice. To study its variance we write $\mathrm{Env}_L^N = T_0 + \delta$ where $\delta \ll T_0$ contains the randomness of Env_L^N. Neglecting the lower order terms in Eq. 3.29 (the second and third terms on the right-hand side), Taylor expanding $-\frac{L^2}{2\mathrm{Env}_L^N} = -\frac{L^2}{2(T_0+\delta)} \approx -\frac{L^2}{2T_0} + \frac{L^2}{2T_0^2}\delta$, and substituting T_0 for Env_L^N in the h and h' expressions (as is again justified by the KPZ scaling theory), we arrive at an approximation for

$$\delta \approx -\frac{2T_0^2}{L^2} \ln\left(e^{h\left(0,\frac{L^4}{T_0^3}\right)} + e^{h'\left(0,\frac{L^4}{T_0^3}\right)}\right).$$

From the above we may extract the following conclusion regarding the asymptotic behaviors for the mean and variance of Env_L^N in the large distance regime:

$$\mathbb{E}^{\mathrm{Asy}}\left[\mathrm{Env}_L^N\right] \approx M_2(L,N) \text{ and } \mathrm{Var}^{\mathrm{Asy}}\!\left(\mathrm{Env}_L^N\right) \approx V_2(L,N)$$

where M_1 and V_1 are defined as

$$\begin{aligned} M_2(L,N) &:= \frac{L^2}{2\ln(N)} \\ V_2(L,N) &:= \frac{L^4\,\mathrm{Var}\!\left(\ln\left(e^{h\left(0,\frac{8(\ln(N))^3}{L^2}\right)} + e^{h'\left(0,\frac{8(\ln(N))^3}{L^2}\right)}\right)\right)}{4(\ln(N))^4}. \end{aligned} \tag{3.30}$$

Notice that for $L = (\ln(N))^{3/2}\hat{\hat{L}}$ (as in the large distance regime scaling) the KPZ equation time $\frac{8(\ln(N))^3}{L^2} = 8/\hat{\hat{L}}^2$. Thus, the calculation of the variance in V_2 requires numerically integration using the exact formula for the one-point distribution for the KPZ equation from [70, 71, 72, 73]. This formula is non-trivial to compute numerically due to its complexity. However, [116] (used in the work of [83]) contains the numerics for the density of $h(0,s)$ for $s \in \{0.25, 0.35, 0.5, 0.75, 1.2, 2, 3.5, 6.5, 13, 25, 50, 100, 250\}$. In the limit where $s \to 0$ or $s \to \infty$ the law of $h(0,s)$ converges to be Gaussian or GUE TW (with appropriate scaling) and thus we can combine these limiting behaviors with the numerical data to produce, via smooth interpolation, a curve

$$s \mapsto \mathrm{Var}\!\left(\ln\left(e^{h(0,s)} + e^{h'(0,s)}\right)\right)$$

for all s that we use to numerically evaluate $V_2(L,N)$.

One-sided case: The same reasoning as in the two-sided case yields expressions for the mean and variance of Env_L^N. Namely, M_2 and V_2 from Eq. 3.30 are replaced now by $\widetilde{M}_2$ and $\widetilde{V}_2$ where $\widetilde{M}_2 = M_2$ and

$$\widetilde{V}_2(L,N) := \frac{L^4\,\mathrm{Var}\Big(h\big(0,\frac{8(\ln(N))^3}{L^2}\big)\Big)}{4(\ln(N))^4}.$$

In this case, the variance in question was numerically computed and plotted in [83].

3.7.4 Stitching Together the Medium and Large Distance Regime Env_L^N Behavior.

We compare the large L (in the $\ln(N)$ scale) behavior of $V_1(L,N)$ to the small L (in the $(\ln(N))^{3/2}$ scale) behavior of $V_2(L,N)$ and show that they match. This justifies defining $\mathrm{Var}^{\mathrm{Asy}}\big(\mathrm{Env}_L^N\big)$ via smoothly stitching these two functions between these two scaling regimes. We then record the very large distance asymptotics that should persist for all L beyond the $(\ln(N))^{3/2}$ regime. We only address the variances below since $M_1(L,N)$ clearly converges to $M_2(L,N)$ when $L \gg \ln(N)$.

Recall $V_1(L,N)$ from Eq. 3.22. Using the discussion after Eq. 3.23, namely Eq. 3.25, we can approximate this as

$$V_1(L,N) \approx \frac{\Big(T_0^{1/3}\sigma\big(\frac{L}{T_0}\big)\Big)^2 \mathrm{Var}\big(\max(\chi,\chi')\big)}{\Big(I\big(\frac{L}{T_0}\big) + T_0\partial_t\, I\big(\frac{L}{t}\big)\big|_{t=T_0}\Big)^2},$$

where χ and χ' are independent GUE TW random variables. Observe the following asymptotic: For $v \to 0$, $\sigma(v) \approx \frac{v^{4/3}}{2^{1/3}}$ while for $L \gg \ln(N)$, $T_0 \approx \frac{L^2}{2\ln(N)}$ and

$$I\left(\frac{L}{T_0}\right) + T_0\partial_t\, I\left(\frac{L}{t}\right)\bigg|_{t=T_0} \approx -2\left(\frac{\ln(N)}{L}\right)^2.$$

Putting these together shows that for $L \gg \ln(N)$,

$$V_1(L,N) \approx \frac{L^{8/3}\mathrm{Var}\big(\max(\chi,\chi')\big)}{2^{1/3}(\ln(N))^2}.$$

Now, let us compare this to the behavior of $V_2(L,N)$ from Eq. 3.30 when $L \ll (\ln(N))^{3/2}$. Observe that the KPZ equation time s in V_2 is given by $s =$

$\frac{8(\ln(N))^3}{L^2}$ which goes to infinity as the ratio $L/(\ln(N))^{3/2}$ tends to zero. Thus, to extract the behavior of V_2 we must use the large time behavior of the KPZ equation one-point distribution which says that the random variable χ_s defined by

$$h(0,s) \approx \chi_s \left(\frac{s}{2}\right)^{1/3} - \frac{s}{24},$$

converges as $s \to \infty$ to a GUE TW random variable [70, 71, 72, 73]. Letting χ and χ' denote the limiting independent GUE TW random variables arising from h and h' in V_2, and using Eq. 3.24, it follows that when $L \ll (\ln(N))^{3/2}$,

$$V_2(L,N) \approx \frac{L^{8/3}\mathrm{Var}\big(\max(\chi,\chi')\big)}{2^{1/3}(\ln(N))^2}$$

which matches the $L \gg \ln(N)$ behavior of $V_1(L,N)$.

This matching of the two expressions V_1 and V_2 justifies stitching them together to provide a single continuous curve for the asymptotic variance of the environmental fluctuations Env_L^N. To do this we use an error function centered at $L = (\ln(N))^{5/4}$ with a width of $(\ln(N))^{6/5}$ to ensure a smooth crossover between the two regimes. The resulting asymptotic variance formulas is then given by

$$\mathrm{Var}^{\mathrm{Asy}}\big(\mathrm{Env}_L^N\big) = \phi(L,N)V_1(L,N) + \big(1-\phi(L,N)\big)V_2(L,N) \tag{3.31}$$

where $V_1(L,N)$ and $V_2(L,N)$ are defined in Eqs. 3.22 and 3.30 respectively, where the interpolation function

$$\phi(L,N) := \frac{1}{2}\left(1 - \mathrm{erf}\left(\frac{L-(\ln(N))^{5/4}}{(\ln(N))^{6/5}}\right)\right) \tag{3.32}$$

with the error function $\mathrm{erf}(x) = \frac{2}{\sqrt{\pi}}\int_0^x e^{-y^2}dy$. We likewise define $\mathbb{E}^{\mathrm{Asy}}\left[\mathrm{Env}_L^N\right]$ via the same interpolation scheme as in Eq. 3.31 using the fact that M_1 and M_2 smoothly crossover too. In fact, since the large L asymptotic of M_1 is precisely in agreement with M_2, the interpolation is essentially unnecessary.

Figure 11 shows how we stitch together in Eq. 3.31 the medium and large distance regimes to produce $\mathrm{Var}^{\mathrm{Asy}}(\mathrm{Env}_L^N)$. It shows that this interpolation scheme provides a smooth crossover between the two regimes and agrees with numerical measurements.

The above asymptotic formula $\mathrm{Var}^{\mathrm{Asy}}(\mathrm{Env}_L^N)$ will be compared to numerical simulations for wide ranges of N and L in Section 3.8. As will become clear there, the crossover $L^{8/3}/(\ln(N))^2$ power-law behavior observed above is something of a ghost. For realistic sizes of N the range between $\ln(N)$ and $(\ln(N))^{3/2}$ is rather narrow. For instance, in Section 3.8 we study the range $N = 10^2$ to $N = 10^{28}$. On the lower end of this range, $\ln(N) \approx 4.6$ and $(\ln(N))^{3/2} \approx 9.9$ while on the upper end $\ln(N) \approx 64$ while $(\ln(N))^{3/2} \approx 517$. So, even for $N = 10^{28}$, there is not even a decade between $\ln(N)$ and $(\ln(N))^{3/2}$.

What is more important in terms of comparison to numerical data is the behavior of the variance of Env_L^N in the limit where $L \gg (\ln(N))^{3/2}$. This unbounded regime demonstrates a novel power-law that will be important to compare to the impact of the Sam_L^N variance.

To probe the behavior of $\mathrm{Var}^{\mathrm{Asy}}(\mathrm{Env}_L^N)$ as $L \gg (\ln(N))^{3/2}$ we need only study the corresponding behavior of $V_2(L, N)$. In that case the KPZ time $s = \frac{8(\ln(N))^3}{L^2}$ goes to zero. Thus, we must make use of the small time (Edwards-Wilkinson) asymptotics that show that the random variable G_s defined by

$$h(0, s) \approx -\frac{s}{24} - \ln(\sqrt{2\pi s}) + \left(\frac{\pi s}{4}\right)^{1/4} G_s \tag{3.33}$$

converges as $s \to 0$ to a standard Gaussian random variable G [70, 71, 72, 73]. Therefore, using $e^x \approx 1 + x$ and $\ln(1 + x) \approx x$ as $x \to 0$, we find that

$$\ln\left(e^{h(0,s)} + e^{h'(0,s)}\right) \approx -\tfrac{s}{24} - \ln\left(\sqrt{\tfrac{\pi s}{2}}\right) + \frac{1}{2}\left(\tfrac{\pi s}{4}\right)^{1/4}(G + G'). \tag{3.34}$$

Substituting $s = \frac{8(\ln(N))^3}{L^2}$ and taking the variance yields

$$\operatorname{Var}\Big(\ln\Big(e^{h\left(0,\frac{8(\ln(N))^3}{L^2}\right)} + e^{h'\left(0,\frac{8(\ln(N))^3}{L^2}\right)}\Big)\Big) \approx \frac{1}{2}\left(\frac{2\pi(\ln(N))^3}{L^2}\right)^{1/2},$$

where we used that $\operatorname{Var}(G+G') = 2$ since G and G' are independent standard Gaussian random variables. Substituting this into Eq. 3.30 shows that where $L \gg (\ln(N))^{3/2}$

$$\operatorname{Var}^{\text{Asy}}\big(\operatorname{Env}_L^N\big) \approx V_2(L,N) \approx \frac{1}{4}\sqrt{\frac{\pi}{2}}\frac{L^3}{(\ln(N))^{5/2}}. \tag{3.35}$$

This power-law behavior will be quite visible in the numerical data from Section 3.8.

One-sided case: The only difference in this case is that we use $\widetilde{V}_1$ and $\widetilde{V}_2$ in place of V_1 and V_2. This crossover behavior between the regime where L is of order $\ln(N)$ and $(\ln(N))^{3/2}$ still matches up and the same interpolation formula Eq. 3.31 can be used. For the $L \gg (\ln(N))^{3/2}$ asymptotics, the right-hand side of Eq. 3.35 ends up being twice as large in the one-sided case as in the two-sided case. This may seem counter-intuitive since there are two Gaussians in the two-sided case versus one in the one-sided case. However, in the calculation in Eq. 3.34, we used $\ln\left(e^{h(0,s)} + e^{h'(0,s)}\right) \approx \ln(2) + \frac{1}{2}\big(h(0,s) + h'(0,s)\big)$. The variance of $\frac{1}{2}\big(h(0,s)+h'(0,s)\big)$ is half that of the variance of $h(0,s)$, thus explaining the factor of 2 difference.

3.7.5 Sam_L^N and Min_L^N Behavior.

We now argue that the environmental and sampling fluctuations Env_L^N and Sam_L^N are asymptotically independent and that the sampling fluctuations are Gumbel distributed. The independence is strongly supported by our numerical data, see for instance Figure 10.

To start, observe that for large N and small $\mathbb{P}^{\mathbf{B}}(\tau_L \leq t)$ we can rewrite Eq. 3.10 as

$$\mathbb{P}^{\mathbf{B}}(\mathrm{Min}_L^N \geq t) \approx e^{-N\mathbb{P}^{\mathbf{B}}(\tau_L \leq t)}. \tag{3.36}$$

Using the non-backtracking approximation in Eq. 3.14 and the medium distance range asymptotic expansion Eq. 3.15 we arrive at the starting formula

$$\begin{aligned}&\ln\left(\mathbb{P}^{\mathbf{B}}(\mathrm{Min}_L^N \geq t)\right) \approx \\ &-N\Big(e^{-tI\left(\frac{L}{t}\right)+t^{1/3}\sigma(\frac{L}{t})\chi_{L,t}} + e^{-tI\left(\frac{L}{t}\right)+t^{1/3}\sigma(\frac{L}{t})\chi_{-L,t}}\Big).\end{aligned} \tag{3.37}$$

We will work here with in the medium distance regime asymptotics. A similar analysis could be performed in the large distance regime and the result would agree with the $L \gg \ln(N)$ behavior derived below so we do not repeat this derivation.

Recalling that $\mathrm{Sam}_L^N = \mathrm{Min}_L^N - \mathrm{Env}_L^N$, we have that $\mathbb{P}^{\mathbf{B}}(\mathrm{Sam}_L^N \geq s) = \mathbb{P}^{\mathbf{B}}(\mathrm{Min}_L^N \geq \mathrm{Env}_L^N + s)$. Thus, $\ln\left(\mathbb{P}^{\mathbf{B}}(\mathrm{Sam}_L^N \geq s)\right)$ is approximately given by the right-hand side of Eq. 3.37 with $t = \mathrm{Env}_L^N + s$. With this in mind, we will use the following Taylor expansion in the exponential on the right-hand side of Eq. 3.37:

$$\begin{aligned}&-(\mathrm{Env}_L^N + s)I\left(\tfrac{L}{\mathrm{Env}_L^N+s}\right)\\ &\quad+(\mathrm{Env}_L^N + s)^{1/3}\sigma\big(\tfrac{L}{\mathrm{Env}_L^N+s}\big)\chi_{L,\mathrm{Env}_L^N+s} \approx\\ &-(\mathrm{Env}_L^N + s)\Big(I\left(\tfrac{L}{\mathrm{Env}_L^N}\right) + s\partial_t\, I\left(\tfrac{L}{t}\right)\big|_{t=\mathrm{Env}_L^N}\Big)\\ &\quad+(\mathrm{Env}_L^N)^{1/3}\sigma\big(\tfrac{L}{\mathrm{Env}_L^N}\big)\chi_{L,\mathrm{Env}_L^N} \approx\\ &\ln\left(\mathbb{P}^{\mathbf{B}}(X(\mathrm{Env}_L^N) \geq L)\right)-\\ &\quad s\Big(I\left(\tfrac{L}{\mathrm{Env}_L^N}\right) + \mathrm{Env}_L^N\partial_t\, I\left(\tfrac{L}{t}\right)\big|_{t=\mathrm{Env}_L^N}\Big)\end{aligned} \tag{3.38}$$

Notice that in the first comparison above we have assumed that $(\mathrm{Env}_L^N + s)^{1/3}\sigma\big(\frac{L}{\mathrm{Env}_L^N+s}\big)\chi_{L,\mathrm{Env}_L^N+s}$ can be replaced by the same term with Env_L^N instead of $\mathrm{Env}_L^N + s$. This is a non-trivial assumption which ultimately implies the Gumbel form of Sam_L^N and its independence from Env_L^N. This should be justifiable based on the KPZ scaling theory and the fact that (as we will see) $\mathbb{E}^{\text{Asy}}\left[\text{Env}_L^N\right] \gg \mathbb{E}^{\text{Asy}}\left[\text{Sam}_L^N\right]$. The second comparison uses Eq. 3.15 and throws out the s^2 term. Of course, the same expansion above applies when $L \mapsto -L$ and $\mathbb{P}^{\mathbf{B}}(X(\text{Env}_L^N) \geq L)$ is replaced by $\mathbb{P}^{\mathbf{B}}(X(\text{Env}_L^N) \leq -L)$. Putting these expansions together with Eq. 3.37 yields

$$\begin{aligned}
&\ln\left(\mathbb{P}^{\mathbf{B}}(\text{Sam}_L^N \geq s)\right) \approx \\
&- N\big(\mathbb{P}^{\mathbf{B}}(X(\text{Env}_L^N) \geq L) + \mathbb{P}^{\mathbf{B}}(X(\text{Env}_L^N) \leq -L)\big) \\
&\times e^{-s\left(I\left(\frac{L}{\text{Env}_L^N}\right) + \text{Env}_L^N \partial_t I\left(\frac{L}{t}\right)\Big|_{t=\text{Env}_L^N}\right)}
\end{aligned} \tag{3.39}$$

Invoking the non-backtracking approximation in Eq. 3.14 and the definition Eq. 3.11 of Env_L^N, it follows that $\mathbb{P}^{\mathbf{B}}(X(\text{Env}_L^N) \geq L) + \mathbb{P}^{\mathbf{B}}(X(\text{Env}_L^N) \leq -L) \approx \mathbb{P}^{\mathbf{B}}(\tau_L \leq \text{Env}_L^N) \approx 1/N$. Using this along with replacing Env_L^N by T_0 as in Eq. 3.18, from Eq. 3.39 we see that

$$\ln\left(\mathbb{P}^{\mathbf{B}}(\text{Sam}_L^N \geq s)\right) \approx -e^{-s\left(I\left(\frac{L}{T_0}\right) + T_0 \partial_t I\left(\frac{L}{t}\right)\Big|_{t=T_0}\right)}.$$

Observe that

$$\begin{aligned}
I\left(\tfrac{L}{T_0}\right) + T_0 \partial_t\, I\left(\tfrac{L}{t}\right)\Big|_{t=T_0} &= I(v) - vI'(v)\Big|_{v=L/T_0} \\
&= \frac{\sqrt{1-v^2}-1}{\sqrt{1-v^2}}\Big|_{v=L/T_0},
\end{aligned}$$

which is negative and behaves like $-v^2/2$ as $v \to 0$. This shows that asymptotically $-\text{Sam}_L^N$ has the law of a Gumbel distribution with location parameter 0 and scale parameter $-\left(I\left(\tfrac{L}{T_0}\right) + T_0 \partial_t\, I\left(\tfrac{L}{t}\right)\Big|_{t=T_0}\right)^{-1}$. From this and the formula for the mean and variance of a Gumbel random variable in terms of its location and scale parameter we see that in the medium distance regime

$$
\begin{aligned}
\mathbb{E}^{\text{Asy}}\left[\text{Sam}_L^N\right] &\approx \frac{\gamma}{\left(I\left(\frac{L}{T_0}\right)+T_0\partial_t\, I\left(\frac{L}{t}\right)\Big|_{t=T_0}\right)},\\
\text{Var}^{\text{Asy}}\!\left(\text{Sam}_L^N\right) &\approx \frac{\pi^2}{6\left(I\left(\frac{L}{T_0}\right)+T_0\partial_t\, I\left(\frac{L}{t}\right)\Big|_{t=T_0}\right)^2},
\end{aligned}
\tag{3.40}
$$

where $\gamma \approx .577$ is the Euler gamma constant. In the limit where $L \gg \ln(N)$ this yields

$$
\begin{aligned}
\mathbb{E}^{\text{Asy}}\left[\text{Sam}_L^N\right] &\approx -\frac{\gamma L^2}{2(\ln(N))^2},\\
\text{Var}^{\text{Asy}}\!\left(\text{Sam}_L^N\right) &\approx \frac{\pi^2}{24}\frac{L^4}{(\ln(N))^4}.
\end{aligned}
\tag{3.41}
$$

Observe that $\mathbb{E}^{\text{Asy}}\left[\text{Sam}_L^N\right] \ll \mathbb{E}^{\text{Asy}}\left[\text{Env}_L^N\right]$ since the former grows like $L^2/(\ln(N))^2$ while the latter like $L^2/\ln(N)$. Thus, we are justified in dropping $\mathbb{E}^{\text{Asy}}\left[\text{Sam}_L^N\right]$ and approximating $\mathbb{E}^{\text{Asy}}\left[\text{Min}_L^N\right] \approx \mathbb{E}^{\text{Asy}}\left[\text{Env}_L^N\right]$ as we will do in Eq. 3.44.

Though the above derivation was done in the medium distance regime, the same could be repeated in the large distance regime and the above asymptotic behavior in Eq. 3.41 would follow (along with the Gumbel scaling limit for Sam_L^N. We do not repeat this calculation here. This, however, justifies using the asymptotic formula from Eq. 3.40 for both the medium and large distance regimes (and $L \gg (\ln(N))^{3/2}$ too).

From the above explained Gumbel limit, observe that the location and scale parameters only depend on the deterministic portion of Env_L^N, given by T_0, and are independent of the higher order, random term, of Env_L^N. This implies the asymptotic independence and hence allows us to represent Min_L^N as a sum of Env_L^N (whose limiting distribution, mean and variance were identified earlier) and Sam_L^N (which is Gumbel distributed as above). This independence implies the following *addition law*

$$\mathrm{Var}^{\mathrm{Asy}}\big(\mathrm{Min}_L^N\big) = \mathrm{Var}^{\mathrm{Asy}}\big(\mathrm{Env}_L^N\big) + \mathrm{Var}^{\mathrm{Asy}}\big(\mathrm{Sam}_L^N\big)\,. \tag{3.42}$$

The same trivially holds for the mean.

Therefore, combining Eq. 3.31 with Eq. 3.40 we conclude (see also Figure 11)

$$\begin{aligned}\mathrm{Var}^{\mathrm{Asy}}\big(\mathrm{Min}_L^N\big) \approx{}& \phi(L,N)V_1(L,N) + \big(1-\phi(L,N)\big)V_2(L,N)\\ &+ \frac{\pi^2}{6\left(I\left(\frac{L}{T_0}\right) + T_0\partial_t\, I\left(\frac{L}{t}\right)\big|_{t=T_0}\right)^2}\end{aligned} \tag{3.43}$$

where $V_1(L,N)$ and $V_2(L,N)$ are defined in Eqs. 3.22 and 3.30 respectively, and the interpolation function ϕ is defined in Eq. 3.32 and the final term comes from Eq. 3.40. Similarly,

$$\mathbb{E}^{\mathrm{Asy}}\left[\mathrm{Min}_L^N\right] \approx M_1(L,N). \tag{3.44}$$

It is worth emphasizing (and will be apparent in the numerical simulation data that follows) that in the asymptotic formula $\mathrm{Var}^{\mathrm{Asy}}\big(\mathrm{Min}_L^N\big)$ in Eq. 3.43, there is a competition between $\mathrm{Var}^{\mathrm{Asy}}\big(\mathrm{Env}_L^N\big)$ and $\mathrm{Var}^{\mathrm{Asy}}\big(\mathrm{Sam}_L^N\big)$. By Eq. 3.35 $\mathrm{Var}^{\mathrm{Asy}}\big(\mathrm{Env}_L^N\big)$ behaves (anywhere past the short lived medium distance regime) according to the power-law $L^3/(\ln(N))^{5/2}$ while by Eq. 3.41, $\mathrm{Var}^{\mathrm{Asy}}\big(\mathrm{Sam}_L^N\big)$ likewise behaves like $L^4/(\ln(N))^{3/2}$. Setting these equal shows a crossover when L is of order $(\ln(N))^{3/2}$, i.e., the large distance regime. For smaller L, $\mathrm{Var}^{\mathrm{Asy}}\big(\mathrm{Env}_L^N\big) \gg \mathrm{Var}^{\mathrm{Asy}}\big(\mathrm{Sam}_L^N\big)$ while for larger L the opposite holds.

One-sided case: The behavior of Sam_L^N is easily seen to be asymptotically the same in this case. The behavior of Min_L^N thus involves combining the one-sided behavior of Env_L^N described earlier with the above behavior of Sam_L^N.

3.7.6 Asymptotic Behavior for the SSRW.

We now derive the extreme first passage time behavior for the SSRW model where the transition biases are deterministic with $B(x,t) = 1/2$. We derive these results using the same techniques and assumptions used for the RWRE model. The methods used in [99, 102] should also yield an alternative derivation of the asymptotics below though we do not pursue that here. To distinguish from the RWRE model, we will use a tilde to label random variables and functions associated to the SSRW model below.

Just as for the RWRE model, we find a trivial short distance behavior for the SSRW model but with a larger cutoff on the short distance length scale. Namely, when $L, N \to \infty$ with $L/\ln(N) \to \hat{L} < 1/\ln(2)$ the mean and variance of the extreme first passage time behaves asymptotically like $\mathbb{E}^{\text{Asy}}\left[\widetilde{\text{Min}}_L^N\right] \approx L$ and $\text{Var}^{\text{Asy}}\left(\widetilde{\text{Min}}_L^N\right) \approx 0$. The $1/\ln(2)$ comes from solving for L such that $(1/2)^L \approx 1/N$ (we do not need to use the law of large numbers here since all $B(x,t) = 1/2$).

The other length regime is when $L, N \to \infty$ with $L/\ln(N) \to \hat{L} > 1/\ln(2)$ (or when $L/\ln(N)$ goes to infinity). Using Stirling's formula (or more generally Cramer's theorem from the large deviation theory) the tail of the probability distribution for the location of a SSRW, $\tilde{X}(t)$, satisfies

$$\mathbb{P}(\tilde{X}(t) \geq x) \approx e^{-t\tilde{I}\left(\frac{x}{t}\right)} \tag{3.45}$$

where $\tilde{I}(v) = \frac{1}{2}\left((1+v)\ln(1+v) + (1-v)\ln(1-v)\right)$ and where we no longer write $\mathbb{P}^{\mathbf{B}}$ since deterministically we have assumed here that all $B(x,t) = 1/2$.

Using the same non-backtracking approximation as in the RWRE case (Eq. 3.14) in conjunction with Eq. 3.45 yields

$$\mathbb{P}(\widetilde{\tau}_L \leq t) \approx 2e^{-t\tilde{I}\left(\frac{L}{t}\right)}. \tag{3.46}$$

We look for $\tilde{T}_0$ such that $\mathbb{P}(\widetilde{\tau_L} \leq \tilde{T}_0) = 1/N$. This is a deterministic analog to Env_L^N and plays the role of the centering of the extreme first passage time. Since $\tilde{T}_0$ is deterministic for the SSRW, there are no environmental fluctuations. Dropping the factor of 2 in Eq. 3.46 (as it is insignificant in the asymptotic regimes we consider here) $\tilde{T}_0$ should satisfy

$$\ln(N) \approx \tilde{T}_0 \cdot \tilde{I}\left(\frac{L}{\tilde{T}_0}\right). \tag{3.47}$$

Although we cannot solve this analytically for $\tilde{T}_0$, we can solve for $\tilde{T}_0$ numerically and asymptotically in the limit $\tilde{T}_0 \to \infty$ (which occurs when L grows fast enough compared to $\ln(N)$) as we show below.

Substituting Eq. 3.46 into Eq. 3.36 and expanding about $\tilde{T}_0$ such that $\widetilde{\mathrm{Min}}_L^N = \tilde{T}_0 + s$ yields

$$\mathbb{P}(\widetilde{\mathrm{Min}}_L^N \geq \tilde{T}_0 + s) \approx e^{-2Ne^{-(\tilde{T}_0+s)\tilde{I}\left(\frac{L}{\tilde{T}_0+s}\right)}}.$$

Expanding about $\tilde{T}_0$ such that $\tilde{I}\left(\frac{L}{\tilde{T}_0+s}\right) \approx \tilde{I}\left(\frac{L}{\tilde{T}_0}\right) + s\partial_t\, \tilde{I}\left(\frac{L}{t}\right)\Big|_{t=\tilde{T}_0}$ gives

$$\mathbb{P}(\widetilde{\mathrm{Min}}_L^N \geq \tilde{T}_0 + s) \approx e^{-e^{-s\left(\tilde{I}\left(\frac{L}{\tilde{T}_0}\right)+\tilde{T}_0\partial_t\,\tilde{I}\left(\frac{L}{t}\right)\big|_{t=\tilde{T}_0}\right)}}$$

This shows $-\widetilde{\mathrm{Min}}_L^N$ is Gumbel distributed with location parameter $-\tilde{T}_0$ and scale parameter $-\left(\tilde{I}\left(\frac{L}{\tilde{T}_0}\right) + \tilde{T}_0\partial_t\, \tilde{I}\left(\frac{L}{t}\right)\Big|_{t=\tilde{T}_0}\right)^{-1}$ (which can be checked to be positive as needed to define a Gumbel distribution). Combining the above calculations we conclude that for the SSRW

$$\begin{aligned} \mathbb{E}^{\mathrm{Asy}}\left[\widetilde{\mathrm{Min}}_L^N\right] &\approx \tilde{T}_0, \\ \mathrm{Var}^{\mathrm{Asy}}\left(\widetilde{\mathrm{Min}}_L^N\right) &\approx \frac{\pi^2}{6\left(\tilde{I}\left(\frac{L}{\tilde{T}_0}\right) + \tilde{T}_0\partial_t\, \tilde{I}\left(\frac{L}{t}\right)\Big|_{t=\tilde{T}_0}\right)^2}. \end{aligned} \tag{3.48}$$

Notice that we have dropped the lower order term $\gamma\left(\tilde{I}\left(\frac{L}{\tilde{T}_0}\right) + \tilde{T}_0\partial_t\, \tilde{I}\left(\frac{L}{t}\right)\Big|_{t=\tilde{T}_0}\right)^{-1}$ from the approximation to $\mathbb{E}^{\mathrm{Asy}}\left[\widetilde{\mathrm{Min}}_L^N\right]$ above, just as we did in the RWRE case.

In the limit $L \gg \ln(N)$ we also have $\tilde{T}_0 \gg L$. Thus, using the expansion $\tilde{I}(v) \approx v^2/2$ as $v \to 0$ we can solve for $\tilde{T}_0$ and thus extract the following asymptotics, valid in the $L \gg \ln(N)$ limit:

$$\begin{aligned} \mathbb{E}^{\text{Asy}}\left[\widetilde{\text{Min}_L^N}\right] &\approx \frac{L^2}{2\ln(N)}, \\ \text{Var}^{\text{Asy}}\Big(\widetilde{\text{Min}_L^N}\Big) &\approx \frac{\pi^2}{24}\frac{L^4}{(\ln(N))^4}. \end{aligned} \tag{3.49}$$

These match the corresponding asymptotic sampling mean and variance formulas for the RWRE in Eq. 3.41.

One-sided case: The same argument and result follows.

3.8 Comparison of Asymptotic and Numerical Results

We find excellent agreement between our asymptotic theory and numerical simulations not only for very large N, but even for as few as $N = 100$ particles. These results are summarized through a number of figures. As a convention we use solid curves (or data points in Figures 10 and 15) to record outcomes of numerical simulations, dashed curves to record our asymptotic theory, and dotted lines to denote relevant power-laws. All plots are in log-log coordinates so power-laws are straight lines. In Figures 10, 12, 13, 14 and 15 each color corresponds to a different value of N while in Figure 9 a single value of N is taken and the colors correspond to numerical and asymptotic curves for the variance of $\text{Min}_L^N, \text{Env}_L^N$ or Sam_L^N.

As discussed earlier, the theoretical curves for $\text{Var}\left(\text{Min}_L^N\right), \text{Var}\left(\text{Env}_L^N\right)$ and $\text{Var}\left(\text{Sam}_L^N\right)$ in Figure 9 closely matches the numerical results except for L very close to $\ln(N)$ where finite size effects dominate. This could be partially remedied by studying the crossover from the short to medium distance regime, for instance using the central limit theorem. In the medium distance regime, the numerical data $\text{Var}^{\text{Num}}\left(\text{Min}_L^N\right)$ closely matches $\text{Var}^{\text{Num}}\left(\text{Env}_L^N\right)$ as well as the asymptotic formula $\text{Var}^{\text{Asy}}(\text{Env}_L^N)$. In the large distance regime, $\text{Var}^{\text{Num}}\left(\text{Min}_L^N\right)$ now closely matches

$\mathrm{Var}^{\mathrm{Num}}\left(\mathrm{Sam}_L^N\right)$ as well as the asymptotic formula $\mathrm{Var}^{\mathrm{Asy}}\left(\mathrm{Sam}_L^N\right)$. This is because in the medium distance regime $\mathrm{Var}\left(\mathrm{Sam}_L^N\right) \ll \mathrm{Var}\left(\mathrm{Env}_L^N\right)$ while in the large distance regime $\mathrm{Var}\left(\mathrm{Sam}_L^N\right) \gg \mathrm{Var}\left(\mathrm{Env}_L^N\right)$. The interpolation curve $\mathrm{Var}^{\mathrm{Asy}}\left(\mathrm{Min}_L^N\right)$ closely matches $\mathrm{Var}^{\mathrm{Num}}\left(\mathrm{Min}_L^N\right)$ over the full medium and long distance regime. For the SSRW, $\mathrm{Var}^{\mathrm{Num}}\left(\widetilde{\mathrm{Min}}_L^N\right)$ closely agrees with $\mathrm{Var}^{\mathrm{Asy}}\left(\widetilde{\mathrm{Min}}_L^N\right)$ (which is quite close to $\mathrm{Var}^{\mathrm{Asy}}\left(\mathrm{Sam}_L^N\right)$ from the RWRE model for L beyond the medium distance regime).

Figure 12 and 13 show the numerically measured variances of Min_L^N and Env_L^N for a range of system sizes as well as the corresponding asymptotic theory results given by Eqs. 3.43 and 3.31, respectively. For large distances, the asymptotic predictions and numerical results match for all system sizes, ranging from $N = 10^2$ to 10^{28}. For $L/\ln(N) \approx 1$ we see additional variance due to finite size effects blunting the transition between the ballistic and diffusive regimes. The ratio of numerics to asymptotic predictions for Min_L^N and Env_L^N are nearly 1 for large $L/\ln(N)$ indicating a good agreement between the numerics and asymptotic predictions. The asymptotic ratio approaches 1 for larger N. However, even for $N = 10^2$ the asymptotic ratio is about .9.

Figure 14 shows the comparison of the numerical measurements and asymptotic theory for the mean of the extreme first passage time Min_L^N for various N. For system sizes ranging from $N = 10^2$ to 10^{28} the data and asymptotic curves are nearly indistinguishable and fall onto the same master curve given by Eq. 3.44. The ratio of $\mathbb{E}^{\mathrm{Num}}\left[\mathrm{Min}_L^N\right]/\mathbb{E}^{\mathrm{Asy}}\left[\mathrm{Min}_L^N\right]$ is nearly 1 for every N indicating the numerics and asymptotic predictions are in agreement. The region with power-law L corresponds to the short distance ballistic regime while the L^2 power-law is valid for all times from the medium distance regime on.

The close agreement between $\mathrm{Var}^{\mathrm{Num}}\left(\mathrm{Min}_L^N\right)$ and $\mathrm{Var}^{\mathrm{Asy}}\left(\mathrm{Min}_L^N\right)$ in Figure 12 provides a verification of the theoretical addition law, Eq. 3.42. Figures 10 and 15 provide further confirmation of the addition law. In particular, Figure 10 shows the power-law of $\mathrm{Var}\left(\mathrm{Env}_L^N\right)$ is clearly recovered, though there is considerably more variation in the ratio of $(\mathrm{Var}^{\mathrm{Num}}\left(\mathrm{Min}_L^N\right) - \mathrm{Var}^{\mathrm{Num}}\left(\mathrm{Sam}_L^N\right))/\mathrm{Var}^{\mathrm{Asy}}\left(\mathrm{Env}_L^N\right)$ than in similar ratios observed in previous figures. This is not so surprising since the difference of two numerical measures introduces additional error. Also for larger N, the number of systems used to estimate the variances is smaller than for small N, thus introducing additional error for large N.

Figure 15 shows another route to measure the environmental variance $\mathrm{Var}\left(\mathrm{Env}_L^N\right)$ by taking the difference $\mathrm{Var}^{\mathrm{Num}}\left(\mathrm{Min}_L^N\right) - \mathrm{Var}^{\mathrm{Asy}}\left(\widetilde{\mathrm{Min}_L^N}\right)$. As we explain in Section 3.9, we use $\mathrm{Var}^{\mathrm{Asy}}\left(\widetilde{\mathrm{Min}_L^N}\right)$ instead of $\mathrm{Var}^{\mathrm{Asy}}\left(\mathrm{Sam}_L^N\right)$ here since in experimental settings it may be possible to estimate the Einstein diffusion coefficient and hence develop a prediction for $\mathrm{Var}^{\mathrm{Asy}}\left(\widetilde{\mathrm{Min}_L^N}\right)$. Since we have shown above that $\mathrm{Var}^{\mathrm{Asy}}\left(\widetilde{\mathrm{Min}_L^N}\right)$ and $\mathrm{Var}^{\mathrm{Asy}}\left(\mathrm{Sam}_L^N\right)$ match beyond the medium distance regime, we thus expect to still be able to recover the power-law behavior of $\mathrm{Var}\left(\mathrm{Env}_L^N\right)$ by studying $\mathrm{Var}^{\mathrm{Num}}\left(\mathrm{Min}_L^N\right) - \mathrm{Var}^{\mathrm{Asy}}\left(\widetilde{\mathrm{Min}_L^N}\right)$.

In Figure 15, the dots record positive values of this difference $\mathrm{Var}^{\mathrm{Num}}\left(\mathrm{Min}_L^N\right) - \mathrm{Var}^{\mathrm{Asy}}\left(\widetilde{\mathrm{Min}_L^N}\right)$ (scaled by $(\ln(N))^{1/2}$, as one should to see a collapse of the data) and the $\times$ records the magnitude of negative values of this difference. Clearly, the presence of negative values contradicts the addition law and recovery of $\mathrm{Var}\left(\mathrm{Env}_L^N\right)$. These values, however, only arise for either small N (10^2 and 10^5) or large L. For large N (10^{12} and 10^{28}) the dots closely follow the asymptotic environmental variance curve $\mathrm{Var}^{\mathrm{Asy}}\left(\mathrm{Env}_L^N\right)$ for just under two decades (as evidenced from the ratio being close to 1) and then peel off following what looks

to be an L^4 power-law (as opposed to the L^3 power-law behavior of $\mathrm{Var}^{\mathrm{Asy}}\big(\mathrm{Env}_L^N\big)$).
The explanation for the lack of agreement for small N or large L likely arises from the presence of higher order corrections to $\mathrm{Var}^{\mathrm{Asy}}\Big(\widetilde{\mathrm{Min}}_L^N\Big)$ which scale like L^4 but with pre-factors that decay with N (the presence of such terms can be seen from [117]). Therefore, for small N or large L these corrections become relevant.

3.9 Conclusion

We consider two models for many-particle diffusion in a common environment. The first treats each particle as an independent SSRW while the second RWRE model treats the environment as a space-time random biasing field within which each particle performs biased random walks. We focus on the extreme first passage time Min_L^N, i.e., the time when the first of N particles passes a barrier distance L from their common starting location. We show that the randomness of Min_L^N splits into two essentially independent pieces, the randomness Env_L^N from the environment and the randomness Sam_L^N from sampling N random walks within that environment.

We determine theoretical predictions (related to the KPZ universality class and equation) for the behavior of each of these contributions based on asymptotic limit theorems in different scaling regimes of N and L. While $\mathrm{Var}\left(\mathrm{Sam}_L^N\right)$ closely matches the variance from sampling in the SSRW model for large L, the $\mathrm{Var}\left(\mathrm{Env}_L^N\right)$ term has no parallel in the SSRW case where the environment is deterministic. We uncover a novel $L^3/(\ln(N))^{5/2}$ power-law describing the large L behavior of $\mathrm{Var}\left(\mathrm{Env}_L^N\right)$. This should be contrasted with the $L^4/(\ln(N))^4$ power-law that we demonstrate describes the large L behavior of $\mathrm{Var}\left(\mathrm{Sam}_L^N\right)$. Thus, for large L, owing to the independence of Env_L^N and Sam_L^N, we see that $\mathrm{Var}\left(\mathrm{Min}_L^N\right) = \mathrm{Var}\left(\mathrm{Env}_L^N\right) + \mathrm{Var}\left(\mathrm{Sam}_L^N\right)$ and only the L^4 power-law is visible.

We numerically verify all of our predictions for system sizes ranging from $N = 10^2$ to $N = 10^{28}$ and, remarkably, see close agreement over this entire range.

Our results point to a potential experimental approach to probe the nature of a random or disordered environment by observing the extreme behavior of many particles diffusing within it. In Figure 15 we show that it is possible to recover, over multiple decades, the L^3 power-law behavior of $\mathrm{Var}\left(\mathrm{Env}_L^N\right)$ by numerically measuring $\mathrm{Var}\left(\mathrm{Min}_L^N\right)$ and then subtracting the asymptotic theory formula for $\mathrm{Var}\left(\widetilde{\mathrm{Min}}_L^N\right)$, the SSRW extreme first passage time variance. This is because the asymptotic behavior of $\mathrm{Var}\left(\widetilde{\mathrm{Min}}_L^N\right)$ for $L \gg \ln(N)$ essentially matches that of $\mathrm{Var}\left(\mathrm{Sam}_L^N\right)$ in the RWRE model. For the SSRW model (or its Brownian analog), a formula for $\mathrm{Var}\left(\mathrm{Min}_L^N\right)$ can be determined asymptotically just by knowing the Einstein diffusion coefficient, which in turn can be estimated experimentally by following the motion of a single particle. Thus, by observing the motion (i.e., extreme first passage time, and Einstein diffusion coefficient) of many particles diffusing in a common environment we are (at least in our numerical simulations) able to recover the power-law that describes the environmental fluctuations. Moreover, with some error, we are also able to estimate the pre-factor of this power-law, which contains further information about the random environment. This pre-factor could be termed the *extreme diffusion coefficient* and in future work we plan to develop a more general map between random environments (beyond the special Uniform on $[0, 1]$ choice) and extreme diffusion coefficients.

In experimental systems such as N colloids or fluorescent dyes diffusing in quasi-1D channels, or photons (here N relates to the laser intensity) diffusing through a quasi-1D tubes filled with scattering media, it should be possible to precisely observe first passage times to various distances, as well as to estimate the Einstein diffusion coefficient for a single particle. Our numerical conclusions suggest a possible route to observe the hidden environment within which these real diffusions occur. Uncovering an L^3 power-law would strongly suggest that the RWRE model more accurately captures the behavior of extreme behavior in many particle diffusions. Moreover, the pre-factor to this power-law would constitute a measurement of the *extreme diffusion coefficient* and thus serve as a microscope through which to view the hidden environment.

3.10 Acknowledgments

This work was funded under the W.M. Keck Foundation Science and Engineering grant on "Extreme Diffusion". I.C. also wishes to acknowledge ongoing support from the NSF through DMS:1811143, DMS:1937254, and DMS:2246576, and the Simons Foundation through a Simons Investigator Grant (Award ID 929852). E.I.C. wishes to acknowledge ongoing support from the Simons Foundation for the collaboration Cracking the Glass Problem via Award No. 454939. We wish to thank S. Prolhac for providing data for the numerically computed density of the one-point distribution for the narrow wedge solution to the KPZ equation that was utilized in producing some of the asymptotic curves herein. We also wish to thank P. Le Doussal for helpful comments on a draft of this paper. This work benefited from access to the University of Oregon high performance computing cluster, Talapas.

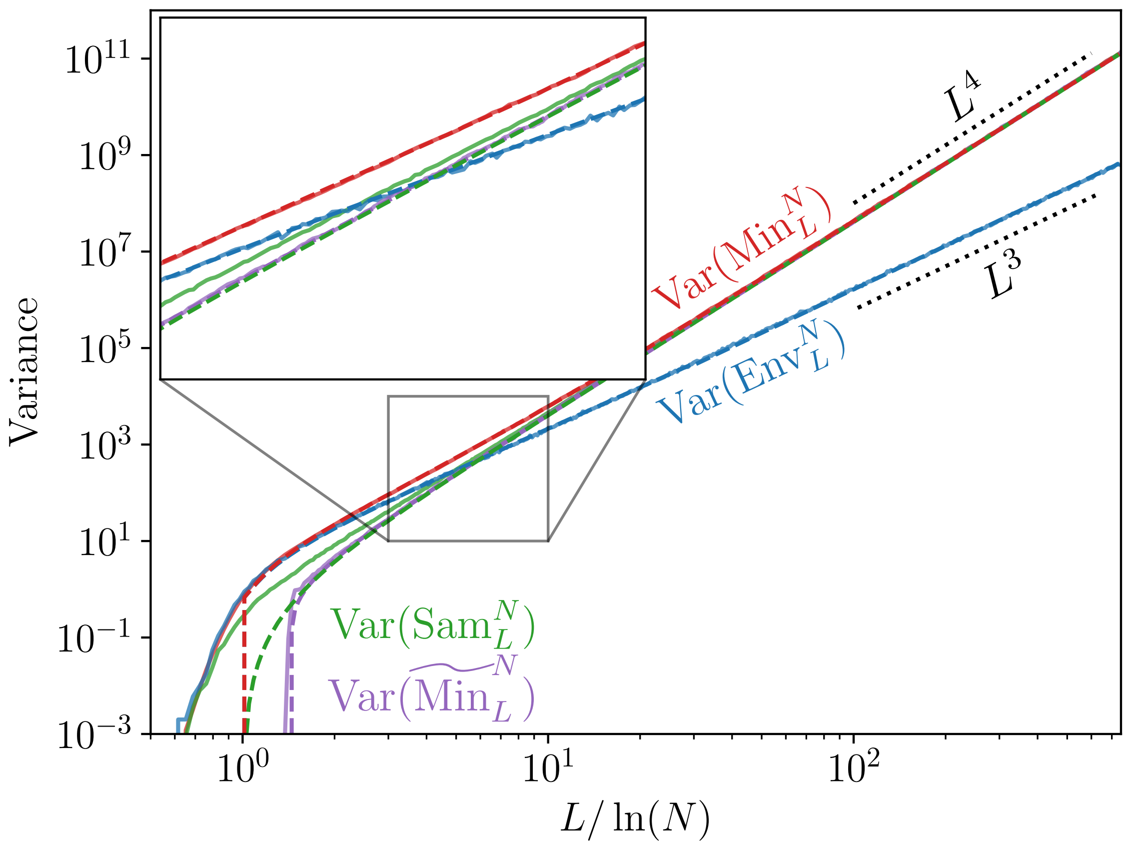

Figure 9. For the RWRE model with $N = 10^{12}$ particles, we plot the numerically measured (solid) and asymptotic theory (dashed) variance of the extreme first passage time $\mathrm{Var}\left(\mathrm{Min}_L^N\right)$ (red); the variance due to the environment $\mathrm{Var}\left(\mathrm{Env}_L^N\right)$ (blue); the variance due to sampling $\mathrm{Var}\left(\mathrm{Sam}_L^N\right)$ (green). For the SSRW model we plot $\mathrm{Var}\left(\widetilde{\mathrm{Min}}_L^N\right)$, where $\widetilde{\mathrm{Min}}_L^N$ is the extreme first passage time for the SSRW model (purple). Note, our asymptotic theory matches our numerics to such precision that they become indistinguishable on this scale.

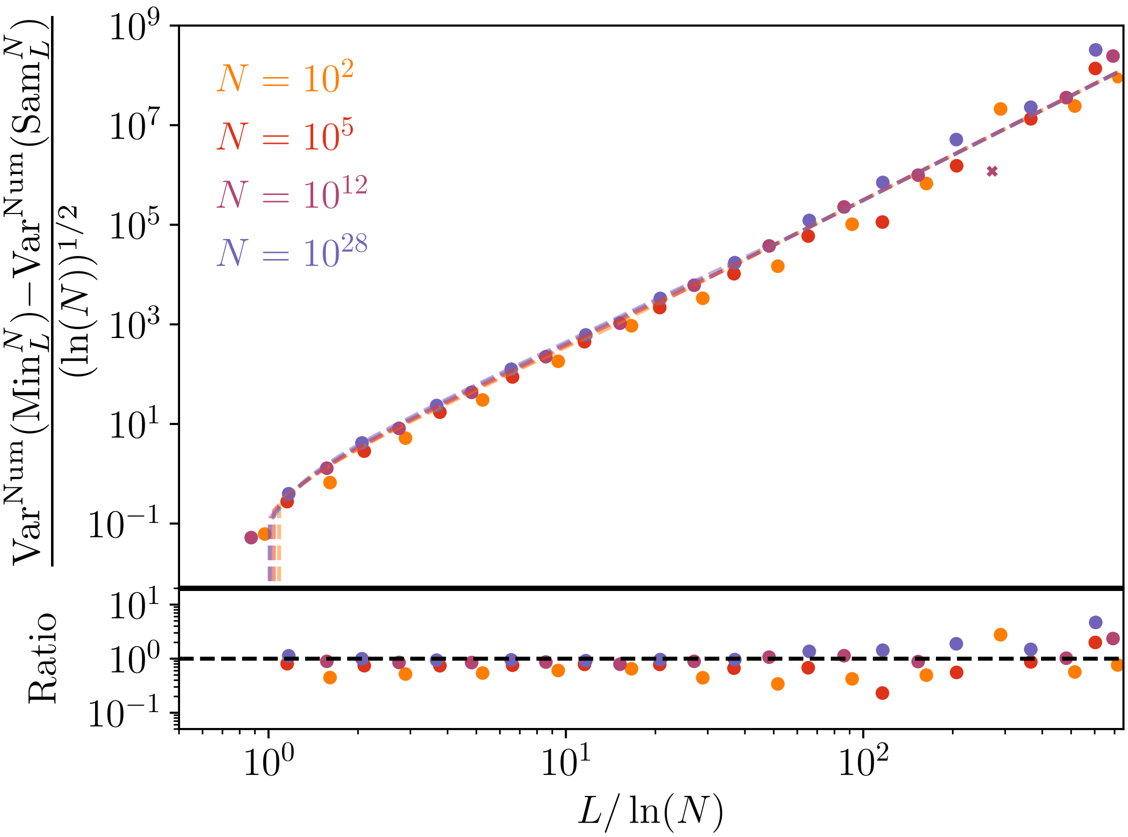

Figure 10. We plot $\mathrm{Var}^{\mathrm{Num}}\left(\mathrm{Min}_L^N\right) - \mathrm{Var}^{\mathrm{Num}}\left(\mathrm{Sam}_L^N\right)$ for $N = 10^2, 10^5, 10^{12}$ and 10^{28} averaged into bins with logarithmically spaced bin edges to achieve 4 bins per decade of L. The dots represent positive values of this difference whereas the $\times$ represents the magnitude of negative values of this difference. The dashed line is $\mathrm{Var}^{\mathrm{Asy}}(\mathrm{Env}_L^N)$ in Eq. 3.31 for each N corresponding to its respective color. The lower plot shows the ratio $\left(\mathrm{Var}^{\mathrm{Num}}\left(\mathrm{Min}_L^N\right) - \mathrm{Var}\left(\mathrm{Sam}_L^N\right)\right)/\mathrm{Var}^{\mathrm{Num}}\left(\mathrm{Env}_L^N\right)$ confirming the close fit.

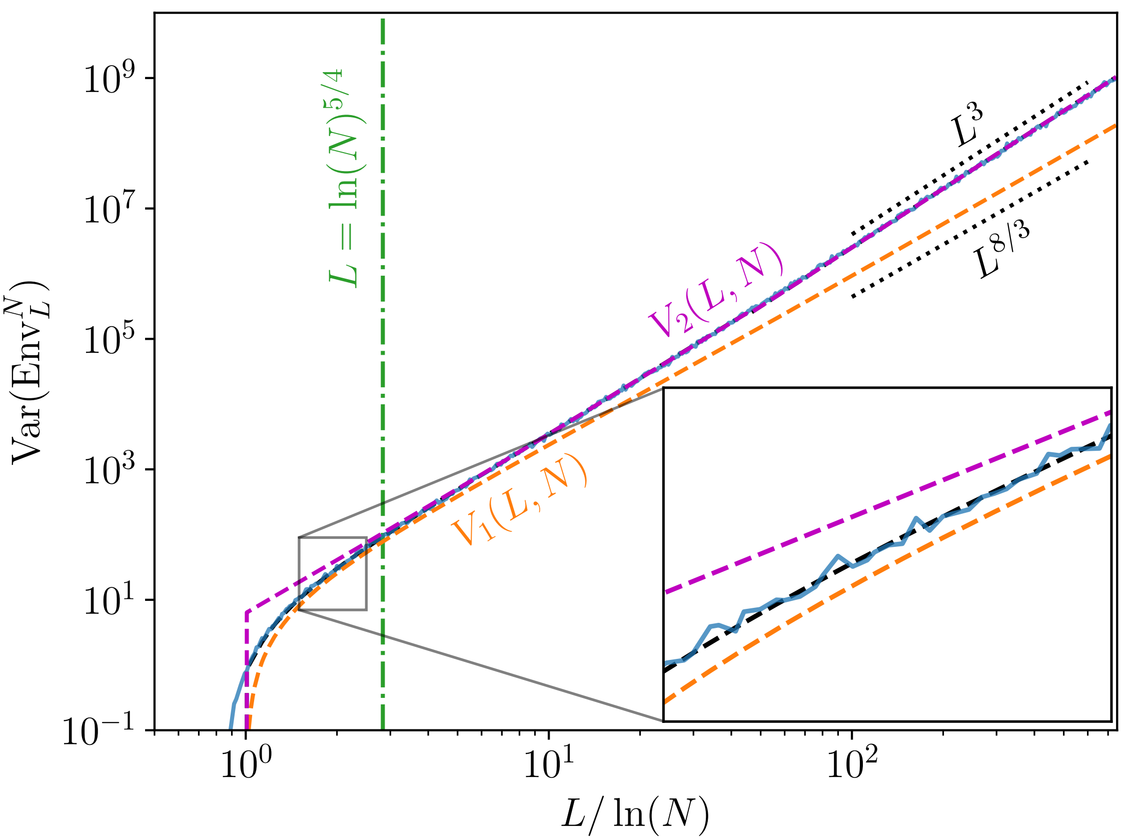

Figure 11. We plot the environmental variance, $\mathrm{Var}^{\mathrm{Num}}\left(\mathrm{Env}_L^N\right)$, for $N = 10^{28}$ particles (blue); the asymptotic variance V_1 for the short time regime given in Eq. 3.22 (orange dashed line); the asymptotic variance V_2 for the long time regime given in Eq. 3.30 (purple dashed line); the interpolation $\mathrm{Var}^{\mathrm{Asy}}\left(\mathrm{Env}_L^N\right)$ between these regimes using Eq. 3.31 (black dashed line); and the power-law asymptotics of V_1 and V_2 (black dotted lines).

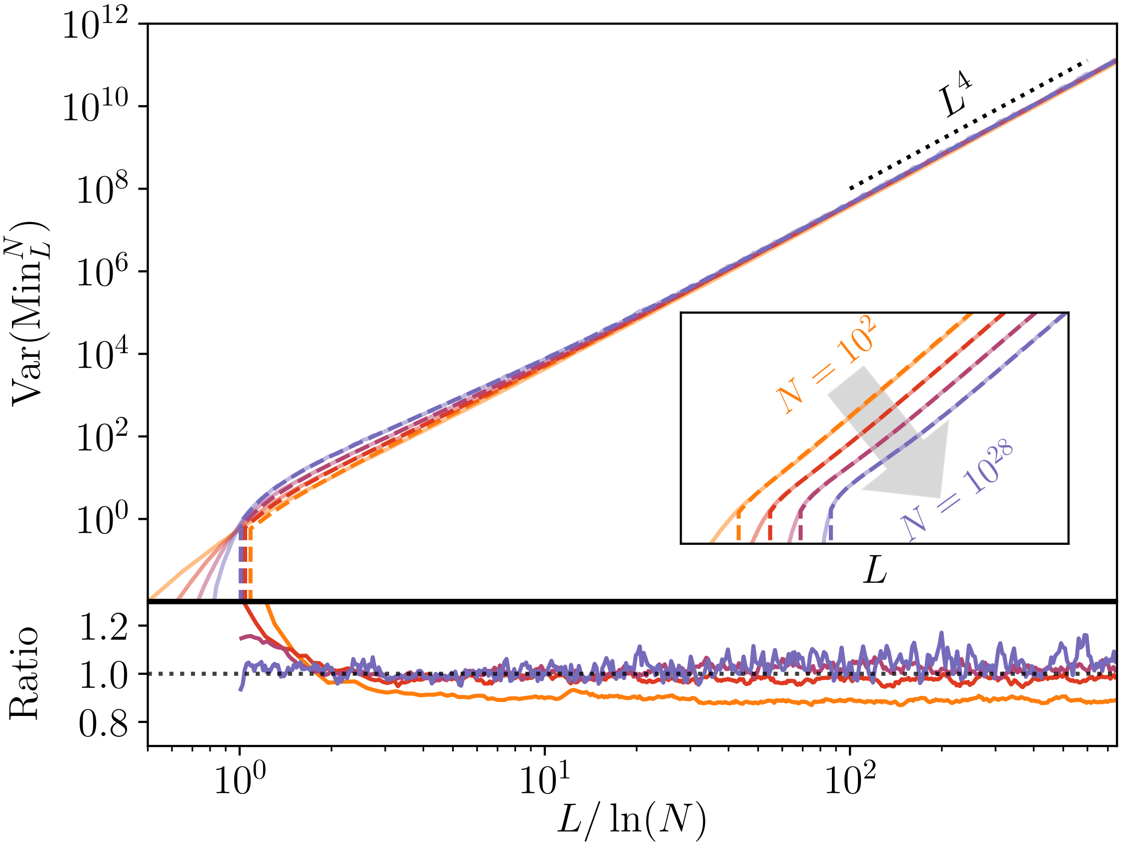

Figure 12. We plot the numerically measured (solid) and asymptotic theory (dashed) variance of the extreme first passage time, $\mathrm{Var}\left(\mathrm{Min}_L^N\right)$, for $N = 10^2, 10^5, 10^{12}$ and 10^{28} (each labeled with a different color). The asymptotic theory variance, $\mathrm{Var}^{\mathrm{Asy}}\!\left(\mathrm{Min}_L^N\right)$, comes from Eq. 3.43. Note, our asymptotic theory matches our numerics to such precision that they are nearly indistinguishable on this scale. The inset shows the same data uncollapsed to better distinguish different N. The lower plot shows the ratio $\mathrm{Var}^{\mathrm{Num}}\left(\mathrm{Min}_L^N\right)/\mathrm{Var}^{\mathrm{Asy}}\!\left(\mathrm{Min}_L^N\right)$.

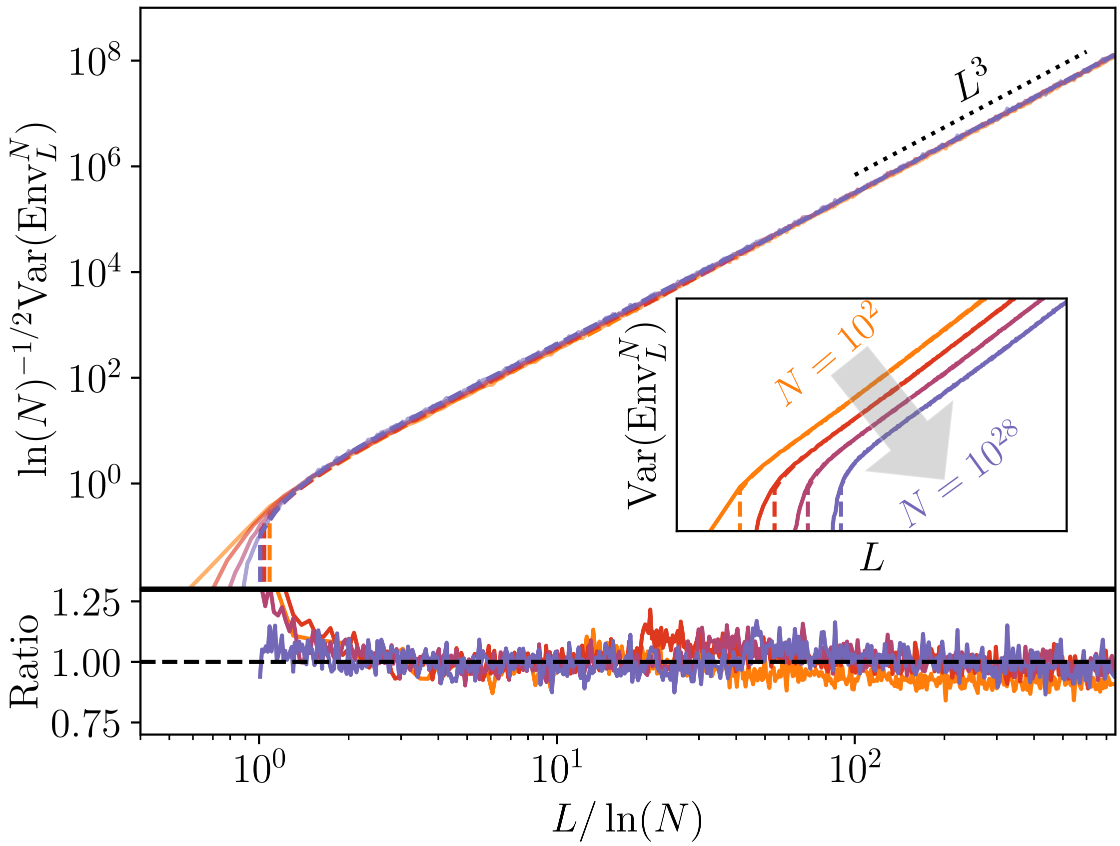

Figure 13. We plot the numerically measured (solid) and asymptotic theory (dashed) environmental variance, $\mathrm{Var}\left(\mathrm{Env}_L^N\right)$, for $N = 10^2, 10^5, 10^{12}$ and 10^{28} (each labeled with a different color). The asymptotic theory variance, $\mathrm{Var}^{\mathrm{Asy}}\left(\mathrm{Env}_L^N\right)$, comes from Eq. 3.31. Note, our asymptotic theory matches our numerics to such precision that they are nearly indistinguishable on this scale. The inset shows the same data uncollapsed to better distinguish different N. The lower plot shows the ratio $\mathrm{Var}^{\mathrm{Num}}\left(\mathrm{Env}_L^N\right)/\mathrm{Var}^{\mathrm{Asy}}\left(\mathrm{Env}_L^N\right)$.

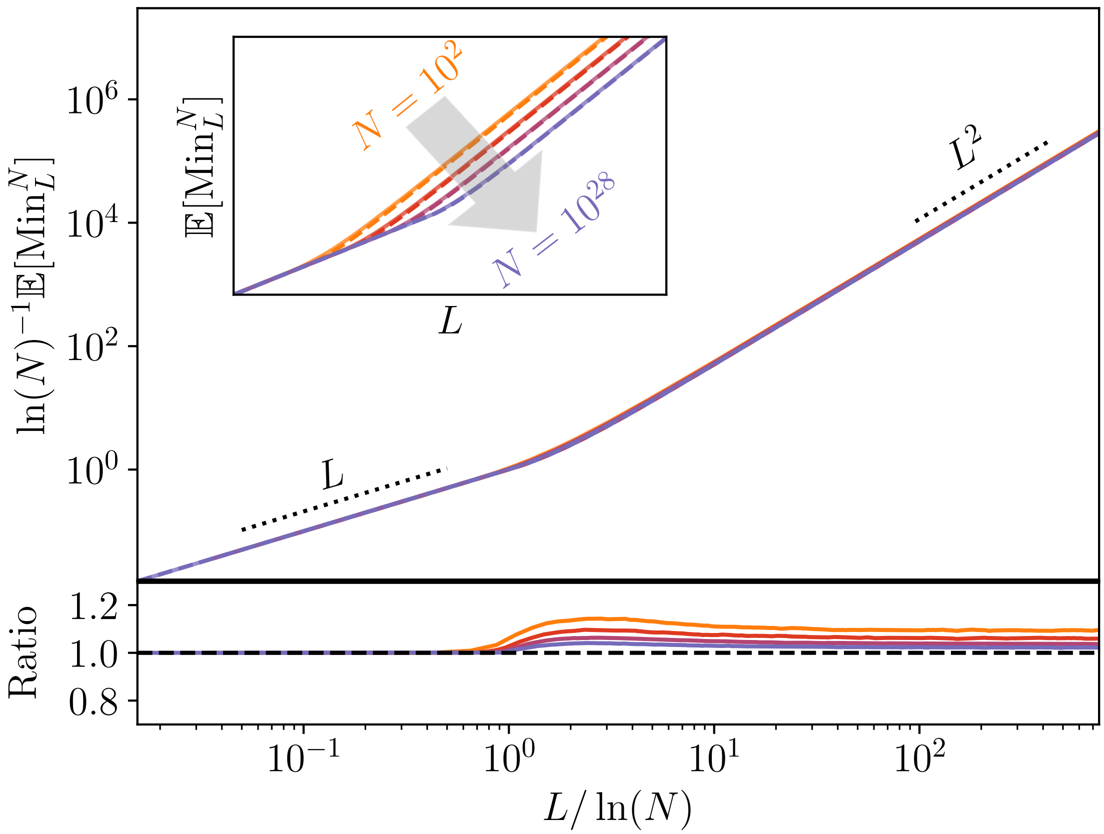

Figure 14. We plot the mean of the extreme first passage time, $\mathbb{E}^{\mathrm{Num}}\left[\mathrm{Min}_L^N\right]$, using solid lines of varying colors for $N = 10^2, 10^5, 10^{12}$ and 10^{28} particles. The dashed lines are the asymptotic curves $\mathbb{E}^{\mathrm{Asy}}\left[\mathrm{Min}_L^N\right]$ from Eq. 3.44. Note, our asymptotic theory matches our numerics to such precision that they are nearly indistinguishable on this scale. The inset shows the uncollapsed data to better distinguish different values of N. The collapse occurs by scaling both the x-axis and y-axis by $\ln(N)$. The lower plot shows the ratio of $\mathbb{E}^{\mathrm{Num}}\left[\mathrm{Min}_L^N\right]/\mathbb{E}^{\mathrm{Asy}}\left[\mathrm{Min}_L^N\right]$ confirming the close fit.

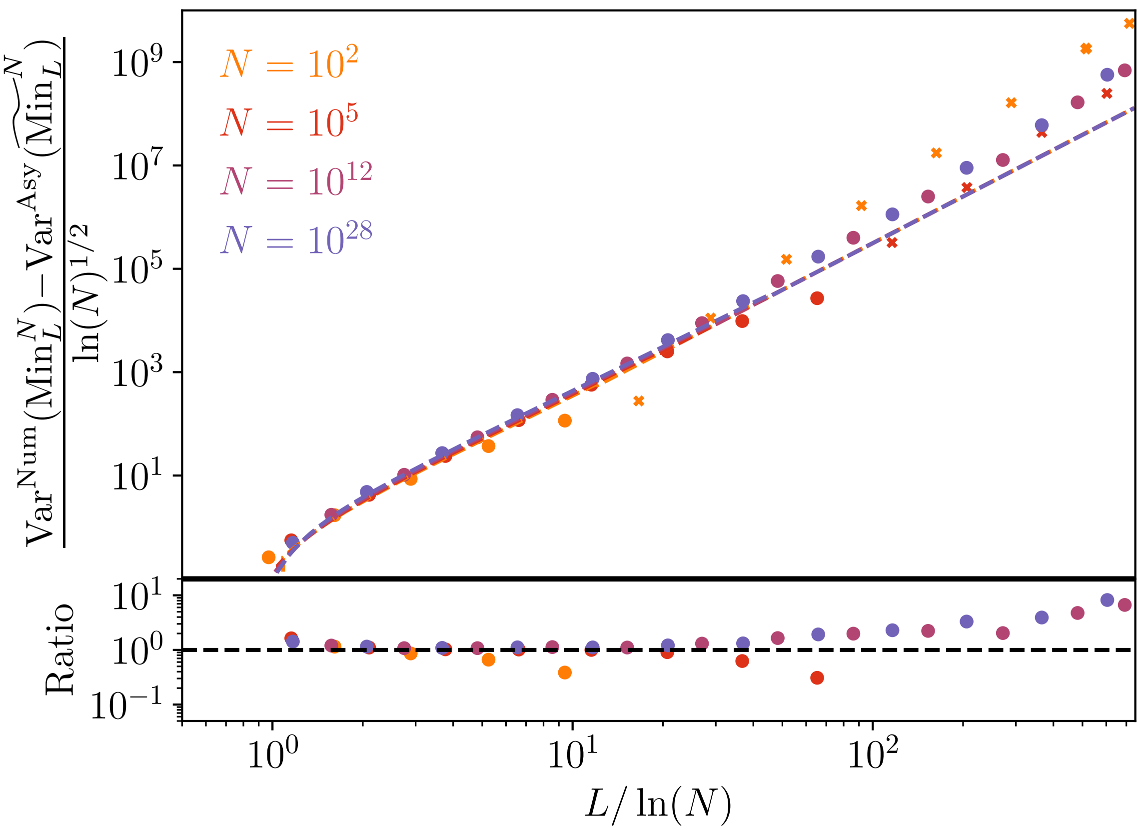

Figure 15. We plot $\mathrm{Var}^{\mathrm{Num}}\left(\mathrm{Min}_L^N\right) - \mathrm{Var}^{\mathrm{Asy}}\left(\widetilde{\mathrm{Min}_L^N}\right)$ for $N = 10^2, 10^5, 10^{12}$ and 10^{28} averaged into bins with logarithmically spaced bin edges to achieve 4 bins per decade of L. The dots represent positive values of this difference whereas the $\times$ represents the magnitude of negative values of this difference. The dashed line is $\mathrm{Var}^{\mathrm{Asy}}\left(\mathrm{Env}_L^N\right)$ in Eq. 3.31 for each N corresponding to its respective color.

CHAPTER IV

EXTREME DIFFUSION MEASURES STATISTICAL FLUCTUATIONS OF THE ENVIRONMENT

This chapter is published as: Hass, J. B., Drillick, H., Corwin, I., & Corwin, E. I. (2024, December). Extreme Diffusion Measures Statistical Fluctuations of the Environment. Physical Review Letters, 133 (26), 267102. doi: 10.1103/PhysRevLett.133.267102. Contrary to the previous two papers, I worked much more independently from Eric and Ivan Corwin on this paper. I developed much of the theoretical results after reading the paper in Ref. [112] and refined these results alongside Hindy Drillick.

4.1 Abstract

We consider many-particle diffusion in one spatial dimension modeled as *Random Walks in a Random Environment* (RWRE). A shared short-range space-time random environment determines the jump distributions that drive the motion of the particles. We determine universal power-laws for the environment's contribution to the variance of the extreme first passage time and extreme location. We show that the prefactors rely upon a single *extreme diffusion coefficient* that is equal to the ensemble variance of the local drift imposed on particles by the random environment. This coefficient should be contrasted with the Einstein diffusion coefficient, which determines the prefactor in the power-law describing the variance of a single diffusing particle and is equal to the jump variance in the ensemble averaged random environment. Thus a measurement of the behavior of extremes in many-particle diffusion yields an otherwise difficult to measure statistical property of the fluctuations of the generally hidden environment in which

that diffusion occurs. We verify our theory and the universal behavior numerically over many RWRE models and system sizes.

4.2 Introduction

Beneath the still surface of a glass of water lies an invisible roiling chaos; thermal motion moves the fluid environment at every time and length scale [2, 30, 31, 29, 28, 25, 21, 22, 23, 26, 27]. It is only through the motion of tracer particles that this molecular storm is rendered visible [2, 31, 30]. The coefficient of the mean-squared displacement power-law for a single tracer particle yields a measurement of the Einstein diffusion coefficient, D. Classical diffusion theory [22, 21, 23, 25, 26, 27, 28, 29] relates this to a microscopic statistic of the environment, namely the square of the mean-free path length divided by the mean collision time. This is far from a complete characterization of the thermal motion within the environment. The introduction of multiple tracer particles offers the possibility of gleaning further statistical information. However, classical diffusion theory stymies such an effort since it treats each particle as independent, thus replacing the richness and chaos of the environment with an ensemble average in which particles are randomly kicked in the same manner and at the same rate everywhere in the system. This erasure is a lie, but one which works well to predict the bulk or typical behavior of many tracer particles. In this paper, we show that at the edges of the bulk, the truth is exposed: the fluctuations of the extremes of many tracer particles are highly sensitive to the disorder of the environment and thus reveal a more complete statistical description of the hidden environment.

Here, we study the statistical behavior of the extreme first passage time past a barrier at location L and of the extreme location at time t for a system of N tracer particles in a general class of *random walk in random environment*

(RWRE) models, see Fig. 16a. These models capture the fact that in real many-particle diffusion, all particles are subject to common and effectively random forces from the thermal fluctuations of the fluid environment. We show theoretically and confirm numerically that (1) the environment's contribution to the variances of these two observables is independent of the variance due to sampling and follows robust power-laws (see, (4.7) and (4.8) below) whose exponents are independent of the choice of environment; (2) the coefficient in these power-laws, as well as the time or location of onset of the power-laws, depends on the Einstein diffusion coefficient, D, as well another parameter D_{ext}, defined in (4.10), that is equal to the ensemble variance of the local drift imposed upon particles by the environment (see Fig. 16b, where D_{ext} records the variance of the black arrows, and see Fig. 17 for numerical results verifying this theory). We call D_{ext} the *extreme diffusion coefficient* as it relates the extreme behavior of many-particle diffusion to a microscopic statistic of the environment. In the RWRE model, the Einstein diffusion coefficient D is related to a different microscopic statistic, namely the jump variance in the ensemble averaged environment. Thus, these two diffusion coefficients—that of Einstein which is observable from a single tracer, and that introduced here which is observable from the extremes of many tracers—offer a refined lens relative to classical diffusion theory through which to measure the statistics of the hidden environment.

4.3 RWRE Models

In place of the independent random walk model of classical diffusion theory, we consider here lattice RWRE models. These play the role of a coarse-grained continuum environment in which particles are chaotically or thermally-randomly biased in their motion by an environment quickly mixing in space and time. As such, we focus on RWRE models whose randomness is short-range correlated in time, see also [56, 57, 58, 59, 60, 61, 62, 118]. This is in contrast to long-range correlated or quenched in time randomness, e.g. as in [50, 39, 51, 52, 53, 54, 55, 119, 46, 120, 121].

To define our RWRE models, we first describe how we specify the environment, and then we describe how random walks evolve therein. Each RWRE model is specified by ν, a choice of probability distribution on the space of probability distributions on $\mathbb{Z}$. There are many ways to produce a random probability distribution on $\mathbb{Z}$. Perhaps the simplest involves choosing a uniform random variable on $[0,1]$ and then assigning that probability to $+1$ and its complementary probability to -1 (and 0 probability assigned to all other values of $\mathbb{Z}$). This *nearest-neighbor* model is a special case of the beta RWRE (where the uniform is replaced by a general beta distribution) introduced and studied recently in [6, 69, 7, 107, 122, 112]. Though our theoretical results apply more generally, for our numerical simulations we will consider a few other specific non-nearest neighbor examples of ν, namely the *Dirichlet* and *random delta* distributions described below; see also [89, 123] for other examples. Let ξ denote a probability distribution on $\mathbb{Z}$ sampled according to ν, so that $\xi(i)$ is the probability mass on $i \in \mathbb{Z}$. For $k \geq 1$ and positive $(\alpha_{-k}, \dots \alpha_k)$ the *Dirichlet* distribution is such that $\xi(i) = X_i/Z$ for $i \in [-k,k]$ (and $\xi(i) \equiv 0$ elsewhere) where the X_i are independent Gamma random variables with shape α_i and rate $\beta = 1$ and $Z = \sum_{j \in [-k,k]} X_i$. The *flat Dirichlet* distribution is when $\alpha_i \equiv 1$ and is uniformly distributed over all probability distributions supported on $[-k,k]$. The *random delta* distribution is solely characterized by the width of the interval k. We first generate two random variables, X_1 and X_2, uniformly and without replacement on the integer interval $[-k, k]$, then we set $\xi(X_1) = \xi(X_2) = 1/2$ and $\xi(i) \equiv 0$ otherwise.

Given ν, we define the random environment as $\boldsymbol{\xi} := \big(\xi_{t,x} : x \in \mathbb{Z}, t \in \mathbb{Z}_{\geq 0}\big)$ where each $\xi_{t,x}$ is a probability distribution on $\mathbb{Z}$ that is sampled independently according to ν. The environment, $\boldsymbol{\xi}$, should be thought of as one instance of an environment in which several particles can diffuse from position x and time t using the transition probabilities $\xi_{t,x}$, i.e. the red arrows in Fig. 16b.

We denote the product measure on the environment $\boldsymbol{\xi}$ by $\mathbb{P}_\nu$ and let $\mathbb{E}_\nu[\bullet]$ and $\mathrm{Var}_\nu(\bullet)$ denote the associated expectation and variance. We restrict our attention to models ν that produce net drift-free systems, i.e. such that $\sum_{j\in\mathbb{Z}} \mathbb{E}_\nu[\xi(j)]\, j = 0$ where ξ is sampled according to ν, and those with finite range, i.e. such that there exists an $M > 0$ so that $\xi(j) = 0$ if $|j| > M$. After going to a suitable moving frame, similar results to ours hold even when there is a net drift, i.e. non-zero expected mean. However, long range, heavy tailed jump distributions may lead to new phenomena related to anomalous diffusion (see, e.g., [121, 124]), deserving of further study.

Given a sample $\boldsymbol{\xi}$ of the environment, we define a probability measure $\mathbb{P}^{\boldsymbol{\xi}}$ on an arbitrary number of independent and identically distributed (i.i.d.) random walks $R^1, R^2, \ldots$ evolving in that environment, and let $\mathbb{E}^{\boldsymbol{\xi}}[\bullet]$ and $\mathrm{Var}^{\boldsymbol{\xi}}(\bullet)$ denote the associated expectation and variance. Each walk starts at $R^i(0) = 0$, where $R^i(t) \in \mathbb{Z}$ denotes its position at time t. The probability that a walk at x at time t transitions to $x + j$ at time $t + 1$ is

$$\mathbb{P}^{\boldsymbol{\xi}}\big(R^i(t+1) = x + j \mid R^i(t) = x\big) = \xi_{t,x}(j).$$

All random walks evolve independently given $\boldsymbol{\xi}$ though notably walkers at the same location x at the same time t are subject to the same jump distribution, $\xi_{t,x}$. We define the transition probabilities given $\boldsymbol{\xi}$ by $p^{\boldsymbol{\xi}}(x,t) = \mathbb{P}^{\boldsymbol{\xi}}(R(t) = x)$ (we drop the superscript i here and elsewhere below since each $R^i(t)$ is i.i.d.); this satisfies $p^{\boldsymbol{\xi}}(x,0) = \mathbf{1}_{x=0}$ and

$$p^{\boldsymbol{\xi}}(x,t+1) = \sum_{j\in\mathbb{Z}} p^{\boldsymbol{\xi}}(x-j,t)\xi_{t,x-j}(j). \tag{4.1}$$

The measure $\mathbb{P}_\nu$ is on the environment $\boldsymbol{\xi}$ and $\mathbb{P}^{\boldsymbol{\xi}}$ is on independent random walks given the environment $\boldsymbol{\xi}$. It is also useful to define $\mathbf{P}$ by $\mathbf{P}(\bullet) = \mathbb{E}_\nu\left[\mathbb{P}^{\boldsymbol{\xi}}(\bullet)\right]$ for any event $\bullet$ defined in terms of the random walks $R^1, R^2, \ldots$, and to let $\mathbf{E}[\bullet]$ and $\mathbf{Var}[\bullet]$ denote the associated expectation and variance. This is the marginal distribution on many-particle diffusion trajectories that is relevant to repeated experimental studies of many-particle diffusion; $\mathbf{P}$ represents the histogram over many experimental samples of the many-particle diffusion trajectories.

Given a random walk R^i, we denote its first passage time past $L > 0$ by τ_L^i. The *extreme first passage time* of N random walkers past location L is defined as

$$\mathrm{Min}_L^N := \min(\{\tau_L^1, \ldots, \tau_L^N\}).$$

Given an environment $\boldsymbol{\xi}$, the walks $R^1, \ldots, R^N$ are i.i.d under the measure $\mathbb{P}^{\boldsymbol{\xi}}$, and thus so are the τ_L^i. Therefore,

$$\mathbb{P}^{\boldsymbol{\xi}}(\mathrm{Min}_L^N \le t) = 1 - \left(1 - \mathbb{P}^{\boldsymbol{\xi}}(\tau_L \le t)\right)^N. \tag{4.2}$$

We also study the *extreme location* of N walks at time t,

$$\mathrm{Max}_t^N := \max\left(\{R^1(t), \ldots R^N(t)\}\right).$$

Given $\boldsymbol{\xi}$, under the measure $\mathbb{P}^{\boldsymbol{\xi}}$ on $R^1, \ldots, R^N$,

$$\mathbb{P}^{\boldsymbol{\xi}}(\mathrm{Max}_t^N \ge x) = 1 - \left(1 - \mathbb{P}^{\boldsymbol{\xi}}(R(t) \ge x)\right)^N. \tag{4.3}$$

We characterize the statistics of Min_L^N and Max_t^N under the measure $\mathbf{P}$, i.e., when the environment is hidden as in real diffusive systems. There are two levels of randomness: first, the randomness due to the environment, Env_t^N, and second, the randomness of sampling walkers in that environment, Sam_L^N. Specifically, we define Env_L^N as the minimum time t such that $\mathbb{P}^{\boldsymbol{\xi}}(\tau_L \leq t) \geq \frac{1}{N}$ and Sam_L^N as the residual, $\mathrm{Sam}_L^N := \mathrm{Min}_L^N - \mathrm{Env}_L^N$. Note that Env_L^N only depends on the environment $\boldsymbol{\xi}$ and by (4.2), Env_L^N satisfies $\mathbb{P}^{\boldsymbol{\xi}}(\mathrm{Min}_L^N \leq \mathrm{Env}_L^N) \approx 1 - e^{-1}$. Thus, Env_L^N is approximately the mean, or median, of Min_L^N in a given environment and Sam_L^N captures fluctuations about Env_L^N due to sampling N random walks in that environment. If one were to sample many systems of N independent random walks in the *same* environment, one could compute the mean value of Min_L^N (i.e. the mean extreme first passage time) and find that it is well approximated by Env_L^N. The fluctuations of the many different measured values of Min_L^N, in the same environment, will in turn be captured by Sam_L^N. We similarly define Env_t^N as the maximum position x satisfying $\mathbb{P}^{\boldsymbol{\xi}}(R(t) \geq x) \geq \frac{1}{N}$ and $\mathrm{Sam}_t^N := \mathrm{Max}_t^N - \mathrm{Env}_t^N$. Note the subscript of Env_L^N, Env_t^N, Sam_L^N and Sam_t^N distinguishes between measurements of the first passage at a distance L (subscript L) and location of extreme particle at time t (subscript t).

4.4 Theoretical Results

The Einstein diffusion coefficient,

$$D := \frac{1}{2} \sum_{j \in \mathbb{Z}} \mathbb{E}_\nu \left[\xi(j)\right] j^2, \tag{4.4}$$

for the RWRE is defined as the variance of the ensemble averaged jump distribution (recall that we have assumed a net drift-free system, i.e. $\sum_{j \in \mathbb{Z}} \mathbb{E}_\nu \left[\xi(j)\right] j = 0$). The following results are derived under the assumption that $L \gg \lambda_{\text{ext}} \ln(N)^{3/2}$ or $t \gg \frac{\lambda_{\text{ext}}^2}{D} \ln(N)^2$ (where λ_{ext} is defined in (4.10)), and $N \gg 1$. We find that

$$\mathbf{E}\left[\mathrm{Min}_L^N\right] \approx \frac{L^2}{4D\ln(N)}, \quad \mathbf{E}[\mathrm{Max}_t^N] \approx \sqrt{4D\ln(N)t}$$

matching the classical theory of diffusion, i.e., where the RWRE is replaced by independent random walks with Einstein diffusion coefficient D, see, e.g. [95, 100, 102, 106, 104, 125, 126].

The variance of Min_L^N and Max_t^N reveals more interesting behavior. The environmental and sampling contributions to Min_L^N and Max_t^N are roughly independent:

$$\mathbf{Var}\left(\mathrm{Min}_L^N\right) \approx \mathbf{Var}\left(\mathrm{Env}_L^N\right) + \mathbf{Var}\left(\mathrm{Sam}_L^N\right), \tag{4.5}$$

$$\mathbf{Var}\left(\mathrm{Max}_t^N\right) \approx \mathbf{Var}\left(\mathrm{Env}_t^N\right) + \mathbf{Var}\left(\mathrm{Sam}_t^N\right). \tag{4.6}$$

The sampling fluctuations are centered Gumbel with

$$\mathbf{Var}(\mathrm{Sam}_L^N) \approx \frac{\pi^2 L^4}{96 D^2 \ln(N)^4}, \quad \mathbf{Var}(\mathrm{Sam}_t^N) \approx \frac{\pi^2 D t}{6 \ln(N)},$$

in agreement with classical diffusion theory [95, 100, 102, 106, 104, 125, 126]. The environmental fluctuations follow anomalous power-laws

$$\mathbf{Var}(\mathrm{Env}_L^N) \approx \lambda_{\mathrm{ext}} \frac{\sqrt{2\pi} L^3}{8 D^2 \ln(N)^{5/2}} \tag{4.7}$$

$$\mathbf{Var}(\mathrm{Env}_t^N) \approx \lambda_{\mathrm{ext}} \sqrt{2\pi D t}. \tag{4.8}$$

where D is the Einstein diffusion coefficient,

$$\lambda_{\mathrm{ext}} := \frac{1}{2} \frac{D_{\mathrm{ext}}}{(D - D_{\mathrm{ext}})} = \frac{1}{2} \frac{\mathrm{Var}_\nu \left(\mathbb{E}^{\boldsymbol{\xi}}[Y]\right)}{\mathbb{E}_\nu \left[\mathrm{Var}^{\boldsymbol{\xi}}(Y)\right]}, \tag{4.9}$$

and D_{ext} is the *extreme diffusion coefficient*:

$$D_{\mathrm{ext}} := \frac{1}{2} \mathrm{Var}_\nu \left(\mathbb{E}^{\boldsymbol{\xi}}[Y]\right) = \frac{1}{2} \mathbb{E}_\nu \left[\Big(\sum_{j \in \mathbb{Z}} \xi(j) j \Big)^2 \right]. \tag{4.10}$$

See the “End Matter” for a brief discussion of our theoretical methods and [89] for a derivation of our results.

Here and below, Y is a random jump distributed according to ξ. Thus D_{ext} is the variance over the random environment of the drift of a single jump, i.e. how much the black arrows fluctuate over space and time in Fig 16b. Then λ_{ext} is the ratio of that to the mean over the random environment of the variance of a single jump. The formula in (4.9) is derived in [89] under the assumptions

$$\mathbb{E}_\nu\left[\xi(i)\xi(j)\right] = c\mathbb{E}_\nu\left[\xi(i)\right]\mathbb{E}_\nu\left[\xi(j)\right] \quad \text{for all } i \neq j \tag{4.11}$$

with some fixed $c \in (0,1)$, and the RWRE is aperiodic (i.e., it does not live on a strict space-time sublattice). In terms of c, $\lambda_{\text{ext}} = \frac{1-c}{2c}$. When (4.11) fails, there is a more involved formula for λ_{ext}, see [123, 127, 89]. When aperiodicity fails, e.g. for the nearest-neighbor RWRE, an additional factor arises in (4.9), see [89].

The extreme diffusion coefficient necessarily satisfies $D_{\text{ext}} \in [0, D]$. When $D_{\text{ext}} = D$ (hence $\lambda_{\text{ext}} = \infty$), ξ is supported at a single, yet random site, hence a perfectly sticky environment of coalescing random walkers. There is a scaling limit where $D_{\text{ext}} \to D$ as time is rescaled which leads to sticky Brownian motions as studied, for instance, in [76, 7, 128, 123]. When $D_{\text{ext}} = 0$, (hence $\lambda_{\text{ext}} = 0$), the drift $\mathbb{E}^{\boldsymbol{\xi}}[Y]$ becomes deterministic, thus with probability 1 under $\mathbb{P}_\nu$, $\sum_j \xi(j)j$ is constant, and (by the net drift-free assumption) equal to 0, see [123, 129].

The quantities D and D_{ext} have units of area per time, while λ_{ext} has units of length. This is shown by rescaling the lattice so as to endow it with length and time units, see [89], or by studying certain continuum versions of our model such as sticky Brownian motions [76, 7, 128, 123] or Langevin dynamics in a random environment [69, 111].

4.5 Numerical Results

Figs. 17a,e show that our theoretical prediction for each relevant variance is asymptotically accurate and that the addition laws in (4.5) and (4.6) are justified. Figs 17b,f show the collapse of the scaled environmental variance for several choices of ν. Although our predictions assume N is large, they are accurate for systems as small as $N = 100$. This is also shown in Figs. 17d,h since the ratio of the measured environmental variance to the theoretical prediction goes to 1, asymptotically. Figs. 17c,g show that our numerically computed values of D_{ext} from both kinds of measurements match the theoretical value, falling onto the line of equality. Since $\mathbf{Var}\left(\text{Sam}_L^N\right)$, and similarly $\mathbf{Var}\left(\text{Sam}_t^N\right)$, rely only on D, a measurement of Min_L^N, or Max_t^N can be translated to a measurement of D_{ext}. See the "End Matter" for our numerical methods.

4.6 Conclusion

While we have focused herein on lattice models, the theory of extreme diffusion should extend to systems with continuous space and time dimensions provided sufficiently fast mixing of the random environment in both dimensions. Besides demonstrating a universality result, the key contribution of this work is the link shown between the extreme diffusion coefficient and the statistics of the environment. Previous works on extreme diffusion have considered nearest neighbor RWREs [6, 69, 7, 107, 122, 112] which are too simple to reveal this relationship, or the continuum sticky Brownian motions where there is no clear notion of an environment [76, 7, 128, 123]). In light of the universality we demonstrate here, we expect this model to be applicable to all physical systems in which particles (or more generally, agents) move in response to the forcing present within a shared space-time chaotic environment. There are several outstanding theoretical challenges including 1) establishing the role of correlation length and time scales in defining the continuum extreme diffusion coefficient, 2) extending extreme diffusion theory to higher spatial dimensions, 3) understanding whether there exists a fluctuation-dissipation type relation for the extreme diffusion coefficient, and if so, what is the relevant notion of extreme drag, and 4) testing extreme diffusion in experimental systems.

Acknowledgements. This work was funded by the W.M. Keck Foundation Science and Engineering grant on "Extreme Diffusion". I.C. also wishes to acknowledge ongoing support from NSF DMS:1811143, 1937254, and 2246576, and the Simons Foundation Investigator Grant 929852. E.I.C. wishes to acknowledge ongoing support from the Simons Foundation for the collaboration Cracking the Glass Problem via Award No. 454939. H.D. wishes to acknowledge ongoing support from the NSF GRFP DGE:2036197. We thank Shalin Parekh for many helpful discussion and Pierre Le Doussal and Guillaume Barraquand for their helpful feedback. This work benefited from access to the University of Oregon high performance computing cluster, Talapas.

4.7 End Matter

4.7.1 Theoretical Methods.. Our derivation [89] of the extreme first passage and location statistics closely follows [107, 122] and relies on moderate deviation asymptotics for the tail probability $\mathbb{P}^{\boldsymbol{\xi}}(R(t) \geq x)$ with $x \propto t^{3/4}$, where $\boldsymbol{\xi}$ is distributed according to $\mathbb{P}_\nu$. We rely on results from [123, 127] that prove convergence in this regime of the tail probability to the KPZ equation [1, 66]. The occurrence of the KPZ equation under moderate deviation scaling was predicted (without a formula for the KPZ coefficients) first in [69] and confirmed with coefficients for the beta RWRE in [7] and general nearest-neighbor RWRE in [112], all prior to the general case addressed in [123, 127].

To see this convergence, first observe that the master equation (4.1) implies the tail probability $\mathbb{P}^{\boldsymbol{\xi}}(R(t) \geq x)$ is the partition function for a directed polymer model. The polymer replica method, developed first in the continuum setting (and related to the KPZ equation) [130, 131], expresses the k^{th} moment of the tail probability as the expected value over k independent random walks of a certain interaction energy. In the continuum limit, this interaction energy becomes equal to the coefficient λ_{ext} times the sum of the pair local times (i.e., coming from a Dirac delta interaction potential) of k Brownian motions, and thus recovering the k^{th} moment of the continuum directed polymer, i.e., the multiplicative stochastic heat equation. The coefficient λ_{ext} can already be determined from the $k = 2$ case and involves the two-point motion, i.e. the law of R^1 and R^2 under $\mathbf{P}$, via the expected change in its difference $|R^1(t) - R^2(t)|$ in a unit of time when initialized under its invariant measure. This is derived in [127] (see also [123]) using a discrete *Tanaka formula* to relate the discrete and continuum interaction potential. Under (4.11), the invariant measure for the two-point motion becomes constant away from the origin and λ_{ext} simplifies to yield (4.9).

As in [107, 122], the tail probability $\mathbb{P}^{\boldsymbol{\xi}}(R(t) \geq x)$ can be inverted to approximately recover Env_L^N and Env_t^N. By the KPZ convergence, this readily implies that

$$\begin{aligned}
\mathbf{Var}\left(\text{Env}_L^N\right) &\approx \frac{L^4}{(4D)^2 \ln(N)^4} \text{Var}\left(h\left(\frac{32\lambda_{\text{ext}}^2 \ln(N)^3}{L^2}, 0\right)\right), \\
\mathbf{Var}\left(\text{Env}_t^N\right) &\approx \frac{Dt}{\ln(N)} \text{Var}\left(h\left(\frac{8\lambda_{\text{ext}}^2 \ln(N)^2}{Dt}, 0\right)\right),
\end{aligned}$$

where $h(t, x)$ is the narrow-wedge solution to the KPZ equation. The power-laws and their regime of applicability come from the short-time Edwards-Wilkinson asymptotics of the KPZ equation, see e.g. [73, 71].

4.7.2 Numerical Methods..

We describe how we numerically measure the mean and variance of Env_L^N, Sam_L^N and Min_L^N. We begin by numerically computing the probability mass function of the first passage time for a single particle (we drop the superscript and just call it $R(t)$), defined as $\tau_L = \min(t : R(t) \geq L)$. To do so, we consider $R_L(t) = R(\min(t, \tau_L))$, the random walk stopped (or absorbed) when $R(t) \geq L$. We denote the probability mass function of $R_L(t)$ as $p_L^{\boldsymbol{\xi}}(x,t) = \mathbb{P}^{\boldsymbol{\xi}}(R_L(t) = x)$. Given an environment $\boldsymbol{\xi}$, $p_L^{\boldsymbol{\xi}}(x,t)$ uniquely solves

$$p_L^{\boldsymbol{\xi}}(x,t+1) = \sum_{i<L} p_L^{\boldsymbol{\xi}}(i,t)\xi_{t,i}(x-i) \tag{4.12}$$

for $x \in (-\infty, L) \cap \mathbb{Z}$ and $t \geq 0$, subject to the absorbing boundary condition

$$p_L^{\boldsymbol{\xi}}(L,t+1) = p_L^{\boldsymbol{\xi}}(L,t) + \sum_{i<L} p_L^{\boldsymbol{\xi}}(i,t) \sum_{j \geq L} \xi_{t,i}(j-i) \tag{4.13}$$

and initial condition $p_L^{\boldsymbol{\xi}}(x,t) = \mathbb{1}_{x=0}$. The probability of τ_L occurring before time t is given by the probability of $R_L(t)$ being absorbed before time t, which is to say

$$\mathbb{P}^{\boldsymbol{\xi}}(\tau_L \leq t) = p_L^{\boldsymbol{\xi}}(L,t). \tag{4.14}$$

For a given environment distribution ν, we numerically sample ν to generate an environment, $\boldsymbol{\xi}$, and then we use this environment to compute $\mathbb{P}^{\boldsymbol{\xi}}(\tau_L \leq t)$ via (4.12) and (4.13). We measure Env_L^N in this environment by finding the minimum time t such that $\mathbb{P}^{\boldsymbol{\xi}}(\tau_L \leq t) \geq 1/N$. We then numerically compute the distributions of Min_L^N and Sam_L^N in the given environment. For Min_L^N we use (4.2) and for Sam_L^N we combine (4.2) and our definition $\mathrm{Sam}_L^N := \mathrm{Min}_L^N - \mathrm{Env}_L^N$ and thus compute the distribution of Sam_L^N as

$$\mathbb{P}^{\boldsymbol{\xi}}(\mathrm{Sam}_L^N \leq t) = 1 - \left(1 - \mathbb{P}^{\boldsymbol{\xi}}(\tau_L \leq t + \mathrm{Env}_L^N)\right)^N. \tag{4.15}$$

Since N is quite large, we use arbitrary precision floating point arithmetic to compute the N^{th} power in (4.2) and (4.15). Now, given these computed distribution functions we compute $\mathbb{E}^{\boldsymbol{\xi}}[\mathrm{Min}_L^N]$ and $\mathrm{Var}^{\boldsymbol{\xi}}(\mathrm{Min}_L^N)$, $\mathbb{E}^{\boldsymbol{\xi}}[\mathrm{Sam}_L^N]$ and $\mathrm{Var}^{\boldsymbol{\xi}}(\mathrm{Sam}_L^N)$. Finally, we repeat this procedure for many different samples of $\boldsymbol{\xi}$. We compute $\mathbf{E}\left[\mathrm{Env}_L^N\right]$ and $\mathbf{Var}\left(\mathrm{Env}_L^N\right)$ by taking the mean and variance of Env_L^N over these samples. For Min_L^N and Sam_L^N we utilize the law of total expectation, i.e.,

$\mathbf{E}\left[\mathrm{Min}_L^N\right] = \mathbb{E}_\nu\left[\mathbb{E}^{\boldsymbol{\xi}}[\mathrm{Min}_L^N]\right]$ (likewise for Sam_L^N) and the total law of variance $\mathbf{Var}\left(\mathrm{Min}_L^N\right) = \mathrm{Var}_\nu\left(\mathbb{E}^{\boldsymbol{\xi}}\left[\mathrm{Min}_L^N\right]\right) + \mathbb{E}_\nu\left[\mathrm{Var}^{\boldsymbol{\xi}}\left(\mathrm{Min}_L^N\right)\right]$.

We use a nearly identical procedure to numerically compute the mean and variance of the corresponding extreme location quantities Env_t^N, Sam_t^N and Max_t^N. Given an environment $\boldsymbol{\xi}$ we start by numerically computing $p^{\boldsymbol{\xi}}(x,t)$ using the recurrence relation given in (4.1). We then calculate Env_t^N by finding the maximum position x such that $\mathbb{P}^{\boldsymbol{\xi}}(R(t) \geq x) \geq 1/N$. We compute the distribution of Max_t^N using (4.3), and the distribution of Sam_t^N by combining (4.3) and our definition $\mathrm{Sam}_t^N := \mathrm{Max}_t^N - \mathrm{Env}_t^N$ to find

$$\mathbb{P}^{\boldsymbol{\xi}}(\mathrm{Sam}_t^N \leq x) = (1 - \mathbb{P}^{\boldsymbol{\xi}}(R(t) \leq x + \mathrm{Env}_t^N))^N. \tag{4.16}$$

From these we compute $\mathbb{E}^{\boldsymbol{\xi}}[\mathrm{Max}_t^N]$, $\mathrm{Var}^{\boldsymbol{\xi}}(\mathrm{Max}_t^N)$, $\mathbb{E}^{\boldsymbol{\xi}}[\mathrm{Sam}_t^N]$ and $\mathrm{Var}^{\boldsymbol{\xi}}(\mathrm{Sam}_t^N)$. Finally, by repeating for several samples of $\boldsymbol{\xi}$, as above, we compute $\mathbf{E}\left[\mathrm{Env}_t^N\right]$ and $\mathbf{Var}\left(\mathrm{Env}_t^N\right)$, and then $\mathbf{E}[\mathrm{Max}_t^N]$, $\mathbf{E}[\mathrm{Sam}_t^N]$, $\mathbf{Var}\left(\mathrm{Max}_t^N\right)$ and $\mathbf{Var}\left(\mathrm{Sam}_t^N\right)$.

One could measure Min_L^N and Max_t^N using agent based simulations in contrast to generating their probability distributions as we do here. By generating the probability distributions, we are also able to measure the environmental and sampling fluctuations.

The extreme diffusion coefficient, D_{ext}, can be independently measured from both the extreme first passage and extreme location statistics. Using (4.9) we find $D_{\text{ext}} = \frac{2\lambda_{\text{ext}} D}{1+2\lambda_{\text{ext}}}$ (D is computed using (4.4) though it could also be recovered numerically). For the extreme first passage time, λ_{ext} is computed as $\frac{8D^2 \ln(N)^{5/2}}{\sqrt{2\pi L^3}}\left(\mathbf{Var}\left(\mathrm{Min}_L^N\right) - \mathbf{Var}\left(\mathrm{Sam}_L^N\right)\right)$, whereas for the extreme location, λ_{ext} is computed as $\frac{1}{\sqrt{2\pi D t}}\left(\mathbf{Var}\left(\mathrm{Max}_t^N\right) - \mathbf{Var}\left(\mathrm{Sam}_t^N\right)\right)$.

We simulate a Dirichlet distribution with $\vec{\alpha} = (12, 1, 12)$ which is peaked at -1 and 1 with particles having a small probability of staying at the same location.

We also simulate a Dirichlet distribution with $\vec{\alpha} = (2, 1, 1/4, 4, 1/2)$ to study a distribution that is not symmetric in the average environment. We consider the flat Dirichlet distribution on the interval $[-k, k]$ for $k = 1, 2, 5$. Recall that the flat Dirichlet distribution is a special case of the Dirichlet distribution with all $\alpha_i = 1$. Lastly, we consider the random delta distribution on the interval $[-k, k]$ for $k = 1, 2, 5$.

4.8 Supplementary Material

4.8.1 Examples of Distributions ν. The *Dirichlet* distribution for ν is specified by a choice of $k \in \mathbb{Z}_{\geq 1}$ and $\vec{\alpha} = (\alpha_{-k}, \ldots, \alpha_k) \in \mathbb{R}_{>0}^{2k+1}$. It assigns probability density proportional to $\prod_{j=-k}^{k} \xi(j)^{\alpha_j}$ to each vector $\xi = (\xi(-k), \ldots, \xi(k)) \in \mathbb{R}_{\geq 0}^{k}$ satisfying $\sum_{j=-k}^{k} \xi(j) = 1$. Then, we set $\xi(i) = 0$ for $i \notin [-k, k]$ so that ξ is defined on $\mathbb{Z}$. Note that a sample ξ under ν defines a probability distribution on $\mathbb{Z}$ due to the imposed normalization and non-negativity. When $\alpha_j \equiv 1$ for all $-k \leq j \leq k$, we call the resulting Dirichlet distribution *uniform*(k) since $(\xi(-k), \ldots, \xi(k))$ is uniformly distributed over vectors in $\mathbb{R}_{\geq 0}^{k}$ that sum up to 1.

The *normalized i.i.d.* distribution for ν is specified by a choice of $k \in \mathbb{Z}_{\geq 1}$ and a choice of probability distribution on $\mathbb{R}_{\geq 0}$. Let $X_{-k}, \ldots, X_k$ be chosen independently according to the specified probability distribution, and then define $\xi(i) = X_i(\sum_{j=-k}^{k} X_j)^{-1}$ for $i \in [-k, k]$ and $\xi(i) = 0$ otherwise. Such ξ are normalized to sum to 1 and are non-negative, and hence define a probability distribution on $\mathbb{Z}$. When the X_i are Gamma distributed with parameter α, the resulting measure on ξ matches the Dirichlet distribution with $\alpha_i \equiv \alpha$.

The *random delta* distribution for ν is specified by $k \in \mathbb{Z}_{\geq 1}$. Two numbers X_1, X_2 are drawn uniformly without replacement from $\{-k, \dots, k\}$. We set $\xi(X_1) = \xi(X_2) = 1/2$ and $\xi(i) = 0$ for all $i \neq X_1, X_2$.

4.8.2 Convergence to the Stochastic Heat Equation.

We begin by summarizing the results in the forthcoming work [127]. These results also follow from [123]. We show that for $N \in \mathbb{Z}_{>0}$, $T \in N^{-1}\mathbb{Z}_{\geq 0}$ and $X \in (2DN)^{-1/2}(\mathbb{Z} - c_N T)$, the scaled moderate deviations of the tail probability for a single random walker converges as $N \to \infty$:

$$\frac{N^{1/4} C_{N,T,X}}{\sqrt{2D}} \mathbb{P}^{\boldsymbol{\xi}}(R^1(NT) \geq c_N T + \sqrt{2DN} X) \Rightarrow \tilde{Z}(T, X) \tag{4.17}$$

with scaling parameters

$$C_{N,T,X} = \frac{\exp\left\{ \dfrac{c_N}{2DN^{1/4}} T + \dfrac{1}{\sqrt{2D}} N^{1/4} X \right\}}{\left(\displaystyle\sum_{i \in \mathbb{Z}} \mathbb{E}_\nu \left[\xi\left(i\right) \right] \exp\left\{ \dfrac{i}{2DN^{1/4}} \right\} \right)^{NT}}, \qquad c_N = N^{3/4} + \frac{\sum_{i \in Z} \mathbb{E}_\nu \left[\xi\left(i\right) \right] i^3}{2(2D)^2} N^{1/2}. \tag{4.18}$$

The convergence is shown in [127] at the level of the first two moments (stronger process-level convergence is shown in [123]), and the limiting process $\tilde{Z}(T, X)$ is the solution to the multiplicative Stochastic Heat Equation (mSHE) with $\tilde{Z}(0, X) = \delta(X)$ initial data:

$$\partial_T \tilde{Z} = \frac{1}{2} \partial_X^2 \tilde{Z} + \sqrt{\frac{2\lambda_{\text{ext}}}{(2D)^{3/2}}} \tilde{Z} \eta. \tag{4.19}$$

Here $\eta(T, X)$ is a space-time Gaussian white noise (i.e. $\mathbb{E}[\eta(T, X)] = 0$ and $\mathbb{E}[\eta(T, X)\eta(T', X')] = \delta(X - X')\delta(T - T')$ where δ is the Dirac delta function). The noise strength is controlled by the Einstein diffusion coefficient D defined in (4.4) and λ_{ext}.

At the full level of generality of RWRE models we introduced in the *RWRE models* section, [127] (see also [123]) provides a somewhat involved formula for λ_{ext}:

$$\lambda_{\text{ext}} := \frac{\mathrm{Var}_{\nu}\left(\mathbb{E}^{\xi}[Y]\right)}{\sum_{l=0}^{\infty} \tilde{\mu}\left(l\right) \mathbf{E}\left[\Delta\left(t+1\right) - \Delta\left(t\right) \mid \Delta\left(t\right) = l\right]}. \tag{4.20}$$

The numerator here is defined in terms of Y, a random jump distributed according to ξ. As in (4.10), this numerator is equal to $2D_{\text{ext}}$. The denominator requires more explanation. Consider two random walks R^1 and R^2 distributed according to the measure $\mathbf{P}$ (i.e., after integrating over the law ν of the environment). These walks are not independent as they are coupled to the same (integrated out) environment—we call these the *two-point motions* as they have the law of two tracer particles when the environment is hidden. Define the gap between them to be

$$\Delta(t) := |R^1(t) - R^2(t)|.$$

There exists a unique (infinite mass) invariant measure for $V(t) := R^1(t) - R^2(t)$ and let $\mu(l)$ be the mass assigned to $l \in \mathbb{Z}$ with the normalization that $\mu(0) = 1$ (see e.g., [132] for background on invariant measures for Markov chains). The corresponding invariant measure for $\Delta(t)$ is therefore

$$\tilde{\mu}\left(l\right) := \begin{cases} 1 & \text{if } l = 0 \\ 2\mu(l) & \text{if } l > 0 \end{cases}. \tag{4.21}$$

This invariant measure can be understood physically as follows. Start two particles near each other and let them diffuse in their common environment. After a relatively long time, measure the distance between them. Repeat this for many different environments, thus building up a histogram of the distances between these two-point motions. The typical distance will be large, but if we cutoff to consider relatively short distances, and normalize the histogram to put weight 1 at distance

0, then it will converge to $\tilde{\mu}(l)$. A slightly different way that this same measure should arise is from surveying the inter-particle distances over all particles in a many-particle diffusion. Normalizing the histogram of these distances to be 1 at distance 0, will yield a histogram that converges to $\tilde{\mu}(l)$ at distance l. This should hold for a single environment since the inter-particle distances (on the short-scale that we are considering) will generally feel different parts of the environment, and hence experience some averaging.

The denominator in (4.20) is independent of t and it has the interpretation as the expected change in the two-point motion gap when started under its invariant measure. For large enough l (since we have assumed a finite range for the jump distribution) the expected change of the gap will be zero and hence the sum will be a finite one.

We will show that λ_{ext} simplifies considerably for a wide class of distributions ν in Section 4.8.6, and (before that) in the next section we will explain (in the spirit of [107, 122]) how we go from this mSHE convergence result to our extreme diffusion theoretical predictions.

However, let us first briefly summarize the approach used in [127] to derive this mSHE convergence result. First of all, (4.17) is only demonstrated therein at the level of convergence of first and second moments. Convergence of higher moments follows similarly as noted below. Since the moments of the mSHE do not characterize its distribution, more work is needed, as in [123], to show convergence in distribution, or convergence of the space-time process.

The second moment of the LHS in (4.17) can be expressed via a discrete Feynman-Kac formula in terms of the expectation of the exponential of the self-intersection time for the two-point motion (R^1, R^2) under a tilting of the measure $\mathbf{P}$

(high integer moments involve higher order self-intersection times). For the mSHE, all integer moments can be expressed in terms of the expectation of the exponential of the pair local times at zero for independent Brownian motions (this is the replica method, see [130, 131]). The k-point motion converges diffusively to k independent Brownian motions, yet the discrete self-intersection time does not converge to the local time at zero for the Brownian motions.

This failure of self-intersection time to local time convergence may seem surprising, but a very simple example should convince the reader that such convergence is more subtle. For instance, imagine two independent SSRWs, one started at 0 and one started at 1. They converge jointly to two Brownian motions, yet their intersection time is always 0 (they are on different sublattices) and hence does not converge to the local time at 0 for the Brownian motions.

A discrete version of the Tanaka formula—which, for a Brownian motion B, shows that $|B(t)| = \int_0^t \mathrm{sgn}(B(s))dB(s) + L(t)$ where $\mathrm{sgn}(x)$ is the derivative of the absolute value function $|x|$ (set to be 0 at 0) and where $L(t)$ is the local time at zero up to time t—is used in [127] to identify the discrete quantity that converges to the Brownian local time $L(t)$. That discrete local time involves reweighting the expected change in distance between the two-point motion according to its invariant measure. This allows us to identify the limit of the self-intersection time and leads to the denominator in (4.20).

4.8.3 Approximating the Tail Probability.

After taking logarithms in (4.17), we see that as $N \to \infty$

$$
\begin{aligned}
\ln(\mathbb{P}^{\boldsymbol{\xi}}(R^1(NT) \geq & c_N T + \sqrt{2DN}X)) \\
& \approx -\frac{c_N T}{2DN^{1/4}} - \frac{N^{1/4}X}{\sqrt{2D}} + NT \ln\left(\sum_{i\in\mathbb{Z}} \mathbb{E}_\nu\left[\xi\left(i\right)\right] \exp\left\{\frac{i}{2DN^{1/4}}\right\}\right) \\
& \quad - \ln\left(\frac{N^{1/4}}{\sqrt{2D}}\right) + \tilde{h}(T,X)
\end{aligned}
\tag{4.22}
$$

where $\tilde{h}(T,X) = \ln(\tilde{Z}(T,X))$ solves the KPZ equation with narrow wedge initial data and with λ_{ext}-dependent noise strength (we now also include tildes on the X and T variables to simplify the below change of variables),

$$\partial_{\tilde{T}}\tilde{h} = \frac{1}{2}\partial_{\tilde{X}}^2\tilde{h} + \frac{1}{2}(\partial_{\tilde{X}}\tilde{h})^2 + \sqrt{\frac{2\lambda_{\text{ext}}}{(2D)^{3/2}}}\eta.$$

Defining $h(T,X) = \tilde{h}(\tilde{T},\tilde{X})$ with $T = \frac{4\lambda_{\text{ext}}^2}{(2D)^3}\tilde{T}$ and $X = \frac{2\lambda_{\text{ext}}}{(2D)^{3/2}}\tilde{X}$, h solves the standard coefficient KPZ equation

$$\partial_T h = \frac{1}{2}\partial_X^2 h + \frac{1}{2}(\partial_X h)^2 + \eta.$$

We also have that as $N \to \infty$,

$$\left(\sum_{i\in\mathbb{Z}} \mathbb{E}_\nu\left[\xi\left(i\right)\right] \exp\left\{\frac{i}{2DN^{1/4}}\right\}\right) \approx \frac{N^{-1/2}}{4D} + \frac{\sum_{i\in\mathbb{Z}}\mathbb{E}_\nu\left[\xi\left(i\right)\right] i^3}{6(2D)^3}N^{-3/4} + \mathcal{O}\left(N^{-1}\right).$$

Substituting this into (4.22) and using our transformation to the KPZ equation, we find

$$
\begin{aligned}
\ln\left(\mathbb{P}^{\boldsymbol{\xi}}\left(R^1(NT) \geq N^{3/4}T + \frac{m_3 N^{1/2}T}{2(2D)^2} + \sqrt{2DN}X\right)\right) & \\
\approx -\frac{N^{1/2}T}{4D} - \frac{N^{1/4}X}{\sqrt{2D}} - \frac{N^{1/4}Tm_3}{3(2D)^3} + \ln\left(\frac{N^{1/4}}{\sqrt{2D}}\right) & \\
+ h\left(\frac{4\lambda_{\text{ext}}^2}{(2D)^3}T, \frac{2\lambda_{\text{ext}}}{(2D)^{3/2}}X\right) + \mathcal{O}(T) &
\end{aligned}
$$

where $m_3 = \sum_{i\in\mathbb{Z}} \mathbb{E}_\nu [\xi(i)] i^3$. We now introduce the time $t := NT$, velocity $v := T^{1/4}$, and rescaled position $y = \frac{X}{v^2}$. Making these substitutions, we find

$$\begin{aligned}\ln\left(\mathbb{P}^{\boldsymbol{\xi}}\left(R^1(t) \geq vt^{3/4} + \frac{m_3}{2(2D)^2}v^2t^{1/2} + \sqrt{2Dt}y\right)\right)& \\ \approx -\frac{v^2}{4D}t^{1/2} - \frac{vy}{\sqrt{2D}}t^{1/4} - \frac{v^3 m_3}{3(2D)^3}t^{1/4} + \ln\left(\frac{t^{1/4}}{\sqrt{2D}v}\right)& \\ +h\left(\frac{4\lambda_{\text{ext}}^2}{(2D)^3}v^4, \frac{2\lambda_{\text{ext}}}{(2D)^{3/2}}yv^2\right) + \mathcal{O}(v^4).&\end{aligned} \tag{4.23}$$

4.8.4 Extreme First Passage Time Theoretical Predictions.

Here we derive asymptotic predictions for the means and variances of Env_L^N, Sam_L^N and Min_L^N. Much of this analysis follows from [122], where they derived predictions for the nearest neighbor case with a uniform distribution.

We start by substituting $y = 0$ and $L = vt^{3/4}$ into (4.23) such that

$$\begin{aligned}\ln\left(\mathbb{P}^{\boldsymbol{\xi}}\left(R^1(t) \geq L + \frac{m_3L^2}{2(2D)^2t}\right)\right) \approx -\frac{L^2}{4Dt} - \frac{m_3L^3}{3(2D)^3t^2} + \ln\left(\frac{t}{\sqrt{2D}L}\right)& \\ + h\left(\frac{4\lambda_{\text{ext}}^2L^4}{(2D)^3t^3}, 0\right) + \mathcal{O}\left(\frac{L^4}{t^3}\right).&\end{aligned}$$

We can now drop all subdominant terms as they will not contribute to the asymptotic predictions (though they could offer some higher-order corrections that we do not probe here). This yields a rougher approximation where we do not track the order of the error

$$\ln\left(\mathbb{P}^{\boldsymbol{\xi}}\left(R^1(t) \geq L\right)\right) \approx -\frac{L^2}{4Dt} + h\left(\frac{4\lambda_{\text{ext}}^2L^4}{(2D)^3t^3}, 0\right). \tag{4.24}$$

We now utilize the non-backtracking approximation $\mathbb{P}^{\boldsymbol{\xi}}(R^1(t) \geq L) \approx \mathbb{P}^{\boldsymbol{\xi}}(\tau_L \leq t)$ (as discussed in [122]) as L gets large to yield

$$\ln\left(\mathbb{P}^{\boldsymbol{\xi}}\left(\tau_L \leq t\right)\right) \approx -\frac{L^2}{4Dt} + h\left(\frac{4\lambda_{\text{ext}}^2L^4}{(2D)^3t^3}, 0\right). \tag{4.25}$$

We now substitute Env_L^N into this equation, recalling that Env_L^N is approximately the time t such that $\mathbb{P}^{\boldsymbol{\xi}}(\tau_L \leq t) = 1/N$ (in fact, the minimum time t satisfying

$\mathbb{P}^{\boldsymbol{\xi}}(\tau_L \leq t) \geq 1/N$ though this difference is negligible):

$$-\ln(N) \approx -\frac{L^2}{4D\mathrm{Env}_L^N} + h\left(\frac{4\lambda_{\mathrm{ext}}^2 L^4}{(2D)^3\left(\mathrm{Env}_L^N\right)^3}, 0\right). \tag{4.26}$$

We can solve this equation perturbatively for Env_L^N. The term $-\frac{L^2}{4D\mathrm{Env}_L^N}$ in (4.26) is dominant for large L, which yields the first-order estimate

$$\mathrm{Env}_L^N \approx T_L^N := \frac{L^2}{4D\ln(N)}. \tag{4.27}$$

We now consider a small perturbation about T_L^N such that $\mathrm{Env}_L^N = T_L^N + \delta$ where $\delta \ll T_L^N$ contains the randomness of Env_L^N. Substituting this into (4.26), we find

$$-\ln(N) \approx -\frac{L^2}{4D(T_L^N + \delta)} + h\left(\frac{4\lambda_{\mathrm{ext}}^2 L^4}{(2D)^3\left(T_L^N + \delta\right)^3}, 0\right). \tag{4.28}$$

Since $\delta \ll T_L^N$, we approximate $-\frac{L^2}{4D(T_L^N+\delta)} \approx -\frac{L^2}{4DT_L^N} + \frac{L^2}{4D(T_L^N)^2}\delta$ and $\frac{4\lambda_{\mathrm{ext}}^2 L^4}{(2D)^3\left(T_L^N+\delta\right)^3} \approx \frac{4\lambda_{\mathrm{ext}}^2 L^4}{(2D)^3\left(T_L^N\right)^3}$. As such we can solve for δ, yielding

$$\delta \approx -\frac{L^2}{4D\ln(N)^2} \cdot h\left(\frac{4\lambda_{\mathrm{ext}}^2 L^4}{(2D)^3 (T_L^N)^3}, 0\right) = -\frac{L^2}{4D\ln(N)^2} \cdot h\left(\frac{32\lambda_{\mathrm{ext}}^2 (\ln(N))^3}{L^2}, 0\right).$$

Therefore, the mean and variance of Env_L^N is given by

$$\mathbf{E}\left[\mathrm{Env}_L^N\right] \approx \frac{L^2}{4D\ln(N)} \tag{4.29}$$

$$\mathbf{Var}\left(\mathrm{Env}_L^N\right) \approx \frac{L^4}{(4D)^2\ln(N)^4}\mathbf{Var}\left(h\left(\frac{32\lambda_{\mathrm{ext}}^2(\ln(N))^3}{L^2}, 0\right)\right). \tag{4.30}$$

We now consider the limit where $L \gg (\ln(N))^{3/2}$. In this limit, we simplify (4.30) using the small-time KPZ Gaussian approximation

$$h(s, 0) \approx -\frac{s}{24} - \ln\left(\sqrt{2\pi s}\right) + \left(\frac{\pi s}{4}\right)^{1/4} G_s \tag{4.31}$$

where G_s converges as $s \to 0$ to a standard Gaussian, see for instance [73, 71]. Thus, for $L \gg \lambda_{\mathrm{ext}}(\ln(N))^{3/2}$ we find

$$\mathbf{Var}\left(\mathrm{Env}_L^N\right) \approx \lambda_{\mathrm{ext}} \frac{\sqrt{2\pi}L^3}{8D^2\ln(N)^{5/2}}. \tag{4.32}$$

We now derive the distribution, and subsequently the mean and variance, for the randomness due to sampling random walks, Sam_L^N. We begin by using the approximation, $(1+x)^N \approx e^{xN}$ for $x \ll 1$ and $N \to \infty$. Therefore, for $N \to \infty$ and small $\mathbb{P}^{\boldsymbol{\xi}}(\tau_L \leq t)$, we approximate (4.15) as

$$\ln\left(\mathbb{P}^{\boldsymbol{\xi}}(\mathrm{Sam}_L^N > t)\right) \approx -N\mathbb{P}^{\boldsymbol{\xi}}(\tau_L \leq t + \mathrm{Env}_L^N). \tag{4.33}$$

Substituting (4.25) yields

$$\ln\left(\mathbb{P}^{\boldsymbol{\xi}}(\mathrm{Sam}_L^N > t)\right) \approx -N\mathrm{exp}\left\{-\frac{L^2}{4D(t+\mathrm{Env}_L^N)}\right\} \tag{4.34}$$

where we have dropped all but the leading order term. We now assume $\mathrm{Env}_L^N \gg t$, which is justified because, as we will show, $\mathbf{E}\left[\mathrm{Env}_L^N\right] \gg \mathbf{E}\left[\mathrm{Sam}_L^N\right]$. When $\mathrm{Env}_L^N \gg t$, we approximate $(t+\mathrm{Env}_L^N)^{-1} \approx \frac{1}{\mathrm{Env}_L^N}\left(1 - \frac{t}{\mathrm{Env}_L^N}\right)$ such that

$$\ln\left(\mathbb{P}^{\boldsymbol{\xi}}(\mathrm{Sam}_L^N > t)\right) \approx -N\mathrm{exp}\left\{-\frac{L^2}{4D\mathrm{Env}_L^N} - \frac{tL^2}{4D\left(\mathrm{Env}_L^N\right)^2}\right\}. \tag{4.35}$$

Now replacing Env_L^N with its leading order approximation, T_L^N, from (4.27), we find

$$\ln\left(\mathbb{P}^{\boldsymbol{\xi}}(\mathrm{Sam}_L^N \leq t)\right) \approx -\mathrm{exp}\left\{-\frac{4D\ln(N)^2 t}{L^2}\right\}.$$

By replacing Env_L^N with T_L^N we have assumed that Sam_L^N and Env_L^N are independent since Sam_L^N no longer depends on the randomness of Env_L^N. Though likely theoretically justifiable, this approximation is a fortiori justified by our numerics as shown in Figure 17. From this we find that $-\mathrm{Sam}_L^N$ is Gumbel distributed with mean and variance

$$\mathbf{E}[\mathrm{Sam}_L^N] \approx -\frac{\gamma L^2}{4D\ln(N)^2} \tag{4.36}$$

$$\mathbf{Var}(\mathrm{Sam}_L^N) \approx \frac{\pi^2 L^4}{96D^2\ln(N)^4} \tag{4.37}$$

where $\gamma \approx 0.577$ is the Euler-Mascheroni constant. Notice that as L and N tend to infinity with $L \gg \ln(N)^{3/2}$, $\mathbf{E}\left[\mathrm{Sam}_L^N\right] \ll \mathbf{E}\left[\mathrm{Env}_L^N\right]$ which justifies the approximation used in (4.35).

We solve for the mean and variance of Min_L^N by rearranging our definition of Sam_L^N such that $\mathrm{Min}_L^N = \mathrm{Sam}_L^N + \mathrm{Env}_L^N$. Since $\mathbf{E}\left[\mathrm{Sam}_L^N\right] \ll \mathbf{E}\left[\mathrm{Env}_L^N\right]$,

$$\mathbf{E}\left[\mathrm{Min}_L^N\right] \approx \frac{L^2}{4D\ln(N)}. \tag{4.38}$$

Since Env_L^N and Sam_L^N are independent, $\mathbf{Var}\left(\mathrm{Min}_L^N\right) = \mathbf{Var}\left(\mathrm{Sam}_L^N\right) + \mathbf{Var}\left(\mathrm{Env}_L^N\right)$ such that

$$\mathbf{Var}\left(\mathrm{Min}_L^N\right) \approx \frac{\pi^2 L^4}{96D^2\ln(N)^4} + \lambda_{\mathrm{ext}}\frac{\sqrt{2\pi}L^3}{8D^2\ln(N)^{5/2}} \tag{4.39}$$

in the limit $L \gg \ln(N)^{3/2}$.

4.8.5 Extreme Location Theoretical Predictions.

Here we derive asymptotic predictions for the means and variances of Env_t^N, Sam_t^N and Max_t^N. As above, much of this analysis follows from [107], where they derived predictions for the nearest neighbor case with a uniform distribution. The argument proceeds similarly to the first passage time analysis. Starting at (4.24), we substitute Env_t^N for the position L such that $\mathbb{P}^{\boldsymbol{\xi}}(R^1(t) \geq L) = 1/N$, thus yielding

$$-\ln(N) \approx -\frac{\left(\mathrm{Env}_t^N\right)^2}{4Dt} + h\left(\frac{4\lambda_{\mathrm{ext}}^2\left(\mathrm{Env}_t^N\right)^4}{(2D)^3t^3}, 0\right). \tag{4.40}$$

The first term on the right-hand side dominates and yields the first-order estimate

$$\mathrm{Env}_t^N \approx X_t^N := \sqrt{4Dt\ln(N)}. \tag{4.41}$$

We consider a small perturbation, δ, about X_t^N such that $\mathrm{Env}_t^N = X_t^N + \delta$ where $\delta \ll X_t^N$. Substituting this into (4.40) and only taking the highest order terms yields

$$\delta \approx \sqrt{\frac{Dt}{\ln(N)}}h\left(\frac{8\lambda_{\mathrm{ext}}^2\ln(N)^2}{Dt}, 0\right). \tag{4.42}$$

Therefore, the mean and variance of Env_t^N satisfy

$$\mathbf{E}\left[\mathrm{Env}_t^N\right] \approx \sqrt{4Dt\ln(N)} \tag{4.43}$$

$$\mathbf{Var}\left(\mathrm{Env}_t^N\right) \approx \frac{Dt}{\ln(N)}\mathbf{Var}\left(h\left(\frac{8\lambda_{\mathrm{ext}}^2\ln(N)^2}{Dt}, 0\right)\right). \tag{4.44}$$

When $t \gg \frac{\lambda_{\mathrm{ext}}^2}{D}\ln(N)^2$, we use the small argument expansion of the KPZ equation in (4.31) to approximate

$$\mathbf{Var}\left(\mathrm{Env}_t^N\right) \approx \lambda_{\mathrm{ext}}\sqrt{2\pi Dt}. \tag{4.45}$$

We now derive the distribution for the randomness due to sampling random walks, Sam_t^N. For $N \to \infty$ and small $\mathbb{P}^{\boldsymbol{\xi}}(R(t) \leq x + \mathrm{Env}_t^N)$, we approximate (4.16) as

$$\ln(\mathbb{P}^{\boldsymbol{\xi}}(\mathrm{Sam}_t^N \leq x)) \approx -N\mathbb{P}^{\boldsymbol{\xi}}(R(t) \leq x + \mathrm{Env}_t^N). \tag{4.46}$$

Substituting (4.24) yields

$$\ln(\mathbb{P}^{\boldsymbol{\xi}}(\mathrm{Sam}_t^N \leq x)) \approx -N\exp\left\{-\frac{(x+\mathrm{Env}_t^N)^2}{4Dt}\right\} \tag{4.47}$$

where we have only kept the leading order term of $\mathbb{P}^{\boldsymbol{\xi}}(R(t) \leq x)$. We assume $\mathrm{Env}_t^N \gg x$ which is justified because, as we will show, $\mathbf{E}\left[\mathrm{Env}_t^N\right] \gg \mathbf{E}\left[\mathrm{Sam}_t^N\right]$. We use this to approximate $(x+\mathrm{Env}_t^N)^2 \approx (\mathrm{Env}_t^N)^2 + 2\mathrm{Env}_t^N x$ such that

$$\ln(\mathbb{P}^{\boldsymbol{\xi}}(\mathrm{Sam}_t^N \leq x)) \approx -N\exp\left\{-\frac{(\mathrm{Env}_t^N)^2}{4Dt} - \frac{\mathrm{Env}_t^N x}{2Dt}\right\}. \tag{4.48}$$

Replacing Env_t^N with its first-order approximation, X_t^N, in (4.41), we find

$$\ln(\mathbb{P}^{\boldsymbol{\xi}}(\mathrm{Sam}_t^N \leq x)) \approx -\exp\left\{-\sqrt{\frac{\ln(N)}{Dt}}x\right\}. \tag{4.49}$$

Therefore, Sam_t^N is Gumbel distributed with mean and variance

$$\mathbf{E}[\mathrm{Sam}_L^N] \approx \gamma\sqrt{\frac{Dt}{\ln(N)}} \tag{4.50}$$

$$\mathbf{Var}(\mathrm{Sam}_L^N) \approx \frac{\pi^2 Dt}{6\ln(N)}. \tag{4.51}$$

Notice that as $t \to \infty$, $\mathbf{E}\left[\mathrm{Env}_t^N\right] \gg \mathbf{E}\left[\mathrm{Sam}_t^N\right]$ which justifies our approximation in (4.48).

We solve for the mean and variance of Max_t^N by rearranging our definition of Sam_t^N such that $\mathrm{Max}_t^N = \mathrm{Sam}_t^N + \mathrm{Env}_t^N$. Since $\mathbf{E}\left[\mathrm{Env}_t^N\right] \gg \mathbf{E}\left[\mathrm{Sam}_t^N\right]$,

$$\mathbf{E}\left[\mathrm{Max}_t^N\right] \approx \sqrt{4Dt\ln(N)}. \tag{4.52}$$

Since Env_t^N and Sam_t^N are assumed to be asymptotically independent, $\mathbf{Var}\left(\mathrm{Max}_t^N\right) = \mathbf{Var}\left(\mathrm{Env}_t^N\right) + \mathbf{Var}\left(\mathrm{Sam}_t^N\right)$ so

$$\mathbf{Var}\left(\mathrm{Max}_t^N\right) \approx \frac{\pi^2 Dt}{6\ln(N)} + \lambda_{\mathrm{ext}}\sqrt{2\pi Dt} \tag{4.53}$$

when $t \gg \lambda_{\mathrm{ext}}^2 \ln(N)^2$.

4.8.6 Calculating the Coefficient for Several Distributions.

We demonstrate that the coefficient λ_{ext} in the mSHE/KPZ equation limit (4.17) simplifies to the expression in (4.9) for a class of distributions ν including those introduced earlier (i.e., the Dirichlet, normalized i.i.d., and random delta distributions), as well as all nearest neighbor distributions.

4.8.6.1 General Model. We study the following class of distributions such that:

$$\text{There exists some } c \in (0,1) \text{ such that for all } i \neq j \qquad \mathbb{E}_\nu\left[\xi(i)\xi(j)\right] = c\mathbb{E}_\nu\left[\xi(i)\right]\mathbb{E}_\nu\left[\xi(j)\right]. \tag{4.54}$$

We will also initially assume that the difference walk $V(t) = R^1(t) - R^2(t)$ (where R^1 and R^2 are distributed according to $\mathbf{P}$) is irreducible (i.e., $V(t)$ can reach any location on $\mathbb{Z}$ when started from 0), although we will later also consider the nearest neighbor model in Section 4.8.6.5, which does not satisfy this condition as the difference walk $V(t)$ in that case is restricted to the even integer sublattice. A sufficient condition for $V(t)$ to be irreducible is that

$$\mathbb{E}_\nu\left[\xi\left(i\right)\right] > 0 \text{ for all } i \in \{-1, 0, 1\}. \tag{4.55}$$

We compute λ_{ext} by simplifying the numerator and denominator of (4.20) in terms of c and then matching this to (4.9). The numerator of (4.20) simplifies to

$$\operatorname{Var}_\nu\left(\mathbb{E}^{\boldsymbol{\xi}}[Y]\right) = \sum_{i\in\mathbb{Z}}(1-c)\mathbb{E}_\nu\left[\xi(i)\right] i^2. \tag{4.56}$$

Simplifying the denominator of (4.20) is much more involved. We do this in three steps. First, we compute the invariant measure, $\tilde{\mu}\left(l\right)$ and show that

$$\tilde{\mu}\left(l\right) = \begin{cases} 1 & \text{if } i = 0 \\ \\ 2c & \text{if } i \neq 0 \end{cases}. \tag{4.57}$$

Then we simplify the expression $\mathbf{E}\left[\Delta\left(t+1\right) - \Delta\left(t\right) \mid \Delta\left(t\right) = l\right]$ and show that (without using the assumption (4.54))

$$\mathbf{E}\left[\Delta\left(t+1\right) - \Delta\left(t\right) \mid \Delta\left(t\right) = l\right] = \begin{cases} \displaystyle\sum_{i,j\in\mathbb{Z}} |i-j|\mathbb{E}_\nu\left[\xi(i)\xi(j)\right] & l = 0 \\ \displaystyle\sum_{|i-j|>l} (|i-j|-l)\mathbb{E}_\nu\left[\xi\left(i\right)\right]\mathbb{E}_\nu\left[\xi\left(j\right)\right] & l > 0 \end{cases}. \tag{4.58}$$

Lastly, we combine these two results to compute the sum over l and show that

$$\sum_{l=0}^{\infty}\mathbf{E}\left[\Delta\left(t+1\right) - \Delta\left(t\right) \mid \Delta\left(t\right) = l\right]\tilde{\mu}\left(l\right) = 2c\sum_{i\in\mathbb{Z}} i^2\mathbb{E}_\nu\left[\xi\left(i\right)\right]. \tag{4.59}$$

The invariant measure: We now compute the invariant measure for the walk $V(t)$. The transition probabilities of V are given by

$$p(i,j) := \mathbf{P}(V(t+1) = j \mid V(t) = i) = \begin{cases} \sum_{k\in\mathbb{Z}}\mathbb{E}_\nu\left[\xi(k)\xi(k-j)\right] & \text{if } i = 0 \\ \sum_{k\in\mathbb{Z}}\mathbb{E}_\nu\left[\xi\left(k\right)\right]\mathbb{E}_\nu\left[\xi\left(k-j+i\right)\right] & \text{if } i \neq 0. \end{cases} \tag{4.60}$$

Notice that if $i, j \neq 0$, then by a change of variables, we have

$$\begin{aligned} p(i,j) &= \sum_{k \in \mathbb{Z}} \mathbb{E}_\nu \left[\xi \left(k - j + i \right) \right] \mathbb{E}_\nu \left[\xi \left(k \right) \right] \\ &= \sum_{\tilde{k} \in \mathbb{Z}} \mathbb{E}_\nu \left[\xi \left(\tilde{k} \right) \right] \mathbb{E}_\nu \left[\xi \left(\tilde{k} - i + j \right) \right] \\ &= p(j,i). \end{aligned} \tag{4.61}$$

It also follows from (4.54) that

$$p(0,j) = cp(j,0). \tag{4.62}$$

We claim that the unique invariant measure of $V(t)$ (up to multiplication by a constant coefficient) is given by $\mu(l) = c$ for all $l \neq 0$ and $\mu(0) = 1$. We check this by showing $\mu(\cdot)$ satisfies the detailed balance equation,

$$\mu(i)p(i,j) = \mu(j)p(j,i) \tag{4.63}$$

for all $i, j \in \mathbb{Z}$. This also shows that the walk $V(t)$ is reversible with respect to $\mu(\cdot)$.

The detailed balance condition is clearly true for the case $i = j = 0$, and for $i, j \neq 0$ it follows from (4.61). We now consider the case when $i = 0$ and $j \neq 0$. Substituting $\mu(j) = c$ and $\mu(0) = 1$ into (4.63), we obtain

$$p(0,j) = cp(j,0),$$

which is true by (4.62). Therefore, our claim that $\mu(l) = c$ for $l \neq 0$ and $\mu(0) = 1$ is justified.

It follows from (4.21) that

$$\tilde{\mu}\left(l\right) = \begin{cases} 1 & \text{if } i = 0 \\ 2c & \text{if } i \neq 0 \end{cases} \tag{4.64}$$

as desired.

Simplification of the expectation value: We now simplify

$\mathbf{E}\left[\Delta\left(t+1\right)-\Delta\left(t\right)\mid\Delta\left(t\right)=l\right]$ to show it is given by (4.58). For $l=0$, the two walkers R^1 and R^2 are both at the same site; therefore, they use the same jump rate such that

$$\mathbf{E}\left[\Delta\left(t+1\right)-\Delta\left(t\right)\mid\Delta\left(t\right)=0\right]=\sum_{i,j\in\mathbb{Z}}|i-j|\mathbb{E}_{\nu}\left[\xi(i)\xi(j)\right],$$

which agrees with (4.58).

For $l>0$, the two walkers R^1 and R^2 are at different sites; therefore, they use independent jump rates such that

$$\mathbf{E}\left[\Delta\left(t+1\right)-\Delta\left(t\right)\mid\Delta\left(t\right)=l\right]=\sum_{i,j\in\mathbb{Z}}(|l+i-j|-l)\mathbb{E}_{\nu}\left[\xi\left(i\right)\right]\mathbb{E}_{\nu}\left[\xi\left(j\right)\right]. \qquad (4.65)$$

We now break this sum up into two parts: when $|i-j|\leq l$ and $|i-j|>l$. For $|i-j|\leq l$, we simplify

$$|l+i-j|-l=\begin{cases} i-j & \text{if } i\geq j \\ j-i & \text{if } i<j, \end{cases}.$$

Therefore,

$$\begin{aligned}\sum_{|i-j|\leq l}(|l+i-j|-l)\mathbb{E}_{\nu}\left[\xi\left(i\right)\right]\mathbb{E}_{\nu}\left[\xi\left(j\right)\right]&=\sum_{i<j}(j-i)\mathbb{E}_{\nu}\left[\xi\left(i\right)\right]\mathbb{E}_{\nu}\left[\xi\left(j\right)\right]\\&\quad+\sum_{i\geq j}(i-j)\mathbb{E}_{\nu}\left[\xi\left(i\right)\right]\mathbb{E}_{\nu}\left[\xi\left(j\right)\right]\\&=0\end{aligned}$$

after swapping the indices of the second sum.

For $|i-j|>l$, we find

$$|l+i-j|-l=\begin{cases} i-j & \text{if } i\geq j \\ j-i-2l & \text{if } i<j \end{cases}.$$

Substituting this into (4.65), we are left with

$$\begin{aligned}\mathbf{E}\left[\Delta(t+1)-\Delta(t)\mid\Delta(t)=l\right] &= \sum_{|i-j|>l}(|l+i-j|-l)\mathbb{E}_\nu\left[\xi(i)\right]\mathbb{E}_\nu\left[\xi(j)\right] \\ &= \sum_{i-j>l}(|i-j|)\mathbb{E}_\nu\left[\xi(i)\right]\mathbb{E}_\nu\left[\xi(j)\right] \\ &\qquad + \sum_{j-i>l}(|i-j|-2l)\mathbb{E}_\nu\left[\xi(i)\right]\mathbb{E}_\nu\left[\xi(j)\right] \\ &= \sum_{|i-j|>l}(|i-j|-l)\mathbb{E}_\nu\left[\xi(i)\right]\mathbb{E}_\nu\left[\xi(j)\right].\end{aligned}$$

Thus, $\mathbf{E}\left[\Delta(t+1)-\Delta(t)\mid\Delta(t)=l\right]$ is given by (4.58).

Computing λ_{ext}: We now compute λ_{ext} using our formula for $\tilde{\mu}(l)$ and $\mathbf{E}\left[\Delta(t+1)-\Delta(t)\mid\Delta(t)=l\right]$. Substituting (4.64) and (4.58), we find

$$\begin{aligned}&\sum_{l=0}^{\infty}\mathbf{E}\left[\Delta(t+1)-\Delta(t)\mid\Delta(t)=l\right]\tilde{\mu}(l) \\ &= c\sum_{i,j\in\mathbb{Z}}|i-j|\mathbb{E}_\nu\left[\xi(i)\right]\mathbb{E}_\nu\left[\xi(j)\right] \\ &\qquad + 2c\sum_{l=1}^{\infty}\sum_{|i-j|>l}(|i-j|-l)\mathbb{E}_\nu\left[\xi(i)\right]\mathbb{E}_\nu\left[\xi(j)\right] \\ &= c\sum_{l=0}^{\infty}\sum_{|i-j|>l}(2-\mathbb{1}_{l=0})(|i-j|-l)\mathbb{E}_\nu\left[\xi(i)\right]\mathbb{E}_\nu\left[\xi(j)\right]\end{aligned} \tag{4.66}$$

after combining the two sums. Now we break up the second sum over i and j such that

$$\begin{aligned}
&\sum_{l=0}^{\infty}\mathbf{E}\left[\Delta\left(t+1\right)-\Delta\left(t\right)\mid\Delta\left(t\right)=l\right]\tilde{\mu}\left(l\right)\\
&\qquad=c\sum_{l=0}^{\infty}\sum_{j\in\mathbb{Z}}\left[\sum_{i=j+l+1}^{\infty}(2-\mathbb{1}_{l=0})(i-j-l)\mathbb{E}_{\nu}\left[\xi\left(i\right)\right]\mathbb{E}_{\nu}\left[\xi\left(j\right)\right]\right.\\
&\qquad\qquad\left.+\sum_{i=-\infty}^{j-l-1}(2-\mathbb{1}_{l=0})(j-i-l)\mathbb{E}_{\nu}\left[\xi\left(i\right)\right]\mathbb{E}_{\nu}\left[\xi\left(j\right)\right]\right]\\
&\qquad=c\sum_{j\in\mathbb{Z}}\left[\sum_{i=j+1}^{\infty}\sum_{l=0}^{i-j-1}(2-\mathbb{1}_{l=0})(i-j-l)\mathbb{E}_{\nu}\left[\xi\left(i\right)\right]\mathbb{E}_{\nu}\left[\xi\left(j\right)\right]\right.\\
&\qquad\qquad\left.+\sum_{i=-\infty}^{j-1}\sum_{l=0}^{j-i-1}(2-\mathbb{1}_{l=0})(j-i-l)\mathbb{E}_{\nu}\left[\xi\left(i\right)\right]\mathbb{E}_{\nu}\left[\xi\left(j\right)\right]\right],
\end{aligned}$$

where in the second step, we switch the order of the sums (which is justified by our assumption that ξ is finite range). Notice that since $\mathbb{E}_{\nu}\left[\xi\left(i\right)\right]$ does not depend on l we can now evaluate the sums over l. This yields

$$\begin{aligned}
\sum_{l=0}^{\infty}\mathbf{E}\left[\Delta\left(t+1\right)-\Delta\left(t\right)\mid\Delta\left(t\right)=l\right]\tilde{\mu}\left(l\right)&=c\sum_{j\in\mathbb{Z}}\left[\sum_{i=j+1}^{\infty}(i-j)^2\mathbb{E}_{\nu}\left[\xi\left(i\right)\right]\mathbb{E}_{\nu}\left[\xi\left(j\right)\right]\right.\\
&\qquad\left.+\sum_{i=-\infty}^{j-1}(i-j)^2\mathbb{E}_{\nu}\left[\xi\left(i\right)\right]\mathbb{E}_{\nu}\left[\xi\left(j\right)\right]\right]\\
&=c\sum_{i,j\in\mathbb{Z}}(i-j)^2\mathbb{E}_{\nu}\left[\xi\left(i\right)\right]\mathbb{E}_{\nu}\left[\xi\left(j\right)\right]\\
&=c\sum_{i,j\in\mathbb{Z}}(i^2+j^2)\mathbb{E}_{\nu}\left[\xi\left(i\right)\right]\mathbb{E}_{\nu}\left[\xi\left(j\right)\right]\\
&=2c\sum_{i\in\mathbb{Z}}i^2\mathbb{E}_{\nu}\left[\xi\left(i\right)\right]
\end{aligned}$$

after using $\sum_{i\in\mathbb{Z}}\mathbb{E}_{\nu}\left[\xi\left(i\right)\right]i=0$. Thus, we find

$$\lambda_{\text{ext}}=\frac{\operatorname{Var}_{\nu}\left(\mathbb{E}^{\boldsymbol{\xi}}[Y]\right)}{\sum_{l=0}^{\infty}\mathbf{E}\left[\Delta\left(t+1\right)-\Delta\left(t\right)\mid\Delta\left(t\right)=l\right]\tilde{\mu}\left(l\right)}=\frac{1-c}{2c}. \tag{4.67}$$

	Dirichlet Distribution	Normalized i.i.d. Distribution	Random Delta Distribution	Nearest Neighbor Distribution
c	$\dfrac{\alpha}{\alpha+1}$	c	$\dfrac{2k+1}{4k}$	$2(1-2\mathbb{E}[\omega^2])$
D	$\dfrac{1}{2\alpha}\sum_{i=-k}^{k}\alpha_i i^2$	$\dfrac{1}{6}k(k+1)$	$\dfrac{1}{6}k(k+1)$	$\dfrac{1}{2}$
D_{ext}	$\dfrac{\sum_{i=-k}^{k}\alpha_i i^2}{2\alpha(\alpha+1)}$	$\dfrac{1}{6}k(k+1)(1-c)$	$\dfrac{1}{24}(k+1)(2k-1)$	$2\mathbb{E}[\omega^2]-\frac{1}{2}$
λ_{ext}	$\dfrac{1}{2\alpha}$	$\dfrac{1-c}{2c}$	$\dfrac{2k-1}{2(2k+1)}$	$\dfrac{4\mathbb{E}[\omega^2]-1}{2(1-2\mathbb{E}[\omega^2])}$

Table 1. A summary of the relevant coefficients for the examples in Sections 4.8.6.2, 4.8.6.3, 4.8.6.4, and 4.8.6.5.

We now match this to (4.9). We recall that $D = \frac{1}{2}\sum_{i\in\mathbb{Z}} i^2\mathbb{E}_\nu\left[\xi\left(i\right)\right]$ and that $D_{\text{ext}} = \frac{1}{2}\text{Var}_\nu\left(\mathbb{E}^{\boldsymbol{\xi}}[Y]\right)$ where $\text{Var}_\nu\left(\mathbb{E}^{\boldsymbol{\xi}}[Y]\right)$ is given in (4.56). Therefore,

$$\frac{D_{\text{ext}}}{2(D-D_{\text{ext}})} = \frac{1-c}{2c} = \lambda_{\text{ext}}. \tag{4.68}$$

In the next several sections, we use the above simplification to derive λ_{ext} for several explicit examples. See Table 1 for a summary.

4.8.6.2 Dirichlet distribution. We recall our definition of the Dirichlet distribution from Section 4.8.1. The Dirichlet distribution for ν is specified by a choice of $k \in \mathbb{Z}_{\geq 1}$ and $\vec{\alpha} = (\alpha_{-k},\ldots,\alpha_k) \in \mathbb{R}_{>0}^{2k+1}$. It assigns probability density proportional to $\prod_{j=-k}^{k}\xi(j)^{\alpha_j}$ to each vector $\xi = (\xi(-k),\ldots,\xi(k)) \in \mathbb{R}_{\geq 0}^{k}$ satisfying $\sum_{j=-k}^{k}\xi(j) = 1$. Then, we set $\xi(i) = 0$ for $i \notin [-k,k]$ so that ξ is defined on $\mathbb{Z}$.

We have

$$\mathbb{E}_\nu\left[\xi\left(i\right)\right] = \begin{cases} \frac{\alpha_i}{\alpha} & \text{for } -k \le i \le k \\ 0 & \text{else,} \end{cases}$$

and for $i, j \in \mathbb{Z}$, $i \neq j$:

$$\mathbb{E}_\nu\left[\xi(i)\xi(j)\right] = \frac{\alpha_i \alpha_j}{\alpha(\alpha+1)} = \frac{\alpha}{\alpha+1}\mathbb{E}_\nu\left[\xi\left(i\right)\right]\mathbb{E}_\nu\left[\xi\left(j\right)\right].$$

It follows that (4.54) and (4.55) hold for the Dirichlet distribution with $c = \frac{\alpha}{\alpha+1}$ so that the Dirichlet distribution falls into the general class of models considered above. Combining (4.10) and (4.56), we see that

$$D_{\text{ext}} = \frac{1}{2\alpha(\alpha+1)}\sum_{i=-k}^{k}\alpha_i i^2.$$

We calculate the diffusion coefficient from its definition in (4.4),

$$D = \frac{1}{2\alpha}\sum_{i=-k}^{k}\alpha_i i^2.$$

Finally, we see from (4.67) that

$$\lambda_{\text{ext}} = \frac{1}{2\alpha}. \tag{4.69}$$

4.8.6.3 Independent and Identically Distributed Random Variables. We recall our definition of the normalized i.i.d. distribution from Section 4.8.1. The normalized i.i.d. distribution for ν is specified by a choice of $k \in \mathbb{Z}_{\ge 1}$ and a choice of probability distribution on $\mathbb{R}_{\ge 0}$. Let $X_{-k}, \ldots, X_k$ be chosen independently according to the specified probability distribution, and then define $\xi(i) = X_i(\sum_{j=-k}^{k} X_j)^{-1}$ for $i \in [-k, k]$ and $\xi(i) = 0$ otherwise.

We have

$$\mathbb{E}_\nu\left[\xi\left(i\right)\right] = \begin{cases} \frac{1}{2k+1} & \text{for } -k \le i \le k \\ 0 & \text{else,} \end{cases}$$

and for $i, j \in \mathbb{Z}$, $i \neq j$:

$$\mathbb{E}_\nu\left[\xi(i)\xi(j)\right] = \frac{c}{(2k+1)^2}$$

for some constant $c \in (0,1)$. Therefore, (4.54) and (4.55) are satisfied. Combining (4.10) and (4.56), we see that

$$D_{\text{ext}} = \frac{1-c}{2(2k+1)} \sum_{i=-k}^{k} i^2 = \frac{1}{6}k(k+1)(1-c)$$

We calculate the diffusion coefficient from its definition in (4.4),

$$D = \frac{1}{2(2k+1)} \sum_{i=-k}^{k} i^2 = \frac{1}{6}k(k+1).$$

Finally, we see from (4.67) that

$$\lambda_{\text{ext}} = \frac{1-c}{2c}. \tag{4.70}$$

4.8.6.4 Random Delta Distribution. We recall our definition of the random delta distribution from Section 4.8.1. The *random delta* distribution for ν is specified by $k \in \mathbb{Z}_{\geq 1}$. Two numbers X_1, X_2 are drawn uniformly without replacement from $\{-k, \ldots, k\}$. We set $\xi(X_1) = \xi(X_2) = 1/2$ and $\xi(i) = 0$ for all $i \neq X_1, X_2$.

We have

$$\mathbb{E}_\nu\left[\xi\left(i\right)\right] = \begin{cases} \frac{1}{2k+1} & \text{for } -k \leq i \leq k \\ 0 & \text{else,} \end{cases}$$

and for $i, j \in \mathbb{Z}$, $i \neq j$:

$$\mathbb{E}_\nu\left[\xi(i)\xi(j)\right] = \frac{1}{4k(2k+1)}.$$

It follows that (4.54) and (4.55) are satisfied with $c = \frac{2k+1}{4k}$. Combining (4.10) and (4.56), we see that

$$D_{\text{ext}} = \frac{2k-1}{8k(2k+1)} \sum_{i=-k}^{k} i^2 = \frac{1}{24}(k+1)(2k-1).$$

We calculate the diffusion coefficient from its definition in (4.4),

$$D = \frac{1}{6}k(k+1).$$

Finally, we see from (4.67) that

$$\lambda_{\text{ext}} = \frac{2k-1}{2(2k+1)}. \tag{4.71}$$

4.8.6.5 Nearest Neighbor Distribution. We define the nearest neighbor distribution as follows. Let ω be any random variable taking values in the interval $[0,1]$ such that $\mathbb{E}[\omega] = \frac{1}{2}$. We set $\xi(1) = \omega$, $\xi(-1) = 1-\omega$ and all other $\xi(i) = 0$.

We have

$$\mathbb{E}_\nu\left[\xi\left(1\right)\right] = \mathbb{E}_\nu\left[\xi\left(-1\right)\right] = \frac{1}{2}$$

and

$$\mathbb{E}_\nu\left[\xi(1)\xi(-1)\right] = \frac{1}{2} - \mathbb{E}[\omega^2].$$

It follows that (4.54) is satisfied with $c = 2(1-2\mathbb{E}[\omega^2])$; however, the walk $V(t)$ is no longer irreducible. In fact, when started from 0, it remains restricted to the sublattice $2\mathbb{Z}$. Therefore, $\mu(\cdot) = 0$ for all $l \notin 2\mathbb{Z}$, $\mu(0) = 1$ and $\mu(l) = c$ for $l \in 2\mathbb{Z}$. This slightly changes the analysis performed above since up until now, we were assuming that $\mu(l) = c$ for all $l \neq 0$. In particular, (4.66) is replaced by

$$\begin{aligned} &\sum_{l=0}^{\infty} \mathbf{E}\left[\Delta\left(t+1\right) - \Delta\left(t\right) \mid \Delta\left(t\right) = l\right] \tilde{\mu}\left(l\right) \\ &= c \sum_{l \in 2\mathbb{Z}_{\geq 0}} \sum_{|i-j|>l} (2 - \mathbb{1}_{l=0})(|i-j| - l)\mathbb{E}_\nu\left[\xi\left(i\right)\right]\mathbb{E}_\nu\left[\xi\left(j\right)\right]. \end{aligned} \tag{4.72}$$

In other words, we are only summing over even integers l. This can be further simplified in the same manner as above such that

$$\sum_{l=0}^{\infty} \mathbf{E}\left[\Delta\left(t+1\right)-\Delta\left(t\right) \mid \Delta\left(t\right)=l\right] \tilde{\mu}\left(l\right)=c\sum_{i\in\mathbb{Z}} i^2\mathbb{E}_{\nu}\left[\xi\left(i\right)\right]=c.$$

Note that this is simply half of what we obtained when summing over all integers instead of just even ones. We can also see this more directly by noticing that $\mathbf{E}\left[\Delta\left(t+1\right)-\Delta\left(t\right) \mid \Delta\left(t\right)=l\right]=0$ for $l\geq 2$. Therefore,

$$\begin{aligned}&\sum_{l=0}^{\infty} \mu(l)\mathbb{E}_{\nu}\left[\Delta\left(t+1\right)-\Delta\left(t\right) \mid \Delta\left(t\right)=l\right]\\&=\mathbb{E}_{\nu}\left[\Delta\left(t+1\right)-\Delta\left(t\right) \mid \Delta\left(t\right)=0\right]=2(1-2\mathbb{E}[\omega^2])=c.\end{aligned}$$

We compute $\mathrm{Var}_{\nu}\left(\mathbb{E}^{\boldsymbol{\xi}}[Y]\right)=4\mathbb{E}[\omega^2]-1=1-c$ so that

$$\lambda_{\text{ext}}=\frac{\mathrm{Var}_{\nu}\left(\mathbb{E}^{\boldsymbol{\xi}}[Y]\right)}{\sum_{l=0}^{\infty}\mathbf{E}\left[\Delta\left(t+1\right)-\Delta\left(t\right) \mid \Delta\left(t\right)=l\right]\tilde{\mu}\left(l\right)}=\frac{4\mathbb{E}[\omega^2]-1}{2(1-2\mathbb{E}[\omega^2])}=\frac{1-c}{c}. \quad (4.73)$$

This matches with the results in [112]. Since $D=1/2$, we have that

$$\lambda_{\text{ext}}=\frac{\mathrm{Var}_{\nu}\left(\mathbb{E}^{\boldsymbol{\xi}}[Y]\right)}{\left(2D-\mathrm{Var}_{\nu}\left(\mathbb{E}^{\boldsymbol{\xi}}[Y]\right)\right)}, \quad (4.74)$$

which is twice that of the irreducible cases. Similar extensions are possible if $V(t)$ is restricted to other sublattices, but we do not write out the details here.

4.8.7 Units of Variables.

We now introduce a lattice spacing dx and time step dt to understand the units of each variable. We do this by rescaling space and time such that $x\in dx\mathbb{Z}$ and $t\in dt\mathbb{Z}$. Note, that the environment is now defined on the new lattice meaning $\xi_{t,x}$ is a probability distribution on $dx\mathbb{Z}$. With the rescaled space and time,

$$D = \frac{1}{2dt} \sum_{i \in dx\mathbb{Z}} \mathbb{E}_{\nu} \left[\xi\left(i\right)\right] i^2 \tag{4.75}$$

$$= \frac{1}{2dt} \sum_{i \in \mathbb{Z}} \mathbb{E}_{\nu} \left[\xi\left(idx\right)\right] \left(idx\right)^2 \tag{4.76}$$

$$= \frac{dx^2}{2dt} \sum_{i \in \mathbb{Z}} \mathbb{E}_{\nu} \left[\xi\left(idx\right)\right] i^2 \tag{4.77}$$

which shows D has units area per time. The extreme diffusion coefficient, D_{ext}, has units of area per time as well since

$$D_{\text{ext}} = \frac{1}{2dt} \mathbb{E}_{\nu} \left[\left(\sum_{i \in dx\mathbb{Z}} \xi_{x,t}(i) i \right)^2 \right] \tag{4.78}$$

$$= \frac{dx^2}{2dt} \mathbb{E}_{\nu} \left[\left(\sum_{i \in \mathbb{Z}} \xi_{x,t}(idx) i \right)^2 \right]. \tag{4.79}$$

We show that λ_{ext} should be a length scale via its definition in (4.20). Notice the numerator of (4.20) has units of area per time. The denominator has units of length per time since $\tilde{\mu}\left(l\right)$ is unitless and $\mathbf{E}\left[\Delta\left(t+dt\right) - \Delta\left(t\right) \mid \Delta\left(t\right) = l\right]$ is the change in the distance between two random walks in a single timestep. Therefore, λ_{ext} has units length. By tracking the units in our simplification of λ_{ext} in Section 4.8.6, we find the simplified form of λ_{ext} in (4.9) becomes

$$\lambda_{\text{ext}} = \frac{1}{2} \frac{D_{\text{ext}}}{\left(D - D_{\text{ext}}\right)} dx = \frac{1}{2} \frac{\operatorname{Var}_{\nu}\left(\mathbb{E}^{\boldsymbol{\xi}}[Y]\right)}{\mathbb{E}_{\nu}\left[\operatorname{Var}^{\boldsymbol{\xi}}(Y)\right]} dx. \tag{4.80}$$

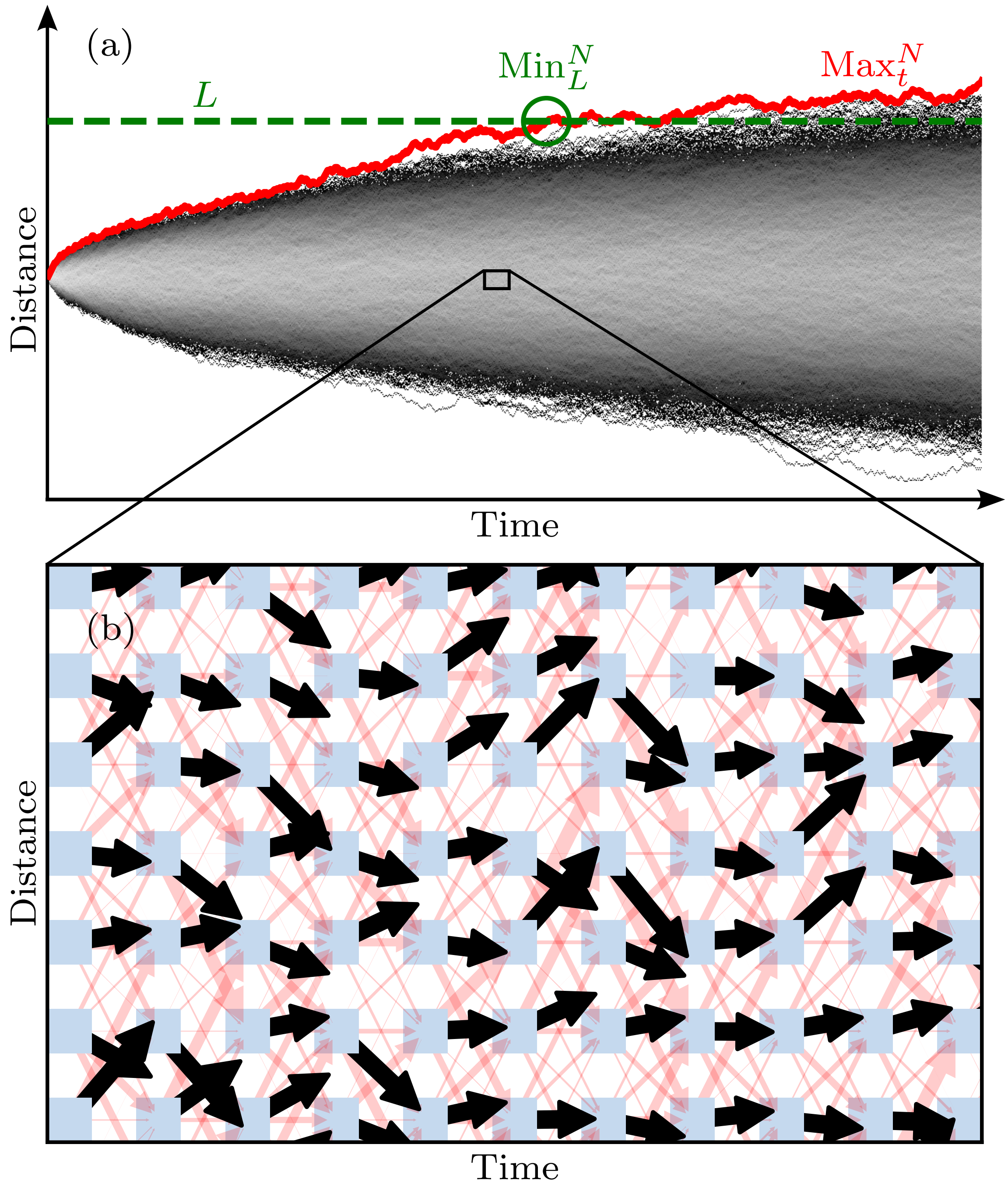

Figure 16. (a) Space-time trajectories of $N = 10^5$ particles evolving in a random environment generated by the flat Dirichlet distribution on the interval $\{-2, \ldots, 2\}$. The solid red line denotes the extreme location Max_t^N, and the green circle denotes the extreme first passage time Min_L^N. (b) The random environment driving the evolution in (a): blue boxes are sites, the width of the red arrows shows the probability of jumping between sites and black arrows are average drifts from sites.

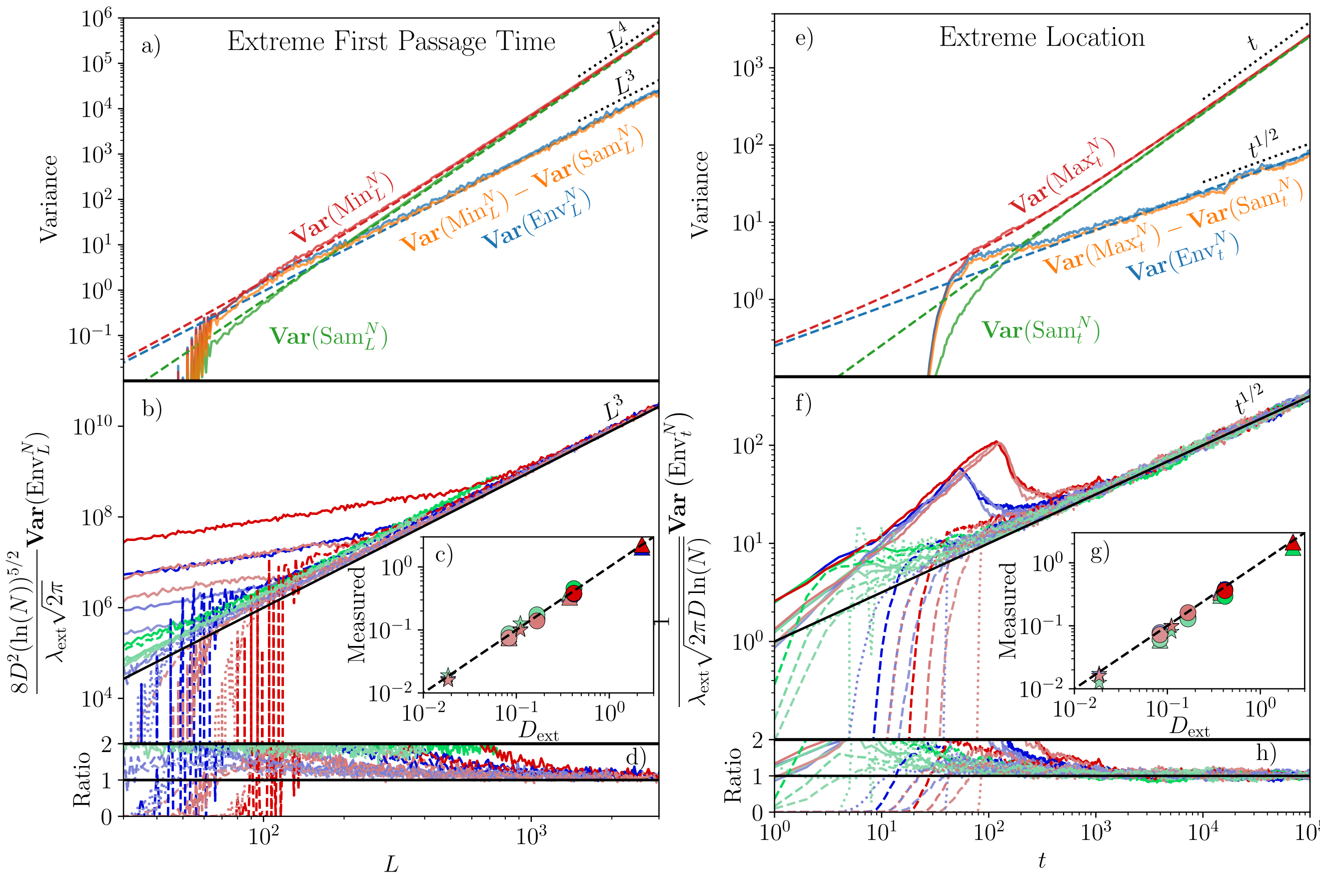

Figure 17. Plot of the measured variances for the extreme first passage time (a) and extreme location (e) for systems of $N = 10^{28}$ and the flat Dirichlet distribution with $D = 1$. b,f) Collapse of the environmental variance as a function of L and t, resp. $N = 10^2, 10^{14}$ and 10^{28} is plotted in red, blue and green resp.; the Dirichlet, flat Dirichlet and random delta distributions for ν are rendered as dotted, dashed and solid lines resp.; the color saturation is proportional to the Einstein diffusion coefficient D. Inset, c,g) Plot of the measured D_{ext} against the true value of D_{ext}. The dashed line represents equality. The Dirichlet, flat Dirichlet, and random delta distributions are labeled with a star, circle and triangle, resp. d,h) Plot of ratios of measured environmental variance vs. theoretical prediction in (4.7) and (4.8) as a function of L and t, resp. All reported quantities are measured by simulating 500 different systems for a given ν and N.

CHAPTER V

UNIVERSAL KPZ FLUCTUATIONS FOR MODERATE DEVIATIONS OF RANDOM WALKS IN RANDOM ENVIRONMENTS

This chapter is published as: Hass, J., Drillick, H., Corwin, I., & Corwin, E. (2025, March). Universal KPZ Fluctuations for Moderate Deviations of Random Walks in Random Environments (No. arXiv:2504.00266). arXiv. doi:10.48550/arXiv.2504.00266 but is currently in production with Physical Review E. My contribution was the theoretical results which were made more rigorous with the help of Hindy Drillick and Ivan Corwin.

5.1 Abstract

The theory of diffusion seeks to describe the motion of particles in a chaotic environment. Classical theory models individual particles as independent random walkers, effectively forgetting that particles evolve together in the same environment. *Random Walks in a Random Environment* (RWRE) models treat the environment as a random space-time field that biases the motion of particles based on where they are in the environment. We provide a universality result for the moderate deviations of the transition probability of this model over a wide class of choices of random environments. In particular, we show the convergence of moments to those of the multiplicative noise stochastic heat equation (SHE), whose logarithm is the Kardar-Parisi-Zhang (KPZ) equation. The environment only filters into the scaling limit through one parameter, which depends explicitly on the statistical description of the environment. This forms the basis for our introduction, in [133], of the extreme diffusion coefficient.

5.2 Introduction

Classical diffusion theory is used to describe the statistical behavior of agents in a wide variety of systems with random/chaotic fluctuations such as stock prices [134, 5], the movement of photons in a scattering medium [135] and the spread of viruses [4]. The theory is built upon the assumption that each particle can be modeled as effectively independent random walkers [22, 21, 23, 25, 26, 27, 28, 29], thus reducing everything to one parameter—the Einstein diffusion coefficient—that characterizes the variance per unit time of those walkers. Despite the simplicity of this model, it is remarkably effective in describing the statistics of the bulk, or typical diffusing particle in a system of many particles [31, 30, 2]. However, a recent series of works [6, 108, 69, 7, 107, 122, 133, 112, 123, 129] has provided evidence that the independent random walkers model for many-particle diffusion fails to accurately predict the behavior of extreme particles, i.e., those that travel the farthest or fastest and are often of considerable interest [95, 100, 102, 106, 104, 125, 8, 96, 94, 97, 98]. Those works have focused on models of *Random Walks in a Random Environment* (RWRE) with environments that are quickly mixing in space and time. Whereas typical particles in such models for many-particle diffusion behave as if the environment was statistically averaged, i.e., reduced to the independent random walker model, the extreme particles manifest novel behavior in the presence of a common random environment. The purpose of this paper is to unwind how the statistical description of the random environment translates into the statistical behavior of the extreme particles.

In the model considered here, an environment is a collection of transition probabilities, indexed by discrete one-dimensional space and time. At each time, particles choose their next spatial location independently according to the transition probabilities at that space-time point. The random environment comes from choosing those transition probability distributions randomly so as to be independent and identically distributed over all of space and time. We consider the many-step transition probability—which is random in light of the random environment. We show that as the time span grows in a scale N, the *moderate deviations* of this transition probability in a spatial scale $N^{3/4}$ (i.e., the probability of a single particle moving $N^{3/4}$ to the right of its mean velocity) converges to the solution of the *stochastic heat equation* (SHE), whose logarithm solves the *Kardar-Parisi-Zhang equation*, and which is given by

$$\partial_T Z = \frac{1}{2}\partial_X^2 Z + \sqrt{2D_0} Z\eta, \tag{5.1}$$

where X is distance and T is time. Above we have $Z(0, X) = \delta(X)$ (Dirac delta function) initial data, and take $\eta(X, T)$ to be space-time Gaussian white noise (i.e., $\mathbb{E}[\eta(X, T)] = 0$ and $\mathbb{E}[\eta(X, T)\eta(X', T')] = \delta(X - X')\delta(T - T')$).

The only parameter in this limit is the *noise strength* $D_0 \in \mathbb{R}_{>0}$, which we determine in Eq. 5.4 explicitly in terms of the statistical description of the random environment. We show convergence at the level of moments, and, though our methods can be applied to general moments, we restrict ourselves to the first and second moments which suffice to pin down the value of D_0. Similar results have been demonstrated recently in the mathematics literature in work of Parekh [123]. That work, as well as ours, can be seen as a generalization of the nearest neighbor or sticky-Brownian motion models studied in [7, 112, 128] to arbitrary random environments. Since moderate deviations translate into the behavior of the maximum of many draws from a probability distribution, our results translate into results about the statistical behavior of the extreme particles under certain scalings of time and the number of particles [133, 107, 69], as well as the location of first passage barriers [133, 122, 69] and the correlations between the positions of particles [136].

The remainder of the paper proceeds as follows. In Section 5.3, we clearly describe the RWRE model and some relevant notation. Section 5.4 contains our main results, namely the convergence of the first two moments and the determination of D_0. Our approach is explained in Section 5.5—in particular we use a variant of the replica method to relate moments to discrete local times, and then employ two probabilistic tools—the Tanaka formula for Brownian local times, and the stationary measures for certain Markov chains—to relate this to the replica formulas for the SHE moments. Section 5.7 fleshes out this local time convergence approach, and Section 5.8 relates those calculations back to the moments of the moderate deviations.

5.3 The RWRE Model

The random environment in which we will consider random walks is defined as $\boldsymbol{\xi} \coloneqq \{\xi_{t,x} : x \in \mathbb{Z}, t \in \mathbb{Z}_{\geq 0}\}$ where each $\xi_{t,x}$ is a probability distribution on $\mathbb{Z}$. The $\xi_{t,x}$ are themselves random, chosen to be independent and identically distributed over all choices of t and x, with a distribution ν that completely determines the RWRE model. Since $\xi_{t,x}$ are not correlated in time, the environment is memoryless. Given an environment $\boldsymbol{\xi}$, we will consider N independent random walkers; when a walker is at position x and t time, they choose how far to jump in the next time interval according to the distribution $\xi_{t,x}$. Different walkers at the same site use the same distribution $\xi_{t,x}$ but sample from it independently. Thus, there are two levels of randomness in the model, that of the environment in which all particles evolve together and that of the independently sampled walker trajectories. We introduce some notation to keep track of these two levels of randomness and illustrate it with an example.

We let $\mathcal{M}_1(\mathbb{Z})$ denote the space of probability distributions on $\mathbb{Z}$ and ν a probability distribution on $\mathcal{M}_1(\mathbb{Z})$. Each choice of ν corresponds to a different law on the random environment $\boldsymbol{\xi}$, where we sample $\xi_{t,x} \in \mathcal{M}_1(\mathbb{Z})$ according to ν, independently for each (t,x). We will restrict ourselves to only consider ν which are supported on finite range probability distributions, i.e., if ξ is distributed according to ν then for some M sufficiently large, $\xi(j) = 0$ for all $j > M$. We let $\mathbb{E}_\nu[\bullet]$ denote the expectation of a function $\bullet$ of $\boldsymbol{\xi}$ with respect to the product measure where each $\xi_{t,x}$ is independent with distribution ν. To illustrate this notation, let us note one example. For integer $k > 0$, and $\alpha_{-k}, \ldots, \alpha_k > 0$, let $\big(\xi(-k), \ldots, \xi(k)\big)$ be Dirichlet distributed with the specified α parameters (and let all other $\xi(j) = 0$ for $j \notin \{-k, k\}$). Precisely, restricted to the simplex where $\xi(-k), \ldots, \xi(k) \in [0,1]$ and $\xi(-k) + \cdots + \xi(k) = 1$, the probability density function is proportional to $\prod_{j=-k}^{k} \xi(j)^{\alpha_j - 1}$. This defines a random probability distribution on $\mathbb{Z}$ (or rather, $\{-k, \ldots, k\}$) and hence defines one choice of ν.

Given an instance of the environment $\boldsymbol{\xi}$, we will consider $N \in \mathbb{N}$ random walkers evolving independently with jump distributions determined by $\boldsymbol{\xi}$, and denote the corresponding probability measure by $\mathbb{P}^{\boldsymbol{\xi}}$. Such a model naturally lends itself to the study of extreme particles and allows one to extract extreme value statistics such as those of the particle which is at the maximum distance at a given time, $\max\big(\{R^1(t), \ldots, R^N(t)\}\big)$, or that which is first to cross a given boundary [133].

More precisely, $\mathbb{P}^{\boldsymbol{\xi}}$ is a probability measure on the sample space $(\mathbb{Z}^N)^{\mathbb{Z}_{\geq 0}}$, where we think of an element $\mathbf{R} = (R^1, \ldots, R^N)$ of this space as the time-indexed spatial trajectory of N walkers $R^1(t), \dots, R^N(t)$ for $t \in \mathbb{Z}_{\geq 0}$. For a given realization $\boldsymbol{\xi}$ of the environment, we define $\mathbb{P}^{\boldsymbol{\xi}}$ to be the measure on $(\mathbb{Z}^N)^{\mathbb{Z}_{\geq 0}}$ such that $(R^1, \dots, R^N)$ are distributed as N independent random walks all started at 0, with independent increments given, for each $k \in \{1, \dots, N\}$ by

$$\mathbb{P}^{\boldsymbol{\xi}}(R^k(t+1) = x + i \mid R^k(t) = x) = \xi_{x,t}(i).$$

In other words, each walker uses the jump distribution at their current time and position to determine the size of their next jump. When the environment $\boldsymbol{\xi}$ is random, the measure $\mathbb{P}^{\boldsymbol{\xi}}$ is random as well. We will be interested below in understanding the random probability distribution of a single walker, i.e., $\mathbb{P}^{\boldsymbol{\xi}}(R^k(t) = x)$. In that case, we will adopt the notation $R(t) = R^1(t)$, dropping the superscript.

We define the *annealed* probability measure $\mathbf{P}_\nu$ on the same N-path sample space $(\mathbb{Z}^N)^{\mathbb{Z}_{\geq 0}}$ by averaging $\mathbb{P}^{\boldsymbol{\xi}}$ over $\boldsymbol{\xi}$, according to the earlier described ν-dependent product measure $\mathbb{E}_\nu$. In other words, we define the annealed probability measure $\mathbf{P}_\nu(\cdot) := \mathbb{E}_\nu\left[\mathbb{P}^{\boldsymbol{\xi}}(\cdot)\right]$ and the corresponding expectation $\mathbf{E}_\nu[\cdot] = \mathbb{E}_\nu\left[\mathbb{E}^{\boldsymbol{\xi}}[\cdot]\right]$. For any $k \leq N$, we call the process $(R^1, \dots, R^k)$ with law given by $\mathbf{P}_\nu$ the *k-point motion.*

We denote the *average* environment as $\bar{\xi} = \mathbb{E}_\nu\left[\xi_{t,x}\right]$, which can also be thought of as the ensemble-averaged environment, meaning what you see if you average over a large swath of space and time. This average is the same at each site, hence, no t, x subscript is needed. For simplicity, we will only consider models with ν that have a drift-free average environment, i.e., such that $\sum_{i \in \mathbb{Z}} \bar{\xi}(i) i = 0$, though we expect similar results to hold for general ν after changing to a suitable moving reference frame.

Since we will make extensive use of them, we describe here the one- and two-point motions R^1 and (R^1, R^2) under the annealed measure $\mathbf{P}_\nu$. The one-point motion R^1 is an independent and identically distributed (i.i.d.) increment random walk that jumps from position x to position $x+j$ with probability $\bar{\xi}(j)$ for all $j \in \mathbb{Z}$. The same is true marginally of R^2, however, it is not quite true that R^1 and R^2 are independent. When $R^1(t) \neq R^2(t)$, (R^1, R^2) evolves according to independent $\bar{\xi}$ distributed increments, i.e., if $R^1(t) = x$ and $R^2(t) = y$ then $R^1(t+1) = x + j$ and $R^2(t+1) = y + k$ with probability given by the product $\bar{\xi}(j)\bar{\xi}(k)$. However, when $R^1(t) = R^2(t) = x$, the probability that $R^1(t+1) = x + j$ and $R^2(t+1) = x + k$ is equal to $\mathbb{E}_\nu\left[\xi_{t,x}(j)\xi_{t,x}(k)\right]$.

It follows from the above two-point motion transition formulas that we can think of them as a pair of *sticky* random walks since when the two walkers are at the same site at time t, they are more likely to also be at the same site at time $t+1$ than two independent random walks. An important object in our analysis will be the difference $V(t) := R^1(t) - R^2(t)$ between the two-point motion (R^1, R^2). In particular, we will study the gap $\Delta(t) := |V(t)|$. The walk $V(t)$ is a Markov chain on $\mathbb{Z}$ where the transition probability from state i to j is

$$p(i,j) = \begin{cases} \sum_{k\in\mathbb{Z}} \mathbb{E}_\nu\left[\xi_{t,x}(k)\xi_{t,x}(k-j)\right] & \text{if } i = 0 \\ \sum_{k\in\mathbb{Z}} \bar{\xi}(k)\bar{\xi}(k+j-i) & \text{if } i \neq 0, \end{cases} \tag{5.2}$$

which only depends on $j - i$ and whether or not $i = 0$. Furthermore, for $i, j \neq 0$, we have $p(i,j) = p(j,i)$.

For clarity, we now summarize the class of models we study. We consider RWRE models with the following assumptions

1. Particles take finite-range jumps.

2. The environment is given by an i.i.d. family of random probability distributions $\xi_{t,x}$, indexed by times t and positions x.

3. The average environment is drift free such that $\sum_{i\in\mathbb{Z}} \bar{\xi}(i)i = 0$.

5.4 Main result: RWRE limit to SHE

Based on previous results for nearest neighbor RWRE jump models [108, 7, 69, 112], we expect that in the moderate deviation regime, the tail probability will have environmental dependent fluctuations that have a SHE scaling limit. We will precisely state the scaling of this tail probability and demonstrate convergence to the SHE at the level of the first and second moments. Our methods can be readily generalized to show convergence of higher moments, but the first and second moments suffice in identifying the apriori unknown noise strength coefficient D_0.

We study the (random) tail probability (recalling our shorthand convention that $R(t) = R^1(t)$)

$$\mathbb{P}^{\boldsymbol{\xi}}\left(R(NT) \geq N^{3/4}T + \frac{\sum_{i\in Z} \bar{\xi}(i)i^3}{2(2D)^2} N^{1/2}T + \sqrt{2DN}X\right) \tag{5.3}$$

in the limit that $N \to \infty$, where $N \in \mathbb{Z}_{>0}$, $T \in N^{-1}\mathbb{Z}_{\geq 0}$, $X \in \mathbb{R}$, and $D := \frac{1}{2}\sum_{i\in\mathbb{Z}} \bar{\xi}(i)i^2$ is the diffusion coefficient of a random walk in the average environment. Note that here and below we use x and t to represent discrete positions in space and time while X and T represent continuous variables corresponding to the KPZ equation. We have dropped the superscript on the random walk in Eq. 5.3 since all N random walks are i.i.d.

Our main result, given by Eq. 5.40, states that the fluctuations of Eq. 5.3 converge to the SHE in Eq. 5.1 with time T, position X and noise strength

$$D_0 = \frac{\lambda_{\text{ext}}}{(2D)^{3/2}} \tag{5.4}$$

where λ_{ext} is a characteristic length defined as follows. Let Y be a random variable distributed according to $\xi_{t,x}$, which can be thought of as a single step of a random walk R^1. Further let $\mu(l)$ be the unique invariant measure of $V(t)$ with the normalization $\mu(0) = 1$ (we address the necessary modifications for the case where the invariant measure of $V(t)$ is not unique in Section 5.7.1.1). We then have

$$\lambda_{\text{ext}} = \frac{\operatorname{Var}_\nu\left(\mathbb{E}^{\boldsymbol{\xi}}[Y]\right)}{\sum_{l=0}^{\infty} \tilde{\mu}\,(l)\,\mathbf{E}_\nu[\Delta\,(t+1) - \Delta\,(t) \mid \Delta\,(t) = l]}, \tag{5.5}$$

where

$$\operatorname{Var}_\nu\left(\mathbb{E}^{\boldsymbol{\xi}}[Y]\right) = \mathbb{E}_\nu\left[\left(\sum_{i\in\mathbb{Z}} \xi_{t,x}(i)i\right)^2\right],$$

$$\tilde{\mu}\,(l) = \begin{cases} 1 & \text{if } l = 0 \\ 2\mu(l) & \text{if } l > 0. \end{cases}$$

Although the form of λ_{ext} is rather complex, it simplifies significantly for a number of distributions, which we discuss in [133].

The term $\operatorname{Var}_\nu\left(\mathbb{E}^{\boldsymbol{\xi}}[Y]\right)$ satisfies $\operatorname{Var}_\nu\left(\mathbb{E}^{\boldsymbol{\xi}}[Y]\right) \in [0, 2D]$ and represents the variance, over all environments, of the drift of a single jump of a random walk. When $\operatorname{Var}_\nu\left(\mathbb{E}^{\boldsymbol{\xi}}[Y]\right) = 2D$, the jump distribution is only supported on a single site, so the walks are perfectly sticky. In the limit that $\operatorname{Var}_\nu\left(\mathbb{E}^{\boldsymbol{\xi}}[Y]\right) \to 2D$, sticky Brownian motion can be recovered as studied in [128]. When $\operatorname{Var}_\nu\left(\mathbb{E}^{\boldsymbol{\xi}}[Y]\right) = 0$, the drift of the system is deterministic. Since we only study environments that are net drift free, this means $\mathbb{E}^{\boldsymbol{\xi}}[Y] = 0$ with probability 1 (see [123, 129] for a discussion of this case).

The invariant measure, $\tilde{\mu}\,(l)$, can be interpreted as how much time two particles spend a distance l apart as compared to being at the same site in the long time limit. One could potentially extract the invariant measure using microrheology as follows [137, 138]. Start two particles in the same environment. Let them diffuse for a long time and then measure their distance apart. Repeat this many times in different environments to build a histogram of the distance apart. After normalizing the histogram to 1 when the particles are at the same location, the histogram represents the invariant measure, $\tilde{\mu}(l)$. Alternatively, the invariant measure could be measured by observing a large system of diffusing particles. Letting the system run for a long time and then building a histogram of the distances between pairs of particles yields the invariant measure, $\tilde{\mu}(l)$.

The term $\mathbf{E}_{\nu}[\Delta(t+1) - \Delta(t) | \Delta(t) = l]$ does not depend on t as we are conditioning on $\Delta(t) = l$. This term quantifies the change in the distance between two random walks. The expectation value could be extracted using microrheology as follows. Start two particles a distance l apart and record how much farther apart they are after a small time step. Repeating this for many trials yields the expectation value. Since we are assuming a finite size jump distribution, the expected value will be 0 for large enough l, and thus, the sum in the denominator will be finite.

Our main result makes a remarkable connection between the microrheological quantity, λ_{ext}, and extreme values. Our results agree with those for nearest neighbor RWRE models [7, 112] and a specific case of a more general class of RWRE models studied in [123].

5.5 Overview of Our Derivation

To show convergence of the tail probability to the SHE, we work with a more general setup of which the tail probability in Eq. 5.3 is a special case. We study the probability mass function smoothed by a spatial test function. We include this smoothing because the probability mass distribution at a single lattice site is too noisy to work with (i.e., it depends on the order one behavior of the noise). The tail probability can be recovered by choosing the spatial test function to sum over all lattice sites in the tail, as discussed below. Of course, any physical measurement of diffusion involves some smoothing, so this is a natural lens through which to study the model.

Since the RWRE probability mass function is given in terms of a discrete path integral through the random environment, its moments admit representations in terms of interacting random walks, where the interaction relates to the law of the environment and is active when the walks coincide. This description is a discrete analog of the replica method formulas for moments of the SHE in terms of Brownian motions interacting through their local times. The argument presented below identifies a scaling under which the discrete moment formulas converge to their continuum SHE counterparts.

As shown below, the fluctuations of the RWRE tail probability converge to that of the KPZ equation when at lattice positions which scale like $N^{3/4}$. This scaling regime is called the "moderate deviation regime" [7].The central limit regime is found for lattice positions which scale like $N^{1/2}$. In this regime, we expect fluctuations in the tail probability to be determined by the Edward-Wilkinson universality class. The large deviation regime is found for lattice positions of order N. In the large deviation regime, fluctuations in the tail probability have been conjectured to be Tracy-Widom distributed [6, 69, 108]. However, this has only been proven rigorously for a specific choice of environment [6]. If one assumes that there are no abrupt changes in the distribution of fluctuations then one would expect the distribution in the moderate deviation regime to smoothly interpolate between the Gaussian and Tracy-Widom distributions. As the SHE is known to do precisely this it is natural that we find the fluctuations of the tail probability in the moderate deviation regime converge to the SHE.

We now introduce a smoothed out version of the probability mass function under this moderate deviations scaling. To start, we re-express the location about which we are studying the tail probability as a window of size $\sqrt{2DN}$ about $x = c(N)T$, where

$$c(N) = N^{3/4} + \frac{\sum_{i\in\mathbb{Z}} \bar{\xi}(i) i^3}{2(2D)^2} N^{1/2}.$$

This specific choice places us in the moderate deviation regime and is justified in detail below. The probability mass distribution at this location in the tail decays to first order like a Gaussian as $N \to \infty$, mimicking the behavior of the tail in the central limit regime. About this Gaussian behavior there are random fluctuations in the probability mass function. To study these fluctuations, we rescale the probability mass function by the first-order Gaussian behavior so the fluctuations stay of order one. This asymptotic Gaussian behavior is encoded in the prefactor $C(N, T, X)$, whose particular functional form is chosen for future mathematical convenience. Since the fluctuations at a single lattice point are too noisy to work with directly, we smooth the probability mass function in space by a spatial test function, ϕ.

Putting all of these elements together, we study

$$\mathscr{U}_N(T, \phi) := \mathbb{E}^{\boldsymbol{\xi}} \left[C\left(N, T, \frac{R(NT) - c(N)T}{\sqrt{2DN}}\right) \phi\left(\frac{R(NT) - c(N)T}{\sqrt{2DN}}\right)\right], \tag{5.6}$$

where $\phi : \mathbb{R} \to \mathbb{R}$ is a spatial test function (i.e. a smooth and compactly supported function), $R = R^1$ is a single random walk in the random environment $\boldsymbol{\xi}$ and

$$C(N,T,X) \coloneqq \frac{\exp\left\{\frac{c(N)}{2DN^{1/4}}T + \frac{1}{\sqrt{2D}}N^{1/4}X\right\}}{\left(\sum_{i\in\mathbb{Z}} \bar{\xi}(i)\exp\left\{\frac{i}{2DN^{1/4}}\right\}\right)^{NT}}$$

encodes the first-order Gaussian behavior of the probability mass distribution in the moderate deviation regime while its higher order terms conspire to yield convergence to the moments of the KPZ equation. Thus, $\mathscr{U}_N(T,\phi)$ is a weighted (by the $C(N,T,X)$ factor) probe of the distribution of $R(NT)$, smoothed by a test function, in the vicinity of $c(N)T$ and in the scale $\sqrt{2DN}$.

We now give our general strategy to show the moments (for different k) $\mathbb{E}_\nu\left[\mathscr{U}_N(T,\phi)^k\right]$ of Eq. 5.6 converge to those of the SHE. We fully realize this for the first and second moments, though the approach works similarly for general moments. Consider the first moment. It is immediate, see 5.9, that $\mathbb{E}_\nu\left[\mathscr{U}_N(T,\phi)\right]$ can be expressed in terms of an expectation over the one-point motion. Then, due to its multiplicative nature, the $C(N,T,X)$ prefactor in the definition of $\mathscr{U}_N(T,\phi)$ can be absorbed as a tilt of the jump distribution of the one-point motion, and hence in the limit yields a Brownian expectation.

Before going to the $k=2$ case, let us note that the k-th moment of the SHE integrated against a spatial test function can be written (via the replica method) in terms of the expectation of the local time of k Brownian motions

$$\mathbb{E}\left[\left(\int_{\mathbb{R}} \phi(X)Z(X,T)dX\right)^k\right] = \mathbf{E}\left[\Phi(\vec{B})\exp\left\{D_0\sum_{i<j} L^{B^i-B^j}(T)\right\}\right] \tag{5.7}$$

where $\mathbb{E}$ on the left is the expectation over the noise η of the SHE, and on the right $\Phi(\vec{x}) := \phi(x_1)\cdots\phi(x_k)$, and the expectation $\mathbf{E}$ is over independent Brownian motions $B^1, \ldots B^k$ with $L^{B^i-B^j}(t)$ their pair local time at zero, defined as follows. The local time of a space-time continuous Brownian motion $B(t)$ with variance $\sigma^2 t$ is

$$L^B(t) := \lim_{\epsilon\to 0^+} \frac{\sigma^2}{2\epsilon} \int_0^t \mathbb{1}_{\{-\epsilon<B(s)<\epsilon\}} ds. \tag{5.8}$$

For $k = 2$ (and higher), the moment is rewritten in terms of an expectation with respect to the 2-point motion. The same tilting argument works provided the two-point motions occupy different spatial locations. When they are at the same site, the two-point motion jump distribution (i.e., $p(i,j)$ from 5.2 with $i = 0$) has some residual effect after tilting which can be written, as in Eq. 5.21, in terms of a local time contribution. The tilted two-point motion clearly converges to independent Brownian motions, so the whole challenge is to understand how the discrete local time converges to a limiting Brownian local time.

To illustrate this challenge, note that a random walk that lives entirely on the odd sublattice of $\mathbb{Z}$ will have zero discrete local time at 0, yet will still converge to a Brownian motion. More relevant to the current situation, the introduction of some stickiness at zero for a random walk will not impact its Brownian limit (provided the stickiness is not tuned in the scaling limit), but will cause the discrete local time at 0 to converge to a constant multiple of the Brownian local time at 0. That constant dilation factor of the local time depends on the degree of stickiness.

Thus, to address the discrete to continuous local time convergence—in particular computing the dilation factor (which translates into the noise strength coefficient D_0)—we develop an argument based on a discrete version of the *Tanaka* *formula* and the *Doob-Meyer decomposition*, both tools based on studying random walks and Brownian motions as *martingales*. This will identify a discrete local time, not entirely concentrated at 0, which converges to the Brownian local time at 0. Then, we will use the invariant measure of the gap between the two-point motion to identify what portion of that discrete local time comes from the discrete local time at 0 (which is what arises in our moment formulas). This will yield the desired dilation factor and explains the form of D_0 given earlier. The details of this argument are presented below.

5.6 Convergence of the First Moment

The convergence of the first moment will show that our choice of $C(N,T,X)$ is the correct prefactor to ensure $\mathscr{U}_N(T,\phi)$ converges to the first moment of the SHE. We begin by averaging $\mathscr{U}_N(T,\phi)$ in Eq. 5.6 over the random environment to obtain

$$\mathbb{E}_\nu\left[\mathscr{U}_N(T,\phi)\right] = \mathbf{E}_\nu\left[C\left(N,T,\frac{R(NT)-c(N)T}{\sqrt{2DN}}\right)\phi\left(\frac{R(NT)-c(N)T}{\sqrt{2DN}}\right)\right]. \tag{5.9}$$

The notation used above should be recalled from Section 5.3. In particular, $R = R^1$ is the one-point motion under the annealed measure $\mathbf{P}_\nu$ and is the expectation with respect to that measure $\mathbf{E}_\nu$.

We now absorb the prefactor into the expectation by interpreting it as an *exponential tilting* of the i.i.d. increments of the one-point motion. We start by breaking up the one-point into its increments, $R(NT) = \sum_{i=1}^{NT} Y_i$ where Y_i are independent and identically distributed according to $\bar{\xi}$. Thus, we can rewrite

$$C\left(N, T, \frac{R(NT) - c(N)T}{\sqrt{2DN}}\right) = \frac{\exp\left\{\frac{R(NT)}{2DN^{1/4}}\right\}}{\left(\sum_{i\in\mathbb{Z}} \bar{\xi}(i) \exp\left\{\frac{i}{2DN^{1/4}}\right\}\right)^{NT}}$$
$$= \prod_{i=1}^{NT} \frac{\exp\left\{\frac{Y_i}{2DN^{1/4}}\right\}}{\sum_{i\in\mathbb{Z}} \bar{\xi}(i) \exp\left\{\frac{i}{2DN^{1/4}}\right\}}.$$

Since the Y_i are independent and identically distributed according to $\bar{\xi}$, this factor can be absorbed as a tilt of the jump distribution for Y_i. Define the tilted measure $\tilde{\mathbf{E}}_\nu$ under which the Y_i are independent and identically distributed but now with the probability that $Y_i = j$ for $j \in \mathbb{Z}$ given by

$$\frac{\bar{\xi}(j) \exp\left\{\frac{j}{2DN^{1/4}}\right\}}{\sum_{i\in\mathbb{Z}} \bar{\xi}(i) \exp\left\{\frac{i}{2DN^{1/4}}\right\}}. \tag{5.10}$$

Notice how the prefactor was chosen to make sure this tilting results in a probability measure Recalling that $R(NT) = \sum_{i=1}^{NT} Y_i$, we thus have shown that Eq. 5.9 can be rewritten in terms of the tilted measure as

$$\mathbb{E}_\nu \left[\mathscr{U}_N(T, \phi)\right] = \tilde{\mathbf{E}}_\nu \left[\phi\left(\frac{R(NT) - c(N)T}{\sqrt{2DN}}\right)\right]. \tag{5.11}$$

Under the tilted measure, the centered and scaled one-point motion converges to a Brownian motion, i.e.,

$$\lim_{N\to\infty} \frac{R(NT) - c(N)T}{\sqrt{2DN}} = B(T) \tag{5.12}$$

where B is a standard unit variance Brownian motion. To see this, since the increments of R are independent and identically distributed, it suffices to check that that $\frac{R(NT)-c(N)T}{\sqrt{2DN}}$ has mean 0 and variance T, at least up to terms that vanish as $N \to \infty$. Under the tilted distribution Eq. 5.10, the increments of $R(NT)$ have mean

$$\frac{\sum_{i\in\mathbb{Z}}\bar{\xi}(i)i\exp\{\frac{i}{2DN^{1/4}}\}}{\sum_{j\in\mathbb{Z}}\bar{\xi}(j)\exp\{\frac{j}{2DN^{1/4}}\}}=\frac{\sum_{i\in\mathbb{Z}}\bar{\xi}(i)i\left(1+\frac{i}{2DN^{1/4}}+\frac{i^2}{4DN^{1/2}}+\mathcal{O}\left(N^{-3/4}\right)\right)}{\sum_{j\in\mathbb{Z}}\bar{\xi}(j)\left(1+\mathcal{O}\left(N^{-1/2}\right)\right)}$$
$$=\sum_{i\in\mathbb{Z}}\bar{\xi}(i)\frac{i^2}{2DN^{1/4}}+\sum_{i\in\mathbb{Z}}\bar{\xi}(i)\frac{i^3}{4D^2N^{1/2}}+\mathcal{O}\left(N^{-3/4}\right)$$
$$=\frac{c(N)}{N}+\mathcal{O}\left(N^{-3/4}\right)$$

where $\mathcal{O}(x)$ denotes terms of order x and lower. The second moment of the increments of $R(NT)$ are

$$\frac{\sum_{i\in\mathbb{Z}}\bar{\xi}(i)i^2\exp\{\frac{i}{2DN^{1/4}}\}}{\sum_{j\in\mathbb{Z}}\bar{\xi}(j)\exp\{\frac{j}{2DN^{1/4}}\}}=\frac{\sum_{i\in\mathbb{Z}}\bar{\xi}(i)i^2\left(1+\mathcal{O}\left(N^{-1/4}\right)\right)}{\sum_{j\in\mathbb{Z}}\bar{\xi}(j)\left(1+\mathcal{O}\left(N^{-1/2}\right)\right)}$$
$$=2D+\mathcal{O}\left(N^{-1/4}\right).$$

Thus, under the tilted measure $R(NT)$ has mean $c(N)T+\mathcal{O}(N^{1/4})$ and variance $2DNT+\mathcal{O}(N^{3/4})$, or equivalently $\frac{R(NT)-c(N)T}{\sqrt{2DN}}$ has a mean of order $\mathcal{O}(N^{-1/4})$ and variance $T+\mathcal{O}(N^{-1/4})$.

Combining Eq. 5.12 with Eq. 5.11, we see the first equality

$$\lim_{N\to\infty}\mathbb{E}_\nu\left[\mathscr{U}_N(T,\phi)\right]=\mathbf{E}\left[\phi(B(T))\right]=\mathbb{E}\left[\int_{\mathbb{R}}\phi(X)Z(X,T)dX\right]. \tag{5.13}$$

Here $\mathbf{E}$ is the expectation with respect to a standard Brownian motion staring at 0, and the second equality (to the the first moment of the SHE) follows from in Eq.5.7.

5.7 Convergence of the Second Moment

We now show that the second moment of $\mathscr{U}(T,\phi)$ converges to the second moment of the SHE with the strength of the noise given by $D_0=\frac{\lambda_{\text{ext}}}{(2D)^{3/2}}$. In doing so, we identify the characteristic length scale λ_{ext}.

Recall that given an instance of the environment $\boldsymbol{\xi}$, the random walks $R^1, R^2, \ldots$ are independent and identically distributed. Thus, in Eq. 5.6, we could have just as well replaced R by R^1 or R^2 without changing anything. Doing that, and owing to the independent (given $\boldsymbol{\xi}$) of R^1 and R^2, it follows that

$$\mathscr{U}_N(T,\phi)^2 = \mathbb{E}^{\boldsymbol{\xi}}\Bigg[C\left(N,T,\frac{R^1(NT)-c(N)T}{\sqrt{2DN}}\right)C\left(N,T,\frac{R^2(NT)-c(N)T}{\sqrt{2DN}}\right) \times \phi\left(\frac{R^1(NT)-c(N)T}{\sqrt{2DN}}\right)\phi\left(\frac{R^2(NT)-c(N)T}{\sqrt{2DN}}\right)\Bigg].$$

This is the first step of the *replica method*.

The next step is to take the expectation over the random environment to get a formula for the second moment. Using the explicit form of the prefactor C, this yields

$$\mathbb{E}_\nu\left[\mathscr{U}_N(T,\phi)^2\right] = \mathbf{E}_\nu\Bigg[\frac{\exp\left\{\frac{R^1(NT)+R^2(NT)}{2DN^{1/4}}\right\}}{\left(\sum_{i\in\mathbb{Z}}\bar{\xi}(i)\exp\left\{\frac{i}{2DN^{1/4}}\right\}\right)^{2NT}}\phi\left(\frac{R^1(NT)-c(N)T}{\sqrt{2DN}}\right) \times \phi\left(\frac{R^2(NT)-c(N)T}{\sqrt{2DN}}\right)\Bigg], \tag{5.14}$$

where the pair (R^1,R^2) is the two-point motion defined earlier. As we did for the first moment, we want to absorb the prefactor as a tilt of the transition probabilities for the two-point motion. When $R^1 \neq R^2$, this works exactly as before since the two random walks take independent jumps. When $R^1 = R^2$, the two jumps are no longer independent, and an additional factor is needed to ensure that the tilting results in a probability measure. This produces a discrete local time at 0 term in our moment formula, see Eq. 5.20 below.

To derive Eq. 5.20, first observe that the denominator inside the expectation in Eq. 5.14 can be broken into NT equal factors with each term given by

$$\left(\sum_{i\in\mathbb{Z}}\bar{\xi}(i)\exp\left\{\frac{i}{2DN^{1/4}}\right\}\right)^2 = \sum_{i,j\in\mathbb{Z}}\bar{\xi}(i)\bar{\xi}(j)\exp\left\{\frac{i+j}{2DN^{1/4}}\right\} \tag{5.15}$$

after expanding into a double sum. When $R^1(t) \neq R^2(t)$, this is the right normalization for the tilting factor needed to produce a probability measure for the increments of R^1 and R^2. When $R^1(t) = R^2(t)$, we require a different normalization to get a tilted probability measure since $\bar{\xi}(i)\bar{\xi}(j)$ should be replaced by $\mathbb{E}_\nu [\xi_{t,x}(i)\xi_{t,x}(j)]$ (as the walks are at the same site).

To account for this, we really should have started with a different prefactor

$$C\left(N, T, \frac{R^1(NT) - c(N)T}{\sqrt{2DN}}\right) C\left(N, T, \frac{R^2(NT) - c(N)T}{\sqrt{2DN}}\right) \\ \times \exp\left\{-g\left((2D)^{-1}N^{-1/4}\right) \sum_{i=0}^{NT-1} \mathbb{1}_{\{R^1(i)=R^2(i)\}}\right\} \tag{5.16}$$

where

$$g(\lambda) = \log\left(\sum_{i,j\in\mathbb{Z}} \mathbb{E}_\nu [\xi_{t,x}(i)\xi_{t,x}(j)]\, e^{\lambda(i+j)}\right) - 2\log\left(\sum_{i\in\mathbb{Z}} \bar{\xi}(i)e^{\lambda i}\right). \tag{5.17}$$

If we use this tilting factor, then we obtain a tilted version of the two-point motion which is a Markov chain with the following transition probabilities: When $R^1(t) \neq R^2(t)$, then $R^1(t+1) = R^1(t) + i$ and $R^2(t+1) = R^2(t) + j$ with probability

$$\frac{\bar{\xi}(i)\bar{\xi}(j)\exp\left\{\frac{i+j}{2DN^{1/4}}\right\}}{\sum_{k,l\in\mathbb{Z}} \bar{\xi}(k)\bar{\xi}(l)\exp\left\{\frac{k+l}{2DN^{1/4}}\right\}}. \tag{5.18}$$

When $R^1(t) = R^2(t) = x$, then $R^1(t+1) = x + i$ and $R^2(t+1) = x + j$ with probability

$$\frac{\mathbb{E}_\nu [\xi_{t,x}(i)\xi_{t,x}(j)] \exp\left\{\frac{i+j}{2DN^{1/4}}\right\}}{\sum_{k,l\in\mathbb{Z}} \mathbb{E}_\nu [\xi_{t,x}(k)\xi_{t,x}(l)] \exp\left\{\frac{k+l}{2DN^{1/4}}\right\}}. \tag{5.19}$$

Noting the overload with the notation from the first moment calculation, we let $\tilde{\mathbf{E}}_\nu [\bullet]$ denote the expectation value with respect to the tilted probability distribution on (R^1, R^2) given by the above transition probability.

Taking into account the g factor we included in Eq. 5.16, we find that

$$\begin{aligned}
\mathbb{E}_\nu\left[\mathscr{U}_N(T,\phi)^2\right] &= \\
&\tilde{\mathbf{E}}_\nu\left[\exp\left\{g\left((2D)^{-1}N^{-1/4}\right)\sum_{i=0}^{NT-1}\mathbb{1}_{\{R^1(i)=R^2(i)\}}\right\}\phi\left(\frac{R^1(NT)-c(N)T}{\sqrt{2DN}}\right)\right. \\
&\qquad\left.\times\,\phi\left(\frac{R^2(NT)-c(N)T}{\sqrt{2DN}}\right)\right].
\end{aligned} \tag{5.20}$$

By Taylor expansion we find that $g((2D)^{-1}N^{-1/4}) = \frac{\mathbb{E}_\nu\left[\left(\sum_{i\in\mathbb{Z}} i\xi_{t,x}(i)\right)^2\right]}{(2D)^2N^{1/2}} + \mathcal{O}(N^{-3/4}) = \frac{\mathrm{Var}_\nu\left(\mathbb{E}^{\boldsymbol{\xi}}[Y]\right)}{(2D)^2N^{1/2}} + \mathcal{O}(N^{-3/4})$ where the second equality comes from observing that $\mathrm{Var}_\nu\left(\mathbb{E}^{\boldsymbol{\xi}}[Y]\right) = \mathbb{E}_\nu\left[\left(\sum_{i\in\mathbb{Z}} i\xi_{t,x}(i)\right)^2\right]$. The fact that this term behaves like $N^{-1/2}$ is key since the discrete local time (i.e., $\sum_{i=0}^{NT-1}\mathbb{1}_{\{R^1(i)=R^2(i)\}}$) needs to be scaled by that factor to have a limit. This consideration is what forces the scaling regime for SHE convergence to be in the $N^{3/4}$-depth moderate deviations of the tail probability.

Substituting this expansion in Eq. 5.20 and using $\approx$ to denote that we have dropped the lower order terms, we have

$$\begin{aligned}
\mathbb{E}_\nu\left[\mathscr{U}_N(T,\phi)^2\right] \approx \tilde{\mathbf{E}}_\nu\left[\exp\left\{\frac{\mathrm{Var}_\nu\left(\mathbb{E}^{\boldsymbol{\xi}}[Y]\right)}{(2D)^2N^{1/2}}\sum_{i=0}^{NT-1}\mathbb{1}_{\{R^1(i)=R^2(i)\}}\right\}\phi\left(\frac{R^1(NT)-c(N)T}{\sqrt{2DN}}\right)\right. \\
\left.\times\phi\left(\frac{R^2(NT)-c(N)T}{\sqrt{2DN}}\right)\right].
\end{aligned} \tag{5.21}$$

Notice that Eq. 5.21 looks like a discrete analog of the second moment of the SHE in Eq. 5.7 since $\sum_{i=0}^{NT-1}\mathbb{1}_{\{R^1(i)=R^2(i)\}}$ is the discrete local time of $R^1(i) - R^2(i)$ at 0. Furthermore, besides their sticky interaction when $R^1 = R^2$, the tilted two-point motion behaves like independent random walks just as in the first moment case. The only way that the sticky interaction could impact the scaling limit is if it is scaled to become stronger as $N \to \infty$ (i.e., so that the time they stay together increases in the scaling limit), or if the size of the jump from $R^1 = R^2$ were scaled to become longer as $N \to \infty$ (i.e., so as to result in a discontinuous jump in the limit process). This is not the case, and hence under the measure $\tilde{\mathbf{E}}_\nu$, the pair $\left(\frac{R^1(NT)-c(N)T}{\sqrt{2DN}}, \frac{R^2(NT)-c(N)T}{\sqrt{2DN}}\right)$ converge to independent variance one Brownian motions, as in the first moment case.

Our final step is to identity the scaling limit of the discrete local time $\sum_{i=0}^{NT-1} \mathbb{1}_{\{R^1(i)=R^2(i)\}}$, namely that it converges to a constant (which we identity) times the local time of the difference of two independent standard Brownian motions. This is the most subtle and interesting part of the argument since it more broadly explains in what sense discrete local times converge to their continuum Brownian analogs. In particular, although the discrete random walks converge to independent Brownian motions, the discrete local time need not converge to the local time of their Brownian motion limits. For example, consider a simple symmetric random walk on $\mathbb{Z}$ modified so as to stay at 0 with probability 1/2 and go to ± 1 each with probability 1/4 (i.e., it is sticky at the origin). The discrete random walks will converge to Brownian motion, but the discrete local time will converge to a constant (explicitly calculable and exceeding one) times the local time of standard Brownian motion. Identifying this constant which rescales the local time limit is the key to identifying the noise strength of the SHE. Specifically, in what follows, we show that

$$\lim_{N\to\infty} \frac{1}{\sqrt{2DN}} \sum_{i=0}^{NT-1} \mathbb{1}_{\{R^1(i)=R^2(i)\}} = \frac{1}{\sum_{l=0}^{\infty} \tilde{\mu}(l)\, \mathbf{E}_\nu\left[\Delta(t+1) - \Delta(t) \mid \Delta(t) = l\right]} L_0^{B^1-B^2}(T). \tag{5.22}$$

where B^1 and B^2 are independent standard Brownian motions starting at 0. Notice that the prefactor of the local time on the right-hand side is the denominator of λ_{ext} in Eq. 5.5. We show this in Section 5.7.1.

Putting the above together, we conclude that

$$\lim_{N\to\infty} \mathbb{E}_\nu \left[\mathscr{U}_N(T,\phi)^2 \right] = \mathbf{E}\left[e^{\frac{\lambda_{\text{ext}}}{(2D)^{3/2}} L_0^{B^1-B^2}(T)} \phi(B^1(T))\phi(B^2(T)) \right]$$

where $\mathbf{E}$ is the expectation with respect to two independent Brownian motions B^1 and B^2 start at 0 and with variance 1; and λ_{ext} is given by Eq. 5.5. This is indeed the second moment of the multiplicative stochastic heat equation defined in Eq. 5.7 with noise strength given by Eq. 5.4.

A similar argument applies for the case of general moments. A priori, when dealing with higher moments, there are terms that come from multi-particle interactions, e.g., when $R^1 = R^2 = R^3$. Each of these contributions needs to be accounted for when writing down the tilted measure and contribute differently to the local time factor. However, in our scaling, these different factors end up factorizing as $N \to \infty$ and thus only contribute in the form of two-body local times, as needed to recover the general moment formula Eq. 5.7.

5.7.1 Convergence to Local Time. The purpose of this section is to demonstrate the claimed convergence of Eq. 5.22. Recall $V(t) = R^2(t) - R^1(t)$, so $\sum_{i=0}^{NT-1} \mathbb{1}_{\{R^1(i)=R^2(i)\}} = \sum_{i=0}^{NT-1} \mathbb{1}_{\{|V(i)|=0\}}$ is the sum of occupation times at 0 for the random walk V. To derive Eq. 5.22, we identify a discrete analog of *Tanaka's formula* to identify a smoothed, discrete local time that converges to the local time of Brownian motion. We then use the invariant measure of the two-point gap process, $\Delta(t) = |V(t)|$, to relate the smoothed, discrete local time to the discrete local time at 0.

Before giving Tanaka's formula, we recall the definition of a martingale. A continuous time martingale is a time-parameterized collection of random variables, $(Y_t)_{t\geq 0}$, which obeys the martingale property whereby $\mathbb{E}[Y_t \mid \mathcal{F}_s] = Y_s$ for all $t > s \geq 0$, where $\mathcal{F}_s$ is the σ-algebra generated by Y_r for all $s \geq r \geq 0$. In words, this property says that the expected value at time t, given the history of the process up to time s, is the value at time s. Brownian motion B_t with drift zero is an example of a martingale, as is $B_t^2 - t$ (the quadratic martingale) or $e^{\lambda B_t - \lambda^2 t/2}$ (the exponential martingale) for any λ.

Tanaka's formula gives a decomposition of the absolute value of a Brownian motion into the sum of a martingale and Brownian local time. More precisely, given a Brownian motion $B(t)$, the Tanaka formula states that

$$|B(t)| = \int_0^t \operatorname{sgn}(B_s) dB_S + L^B(t), \tag{5.23}$$

where $L^B(t)$ is the local time at zero, defined in Eq. 5.8, and

$$\operatorname{sgn}(x) = \begin{cases} +1 & x > 0 \\ 0 & x = 0 \cdot \\ -1 & x < 0 \end{cases}$$

The stochastic integral $\int_0^t \operatorname{sgn}(B_s) dB_S$ is a martingale, and, in fact, is another Brownian motion.

Tanaka's formula gives a way to decompose $|B(t)|$ into the sum of a martingale (the stochastic integral) and an increasing *predictable process* (the local time). Such a decomposition is called the *Doob-Meyer decomposition.* A key fact is that the Doob-Meyer decomposition of a *submartingale* (a process such as $Y_t = |B(t)|$ that satisfies $\mathbb{E}[Y_t \mid \mathcal{F}_s] \geq Y_s$ for all $t > s \geq 0$) is unique under fairly general assumptions. Therefore, if we can obtain *any* decomposition of $|B(t)|$ into the sum of a martingale term and an increasing predictable process, we can identify that increasing predictable process as Brownian local time.

Motivated by this fact, we obtain a Doob decomposition for $\Delta(t) = |V(t)|$ by identifying a discrete analogue of Tanaka's formula. This decomposition involves the sum of a martingale and a discrete local time term. We then take the term-by-term limit of this decomposition. We know that $\Delta(t)$ will converge to $|B(t)|$, where $B(t)$ will be a Brownian motion with variance 2. The martingale term will converge to a limiting martingale, and the limit of the discrete local time term will still be an increasing predictable process. Hence, by the uniqueness of the Doob-Meyer decomposition for $|B(t)|$, we will conclude that the limit of the discrete local time term is Brownian local time.

There are several mathematical subtleties that we brush over but quickly note here. From Eq. 5.21, we are concerned with convergence of an expectation with respect to the tilted measure $\tilde{\mathbf{E}}_\nu$ of an expression involving the expectation of the local time at zero for $\Delta(t)$. The argument presented below shows that this local time under the untilted measure $\mathbf{E}_\nu$ converges in distribution to a constant multiple of Brownian local time. The replacement of the tilted measure by its untilted counterpart is mostly out of convenience (the argument could be done under the tilted measure too) and is justified since as $N \to \infty$, the tilted (N-dependent) measure converges to the untilted one. This can be seen by expanding e^x around $x = 0$ to simplify the exponential in the tilted measure. Then the sums in the denominators of (5.18) and (5.19) evaluate to 1, and we recover the transition probabilities of the untilted two-point motion. The issue around convergence of expectations of exponentials would require some further careful justification that we do not pursue here.

Turning to the details of this argument, we decompose $\Delta(t)$ as follows:

$$\Delta(t) = M(t) + \sum_{i=0}^{t-1} \sum_{l=0}^{\infty} \kappa\,(l)\, \mathbb{1}_{\{\Delta(i)=l\}} \tag{5.24}$$

where we define

$$\kappa(l) = \mathbf{E}_\nu\left[\Delta(i+1) - \Delta(i)\middle|\Delta(i) = l\right] \qquad \text{and} \qquad M(t) := \Delta(t) - \sum_{i=0}^{t-1}\sum_{l=0}^{\infty} \kappa\left(l\right) \mathbb{1}_{\{\Delta(i)=l\}}.$$

Note that $\Delta(i+1) - \Delta(i)$ does not actually depend on i since we are conditioning on $\Delta(i) = l$.

To see that $M(t)$ is a martingale with respect to the untilted measure $\mathbf{E}_\nu$, we rewrite $M(t)$ as

$$\begin{aligned} M(t) &= \Delta(t) - \sum_{i=0}^{t-1}\sum_{l=0}^{\infty} \mathbf{E}_\nu\left[\Delta(i+1) - \Delta(i) \mid \Delta(i) = l\right] \mathbb{1}_{\{\Delta(i)=l\}} \\ &= \Delta(t) - \sum_{i=0}^{t-1} \mathbf{E}_\nu\left[\Delta(i+1) - \Delta(i) \mid \Delta(i)\right] \end{aligned}$$

where we have taken the sum over l so that we now condition on the random value $\Delta\left(i\right)$. Notice $\Delta(i+1) - \Delta(i)$ is independent of the values of $\Delta(1), \ldots, \Delta(i-1)$ and only depends on $\Delta(i)$. Thus, we can rewrite

$$M(t) = \Delta(t) - \sum_{i=0}^{t-1} \mathbf{E}_\nu\left[\Delta(i+1) - \Delta(i) \mid \Delta(1), \ldots, \Delta(i)\right].$$

It follows from this and telescoping that $M(t)$ is a martingale.

We now show that the term $\sum_{i=0}^{t-1}\sum_{l=0}^{\infty} \kappa\left(l\right) \mathbb{1}_{\{\Delta(i)=l\}}$ is increasing in t and predictable. We first show that $\kappa(l) \geq 0$. To see this, we use our results from [133] which show $\kappa(l)$ simplifies to

$$\kappa(l) = \begin{cases} \displaystyle\sum_{i,j\in\mathbb{Z}} |i-j|\mathbb{E}_\nu\left[\xi(i)\xi(j)\right] & l = 0 \\ \displaystyle\sum_{|i-j|>l} (|i-j|-l)\bar{\xi}(i)\bar{\xi}(j) & l > 0 \end{cases}. \tag{5.25}$$

Thus, $\kappa(l) \geq 0$ and hence $\sum_{i=0}^{t-1}\sum_{l=0}^{\infty} \kappa\left(l\right) \mathbb{1}_{\{\Delta(i)=l\}}$ is a sum of non-negative terms which increases in time. Furthermore, this process is predictable as it only depends on the values of $\Delta(0)\ldots\Delta(t-1)$. Therefore, (5.24) is a decomposition of $\Delta(t)$ into the sum of a martingale and an increasing predictable process.

We look at the limiting behavior of this decomposition under a diffusive scaling and match it term by term with Tanaka's formula in Eq. 5.23. As argued in the paragraph after Eq. 5.21, the term $\Delta(t) = |R^1(t) - R^2(t)|$ converges under diffusive scaling to $|B^1(t) - B^2(t)|$. Since the term $M(t)$ is a martingale, it should likewise converge to a limiting martingale. Therefore, the second term on the right-hand side of Eq. 5.24 should converge to the local time $L^{B^1-B^2}(t)$ in Eq. 5.23 (where we take $B = B^1 - B^2$). Thus, taking $t = NT$, under the diffusive scaling

$$\lim_{N\to\infty} \frac{1}{\sqrt{2DN}} \sum_{l=0}^{\infty} \kappa\left(l\right) \sum_{i=0}^{NT-1} \mathbb{1}_{\{\Delta(i)=l\}} = L^{B^1-B^2}(T). \tag{5.26}$$

This completes the first step towards establishing Eq. 5.22. Of course, that result calls for taking the limit of the discrete local time at 0,

$$\lim_{N\to\infty} \frac{1}{\sqrt{2DN}} \sum_{i=0}^{Nt-1} \mathbb{1}_{\{\Delta(i)=0\}}, \tag{5.27}$$

whereas Eq. 5.26 is in terms of a combination of local time at every position $l \in \mathbb{Z}_{\geq 0}$.

To compare the limits in Eqs. 5.26 and 5.27, we will show in Section 5.7.1.1 that for $l \geq 0$,

$$\lim_{t\to\infty} \frac{\sum_{i=0}^{t} \mathbb{1}_{\{\Delta(i)=l\}}}{\sum_{i=0}^{t} \mathbb{1}_{\{\Delta(i)=0\}}} = \tilde{\mu}(l), \tag{5.28}$$

where $\tilde{\mu}$ is the normalized invariant measure of $V(t)$, see the discussion after Eq. 5.5. For large t, we can therefore approximately relate the local time at l and at 0 so that

$$\sum_{i=0}^{t} \mathbb{1}_{\{\Delta(i)=l\}} \approx \tilde{\mu}(l) \sum_{i=0}^{t} \mathbb{1}_{\{\Delta(i)=0\}}. \tag{5.29}$$

Using this approximation, we obtain

$$\sum_{l=0}^{\infty} \kappa\left(l\right) \sum_{i=0}^{t-1} \mathbb{1}_{\{\Delta(i)=l\}} \approx \left(\sum_{l=0}^{\infty} \kappa\left(l\right) \tilde{\mu}\left(l\right)\right) \sum_{i=0}^{t-1} \mathbb{1}_{\{\Delta(i)=0\}}$$

Substituting this into Eq. 5.26 and rearranging, we obtain

$$\lim_{N\to\infty} \frac{1}{\sqrt{2DN}} \sum_{i=0}^{Nt-1} \mathbb{1}_{\{\Delta(i)=0\}} = \frac{1}{\sum_{l=0}^{\infty} \kappa\left(l\right) \tilde{\mu}\left(l\right)} L^{B^1-B^2}(t). \tag{5.30}$$

After substituting in our definitions of $\kappa(l)$ and $\Delta\left(t\right)$, we conclude that

$$\lim_{N\to\infty} \frac{1}{\sqrt{2DN}} \sum_{i=0}^{Nt-1} \mathbb{1}_{\{R^1(i)=R^2(i)\}} = \frac{1}{\sum_{l=0}^{\infty} \tilde{\mu}\left(l\right) \mathbf{E}_{\nu}\left[\Delta\left(t+1\right) - \Delta\left(t\right) \mid \Delta\left(t\right) = l\right]} L^{B^1-B^2}(t).$$

which indeed matches Eq. 5.22.

5.7.1.1 Invariant Measure of V. In this section, we demonstrate the claim in Eq. 5.28. If a Markov chain is irreducible (starting from any state, the chain can eventually reach any other state) and recurrent (it returns to every state infinitely many times), then it has a unique invariant measure up to a constant multiple. As explained earlier, we consider V under the untilted measure $\mathbf{E}_{\nu}$ on the two-point motion rather than the tilted probability distribution. We can see that $V(t)$ is recurrent as follows: When $V(t)$ is away from 0 its increments are i.i.d. and have mean 0 and thus, by the Chung-Fuchs theorem [139], the walk will almost surely eventually return to 0. Once at 0, it will eventually leave, and the above argument can be repeated to show that $V(t)$ will return to 0 infinitely many times, which suffices to show recurrence. However, $V(t)$ may not always be irreducible. For example, consider the case where $R^1(t)$ and $R^2(t)$ only take nearest neighbor jumps. Then $V(t)$ can only take jumps that are multiples of 2, so if it starts from 0, it can only visit sites in the sublattice $2\mathbb{Z}$.

Let us first deal with the case where $V(t)$ is irreducible so that it has a unique (up to a constant multiple) invariant measure. Let

$$T_0 = 0, \quad T_k = \inf\{n > T_{k-1} : V(n) = 0\}$$

so that T_k is the kth return time to 0. Define $Y_k^l = \sum_{i=T_k}^{T_{k+1}-1} \mathbb{1}_{\{V(i)=l\}}$. For an irreducible and recurrent Markov chain, we know that the measure μ on $\mathbb{Z}$ defined by $\mu(l) := \mathbb{E}[Y_0^l]$ is an invariant measure for V where $\mathbb{E}$ is the expectation of the walker starting at 0. Furthermore, since V is a Markov chain, the random variables $(Y_k^l)_{k\geq 0}$ are i.i.d. for a fixed l.

We have that

$$\frac{Y_0^l + \cdots + Y_{n-1}^l}{n} = \frac{\sum_{i=0}^{T_n-1} \mathbb{1}_{\{V(i)=l\}}}{\sum_{i=0}^{T_n-1} \mathbb{1}_{\{V(i)=0\}}}. \tag{5.31}$$

The equality in the denominator is due to the fact that we visit 0 exactly n times before time $T_n - 1$. By the law of large numbers for i.i.d. random variables,

$$\lim_{n\to\infty} \frac{Y_0^l + \cdots + Y_n^l}{n} = \mathbb{E}[Y_0^l] = \mu(l). \tag{5.32}$$

almost surely. On the other hand, we have that

$$\lim_{n\to\infty} \frac{\sum_{i=0}^{T_n-1} \mathbb{1}_{\{V(i)=l\}}}{\sum_{i=0}^{T_n-1} \mathbb{1}_{\{V(i)=0\}}} = \lim_{t\to\infty} \frac{\sum_{i=0}^{t} \mathbb{1}_{\{V(i)=l\}}}{\sum_{i=0}^{t} \mathbb{1}_{\{V(i)=0\}}}. \tag{5.33}$$

Thus, by combining Eqs. 5.31, 5.32, and 5.33, we obtain

$$\lim_{t\to\infty} \frac{\sum_{i=0}^{t} \mathbb{1}_{\{V(i)=l\}}}{\sum_{i=0}^{t} \mathbb{1}_{\{V(i)=0\}}} = \mu(l). \tag{5.34}$$

Note that by symmetry $\mu(l) = \mu(-l)$. Furthermore, for $l = 0$, we have

$$\mathbb{1}_{\{\Delta(i)=l\}} = \mathbb{1}_{\{V(i)=l\}}$$

and for $l > 0$,

$$\mathbb{1}_{\{\Delta(i)=l\}} = \mathbb{1}_{\{V(i)=l\}} + \mathbb{1}_{\{V(i)=-l\}}.$$

Putting this all together with Eq. 5.34, we conclude that

$$\lim_{t\to\infty} \frac{\sum_{i=0}^{t} \mathbb{1}_{\{\Delta(i)=l\}}}{\sum_{i=0}^{t} \mathbb{1}_{\{\Delta(i)=0\}}} = \tilde{\mu}(l)$$

where

$$\tilde{\mu}(l) = \begin{cases} 1 & \text{if } l = 0 \\ 2\mu(l) & \text{if } l > 0. \end{cases}$$

Finally, we consider the case where $V(t)$ is not irreducible. We can decompose $\mathbb{Z}$ into the union of finitely many closed and irreducible sets (sublattices) E_i. Let E_0 be the set containing 0. Since we have $V(0) = 0$, we know that $V(t) \in E_0$ for all t. Let μ be the unique invariant measure of the Markov chain $V(t)$ when restricted to the state space E_0. All of the above analysis goes through, but the sum $\sum_{l=0}^{\infty} \kappa(l)\tilde{\mu}(l)$ gets replaced by $\sum_{l \in E_0} \kappa(l)\tilde{\mu}(l)$. An example of this situation is when R^1 and R^2 are nearest neighbor random walks. In this case, $V(t)$ is restricted to the even integer sublattice, i.e., $E_0 = 2\mathbb{Z}$.

5.8 Convergence of the Tail Probability to the SHE

The above discussion shows that the first two moments of the rescaled probability mass distribution converge to the moments of the SHE. In this section, we discuss the convergence of the tail probability, which can be written as

$$\mathbb{P}^{\boldsymbol{\xi}}(R(NT) \geq c(N)T + \sqrt{2DN}X) = \mathbb{E}^{\boldsymbol{\xi}}\left[\mathbb{1}_{\left\{R(NT) \geq c(N)T + \sqrt{2DN}X\right\}}\right] \tag{5.35}$$

Defining (and then simplifying)

$$\phi_N^{\text{tail}}(X') := \frac{C(N,T,X)}{C(N,T,X')}\mathbb{1}_{\{X' \geq X\}} = \exp\left\{-\frac{N^{1/4}}{\sqrt{2D}}(X' - X)\right\}\mathbb{1}_{\{X' \geq X\}} \tag{5.36}$$

we can rewrite Eq. 5.35 as

$$\begin{aligned} \mathbb{P}^{\boldsymbol{\xi}}(R(NT) \geq c(N)T + \sqrt{2DN}X) &= \frac{\mathbb{E}^{\boldsymbol{\xi}}\left[C\left(N, T, \frac{R^1(NT) - c(N)T}{\sqrt{2DN}}\right)\phi_N^{\text{tail}}\left(\frac{R^1(NT) - c(N)T}{\sqrt{2DN}}\right)\right]}{C(N,T,X)} \\ &= \frac{1}{C(N,T,X)}\mathscr{U}_N(T,\phi), \end{aligned} \tag{5.37}$$

where we recall $\mathscr{U}_N(T,\phi)$ from Eq. 5.6. Observe that as $N \to \infty$,

$$\exp\left\{-\frac{N^{1/4}}{\sqrt{2D}}(X'-X)\right\}\mathbb{1}_{\{X'\geq X\}} \approx \delta\left(\frac{N^{1/4}}{\sqrt{2D}}(X'-X)\right)\mathbb{1}_{\{X'\geq X\}}.$$

Note here that the convergence shown earlier was for fixed ϕ while we are now permitting ϕ to vary in N and tend to a Dirac delta function. Thus, in light of the convergence of $\mathscr{U}_N(T,\phi)$ to the SHE, this implies that

$$\mathbb{P}^{\boldsymbol{\xi}}(R(NT) \geq c(N)T + \sqrt{2DN}X) \approx \frac{1}{C(N,T,X)}\int_X^\infty \delta\left(-\frac{N^{1/4}}{\sqrt{2D}}(X'-X)\right)Z(T',X')dX' \tag{5.38}$$

$$= \frac{\sqrt{2D}}{N^{1/4}C(N,T,X)}Z(T,X). \tag{5.39}$$

Moving the prefactor to the left-hand side,

$$\lim_{N\to\infty}\frac{N^{1/4}C(N,T,X)}{\sqrt{2D}}\mathbb{P}^{\boldsymbol{\xi}}(R(NT) \geq c(N)T + \sqrt{2DN}X) = Z(T,X). \tag{5.40}$$

Thus, the tail probability converges to the SHE with the same noise strength but a modified prefactor.

5.9 The distribution of the extreme location

In a system of many diffusing particles, the location of the particle that has moved the furthest is often more important than that of a typical particle, as in oocyte fertilization [94, 95, 96], neuronal activation [8], and the information flow in networks [97, 98]. Thus, understanding the distribution of the extreme particle is of critical importance.

We summarize our main result in [133], where we used the above results for the tail probability to characterize the statistics of the *extreme location*, which is the particle that has traveled the furthest, as a function of time. In that work, we argued that a measurement of the extreme location can be used to reveal microscopic information about the underlying environment through the coefficient

λ_{ext}. To do this, we studied the extreme location of N random walks at time t,

$$\text{Max}_t^N := \max\left(\{R^1(t), \dots R^N(t)\}\right),$$

recalling that $R^1(t), \dots, R^N(t)$ for $t \in \mathbb{Z}_{\geq 0}$ are random walks distributed according to the measure $\mathbb{P}^{\boldsymbol{\xi}}$. Using our results for the distribution of the tail probability in Eq. 5.40, we found that as $t \to \infty$,

$$\text{Max}_t^N \approx \sqrt{4Dt\ln(N)} + \text{Gumbel}\left(0, \sqrt{\frac{\ln(N)}{Dt}}\right) + \sqrt{\frac{Dt}{\ln(N)}} h\left(0, \frac{8\lambda_{\text{ext}}^2 \ln(N)^2}{Dt}\right), \tag{5.41}$$

where Gumbel(μ, β) is a Gumbel random variable with location μ and shape β, $h(X, T)$ solves the Kardar-Parisi-Zhang (KPZ) equation with noise strength $D_0 = 1/2$ and these two random variables are independent.

The first and second term in Eq. 5.41 agree with results from classical diffusion on the distribution of the extreme location [102, 106].The derivation of the third term in Eq. 5.41 is the main result of [133]. Since only the second and third terms are random variables, the variance of Max_t^N has two contributions. We find that as $t \to \infty$

$$\mathbf{Var}(\text{Max}_t^N) \approx \frac{\pi^2 Dt}{6\ln(N)} + \lambda_{\text{ext}}\sqrt{2\pi Dt}$$

where $\mathbf{Var}(\cdot)$ is the variance under the annealed measure $\mathbf{P}_\nu$, the first term is the classical diffusion result which comes from taking the variance of the Gumbel random variable in Eq. 5.41 and the second term comes from taking the variance of the KPZ term and then using the small time expansion of $h(0, T)$ [73, 71].

By measuring the variance of the extreme location and subtracting off the contribution due to classical diffusion, the KPZ term, and subsequently λ_{ext}, can be directly measured. Thus, a macroscopic measurement of the fluctuations of the extreme location over time yields microscopic information about the underlying environment through the coefficient λ_{ext}.

5.10 Conclusion

We have demonstrated that under a moderate deviations scaling, there are universal KPZ fluctuations for a large class of RWRE models. This class of model only includes environments which are delta correlated in space and time making the environment memoryless. However, as our model is a discretized/coarse grained model, it can be equally well applied to environments with memories that decay faster than a power-law by choosing the time steps in the model to be larger than the correlation time of the memory. It should be noted that this excludes a large number of interesting systems with power-law memories [137] which would be expected to deviate even farther from the Einstein model in their extremes.

We show that the strength of the noise of the KPZ equation is characterized by the variable λ_{ext}, which depends on the statistics of the underlying environment. Our results can be extended to characterize the distribution of the extreme value statistics of a system of N diffusing particles as in [107, 122, 133] (e.g., the first time a particle reaches a position L or the position of the farthest particle at time t). Thus, we have established a link between the extreme value statistics of a system of diffusing particles and the microscopic rheological properties of the underlying environment.

5.11 Acknowledgments

We thank Guillaume Barraquand, Pierre Le Doussal, and Shalin Parekh for helpful discussions. This work was funded by the W. M. Keck Foundation Science and Engineering grant on "Extreme Diffusion." I. C. also wishes to acknowledge ongoing support from NSF DMS:1811143, 1937254, and 2246576, and the Simons

Foundation Investigator Grant No. 929852. H. D. wishes to acknowledge support from the NSF GRFP DGE:2036197. This work benefited from access to the University of Oregon high performance computing cluster, Talapas.

CHAPTER VI

SUPER-UNIVERSAL BEHAVIOR OF OUTLIERS DIFFUSING IN A SPACE-TIME RANDOM ENVIRONMENT

This chapter is published as: Hass, J. (2025, May). Super-Universal Behavior of Outliers Diffusing in a Space-Time Random Environment (No. arXiv:2505.01533). arXiv. doi:10.48550/arXiv.2505.01533. This is a single author paper in which I came up with the main idea of the paper and derived all of the theoretical and numerical results.

6.1 Abstract

I characterize the extreme location and extreme first passage time of a system of N particles independently diffusing in a space-time random environment. I show these extreme statistics are governed by the Kardar-Parisi-Zhang (KPZ) equation and derive their mean and variance. I find the scalings of the statistics depend on the moments of the environment. Each scaling regime forms a universality class which is controlled by the lowest order moment which exhibits random fluctuations. When the first moment is random, the environment plays the role of a random velocity field. When the first moment is fixed but the second moment is random, the environment manifests as fluctuations in the diffusion coefficient. As each higher moment is fixed, the next moment determines the scaling behavior. Since each scaling regime forms a universality class, this model for diffusion forms a super-universality class. I confirm my theoretical predictions using numerics for a wide class of underlying environments.

6.2 Introduction

The classical theory of diffusion reduces the stochastic and chaotic motion of particles due to a complex environment to a single parameter – the diffusion coefficient, D. [23, 21, 22, 26, 28]. This simplification relies on two key assumptions: particles evolve independently and the mean and variance of their jump distribution are well defined. When the second assumption is violated, specifically when the variance is not well defined, this leads to phenomenon described by anomalous diffusion and Lévy flights [140, 141, 124, 39]. I study *Random Walks in a Random Environment* (RWRE) models which violates the first assumption, independence, by introducing a space-time random environment that induces correlations in the movement of nearby particles. Here I show the environment effects the fluctuations of particles at the edge of a system of N diffusing particles. I show that the fluctuations in these extreme particles are characterized by the Kardar-Parisi-Zhang (KPZ) equation [1, 66] with universal scalings. In doing so, I derive the prefactors through which the environment controls these statistics. Even if the leading moments of the environment are fixed the higher order moments will control the fluctuations at the edge of the system.

I study RWRE models for diffusion wherein particles evolve on the integer lattice in a space-time random environment as shown in Fig. 18. I derive the mean and variance of the first time a particle passes a barrier at position L, the *extreme first passage time*, and the maximum position at time t, the *extreme location*, for a system of N diffusing particles. Previous work has shown that when the first moment of the environment is random, the distribution of these extreme statistics form a universality class which is governed by the KPZ universality class [6, 69, 7, 111, 107, 122, 133, 127]. Here, I generalize these results to show there are an infinite number of universality classes where the lowest random moment of the environment determines which universality class a RWRE model is governed by.

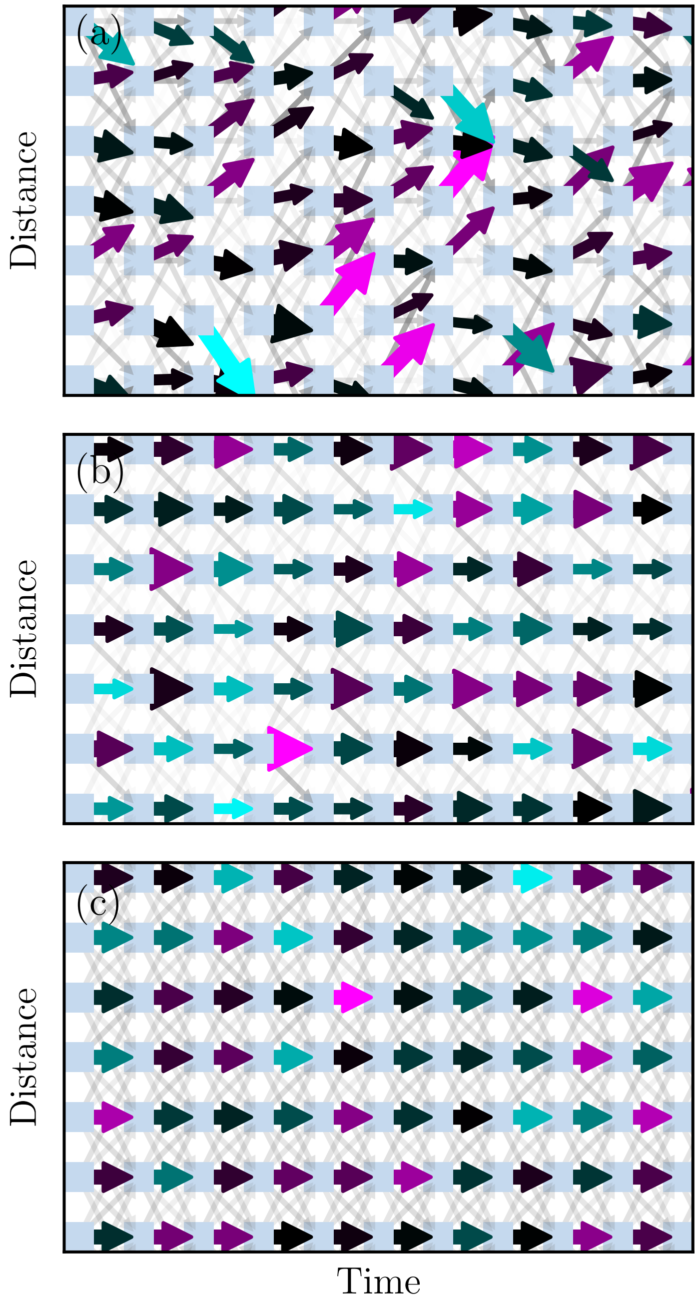

Figure 18. Several examples of random environments. Blue boxes are lattice sites and the opacity of the gray arrows shows the probability of jumping to a site. Large, solid arrows show the average drift at each site. The size of the arrow scales with the variance of the jump distribution and the color denotes the skew (cyan skewed down and pink skewed up). (a) Environment where the drift, variance and skewness are random. (b) Environment with no drift, but the variance and skewness are random. (c) Environment with no drift, a constant variance but a random skewness.

6.3 RWRE Models

I define the class of RWRE models that I study. I begin by defining the space-time random environment as follows. Let ν define a probability distribution on the space of probability distributions on the integers, $\mathbb{Z}$. I define ξ as a probability distribution on $\mathbb{Z}$ which is sampled according to ν. Then $\xi(i)$ denotes the probability mass at $i \in \mathbb{Z}$. Each choice of ν defines a new RWRE model.

Given a distribution ν, I define the environment as $\boldsymbol{\xi} = \{\xi_{x,t} : x \in \mathbb{Z}, t \in \mathbb{Z}_{>0}\}$ where each $\xi_{x,t}$ is a probability distribution on $\mathbb{Z}$ independently sampled from ν for each site (x, t). Three examples of an environment, $\boldsymbol{\xi}$, are given in Fig. 18, where $\xi_{x,t}$ is given by the light grey arrows at each (x, t). Physically, a single instatiation of an experiment of particles diffusing yields a different environment, $\boldsymbol{\xi}$.

I give an example of ν where the first moment of the jump distribution, $\sum_{i\in\mathbb{Z}} \xi_{x,t}(i)i$, is random and another example where the first moment is fixed. Fixing higher moments becomes more nuanced, but I have given several examples in the "End Matter". To achieve an environment where the first moment of the jump distribution is random, I use the *Dirichlet* distribution which is sampled as follows. Begin by generating a list of Gamma distributed random variables, $(X_{-k}, \dots, X_k)$, with shapes $\vec{\alpha} = (\alpha_{-k}, \dots, \alpha_k)$ for $\alpha_i > 0$ and rate $\beta = 1$ where $k \in \mathbb{Z}_{>0}$ determines the width of the distribution. A sample of the Dirichlet distribution is this list of Gamma distributed random variables normalized to sum to 1 by dividing by their sum, $Z = \sum_{i=-k}^{k} X_i$. Then set $\xi(i) = X_i/Z$ for $i \in [-k, k]$ and $\xi = 0$ otherwise. To achieve an environment where the first moment is fixed, but the second moment is random, I study the *symmetric Dirichlet* distribution. A sample of this distribution is generated by sampling the Dirichlet distribution, $\frac{1}{Z}(X_{-k}, \dots, X_k)$, for a given $\vec{\alpha}$ and then setting $\xi(i) = (X_i + X_{-i})/(2Z)$ for

$i \in [-k, k]$ and $\xi = 0$ otherwise. Thus, the first moment is always zero, i.e. $\sum_{i\in\mathbb{Z}} \xi_{x,t}(i)i = 0$, but the second moment is random.

I define $\mathbb{E}_\nu[\bullet]$ and $\mathrm{Var}_\nu(\bullet)$ as the expectation and variance over the probability distribution ν. This expectation and variance is obtained by taking the average over many different environments, $\boldsymbol{\xi}$, sampled via ν. I denote $\mathbb{E}_\nu[\xi]$ as the average probability distribution where I have dropped the subscript x, t because all $\xi_{x,t}$ are sampled independently from ν. Thus, the average of each $\xi_{x,t}$ is the same. I will only consider distributions ν which produce an average of no drift, i.e. $\sum_{i\in\mathbb{Z}} \mathbb{E}_\nu[\xi(i)]i = 0$; although, my results likely hold for models with drift after shifting to a moving reference frame.

I define $\mathbb{P}^{\boldsymbol{\xi}}$ as the probability measure of N independent random walks, $R^1, \ldots, R^N$, evolving in the same environment, $\boldsymbol{\xi}$. I let $\mathbb{E}^{\boldsymbol{\xi}}[\bullet]$ and $\mathrm{Var}^{\boldsymbol{\xi}}(\bullet)$ denote the mean and variance associated with the measure $\mathbb{P}^{\boldsymbol{\xi}}$. This mean and variance corresponds to averaging over many samples of a random variable in the *same* environment. I denote $R^i(t) \in \mathbb{Z}$ as the position of the i^{th} walker at time t and set $R^i(0) = 0$ for all $i \in [1, N]$ so all walkers start at the origin. The transition probabilities of each walker in $\boldsymbol{\xi}$ is given by

$$\mathbb{P}^{\boldsymbol{\xi}}(R(t+1) = x + i \mid R(t) = x) = \xi_{x,t}(i)$$

where I have dropped the super-script i here and below since all walkers are independent and identically distributed (i.i.d). The walkers evolve independently in the same environment, but walks at the same site (x, t) have correlated motion since they sample the same jump distribution, $\xi_{x,t}$.

Given a single random walk, I denote the probability of the walk being at site x at time t as $p^{\boldsymbol{\xi}}(x, t) := \mathbb{P}^{\boldsymbol{\xi}}(R(t) = x)$. By independence, all random walks have the same distribution $p^{\boldsymbol{\xi}}(x,t)$. This distribution obeys the recurrence relation

$$p^{\boldsymbol{\xi}}(x,t+1) = \sum_{j\in\mathbb{Z}} p^{\boldsymbol{\xi}}(x-j,t)\xi_{t,x-j}(j)$$

with initial condition $p^{\boldsymbol{\xi}}(x,0) = \delta_{x,0}$ where $\delta_{x,0}$ is the Kronecker-delta.

I conclude by defining the mean and variance of a random variable averaged over many samples from many different environments which I denote as $\mathbf{E}[\bullet]$ and $\mathbf{Var}(\bullet)$. These are the mean and variance which would be experimentally measurable, as these statistics correspond to averaging over many runs of an experiment where the random, underlying environment is unknown. I relate $\mathbf{E}[\bullet]$ and $\mathbf{Var}(\bullet)$ to my previous definitions using the total law of expectation and variance such that $\mathbf{E}[\bullet] = \mathbb{E}_\nu[\mathbb{E}^{\boldsymbol{\xi}}[\bullet]]$ and $\mathbf{Var}(\bullet) = \mathbb{E}_\nu[\mathrm{Var}^{\boldsymbol{\xi}}(\bullet)] + \mathrm{Var}_\nu(\mathbb{E}^{\boldsymbol{\xi}}[\bullet])$.

6.4 Extreme Value Statistics

For a system of N particles, I study the extreme location and the extreme first passage time. I define the extreme location at time t as

$$\mathrm{Max}_t^N := \max(R^1(t),\ldots,R^N(t)).$$

Since the random walks are independent, the distribution of Max_t^N in $\boldsymbol{\xi}$ is given by

$$\mathbb{P}^{\boldsymbol{\xi}}(\mathrm{Max}_t^N \le x) = (1-\mathbb{P}^{\boldsymbol{\xi}}(R(t)\ge x))^N. \tag{6.1}$$

I define τ_L^i as the first time the i^{th} particle passes position $L \in \mathbb{Z}_{>0}$. Then the extreme first passage time of N particles at a distance L is

$$\mathrm{Min}_L^N := \min(\tau_L^1,\ldots,\tau_L^N).$$

Since the location of the random walks are i.i.d., all τ_L^i are also i.i.d. Thus, the distribution of the extreme first passage time is

$$\mathbb{P}^{\boldsymbol{\xi}}(\mathrm{Min}_L^N \ge t) = (1-\mathbb{P}^{\boldsymbol{\xi}}(\tau_L\le t))^N. \tag{6.2}$$

I derive $\mathbf{E}[\bullet]$ and $\mathbf{Var}(\bullet)$ for Max_t^N and Min_L^N; that is, the mean and variance calculated over many experiments in different environments. I break each extreme value statistic into two sources of randomness: the mean of the statistic in a given environment and fluctuations about that mean.

I begin by discussing the extreme location. I approximate the mean of the extreme location in a given environment, $\mathbb{E}^{\boldsymbol{\xi}}[\mathrm{Max}_t^N]$, with Env_t^N. I define Env_t^N as

$$\mathrm{Env}_t^N := \max\left(x : \mathbb{P}^{\boldsymbol{\xi}}(R(t) \geq x) \geq \frac{1}{N}\right).$$

I argue Env_t^N is a natural approximation for $\mathbb{E}^{\boldsymbol{\xi}}[\mathrm{Max}_t^N]$ because by combining Eq. 6.1 with my definition for Env_t^N, $\mathbb{P}^{\boldsymbol{\xi}}(\mathrm{Max}_t^N \leq \mathrm{Env}_t^N) \approx e^{-1}$ as $N \to \infty$. Therefore, Env_t^N is approximately the median of Max_t^N in a given environment which can further be approximated as $\mathbb{E}^{\boldsymbol{\xi}}[\mathrm{Max}_t^N]$. Notice Env_t^N only captures environmental fluctuations since it only depends on $\boldsymbol{\xi}$. For classical diffusion, Env_t^N is constant since the environment is constant. I define the fluctuations about Env_t^N as $\mathrm{Sam}_t^N := \mathrm{Max}_t^N - \mathrm{Env}_t^N$. Then Sam_t^N represents the effects of sampling Max_t^N in a given environment. Physically, the distribution of Sam_t^N can be constructed by measuring Max_t^N many times in the *same* environment and then subtracting the measured mean, i.e. $\mathbb{E}^{\boldsymbol{\xi}}[\mathrm{Max}_t^N]$.

Similarly, for the extreme first passage time, I approximate $\mathbb{E}^{\boldsymbol{\xi}}[\mathrm{Min}_L^N]$ via

$$\mathrm{Env}_L^N := \min\left(t : \mathbb{P}^{\boldsymbol{\xi}}(\tau_L \leq t) \geq \frac{1}{N}\right)$$

and fluctuations about Env_L^N as $\mathrm{Sam}_L^N := \mathrm{Min}_L^N - \mathrm{Env}_L^N$.

6.5 Theoretical Methods

I generalize the methods presented in [133] to characterize the tail probability, $\mathbb{P}^{\boldsymbol{\xi}}(R(t) \geq x)$, in the limit that $t \to \infty$. I use the replica method to derive the first two moments of the tail probability and show the moments converge to those of the multiplicative stochastic heat equation (SHE),

$$\partial_T Z(X,T) = \partial_X^2 Z(X,T) + \sqrt{2D_0} Z(X,T)\eta$$

where $Z(X,T)$ is the solution to the SHE, $D_0 \in \mathbb{R}_{>0}$ is the noise strength and η is space time white noise with the properties $\mathbb{E}[\eta(X,T)] = 0$, $\mathbb{E}[\eta(X,T)\eta(X',T')] = \delta(X-X',T-T')$ where $\delta(x,t)$ is the Dirac delta function. Here, $\mathbb{E}[\bullet]$ represents and average over the noise, η. The KPZ equation is related to the SHE via a logarithm , $Z(X,T) = e^{h(X,T)}$, where $h(X,T)$ solves the KPZ equation

$$\partial_T h(X,T) = \partial_X^2 h(X,T) + (\partial_X h(X,T))^2 + \sqrt{2D_0}\eta.$$

The crux of my derivation is identifying the noise strength of the SHE in terms of the statistics of the environment. See [89] for the derivation of the first two moments.

The scaling regime where these KPZ fluctuations appear scales as $R(t) \propto t^{\frac{4m-1}{4m}}$ where $m \in \mathbb{Z}_{>0}$ and $m-1$ is the number of deterministic moments of the jump distribution [142]. When $m = 1$, there are no moments fixed in the environment, as shown in Fig. 18a. This corresponds to an environment which acts as a space-time random velocity field creating correlations in the velocity of nearby particles. When $m = 2$, the first moment of the environment is always fixed such that ν only generates distributions where $\sum_{i\in\mathbb{Z}} \xi_{x,t}(i)i = 0$, as shown in Fig. 18b. Since I only consider net drift free environments, the first moment must always be 0. This corresponds to an environment where there are no correlations in the velocity of nearby particles, but the diffusion coefficient is a space-time random value. When $m = 3$, the first moment and second moments are deterministic such that ν only generates distributions where $\sum_{i\in\mathbb{Z}} \xi_{x,t}(i)i = 0$ and $\sum_{i\in\mathbb{Z}} \xi_{x,t}(i)i^2 = 2D$ for $D \in \mathbb{R}_{>0}$, as shown in Fig. 18c.

6.6 Theoretical Results

I define the diffusion coefficient for a RWRE model as half the variance in the average environment,

$$D := \frac{1}{2} \sum_{i \in \mathbb{Z}} \mathbb{E}_{\nu}[\xi(i)] i^2 \tag{6.3}$$

where the mean in the average environment is 0 since I consider net drift free environments. Since the tail probability depends on the number of moments that are fixed, m, the extreme value statistics will as well. I derive the following results for the extreme location and extreme first passage time in the limit that $t^{2m-1} \gg \lambda_{\text{ext}}^2 \ln(N)^{2m}$ and $L^{4m-2} \gg \lambda_{\text{ext}}^2 \ln(N)^{4m-1}$, respectively, where λ_{ext} is defined in Eq. 6.8 and $N \gg 1$.

I find the mean of Max_t^N and Min_L^N are given by

$$\mathbf{E}[\text{Max}_t^N] \approx \sqrt{4Dt \ln(N)} \quad \text{and} \quad \mathbf{E}[\text{Min}_L^N] \approx \frac{L^2}{4D \ln(N)}$$

which match the classical predictions [104, 102, 100, 106, 125, 95, 101]. Notice that the means only depend on the diffusion coefficient of the model and not any other statistics of the environment.

Although the means give the same results as classical predictions, the variances display more interesting behavior. I find the variance of Sam_t^N and Sam_L^N are Gumbel distributed with variances

$$\mathbf{Var}(\text{Sam}_t^N) \approx \frac{\pi^2 D t}{6 \ln(N)} \tag{6.4}$$

$$\mathbf{Var}(\text{Sam}_L^N) \approx \frac{\pi^2 L^4}{96 D^2 \ln(N)^4}. \tag{6.5}$$

These results match the variance of the extreme location and first passage time predicted classically [104, 102, 100, 106, 125, 95, 101] and thus only depend on the diffusion coefficient and no other statistics of the environment. This makes sense because in classical diffusion, the environment is homogeneous and thus the variance only depends on fluctuations due to sampling random walks.

I find the variance of Env_t^N and Env_L^N are given by

$$\mathrm{Var}_\nu(\mathrm{Env}_t^N) \approx \frac{\sqrt{2\pi}}{(m!)^2}\lambda_{\mathrm{ext}} \ln(N)^{m-1}(Dt)^{\frac{3-2m}{2}} \tag{6.6}$$

$$\mathrm{Var}_\nu(\mathrm{Env}_L^N) \approx \frac{\lambda_{\mathrm{ext}}\sqrt{\pi}2^{\frac{4m-9}{2}}}{(m!)^2D^2} \ln(N)^{\frac{4m-9}{2}} L^{5-2m} \tag{6.7}$$

where $m-1$ is the number of deterministic moments and

$$\lambda_{\mathrm{ext}} = \frac{\mathrm{Var}_\nu\left(\mathbb{E}^{\boldsymbol{\xi}}[Y^m]\right)}{2\mathbb{E}_\nu[\mathrm{Var}^{\boldsymbol{\xi}}(Y)]} \tag{6.8}$$

where $Y \sim \xi_{x,t}$ is distributed according to a single step of a random walk such that

$$\begin{aligned}\mathrm{Var}_\nu\left(\mathbb{E}^{\boldsymbol{\xi}}[Y^m]\right) = \mathbb{E}_\nu &\left[\left(\sum_{i\in\mathbb{Z}} \xi_{x,t}(i) i^m\right)^2\right] \\ &- \left(\sum_{i\in\mathbb{Z}} \mathbb{E}_\nu[\xi(i)] i^m\right)^2,\end{aligned} \tag{6.9}$$

$$\mathbb{E}_\nu[\mathrm{Var}^{\boldsymbol{\xi}}(Y)] = 2D - \mathrm{Var}_\nu(\mathbb{E}^{\boldsymbol{\xi}}[Y]). \tag{6.10}$$

Since Env_t^N and Env_L^N are constant in a given environment, I calculate the mean and variance with respect to ν.

Notice that for $m > 1$, the environmental variance for the extreme location, $\mathrm{Var}_\nu(\mathrm{Env}_t^N)$, decreases in t. Similarly, for $m > 2$, the environmental variance for the extreme first passage time, $\mathrm{Var}_\nu(\mathrm{Env}_L^N)$, decreases in L. Thus, any RWRE model with $m > 2$ will yield the same measurements, as $t \to \infty$ for the extreme location and $L \to \infty$ for the extreme first passage time, as the classical predictions since the environmental variance asymptotes to 0 but the sampling variance persists. Luckily, the $m = 1$ and $m = 2$ case have the most physical interpretations as they correspond to an environment which represents an underlying velocity field and random diffusion coefficient, respectively.

For $m = 1$, the form of λ_{ext} in Eq. 6.8 only contains one unknown quantity, $\frac{1}{2}\mathbb{E}_\nu\left[\left(\sum_{i\in\mathbb{Z}}\xi_{x,t}i\right)^2\right]$, which was termed the *extreme diffusion coefficient*, D_{ext}, in [133]. For $m > 1$, I define an analogous extreme diffusion coefficient as $D_{\text{ext}}^{(m)} := \frac{1}{2}\text{Var}_\nu\left(\mathbb{E}^{\boldsymbol{\xi}}[Y^m]\right)$. Thus, the extreme diffusion coefficient is simply the variance of the m^{th} moment of the jump distribution over all environments. For $m = 1$, $D_{\text{ext}}^{(1)}$ is the variance in the drift and for $m = 2$, $D_{\text{ext}}^{(2)}$ is the variance in the diffusion coefficient.

I derive Eq. 6.8 under the condition

$$\mathbb{E}_\nu[\xi_{x,t}(i)\xi_{x,t}(j)] = c\mathbb{E}_\nu[\xi_{x,t}(i)]\mathbb{E}_\nu[\xi_{x,t}(j)] \tag{6.11}$$

for all $i \neq j$ where $c \in (0,1)$. This condition is satisfied for every distribution I consider for $m = 1$. Although this is not the case for the distributions that I consider for $m > 1$, Eq. 6.11 is approximately satisfied in the weak noise limit where $\xi_{x,t}(i) = \mathbb{E}_\nu[\xi_{x,t}(i)] + \sigma_{x,t}(i)$ and $\sigma_{x,t}(i) \ll \mathbb{E}_\nu[\xi_{x,t}(i)]$ for all $i \in \mathbb{Z}$.

In finding the first two moments of Env_t^N and Sam_t^N, I find they are independent as $t \to \infty$. Similarly, Env_L^N and Sam_L^N are independent as $L \to \infty$. By this independence, I find

$$\mathbf{Var}(\text{Max}_t^N) \approx \text{Var}_\nu(\text{Env}_t^N) + \mathbf{Var}(\text{Sam}_t^N) \tag{6.12}$$

$$\mathbf{Var}(\text{Min}_L^N) \approx \text{Var}_\nu(\text{Env}_L^N) + \mathbf{Var}(\text{Sam}_L^N). \tag{6.13}$$

6.7 Numerical Results

Figs. 2a,d) show the collapse of each variance to their numerically measured counterpart in the limit that $t \to \infty$ and $L \to \infty$. I find $\text{Var}_\nu(\mathbb{E}^{\boldsymbol{\xi}}[\text{Max}_t^N])$ is well approximated by $\text{Var}_\nu(\text{Env}_t^N)$ and $\mathbb{E}_\nu\left[\text{Var}_\nu(\text{Max}_t^N)\right]$ is well approximated by $\text{Var}_\nu(\text{Sam}_t^N)$. The same is true for the analogous variances of the extreme first passage time. This collapse confirms the independence of the environmental and sampling variance and thus the addition laws in Eq. 6.12 and 6.13. Figs. b,e) show the numerically measured environmental variance asymptotes to my theoretical predictions for a wide range of distributions and m. For $m \geq 2$, Eq. 6.11 is not satisfied for any of the show distributions. However, I still use the simplified form of λ_{ext} in Eq. 6.8 under the assumption that these distributions are in the weak noise limit. This appears to be a reasonable approximation because my predictions match the numerics quite well. For the extreme first passage time and $m > 3$, my theoretical predictions break down. This is because my predictions for the extreme first passage time are derived by translating the KPZ fluctuations at $R(t) \propto t^{\frac{4m-1}{4m}}$ to the bulk regime where $R(t) \propto \mathcal{O}(1)$. In the bulk regime, [143] predicts that there are Gaussian fluctuations with scaling behavior that is not captured by the short-time Gaussian statistics of the KPZ equation.

6.8 Conclusion

I have shown the extreme value statistics of RWRE models for diffusion form a super-universality class which is governed by the KPZ equation. I find the variance of the extreme statistics display anomalous power laws given in Eq. 6.6 and 6.7 not captured by classical diffusion. The prefactor of the statistics depends on a single unknown quantity , λ_{ext}, in Eq. 6.8 which is defined in terms of the variance of the lowest random moment of the environment. Thus, a measurement of the extreme location or extreme first passage time could be used to measure microscopic fluctuations of the environment which are ignored in classical diffusion. The diffusive environment I study is quite general so I expect this to apply to a wide number of physical systems. This includes particles diffusing in a space-time random velocity field and systems with a space-time random diffusion coefficient.

6.9 Acknowledgments

This work was funded by the W.M. Keck Foundation Science and Engineering grant on "Extreme Diffusion". This work benefited from access to the University of Oregon high performance computing cluster, Talapas. I would also like to thank Eric Corwin, Ivan Corwin, Hindy Drillick and Shalin Parekh for their helpful discussion.

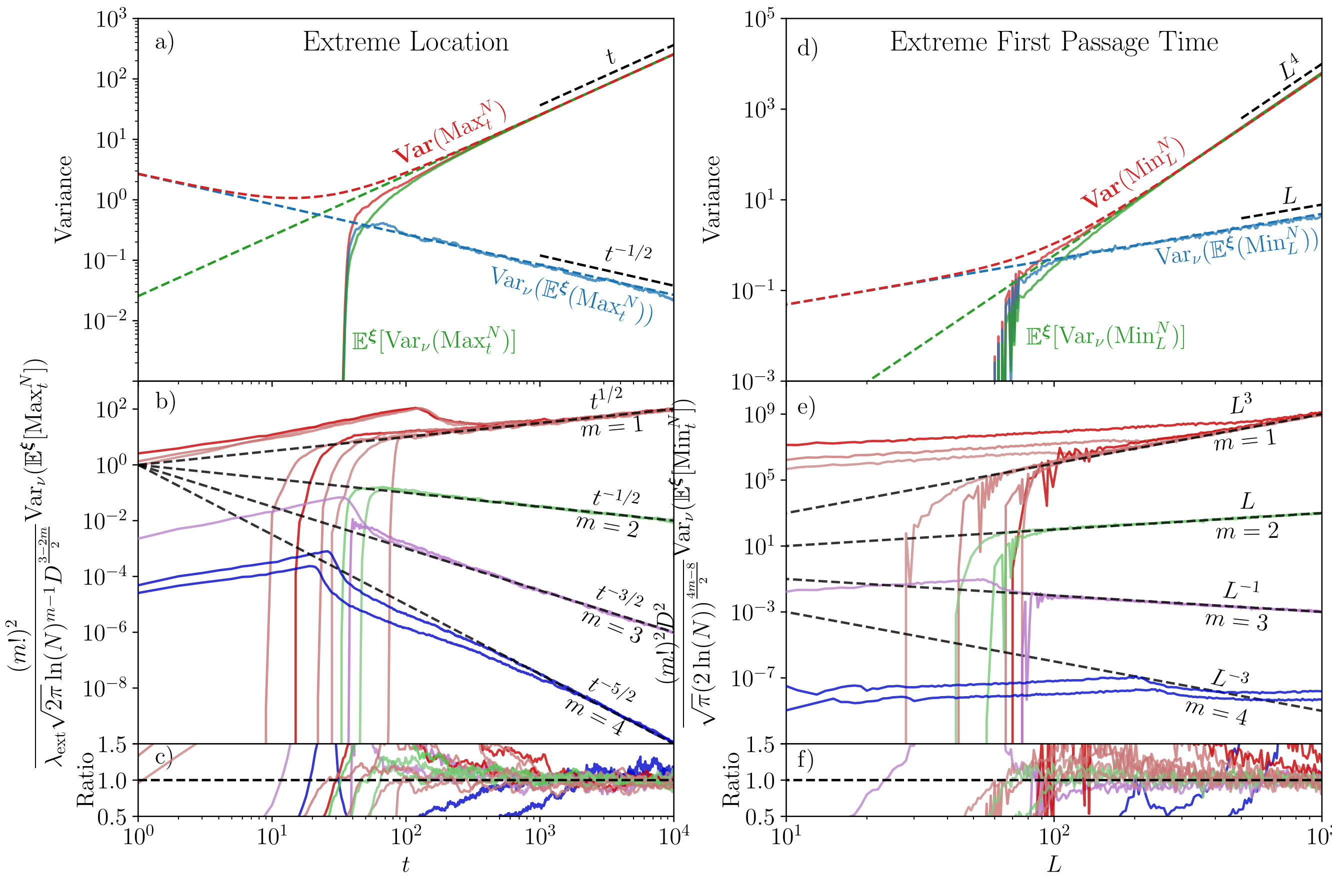

Figure 19. Plot of the different variances for the extreme location (a) and the extreme first passage time (d), for the symmetric Dirichlet distribution and systems of size $N = 10^{28}$. Dashed lines represent my theoretical predictions and solid lines are numerically measured values. Collapse of the environmental fluctuations of the extreme location (b) and extreme first passage time (e) for $m = 1$ (red), $m = 2$ (green), $m = 3$ (purple) and $m = 4$ (blue). I plot a number of different distributions listed in the "End Matter". The saturation of each curve is scaled by the diffusion coefficient, D. The ratio of measured Env_t^N (c) and Env_L^N (f) to their theoretical predictions in Eq. 6.6 and 6.7, respectively. All curves are computed over 500 independent environments.

End Matter

6.1 Distributions for ν in Figure 19

Here I list the various distributions for ν I used for the numerics in Fig. 19. I begin by defining the distributions I study where the first moment is random, i.e. $m = 1$. I then move onto $m = 2, 3$ and 4 where I fix more moments of the jump distribution.

For $m = 1$, I use the same distributions we studied in [133]. This includes the Dirichlet distribution for $\vec{\alpha} = (12, 1, 12)$ and $\vec{\alpha} = (2, 1, 1/4, 4, 1/2)$. I also studied the *flat Dirichlet distribution* which is the Dirichlet distribution with all $\alpha_i = 1$ on the interval $[-k, k]$. I used the flat Dirichlet distribution with $k = 3, 5$ and 11.

I also studied the *random delta* distribution defined as follows. The random delta distribution is controlled by a choice of $k \in \mathbb{Z}_{>0}$. Then the random delta distribution is sampled by drawing two numbers X_1 and X_2 uniformly and without replacement from $\{-k, \ldots k\}$. I then set $\xi(X_1) = \xi(X_2) = 1/2$ and $\xi(i) = 0$ for all $i \neq X_1, X_2$. I used the random delta distribution with parameter $k = 3, 5$ and 11.

For $m = 2$, I use the symmetric Dirichlet distribution with $\vec{\alpha} = (1, 1, 1)$ and $\vec{\alpha} = (1, 1, 1, 1, 1)$.

For $m = 3$, I study two distributions where the first moment is always zero, the second moment is constant, and the third moment is random. The first way I do this is to first construct a distribution which has a mean of zero and a finite second and third moment. Then by flipping the distribution, i.e. swapping $\xi_{x,t}(i)$ and $\xi_{x,t}(-i)$, randomly the mean and second moment stay the same, but the third moment changes sign. In this spirit, I define the *randomly flipped Beta Binomial* distribution as follows. I define the vector

$$\vec{X} = \left(\frac{1}{14}, \frac{3}{14}, \frac{5}{14}, \frac{5}{14}, 0\right).$$

I then flip a coin, and if heads let $\xi_{x,t}(i) = \vec{X}(i)$ for $i \in [-2, 2]$ and tails let $\xi_{x,t}(i) = \vec{X}(-i)$. I set $\xi_{x,t}(i) = 0$ otherwise. This ensures $\xi_{x,t}$ has the properties $\sum_{i\in\mathbb{Z}} \xi_{x,t}(i)i = 0$, $\sum_{i\in\mathbb{Z}} \xi_{x,t}(i)i^2 = 6/7$ and $\sum_{i\in\mathbb{Z}} \xi_{x,t}(i)i^3 = \pm 3/7$ depending on if coin lands heads or tails. I call this the randomly flipped Beta Binomial distribution because $\vec{X}$, ignoring the last term that is 0, is the probability mass function of the Beta-binomial distribution with number of trials $n = 3$ and parameters $\alpha = 3$ and $\beta = 4$.

Although the randomly flipped Beta Binomial distribution has a third moment which is random, I construct a more general distribution which has a random third moment. I first constrain the distribution $\xi_{x,t}$, to be nonzero on the interval $[-2, 2]$, and zero otherwise. I have three constraints on the distribution: $\sum_{i\in\mathbb{Z}} \xi_{x,t}(i) = 1$, $\sum_{i\in\mathbb{Z}} \xi_{x,t}(i)i = 0$ and $\sum_{i\in\mathbb{Z}} \xi_{x,t}(i)i^2 = 2D$ for $D > 0$. Since $\xi_{x,t}$ has fine non-zero values and I have three constraints, there are two degrees of freedom in the distribution. One way to interpret this, is that there are two random values in the distribution $\xi_{x,t}$ and the other elements are functions of these random values. For example, I define the *random two DOF* distribution as

$$\xi_{x,t} = \left(\frac{1}{6}(2 - 3a - b), a, b, \frac{1}{3}(2 - 3a - 4b), \frac{a+b}{2}\right)$$

where a and b are uniform random variables on the interval $\left[\frac{2}{15}, \frac{4}{15}\right]$. This ensures that $\sum_{i\in\mathbb{Z}} \xi_{x,t}(i)i = 0$, $\sum_{i\in\mathbb{Z}} \xi_{x,t}(i)i^2 = 2$ but the third moment is random.

Lastly, for $m = 4$, I construct a distribution where the first three moments are deterministic. An easy way to keep the first and third moments constant is to make the distribution symmetric such that $\xi_{x,t}(i) = \xi_{x,t}(-i)$. In this spirit, I define the *random three step* distribution as follows. I construct this distribution to have a constant diffusion coefficient of $D = 5$. To sample this distribution, I draw a random integer, X, uniformly on the interval $[4, k]$ for $k \in \mathbb{Z}_{>4}$. Note that the distribution is determined by the choice of k. I then set $\xi_{x,t}(X) = \xi_{x,t}(-X) = 5/X^2$ and $\xi_{x,t}(0) = 1 - 10/X^2$. Note that I do not allow X to be less than four, because if $X < 4$, then $\xi_{x,t}$ cannot be both a probability distribution and have a diffusion coefficient of $D = 5$. Since the $\xi_{x,t}$ is always symmetric, the first and third moments are zero. One can easily check that $D = 5$ regardless of the choice of X. However, the fourth moment is random. I study the random three step distribution for $k = 10$ and $k = 15$.

6.2 Supplementary Material

6.2.1 Overview of Derivation. Here, I provide an outline of my strategy to show convergence of the first two moments of the tail probability to the first two moments of the multiplicative stochastic heat equation. This derivation generalizes the methods in [127] but follows in parallel. Thus, I defer to [127] for a more pedagogical approach.

Before continuing, it is important to more rigorously define some properties of RWRE models. For convenience, I will introduce the notation for the jump distribution in the average environment, $\bar{\xi}(i) = \mathbb{E}_{\nu}[\xi_{x,t}(i)]$. I now define the *annealed* probability measure of N independent random walks, $R^1, \ldots, R^N$ as $\mathbf{P}(\bullet) = \mathbb{E}_{\nu}\left[\mathbb{P}^{\boldsymbol{\xi}}(\bullet)\right]$. This probability measure is simply the probability measure $\mathbb{P}^{\boldsymbol{\xi}}$ averaged over all environments, $\boldsymbol{\xi}$, sampled via ν. I define the expectation value and variance with respect to the annealed measure as $\mathbf{E}[\bullet]$ and $\mathbf{Var}(\bullet)$. As discussed in the main text, this mean and variance corresponds to averaging a random variable over many samples from many different environments. I define the *k-point motion* as $R^1, \ldots, R^k$ for $k \leq N$ with the measure $\mathbf{P}$. The one-point motion is a single random walk, R^1, where $R^1(t+1) = R^1(t) + i$ with probability $\bar{\xi}(i)$. The two-point motion is two random walks, (R^1, R^2), which are i.i.d. when they are apart but are coupled when they are at the same site. When $R^1(t) \neq R^2(t)$, $R^1(t+1) = R^1(t)+i$ with probability $\bar{\xi}(i)$ and $R^2(t+1) = R^2(t)+j$ with probability $\bar{\xi}(j)$. In other words, when $R^1(t) \neq R^2(t)$, the random walks behave as if they were in the average environment. When $R^1(t) = R^2(t) = x$, then $R^1(t+1) = x+i$ and $R^2(t+1) = x+j$ with probability $\mathbb{E}_\nu\left[\xi_{x,t}(i)\xi_{x,t}(j)\right]$.

Rather than studying the tail probability directly, it is easier to work with a more general setup in which the tail probability is a special case. This general setup is the probability mass distribution smoothed against a spatial test function. I include this smoothing because the probability mass distribution is too noisy to work with directly. The probability mass distribution decays like a Gaussian for large times, so I rescale to ensure the fluctuations remain finite. Putting these elements together, I study

$$\mathscr{U}_N(T,\phi) := \sum_{x\in\mathbb{Z}} C\left(N, T, \frac{x - c(N)T}{\sqrt{2DN}}\right)\phi\left(\frac{x-c(N)T}{\sqrt{2DN}}\right) P^{\boldsymbol{\xi}}(x, NT) \tag{S1}$$

where $\phi : \mathbb{R} \to \mathbb{R}$ is a spacial test function,

$$C(N,T,X) := \frac{\exp\left\{\dfrac{c(N)}{2DN^{1/4m}}T + \dfrac{1}{\sqrt{2D}}N^{\frac{2m-1}{4m}}X\right\}}{\left(\displaystyle\sum_{i\in\mathbb{Z}}\bar{\xi}(i)\exp\left\{\dfrac{i}{2DN^{1/4m}}\right\}\right)^{NT}} \tag{S2}$$

encodes the long time Gaussian behavior where $m-1$ is the number of deterministic moments of the environment and

$$c(N) := N\frac{\displaystyle\sum_{j\in\mathbb{Z}} j\bar{\xi}(j)\exp\left\{\frac{j}{2DN^{\frac{1}{4m}}}\right\}}{\displaystyle\sum_{i\in\mathbb{Z}}\bar{\xi}(i)\exp\left\{\frac{i}{2DN^{\frac{1}{4m}}}\right\}}.$$

By centering the spatial test function at $c(N)T$ and dividing by $\sqrt{2DN}$, I probe the probability distribution at $c(N)T$ around a window of size $\sqrt{2DN}$. It's useful to express Eq. S1 as an expectation over an environment $\boldsymbol{\xi}$, such that

$$\mathscr{U}_N(T,\phi) \coloneqq \mathbb{E}^{\boldsymbol{\xi}}\left[C\left(N,T,\frac{R^1(NT)-c(N)T}{\sqrt{2DN}}\right)\phi\left(\frac{R^1(NT)-c(N)T}{\sqrt{2DN}}\right)\right]. \qquad \text{(S3)}$$

where $R^1(NT)$ is a random walk in the environment $\boldsymbol{\xi}$.

I will show $\mathbb{E}_\nu\left[\mathscr{U}_N(T,\phi)\right]$ and $\mathbb{E}_\nu\left[\mathscr{U}_N(T,\phi)^2\right]$ converge to the first and second moment of the SHE. The k^{th} moment of the SHE is given in terms of the expectation of the local time of k independent Brownian motions [130, 131]

$$\mathbb{E}\left[\left(\int_{\mathbb{R}}\phi(X)Z(X,T)dX\right)^k\right] = \mathbf{E}\left[\Phi(\vec{B})\exp\left\{D_0\sum_{i<j}L^{B^i-B^j}(T)\right\}\right] \qquad \text{(S4)}$$

where $\mathbb{E}$ on the left is the expectation over the noise η of the SHE, and on the right $\Phi(\vec{x}) \coloneqq \phi(x_1)\cdots\phi(x_k)$, and the expectation $\mathbf{E}$ is over independent Brownian motions $B^1,\dots B^k$ starting at 0 and $L^{B^i-B^j}(t)$ is their pair local time at zero, defined as follows. The local time of a space-time continuous Brownian motion $B(t)$ with variance $\sigma^2 t$ is

$$L^B(t) \coloneqq \lim_{\epsilon\to 0^+}\frac{\sigma^2}{2\epsilon}\int_0^t \mathbb{1}_{\{-\epsilon<B(s)<\epsilon\}}ds.$$

My general strategy will be to absorb the prefactor, $C(N,T,X)$, into the expectation in Eq. S3 by interpreting it as a tilting of the increments of the random walk. The first moment can be readily identified as that of the SHE after this tilting. The second moment is more nuanced because it depends on two random walks in the same environment. When these random walks are apart, the tilting works, but when they are at the same site their movement is coupled. This coupling introduces a term which is proportional to a discrete version of the local time. I then take a Taylor expansion of the prefactor on the discrete local time. This Taylor expansion deviates from that in [127] because it depends on the number of fluctuating moments of the environment. I conclude by using results from [127] to relate the discrete local time to the local time of continuous Brownian motion. This culminates in identifying the noise strength of the SHE as

$$D_0 = \frac{\lambda_{\text{ext}}}{(m!)^2 (2D)^{\frac{4m-1}{2}}} \tag{S5}$$

where

$$\lambda_{\text{ext}} = \frac{\text{Var}_\nu\left(\mathbb{E}^{\boldsymbol{\xi}}[Y^m]\right)}{\sum_{l=0}^{\infty} \tilde{\mu}\,(l)\, \mathbf{E}_\nu[\Delta\,(t+1) - \Delta\,(t) \mid \Delta\,(t) = l]} \tag{S6}$$

where

$$\begin{aligned} \text{Var}_\nu\left(\mathbb{E}^{\boldsymbol{\xi}}[Y^m]\right) &= \mathbb{E}_\nu\left[\left(\sum_{i\in\mathbb{Z}} \xi_{t,x}(i) i^m\right)^2\right] - \left(\sum_{i\in\mathbb{Z}} \bar{\xi}(i) i^m\right)^2, \\ \tilde{\mu}\,(l) &= \begin{cases} 1 & \text{if } l = 0 \\ 2\mu(l) & \text{if } l > 0 \end{cases} \end{aligned} \tag{S7}$$

and $\mu(l)$ is the unique invariant measure, up to a constant, of the difference random walk $R^1(t) - R^2(t)$, $\Delta\,(t) = |R^1(t) - R^2(t)|$ and $Y \sim \xi_{t,x}$ is a random variable that can be thought of as a single step of a random walk R^1. Although the form of λ_{ext} is rather complex, it simplifies significantly for a number of distributions, which I discuss in the main text and in more detail in [133].

After showing the convergence of the first and second moments of $\mathscr{U}_N(T,\phi)$, I convert these results to show the tail probability also converges to the SHE except with a modified prefactor.

6.2.2 Convergence of the first moment. I show the first moment of $\mathscr{U}\,(T,\phi)$ converges, as $N \to \infty$ to the first moment of the SHE. I begin by taking the average over all environments of Eq. S3,

$$\mathbb{E}_\nu\left[\mathscr{U}_N(T,\phi)\right] = \mathbf{E}\left[C\left(N, T, \frac{R^1(NT) - c(N)T}{\sqrt{2DN}}\right)\phi\left(\frac{R^1(NT) - c(N)T}{\sqrt{2DN}}\right)\right].$$

where R^1 is now the one-point motion. I now interpret the coefficient as a tilting of the increments of the random walk $R^1(NT)$. Simplifying the coefficient, I find

$$C\left(N, T, \frac{R(NT) - c(N)T}{\sqrt{2DN}}\right) = \frac{\exp\left\{\dfrac{R(NT)}{2DN^{1/4m}}\right\}}{\left(\displaystyle\sum_{i \in \mathbb{Z}} \bar{\xi}(i) \exp\left\{\dfrac{i}{2DN^{1/4m}}\right\}\right)^{NT}}$$

$$= \frac{\displaystyle\prod_{i=0}^{NT-1} \exp\left\{\dfrac{Y_i}{2DN^{1/4m}}\right\}}{\left(\displaystyle\sum_{i \in \mathbb{Z}} \bar{\xi}(i) \exp\left\{\dfrac{i}{2DN^{1/4m}}\right\}\right)^{NT}}$$

after breaking up the random walk into its increments, $R(NT) = \sum_{i=0}^{NT-1} Y_i$, where Y_i are independent and identically distributed according to $\bar{\xi}$. Notice that there are NT terms in the numerator and denominator. Thus, I can interpret each term as a tilting of the increments of the random walk. The increments of the tilted random walk are independent and identically distributed where now $Y_i = j$ for $j \in \mathbb{Z}$ with probability

$$\frac{\bar{\xi}(i) \exp\left\{\dfrac{i}{2DN^{1/4m}}\right\}}{\displaystyle\sum_{j \in \mathbb{Z}} \bar{\xi}(j) \exp\left\{\dfrac{j}{2DN^{1/4m}}\right\}}.$$

I chose the denominator of $C(N, T, X)$ in Eq. S2 so this tilting argument yields increments distributed according to a probability mass distribution.

Tilting the expectation value to the new probability mass distribution, I find

$$\mathbb{E}_\nu \left[\mathscr{U}_N(T, \phi)\right] = \tilde{\mathbf{E}}\left[\phi\left(\frac{R^1(NT) - c(N)T}{\sqrt{2DN}}\right)\right]. \tag{S8}$$

where $\tilde{\mathbf{E}}[\bullet]$ is the tilted expectation value. Under the tilted probability mass distribution, $(R(NT) - c(N)T)/\sqrt{2DN}$ has mean 0 and variance $T + \mathcal{O}(N^{-1/4m})$ in the limit $N \to \infty$ where I have dropped higher order terms in the variance. Thus, under the tilted probability mass distribution, the centered and rescaled random walk converges to Brownian motion, i.e.

$$\lim_{N\to\infty} \frac{R(NT)-c(N)T}{\sqrt{2DN}} \to B(T)$$

where $B(T)$ is standard Brownian motion at time T. Substituting this into Eq. S8, I find

$$\lim_{N\to\infty} \mathbb{E}_\nu \left[\mathscr{U}_N(T,\phi)\right] = \mathbf{E}\left[\phi\left(B(T)\right)\right]$$

where $\mathbf{E}[\bullet]$ is the expectation value with respect to a Brownian motion starting at position 0. This is indeed the first moment of the SHE in Eq. S4.

6.2.3 Convergence of the Second Moment. I now show the second moment of $\mathscr{U}_N(T,\phi)$ converges, as $N\to\infty$ to the second moment of the SHE. In doing so, I identify the noise strength of the SHE in Eq. S5.

I begin by squaring Eq. S3 and averaging over all environments such that

$$\begin{aligned}
&\mathbb{E}_\nu\left[\mathscr{U}_N(T,\phi)^2\right] = \\
&\quad \mathbf{E}\Bigg[C\left(N,T,\frac{R^1(NT)-c(N)T}{\sqrt{2DN}}\right)C\left(N,T,\frac{R^2(NT)-c(N)T}{\sqrt{2DN}}\right) \\
&\qquad\qquad \times\phi\left(\frac{R^1(NT)-c(N)T}{\sqrt{2DN}}\right)\phi\left(\frac{R^2(NT)-c(N)T}{\sqrt{2DN}}\right)\Bigg].
\end{aligned} \tag{S9}$$

where (R^1,R^2) is the two point motion. I now simplify the prefactors to find

$$\begin{aligned}
&C\left(N,T,\frac{R^1(NT)-c(N)T}{\sqrt{2DN}}\right)C\left(N,T,\frac{R^2(NT)-c(N)T}{\sqrt{2DN}}\right) \\
&= \frac{\exp\left\{\dfrac{R^1(NT)+R^2(NT)}{2DN^{1/4m}}\right\}}{\left(\displaystyle\sum_{i\in\mathbb{Z}}\bar{\xi}(i)\exp\left\{\frac{i}{2DN^{1/4m}}\right\}\right)^{2NT}}.
\end{aligned} \tag{S10}$$

As in the first moment, I want to interpret this prefactor as a tilting of the increments of the two-point motion. This argument follows if the two random walks are at different sites, but doesn't account for the coupled motion when the walks are together. To see this, I break up the denominator of Eq. S10 into NT terms of

$$\left(\sum_{i\in\mathbb{Z}}\bar{\xi}(i)\exp\left\{\frac{i}{2DN^{1/4m}}\right\}\right)^2=\sum_{i,j\in\mathbb{Z}}\bar{\xi}(i)\bar{\xi}(j)\exp\left\{\frac{i+j}{2DN^{1/4m}}\right\}. \tag{S11}$$

When $R^1(t)\neq R^2(t)$, this correctly normalizes the terms in the numerator of Eq. S10 so the increments of the tilted random walks obey a probability mass distribution. When $R^1(t)=R^2(t)$, the motion of the random walks is coupled and the increments of the tilted random walks no longer obey a probability mass distribution. This coupling can be accounted for by changing $\bar{\xi}(i)\bar{\xi}(j)$ to $\mathbb{E}_\nu\left[\xi_{x,t}(i)\xi_{x,t}(j)\right]$ in Eq. S11. This can be accomplished by including an additional term to the prefactors,

$$C\left(N,T,\frac{R^1(NT)-c(N)T}{\sqrt{2DN}}\right)C\left(N,T,\frac{R^2(NT)-c(N)T}{\sqrt{2DN}}\right)$$
$$\times\exp\left\{-g\left(\frac{1}{2DN^{1/4m}}\right)\sum_{i=0}^{t-1}\mathbb{1}_{\{R^1(i)=R^2(i)\}}\right\}$$

where $\mathbb{1}_{\{x=y\}}$ is the indicator function and

$$g(\lambda)=\log\left(\sum_{i,j\in\mathbb{Z}}\mathbb{E}_\nu\left[\xi_{t,x}(i)\xi_{t,x}(j)\right]e^{\lambda(i+j)}\right)-2\log\left(\sum_{i\in\mathbb{Z}}\bar{\xi}(i)e^{\lambda i}\right).$$

The extra term proportional $g(\lambda)$ ensures that when $R^1(t)=R^2(t)$ the increments of the tilted random walks obey a probability mass distribution. Including this factor, I can tilt the expectation value in Eq. S9 to the new tilted probability mass distribution defined as follows. When $R^1(t)\neq R^2(t)$, $R^1(t+1)=R^1(t)+i$ and $R^2(t+1)=R^2(t)+j$ with probability

$$\frac{\bar{\xi}(i)\bar{\xi}(j)\exp\left\{\dfrac{i+j}{2DN^{1/4m}}\right\}}{\displaystyle\sum_{k,l\in\mathbb{Z}}\bar{\xi}(k)\bar{\xi}(l)\exp\left\{\dfrac{k+l}{2DN^{1/4m}}\right\}}.$$

When $R^1(t) = R^2(t) = x$, $R^1(t+1) = x+i$ and $R^2(t+1) = x+j$ with probability

$$\frac{\mathbb{E}_\nu\left[\xi_{t,x}(i)\xi_{t,x}(j)\right]\exp\left\{\dfrac{i+j}{2DN^{1/4m}}\right\}}{\displaystyle\sum_{k,l\in\mathbb{Z}}\mathbb{E}_\nu\left[\xi_{t,x}(k)\xi_{t,x}(l)\right]\exp\left\{\dfrac{k+l}{2DN^{1/4m}}\right\}}.$$

I denote $\tilde{\mathbf{E}}\left[\bullet\right]$ as the expectation with respect to the tilted probability mass distribution. Tilting the expectation value in Eq. S9, I find

$$\begin{aligned}\mathbb{E}_\nu\left[\mathscr{U}_N(T,\phi)^2\right] = \tilde{\mathbf{E}}\Bigg[&\exp\left\{g\left((2D)^{-1}N^{-1/4m}\right)\sum_{i=0}^{NT-1}\mathbb{1}_{\{R^1(i)=R^2(i)\}}\right\}\\ &\times\phi\left(\frac{R^1(NT)-c(N)T}{\sqrt{2DN}}\right)\phi\left(\frac{R^2(NT)-c(N)T}{\sqrt{2DN}}\right)\Bigg].\end{aligned}\tag{S12}$$

The next step is to take the Taylor expansion of the exponential in the limit that $N\to\infty$. Up until now, I have followed the analysis done in [127], but the expansion of $g(\lambda)$ greatly differs. As I will show in Section 6.2.3.1, as $N\to\infty$,

$$g\left(\frac{1}{2DN^{1/4m}}\right) = \frac{\mathrm{Var}_\nu\left(\mathbb{E}^{\boldsymbol{\xi}}[Y^m]\right)}{(m!)^2(2D)^{2m}\sqrt{N}} + \mathcal{O}\left(\frac{1}{N^{\frac{2m+1}{4m}}}\right).$$

The fact that the leading order term of this expansion scales like $N^{-1/2}$ is quite important. As I will discuss, this scaling ensures the discrete local time converges to the continuous local time. Substituting this expansion into Eq. S12 above yields

$$\begin{aligned}\mathbb{E}_\nu\left[\mathscr{U}_N(T,\phi)^2\right] \approx \tilde{\mathbf{E}}\Bigg[&\exp\left\{\frac{\mathrm{Var}_\nu\left(\mathbb{E}^{\boldsymbol{\xi}}[Y^m]\right)}{(m!)^2(2D)^{2m}\sqrt{N}}\sum_{i=0}^{NT-1}\mathbb{1}_{\{R^1(i)=R^2(i)\}}\right\}\\ &\times\phi\left(\frac{R^1(NT)-c(N)T}{\sqrt{2DN}}\right)\phi\left(\frac{R^2(NT)-c(N)T}{\sqrt{2DN}}\right)\Bigg].\end{aligned}\tag{S13}$$

To conclude, I only need to show that the centered and rescaled random walks converge to independent Brownian motion and the discrete local time, $\frac{1}{\sqrt{N}}\sum_{i=0}^{NT-1}\mathbb{1}_{\{R^1(i)=R^2(i)\}}$ converges to the pair local time at zero of two independent Brownian motions.

As in the first moment, $\left(\frac{R^1(NT)-c_NT}{\sqrt{2DN}}, \frac{R^2(NT)-c_NT}{\sqrt{2DN}}\right)$ will converge to independent Brownian motion in the limit that $N\to\infty$. The two random walks are independent except when $R^1 = R^2$ where their motion is coupled. However, these correlations become negligible in the limit that $N \to \infty$ unless they are tuned to become stronger as $N \to \infty$. This is not the case for my models so the centered and rescaled random walks will converge to independent Brownian motion.

In [127], I show the discrete local time relates to the pair local time via

$$\lim_{N\to\infty} \frac{1}{\sqrt{2DN}} \sum_{i=0}^{NT-1} \mathbb{1}_{\{R^1(i)=R^2(i)\}} = \frac{1}{\sum_{l=0}^{\infty} \tilde{\mu}(l)\, \mathbf{E}_\nu \left[\Delta(t+1) - \Delta(t) \mid \Delta(t) = l\right]} L_0^{B^1-B^2}(T)$$

where $\Delta(t) = |R^1(t) - R^2(t)|$ and

$$\tilde{\mu}(l) = \begin{cases} 1 & \text{if } l = 0 \\ 2\mu(l) & \text{if } l > 0 \end{cases}$$

where $\mu(l)$ is the invariant measure of the difference random walk $R^1(t) - R^2(t)$. Substituting this into Eq. S13 yields

$$\lim_{N\to\infty} \mathbb{E}_\nu \left[\mathscr{U}_N(T,\phi)^2\right] = \tilde{\mathbf{E}} \left[\exp\left\{\frac{\lambda_{\text{ext}}}{(m!)^2 (2D)^{\frac{4m-1}{2}}} L_0^{B^1-B^2}(T)\right\} \phi(B^1(T))\phi(B^2(t))\right],$$

where $\mathbf{E}$ denotes the expectation value of two independent Brownian motion, B^1 and B^2, starting at position 0 and λ_{ext} is defined in Eq. S6. This is indeed the second moment of the SHE in Eq. S4 with noise strength given by Eq. S5.

6.2.3.1 Expansion of $g(\lambda)$***.*** I now expand $g(\lambda)$ in the limit that $\lambda \to 0$. My strategy will be to rewrite g in terms of the cumulant and joint cumulant generating function of two random variables. I will then use properties of the cumulant generating function to simplify this expression. Finally, I will evaluate the simplified expression of g for $m = 1, 2$ and 3 to observe a pattern and generalize this for all m.

I begin by recalling some useful properties of cumulants and joint cumulants. Let X be a random variable with probability distribution $\mathbb{P}$ and expectation value $\mathbb{E}$. Then the Taylor series of the cumulant generating function, $K(\lambda)$, of X is given by

$$K(\lambda) = \log\left(\mathbb{E}\left[e^{\lambda X}\right]\right) = \sum_{n=1}^{\infty} \frac{\lambda^n}{n!}\kappa_n(X) \tag{S14}$$

where

$$\kappa_n(X) = \left.\frac{d^n K(\lambda)}{d\lambda^n}\right|_{\lambda=0}$$

is the n^{th} cumulant of X.

I now consider n random variables, $X_1, \ldots, X_n$ with probability measure $\mathbb{P}$ and expectation $\mathbb{E}$. Then the multivariate cumulant generating function, of $X_1, \ldots, X_n$ is given by

$$K(\lambda_1, \ldots, \lambda_n) = \log\left(\mathbb{E}\left[\exp\left\{\sum_{j=1}^{N} \lambda_i X_i\right\}\right]\right).$$

The joint cumulant of $X_1, \ldots, X_n$ is defined as

$$\kappa(X_1, \ldots, X_n) = \frac{d^n}{d\lambda_1 \cdots d\lambda_n} K(\lambda_1, \ldots, \lambda_n).$$

The n^{th} cumulant of the addition of two random variables can be expressed in terms of the joint cumulant of copies of the two random variables via

$$\kappa_n(X_1 + X_2) = \sum_{j=0}^{n} \binom{n}{j} \kappa(\underbrace{X_1, \ldots, X_1}_{n}, \underbrace{X_2, \ldots, X_2}_{n-j}). \tag{S15}$$

It is convenient to first express $g(\lambda)$ in terms of the increments of the two-point motion. Let $Y_1, Y_2 \in \mathbb{Z}$ be the increments of the two point motion, (R^1, R^2), when $R^1 = R^2$ under the measure $\mathbf{P}$. Then $g(\lambda)$ can be rewritten as

$$g(\lambda) = \log\left(\mathbf{E}\left[e^{\lambda(Y_1+Y_2)}\right]\right) - 2\log\left(\mathbf{E}\left[e^{\lambda Y_1}\right]\right). \tag{S16}$$

In the first term on the right hand side, Y_1 and Y_2 are under the measure of the two-point motion such that $Y_1 = i$ and $Y_2 = j$ with probability $\mathbb{E}_\nu\left[\xi_{x,t}(i)\xi_{x,t}(j)\right]$. Only Y_1 appears in the second term, so Y_1 in that term is under the measure of the one-point motion such that $Y_1 = i$ with probability $\bar{\xi}(i)$. Notice that

$\log\left(\mathbf{E}\left[e^{\lambda Y_1}\right]\right)$ is the cumulant generating function of Y_1 and $\log\left(\mathbf{E}\left[e^{\lambda(Y_1+Y_2)}\right]\right)$is the joint cumulant generating function of Y_1 and Y_2.

Substituting the definition of the cumulant generation function in Eq. S14 into $g(\lambda)$ in Eq. S16, I find

$$g(\lambda) = \sum_{n=1}^{\infty} \frac{\lambda^n}{n!} \kappa_n(Y_1 + Y_2) - 2\sum_{n=1}^{\infty} \frac{\lambda^n}{n!} \kappa_n(Y_1). \tag{S17}$$

I now use Eq. S15 to see

$$\begin{aligned} g(\lambda) &= \sum_{n=1}^{\infty} \frac{\lambda^n}{n!} \sum_{j=0}^{n} \binom{n}{j} \kappa(Y_1, \ldots, Y_2) - 2\sum_{n=1}^{\infty} \frac{\lambda^n}{n!} \kappa_n(Y_1) \\ &= \sum_{n=1}^{\infty} \frac{\lambda^n}{n!} \left[\sum_{j=0}^{n} \binom{n}{j} \kappa(Y_1, \ldots, Y_2) - 2\kappa_n(Y_1)\right] \end{aligned}$$

after combining the sums over n. The $2\kappa_n(Y_1)$ term can be canceled by writing out the $j = 0$ and $j = n$ terms of the sum over j. Doing so I find,

$$g(\lambda) = \sum_{n=1}^{\infty} \frac{\lambda^n}{n!} \left[\kappa(Y_1, \ldots, Y_1) + \kappa(Y_2, \ldots, Y_2) + \sum_{j=1}^{n-1} \binom{n}{j} \kappa(Y_1, \ldots, Y_2) - 2\kappa_n(Y_1)\right]$$

Notice $\kappa(Y_1, \ldots, Y_1) = \kappa(Y_2, \ldots, Y_2)$ because Y_1 and Y_2 are no longer in the same expectation value so they are identically distributed according to $\bar{\xi}$. Furthermore, the n^{th} cumulant is equal to the joint cumulant of n copies of Y_1, i.e. $\kappa_n(Y_1) = \kappa(Y_1, \ldots, Y_1)$. Using these properties, I find

$$g(\lambda) = \sum_{n=2}^{\infty} \frac{\lambda^n}{n!} \sum_{j=1}^{n-1} \binom{n}{j} \kappa(\underbrace{Y_1, \ldots, Y_1}_{j}, \underbrace{Y_2, \ldots, Y_2}_{n-j}). \tag{S18}$$

where the sum over j now runs over $j = 1$ to $j = n - 1$ and I have dropped the $n = 1$ term because it is equal to 0. Further simplification of $g(\lambda)$ proves difficult so I calculate Eq. S18 for various m.

For $m = 1$, I find

$$\lim_{\lambda \to 0} g(\lambda) = \lambda^2 \left(\mathbf{E}[Y_1 Y_2] - \mathbf{E}[Y_1]\mathbf{E}[Y_2]\right) + \mathcal{O}\left(\lambda^3\right).$$

It's now useful to write out the expectation values, which yields

$$\lim_{\lambda\to 0} g(\lambda) = \lambda^2 \left(\sum_{i,j\in\mathbb{Z}} \mathbb{E}_\nu \left[\xi_{x,t}(i)\xi_{x,t}(j)\right] ij - \sum_{i,j\in\mathbb{Z}} \bar{\xi}(i)\bar{\xi}(j) ij \right) + \mathcal{O}\left(\lambda^3\right).$$

Note, the second term is 0 since I only consider net drift free systems. Now let $Y \sim \xi_{x,t}$ such that,

$$\lim_{\lambda\to 0} g(\lambda) = \lambda^2 \mathrm{Var}_\nu(\mathbb{E}^{\boldsymbol{\xi}}[Y]) + \mathcal{O}\left(\lambda^3\right)$$

where $\mathrm{Var}_\nu(\mathbb{E}^{\boldsymbol{\xi}}[Y]) = \sum_{i,j\in\mathbb{Z}} \mathbb{E}_\nu \left[\xi_{x,t}(i)\xi_{x,t}(j)\right] ij$. This agrees with the expansion of $g(\lambda)$ in [127] which studied the $m = 1$ case.

I now consider the case when $m = 2$ where the first moment $\sum_{i\in\mathbb{Z}} \xi_{t,x}(i)i = 0$ with probability 1. Using this property, I find

$$\mathbf{E}[Y_1 Y_2^n] = \sum_{i,j\in\mathbb{Z}} \mathbb{E}_\nu \left[\xi_{x,t}(i)\xi_{x,t}(j)\right] ij^n = \mathbb{E}_\nu \left[\left(\sum_{i\in\mathbb{Z}} \xi_{x,t}(i) i \right) \left(\sum_{j\in\mathbb{Z}} \xi_{x,t}(j) j^n \right) \right] = 0$$

for all $n \in \mathbb{Z}_{\geq 1}$ after separating the sums. With these terms equal to 0, I find

$$\begin{aligned} \lim_{\lambda\to 0} g(\lambda) &= \frac{\lambda^4}{4!}\binom{4}{2}\left(\mathbf{E}_\nu[Y_1^2 Y_2^2] - \mathbf{E}_\nu[Y_1^2]^2\right) + \mathcal{O}\left(\lambda^5\right) \\ &= \frac{\lambda^4}{4!}\binom{4}{2}\left(\sum_{i,j\in\mathbb{Z}} \mathbb{E}_\nu \left[\xi_{x,t}(i)\xi_{x,t}(j)\right] i^2 j^2 - \sum_{i,j\in\mathbb{Z}} \bar{\xi}(i)\bar{\xi}(j) i^2 j^2 \right) + \mathcal{O}\left(\lambda^5\right) \end{aligned}$$

As in the first moment this expression can be made more compact by writing it in terms of $Y \sim \xi_{x,t}$. Doing so yields

$$\lim_{\lambda\to 0} g(\lambda) = \frac{\lambda^4}{(2!)^2} \mathrm{Var}_\nu(\mathbb{E}^{\boldsymbol{\xi}}[Y^2]) + \mathcal{O}\left(\lambda^5\right)$$

where I've used $\binom{4}{2} = 4!/(2!)^2$ and $\mathrm{Var}_\nu(\mathbb{E}^{\boldsymbol{\xi}}[Y^2]) = \sum_{i,j\in\mathbb{Z}} \mathbb{E}_\nu \left[\xi_{x,t}(i)\xi_{x,t}(j)\right] i^2 j^2 - \sum_{i,j\in\mathbb{Z}} \bar{\xi}(i)\bar{\xi}(j) i^2 j^2$.

I now consider the $m = 3$ where $\mathbf{E}[Y_1 Y_2^n] = 0$ for all $n \in \mathbb{Z}_{\geq 1}$ as well as a constant second moment such that $\sum_{i\in\mathbb{Z}} \xi_{x,t}(i) i^2 = 2D$ with probability 1 where D is the diffusion coefficient in Eq. 6.3. Thus,

$$\mathbf{E}[Y_2^2 Y_2^n] = \mathbb{E}_\nu \left[\left(\sum_{i\in\mathbb{Z}} \xi_{x,t}(i) i^2 \right) \sum_{j\in\mathbb{Z}} \xi_{x,t}(j) j^n \right] = 2D\mathbf{E}[Y_2^n]$$

for all $n \in \mathbb{Z}_{\geq 1}$. As expected, $g(\lambda)$ simplifies to

$$\lim_{\lambda \to 0} g(\lambda) = \frac{\lambda^6}{(3!)^2} \mathrm{Var}_\nu(\mathbb{E}^{\boldsymbol{\xi}}[Y^3]) + \mathcal{O}\left(\lambda^7\right)$$

Thus, I extrapolate to higher m,

$$\lim_{\lambda \to 0} g(\lambda) = \frac{\lambda^{2m}}{(m!)^2} \mathrm{Var}_\nu\left(\mathbb{E}^{\boldsymbol{\xi}}[Y^m]\right) + \mathcal{O}\left(\lambda^{2m+1}\right) \tag{S19}$$

as desired.

6.2.4 Convergence of the Tail Probability.

To derive the distribution of the extreme location and extreme first passage time, I convert the probability mass distribution, to the tail probability

$$\mathbb{P}^{\boldsymbol{\xi}}\left(R(NT) \geq c(N)T + \sqrt{2DN}X\right) = \sum_{y \geq c(N)T + \sqrt{2DN}X} \mathbb{P}^{\boldsymbol{\xi}}\left(R(NT) = y\right). \tag{S20}$$

In [127], I do this for the $m = 1$ case and show the tail probability is also characterized by the SHE but with a modified prefactor. The derivation for higher m is nearly identical so I will only provide an overview of the derivation here.

The tail probability in Eq. S20 is a special case of $\mathscr{U}_N(T, \phi)$ where

$$\phi_{\text{tail}}\left(X'\right) = \frac{1}{C(N,T,X)} \exp\left\{-\frac{N^{\frac{2m-1}{4m}}}{\sqrt{2D}}(X' - X)\right\} \mathbb{1}_{\{X' \geq X\}}$$

such that

$$\mathbb{P}^{\boldsymbol{\xi}}\left(R(NT) \geq c(N)T + \sqrt{2DN}X\right) = \mathscr{U}_N(T, \phi_{tail}). \tag{S21}$$

Assuming convergence of $\mathscr{U}_N(T, \phi)$ to the SHE as $N \to \infty$, yields

$$\begin{aligned}
&\mathbb{P}^{\boldsymbol{\xi}}\left(R(NT) \geq c(N)T + \sqrt{2DN}X\right) \\
&= \int_{\mathbb{R}} \phi_{\text{tail}}(X') Z(X', T) dX' \\
&= \frac{1}{C(N,T,X)} \int_{\mathbb{R}} \exp\left\{-\frac{N^{\frac{2m-1}{4m}}}{\sqrt{2D}}(X' - X)\right\} \mathbb{1}_{\{X' \geq X\}} Z(X', T) dX'
\end{aligned}$$

where I've substituted the definition of ϕ_{tail} in the second line. Notice that for $X' > X$, the exponential in the integral vanishes as $N \to \infty$. Due to the indicator function, I only integrate over the random where $X' \geq X$. Thus, I approximate the exponential in the limit that $N \to \infty$ as

$$\exp\left\{-\frac{N^{\frac{2m-1}{4m}}}{\sqrt{2D}}(X'-X)\right\} \approx \delta\left(-\frac{N^{\frac{2m-1}{4m}}}{\sqrt{2D}}(X'-X)\right)$$

where $\delta(x)$ is the Dirac delta function. Making this approximation, I evaluate the integral above to find

$$\mathbb{P}^{\boldsymbol{\xi}}\left(R(NT) \geq c(N)T + \sqrt{2DN}X\right) = \frac{\sqrt{2D}}{N^{\frac{2m-1}{4m}}C(N,T,X)}Z(X,T)$$

as $N \to \infty$. After bringing the prefactor to the left hand side,

$$\lim_{N\to\infty} \frac{N^{\frac{2m-1}{4m}}C(N,T,X)}{\sqrt{2D}}\mathbb{P}^{\boldsymbol{\xi}}\left(R(NT) \geq c(N)T + \sqrt{2DN}X\right) = Z(X,T). \tag{S22}$$

Therefore, the tail probability converges to the SHE with the same noise strength in Eq. S5, but with a different prefactor.

6.2.5 Asymptotic Expansion of the Tail Probability. Before beginning the analysis of the extreme location and first passage time, I first change variables in the tail probability to consider a random walk at time t. In contrast to a random walk at time NT in Eq. S22.

I begin by taking the ln of both sides of Eq. S22 and solving for tail probability, such that

$$\begin{aligned}
&\ln\left(\mathbb{P}^{\boldsymbol{\xi}}\left(R(NT) \geq c(N)T + \sqrt{2DN}X\right)\right) = \\
&\quad -\frac{c(N)T}{2DN^{1/4m}} - \frac{N^{\frac{2m-1}{4m}}X}{\sqrt{2D}} - \ln\left(\frac{N^{\frac{2m-1}{4m}}}{\sqrt{2D}}\right) + NT\ln\left(\sum_{i\in\mathbb{Z}}\bar{\xi}(i)\exp\left\{\frac{i}{2DN^{1/4m}}\right\}\right) \\
&\quad + h(X,T)
\end{aligned} \tag{S23}$$

where $h(X,T) = \ln(Z(X,T))$ now solves the KPZ equation with narrow wedge initial condition and noise strength given by Eq. S5. I now substitute $t \coloneqq NT$ and

$v \coloneqq T^{1/4m}$ to find

$$\ln\left(\mathbb{P}^{\boldsymbol{\xi}}\left(R(t) \geq c\left(\frac{t}{v^{4m}}\right)v^{4m} + \sqrt{\frac{2Dt}{v^{4m}}}X\right)\right) = \\ -\frac{c\left(\frac{t}{v^{4m}}\right)v^{4m+1}}{2Dt^{1/4m}} - \frac{t^{\frac{2m-1}{4m}}X}{v^{2m-1}\sqrt{2D}} - \ln\left(\frac{t^{\frac{2m-1}{4m}}}{v^{2m-1}\sqrt{2D}}\right) \\ + t\ln\left(\sum_{i\in\mathbb{Z}}\bar{\xi}(i)\exp\left\{\frac{iv}{2Dt^{1/4m}}\right\}\right) + h(X, v^{4m}). \tag{S24}$$

To simplify, I expand in the limit that $t \to \infty$. I will only track the lowest order terms in t as higher order terms do not enter the extreme location and extreme first passage time calculations. Expanding the function $c(t/v^{4m})$, I find

$$c\left(\frac{t}{v^{4m}}\right) = \frac{t}{v^{4m}}\frac{\sum_{j\in\mathbb{Z}} j\bar{\xi}(j)\exp\left\{\frac{vj}{2Dt^{1/4m}}\right\}}{\sum_{i\in\mathbb{Z}}\bar{\xi}(i)\exp\left\{\frac{vi}{2Dt^{1/4m}}\right\}} \\ \approx \frac{t}{v^{4m}}\frac{\sum_{j\in\mathbb{Z}} j\bar{\xi}(j)\left(1+\frac{vj}{2Dt^{1/4m}}\right)}{\sum_{i\in\mathbb{Z}}\bar{\xi}(i)\left(1+\mathcal{O}\left(t^{-1/4m}\right)\right)}$$

where I've used the approximation $e^x \approx 1 + x$ as $x \to 0$. Since $\bar{\xi}$ is a probability distribution on $\mathbb{Z}$, $\sum_{i\in\mathbb{Z}}\bar{\xi}(i) = 1$. Furthermore, since I only consider distributions with a zero mean in the average environment, $\sum_{j\in\mathbb{Z}}\bar{\xi}(j)j = 0$. Using these properties, I simplify

$$c\left(\frac{t}{v^{4m}}\right) \approx \frac{t}{v^{4m}}\left(\frac{v}{2Dt^{1/4m}}\sum_{j\in\mathbb{Z}}\bar{\xi}(j)j^2\right) \\ \approx \frac{t^{\frac{4m-1}{4m}}}{v^{4m-1}}.$$

where I've dropped higher order terms in t and used $\sum_{i\in\mathbb{Z}}\bar{\xi}(i)i^2 = 2D$.

I also expand the logarithmic term such that

$$\begin{aligned}
&\ln\left(\sum_{i\in\mathbb{Z}}\bar{\xi}(i)\exp\left\{\frac{iv}{2Dt^{1/4m}}\right\}\right)\\
&\approx \ln\left(\sum_{i\in\mathbb{Z}}\bar{\xi}(i)\left(1+\frac{iv}{2Dt^{1/4m}}+\frac{i^2v^2}{2(2D)^2t^{1/2m}}\right)\right)\\
&= \ln\left(\sum_{i\in\mathbb{Z}}\bar{\xi}(i)+\frac{v}{2Dt^{1/4m}}\sum_{i\in\mathbb{Z}}\bar{\xi}(i)i+\frac{v^2}{2(2D)^2t^{1/2m}}\sum_{i\in\mathbb{Z}}\bar{\xi}(i)i^2\right)
\end{aligned}$$

where I've used the small argument expansion of the exponential. As before, I use the properties $\sum_{i\in\mathbb{Z}}\bar{\xi}(i)=1$, $\sum_{i\in\mathbb{Z}}\bar{\xi}(i)i=0$, and $\sum_{i\in\mathbb{Z}}\bar{\xi}(i)i^2=2D$ to simplify

$$\begin{aligned}
\ln\left(\sum_{i\in\mathbb{Z}}\bar{\xi}(i)\exp\left\{\frac{iv}{2Dt^{1/4m}}\right\}\right) &= \ln\left(1+\frac{v^2}{4Dt^{1/2m}}\right)\\
&\approx \frac{v^2}{4Dt^{1/2m}}.
\end{aligned}$$

where I've used $\ln(1+x)\approx x$ for $x\to 0$.

Substituting these approximations into Eq. S24, I find

$$\ln\left(\mathbb{P}^{\boldsymbol{\xi}}\left(R(t)\geq vt^{\frac{4m-1}{4m}}+\sqrt{\frac{2Dt}{v^{4m}}}X\right)\right)\approx -\frac{v^2t^{\frac{2m-1}{2m}}}{4D}-\frac{t^{\frac{2m-1}{4m}}X}{v^{2m-1}\sqrt{2D}}+h(X,v^{4m})$$

where I've dropped the term proportional to $\ln(t)$.

Recall $h(X,T)$ has noise strength given by Eq. S5. I now transform the space and time variables of the KPZ equation such that the noise strength is 1. I define $\tilde{h}(\tilde{X},\tilde{T})=h(X,T)$ with $\tilde{X}=\frac{2\lambda_{\text{ext}}}{(m!)^2(2D)^{\frac{4m-1}{2}}}X$ and $\tilde{T}=\frac{4\lambda_{\text{ext}}^2}{(m!)^4(2D)^{4m-1}}T$ where $\tilde{h}$ solves the standard coefficient KPZ equation

$$\partial_{\tilde{T}}\tilde{h}=\frac{1}{2}\partial_{\tilde{X}}^2\tilde{h}+\frac{1}{2}\left(\partial_{\tilde{X}}\tilde{h}\right)^2+\eta. \tag{S25}$$

Making these transformations, I find

$$\begin{aligned}
&\ln\left(\mathbb{P}^{\boldsymbol{\xi}}\left(R(t) \geq vt^{\frac{4m-1}{4m}} + \sqrt{\frac{2Dt}{v^{4m}}}X\right)\right) \\
&\approx -\frac{v^2 t^{\frac{2m-1}{2m}}}{4D} - \frac{t^{\frac{2m-1}{4m}}X}{v^{2m-1}\sqrt{2D}} \\
&\quad + \tilde{h}\left(\frac{2\lambda_{\text{ext}}}{(m!)^2(2D)^{\frac{4m-1}{2}}}X, \frac{4\lambda_{\text{ext}}^2}{(m!)^4(2D)^{4m-1}}v^{4m}\right).
\end{aligned} \tag{S26}$$

Note that I will drop the tilde on $\tilde{h}$ as I will always use the standard coefficient KPZ equation in Eq. S25 for now on.

6.2.6 Extreme Position.

Here I derive the large time asymptotics of the extreme location. The analysis follows almost identically from [133, 107] so I provide a summary of the methods here, but refer to [133, 107] for a more in-depth treatment.

I first derive the mean and variance of Env_t^N. Since my definition of Env_t^N is in terms of $\mathbb{P}^{\boldsymbol{\xi}}(R(t) \geq x)$, I first have to transform Eq. S26 to match. I do so by substituting $x = vt^{\frac{4m-1}{4m}}$ and $X = 0$ into Eq. S26, such that

$$\ln(\mathbb{P}^{\boldsymbol{\xi}}(R(t) \geq x)) = -\frac{x^2}{4Dt} + h\left(0, \frac{4\lambda_{\text{ext}}^2}{(m!)^4(2D)^{4m-1}}\frac{x^{4m}}{t^{4m-1}}\right). \tag{S27}$$

I now use the definition of the extreme location to set $\mathbb{P}^{\boldsymbol{\xi}}(R(t) \geq x) = 1/N$ such that

$$\ln(N) \approx \frac{(\mathrm{Env}_t^N)^2}{4Dt} - h\left(0, \frac{4\lambda_{\text{ext}}^2}{(m!)^4(2D)^{4m-1}}\frac{(\mathrm{Env}_t^N)^{4m}}{t^{4m-1}}\right). \tag{S28}$$

Note that Eq. S28 is an approximation because Env_t^N need not occur exactly at the position when $\mathbb{P}^{\boldsymbol{\xi}}(R(t) \geq x) = 1/N$ but the maximum position satisfying $\mathbb{P}^{\boldsymbol{\xi}}(R(t) \geq x) \geq 1/N$.

I approximate Env_t^N in the asyptotic limit that $t^{2m-1} \gg \lambda_{\mathrm{ext}}^2 \ln(N)^{2m}$ and $N \gg 1$ by perturbatively expanding Eq. S28. Specifically, I find

$$\mathrm{Env}_t^N \approx \sqrt{4D\ln(N)t} + \sqrt{\frac{Dt}{\ln(N)}} h\left(0, \frac{8\lambda_{\mathrm{ext}}^2 \ln(N)^{2m}}{(m!)^4 (Dt)^{2m-1}}\right).$$

Since only the term proportional to the KPZ equation is random, the mean and variance of Env_t^N are

$$\mathbb{E}_\nu\left[\mathrm{Env}_t^N\right] \approx \sqrt{4D\ln(N)t} \tag{S29}$$

$$\mathrm{Var}_\nu\left(\mathrm{Env}_t^N\right) = \frac{Dt}{\ln(N)} \mathrm{Var}\left(h\left(0, \frac{8\lambda_{\mathrm{ext}}^2 \ln(N)^{2m}}{(m!)^4 (Dt)^{2m-1}}\right)\right). \tag{S30}$$

where I have only kept the leading order term of the mean.

For $t^{2m-1} \gg \lambda_{\mathrm{ext}}^2 \ln(N)^{2m}$, I derive the asymptotic scaling, in time, of $\mathrm{Var}_\nu\left(\mathrm{Env}_t^N\right)$. In this regime, I use the small time expansion of the KPZ equation

$$h(0,s) \approx -\frac{s}{24} - \ln\left(\sqrt{2\pi s}\right) + \left(\frac{\pi s}{4}\right)^{1/4} G_s \tag{S31}$$

where G_s converges to a standard Gaussian as $s \to \infty$ [73, 71]. Substituting this expansion into Eq. S30, I find

$$\mathrm{Var}_\nu(\mathrm{Env}_t^N) \approx \frac{\sqrt{2\pi}}{(m!)^2} \lambda_{\mathrm{ext}} \ln(N)^{m-1} (Dt)^{\frac{3-2m}{2}}$$

for $t^{2m-1} \gg \ln(N)^{2m}$. For $m = 1$, $\mathrm{Var}_\nu\left(\mathrm{Env}_t^N\right) = \lambda_{\mathrm{ext}}\sqrt{2\pi Dt}$, which matches results in [133].

I now derive the distribution of Sam_t^N and identify the mean and variance. I begin by deriving the tail probability distribution by combining Eq. 6.2 and the definition of Sam_t^N such that

$$\mathbb{P}^{\boldsymbol{\xi}}(\mathrm{Sam}_t^N \leq x) = (1 - \mathbb{P}^{\boldsymbol{\xi}}(R(t) \leq x + \mathrm{Env}_t^N))^N$$

I now use the approximation $(1+x)^N \approx e^{xN}$ for $x \ll 1$ and $N \to \infty$ to find

$$\ln\left(\mathbb{P}^{\boldsymbol{\xi}}(\mathrm{Sam}_t^N \leq x)\right) \approx -N\mathbb{P}^{\boldsymbol{\xi}}(R(t) \leq x + \mathrm{Env}_t^N)$$

after taking the logarithm of both sides. I now substitute Eq. S27 to find

$$\ln\left(\mathbb{P}^{\boldsymbol{\xi}}(\mathrm{Sam}_t^N \leq x)\right) \approx -N \exp\left(-\frac{(x + \mathrm{Env}_t^N)^2}{4Dt}\right)$$

where I've only kept the leading order term. I also assume $x \ll \mathrm{Env}_t^N$, such that $(x + \mathrm{Env}_t^N)^2 \approx (\mathrm{Env}_t^N)^2 + 2x\mathrm{Env}_t^N$. As I will see, $\mathbb{E}_\nu\left[\mathrm{Env}_t^N\right] \gg \mathbb{E}_\nu\left[\mathrm{Sam}_t^N\right]$ which justifies this approximation. Using this approximation, I find

$$\ln\left(\mathbb{P}^{\boldsymbol{\xi}}(\mathrm{Sam}_t^N \leq x)\right) \approx -N \exp\left(-\frac{(\mathrm{Env}_t^N)^2}{4Dt} - \frac{x\mathrm{Env}_t^N}{2Dt}\right).$$

I now approximate Env_t^N with its leading order term, $\sqrt{4Dt\ln(N)}$. In making this approximation, I assume that Sam_t^N and Env_t^N are independent. Although I do not justify this here, my numerics indicate this is a reasonable assumptions. Substituting this approximation, I find

$$\ln\left(\mathbb{P}^{\boldsymbol{\xi}}(\mathrm{Sam}_t^N \leq x)\right) \approx -\exp\left(-\sqrt{\frac{\ln(N)}{Dt}}x\right)$$

after simplifying. Therefore, Sam_t^N is Gumbel distributed with location 0 and scale $\sqrt{\frac{Dt}{\ln(N)}}$. Therefore, the mean and variance of Sam_t^N is

$$\mathbb{E}_\nu\left[\mathrm{Sam}_t^N\right] \approx \sqrt{\frac{Dt}{\ln(N)}}\gamma \tag{S32}$$

$$\mathrm{Var}_\nu(\mathrm{Sam}_t^N) \approx \frac{\pi^2 Dt}{6\ln(N)} \tag{S33}$$

where $\gamma \approx 0.577$ is the Euler-Mascheroni constant. Notice that unlike Env_t^N, Sam_t^N does not depend on m.

With the mean and variance of both Env_t^N and Sam_t^N, I finally derive the mean and variance of Max_t^N. Rearranging my definition of Sam_t^N, I see $\mathrm{Max}_t^N = \mathrm{Sam}_t^N + \mathrm{Env}_t^N$. I find to leading order the mean of Max_t^N is given by $\mathbb{E}_\nu\left[\mathrm{Max}_t^N\right] \approx \mathbb{E}_\nu\left[\mathrm{Env}_t^N\right]$ since $\mathbb{E}_\nu\left[\mathrm{Env}_t^N\right] \gg \mathbb{E}_\nu\left[\mathrm{Sam}_t^N\right]$. I find the variance of Max_t^N is given by $\mathrm{Var}_\nu(\mathrm{Max}_t^N) \approx \mathrm{Var}_\nu(\mathrm{Sam}_t^N) + \mathrm{Var}_\nu(\mathrm{Env}_t^N)$ since Sam_t^N and Env_t^N are independent. Using my asymptotic approximations of the mean and variance of Env_t^N and Sam_t^N, I find

$$\mathbb{E}_\nu\left[\mathrm{Max}_t^N\right] \approx \sqrt{4Dt\ln(N)} \tag{S34}$$

$$\mathrm{Var}_\nu(\mathrm{Max}_t^N) \approx \frac{\pi^2 Dt}{6\ln(N)} + \frac{\sqrt{2\pi}}{(m!)^2}\lambda_{\mathrm{ext}}\ln(N)^{m-1}(Dt)^{\frac{3-2m}{2}} \tag{S35}$$

for $t^{2m-1} \gg \lambda_{\mathrm{ext}}^2 \ln(N)^{2m}$ and $N \gg 1$.

6.2.7 Extreme First Passage Time. Here I derive the large distance asymptotics for the extreme first passage time. The analysis follows almost identically from [133, 122] so I provide a summary of the methods here, but refer to [133, 122] for a more in-depth treatment.

I begin by using the non-backtracking approximation $\mathbb{P}^{\boldsymbol{\xi}}(\tau_L \leq t) \approx \mathbb{P}^{\boldsymbol{\xi}}(R(t) \geq L)$ to convert the distribution of the first passage time to the distribution of the position of a random walker. This assumes that once a particle passes the location L, the particle will not backtrack and cross past position L again. I substitute this approximation into Eq. S27 and find

$$\ln(\mathbb{P}^{\boldsymbol{\xi}}(\tau_L \leq t)) \approx -\frac{L^2}{4Dt} + h\left(0, \frac{4\lambda_{\mathrm{ext}}^2}{(m!)^4(2D)^{4m-1}}\frac{L^{4m}}{t^{4m-1}}\right). \tag{S36}$$

I now use the definition of Env_L^N to set $\mathbb{P}^{\boldsymbol{\xi}}(\tau_L \leq t) = 1/N$ such that

$$\ln(N) \approx \frac{L^2}{4D\mathrm{Env}_L^N} - h\left(0, \frac{4\lambda_{\mathrm{ext}}^2}{(m!)^4(2D)^{4m-1}}\frac{L^{4m}}{(\mathrm{Env}_L^N)^{4m-1}}\right) \tag{S37}$$

Note that this is an approximation since Env_L^N need not occur exactly at the time when $\mathbb{P}^{\boldsymbol{\xi}}(\tau_L \leq t) = 1/N$ but the minimum time satisfying $\mathbb{P}^{\boldsymbol{\xi}}(\tau_L \leq t) \geq 1/N$.

I approximate Env_L^N in the asymptotic limit that $L^{4m-2} \gg \lambda_{\mathrm{ext}}^2 \ln(N)^{4m-1}$ and $N \gg 1$ by perturbatively expanding Eq. S37. Specifically, I find

$$\mathrm{Env}_L^N \approx \frac{L^2}{4D\ln(N)} - \frac{L^2}{4D\ln(N)^2} h\left(0, \frac{2^{4m+1}\lambda_{\mathrm{ext}}^2\ln(N)^{4m-1}}{(m!)^4 L^{4m-2}}\right).$$

Since only the term proportional to the KPZ equation is random, the mean and variance of Env_L^N are

$$\mathbb{E}_\nu\left[\mathrm{Env}_L^N\right] \approx \frac{L^2}{4D\ln(N)} \tag{S38}$$

$$\mathrm{Var}_\nu(\mathrm{Env}_L^N) \approx \frac{L^4}{(4D)^2\ln(N)^2}\mathrm{Var}\left(h\left(0, \frac{2^{4m+1}\lambda_{\mathrm{ext}}^2\ln(N)^{4m-1}}{(m!)^4L^{4m-2}}\right)\right). \tag{S39}$$

For $L^{4m-2} \gg \lambda_{\mathrm{ext}}^2\ln(N)^{4m-1}$, I derive the asymptotic scaling in position of $\mathrm{Var}_\nu(\mathrm{Env}_L^N)$ using the small time approximation of the KPZ equation in Eq. S31. Substituting this expansion into Eq. S39, I find

$$\mathrm{Var}_\nu(\mathrm{Env}_L^N) \approx \frac{\lambda_{\mathrm{ext}}\sqrt{\pi}2^{\frac{4m-9}{2}}}{(m!)^2D^2}\ln(N)^{\frac{4m-9}{2}}L^{5-2m}.$$

For $m = 1$, I see

$$\mathrm{Var}_\nu(\mathrm{Env}_L^N) \approx \lambda_{\mathrm{ext}}\frac{\sqrt{2\pi}L^3}{8D^2\log(N)^{5/2}}$$

which matches results in [133].

I now derive the distribution of Sam_L^N and identify the mean and variance. I begin by deriving the tail probability distribution by combining Eq. 6.2 and the definition of Sam_L^N such that

$$\mathbb{P}^{\boldsymbol{\xi}}(\mathrm{Sam}_L^N \geq t) = (1 - \mathbb{P}^{\boldsymbol{\xi}}(\tau_L \leq t + \mathrm{Env}_L^N))^N.$$

I now use the approximation $(1+x)^N \approx e^{xN}$ for $x \ll 1$ and $N \to \infty$ to find

$$\ln(\mathbb{P}^{\boldsymbol{\xi}}(\mathrm{Sam}_L^N \geq t)) \approx -N\mathbb{P}^{\boldsymbol{\xi}}(\tau_L \leq t + \mathrm{Env}_L^N)$$

after taking the logarithm of both sides. I now substitute Eq. S36 which yields

$$\ln(\mathbb{P}^{\boldsymbol{\xi}}(\mathrm{Sam}_L^N \geq t)) \approx -N\exp\left(-\frac{L^2}{4D(t+\mathrm{Env}_L^N)}\right)$$

where I've only kept the leading order term. I also assume $t \ll \mathrm{Env}_L^N$, such that $\frac{1}{t+\mathrm{Env}_L^N} \approx \frac{1}{\mathrm{Env}_L^N}(1 - \frac{t}{\mathrm{Env}_L^N}) = \frac{1}{\mathrm{Env}_L^N} - \frac{t}{(\mathrm{Env}_L^N)^2}$. As I will show, $\mathbb{E}_\nu\left[\mathrm{Env}_L^N\right] \gg \mathbb{E}_\nu\left[\mathrm{Sam}_L^N\right]$

which justifies this approximation. Using this approximation, I find

$$\ln(\mathbb{P}^{\boldsymbol{\xi}}(\mathrm{Sam}_L^N \geq t)) \approx -N \exp\left(-\frac{L^2}{4D\mathrm{Env}_L^N} + \frac{tL^2}{4D(\mathrm{Env}_L^N)^2}\right).$$

I now approximate Env_L^N with its leading order term $\frac{L^2}{4D\ln(N)}$. In making this approximation, I assume that Sam_L^N and Env_L^N are independent. Although I do not justify this here, my numerics indicate this is a reasonable assumption. Substituting this approximation, I find

$$\ln(\mathbb{P}^{\boldsymbol{\xi}}(\mathrm{Sam}_L^N \geq t)) \approx -\exp\left(\frac{4D\ln(N)^2}{L^2}t\right)$$

after simplifying. Therefore, $-\mathrm{Sam}_L^N$ is Gumbel distributed with location 0 and scale $\frac{L^2}{4D\ln(N)^2}$. Then, the mean and variance of Sam_L^N is

$$\mathbb{E}_\nu\left[\mathrm{Sam}_L^N\right] \approx -\frac{\gamma L^2}{4D\ln(N)^2}$$
$$\mathrm{Var}_\nu(\mathrm{Sam}_L^N) \approx \frac{\pi^2 L^4}{96D^2\ln(N)^4}$$

where γ is the the Euler-Mascheroni constant. Notice that unlike Env_L^N, Sam_L^N does not depend on m.

With the mean and variance of both Env_L^N and Sam_L^N, I finally derive the mean and variance of Min_L^N. Rearranging my definition of Sam_L^N, I see $\mathrm{Min}_L^N = \mathrm{Sam}_L^N + \mathrm{Env}_L^N$. I find to leading order that the mean of Min_L^N is given by $\mathbb{E}_\nu\left[\mathrm{Min}_L^N\right] \approx \mathbb{E}_\nu\left[\mathrm{Env}_L^N\right]$ since $\mathbb{E}_\nu\left[\mathrm{Env}_L^N\right] \gg \mathbb{E}_\nu\left[\mathrm{Sam}_L^N\right]$. I find the variance of Min_L^N is given by $\mathrm{Var}_\nu\left(\mathrm{Min}_L^N\right) \approx \mathrm{Var}_\nu\left(\mathrm{Sam}_L^N\right) + \mathrm{Var}_\nu\left(\mathrm{Env}_L^N\right)$ since Sam_L^N and Env_L^N are independent. Using my asymptotic approximations of the mean and variance of Env_L^N and Sam_L^N, I find

$$\mathbb{E}_\nu\left[\mathrm{Min}_L^N\right] \approx \frac{L^2}{4D\ln(N)} \tag{S40}$$
$$\mathrm{Var}_\nu(\mathrm{Min}_L^N) \approx \frac{\pi^2 L^4}{96D^2\ln(N)^4} + \frac{\lambda_{\mathrm{ext}}\sqrt{\pi}2^{\frac{4m-9}{2}}}{(m!)^2D^2}\ln(N)^{\frac{4m-9}{2}}L^{5-2m} \tag{S41}$$

for $L^{4m-2} \gg \lambda_{\mathrm{ext}}^2\ln(N)^{4m-1}$ and $N \gg 1$.

CHAPTER VII

UNIVERSAL FLUCTUATIONS IN THE TAIL PROBABILITY FOR $D = 2$ RANDOM WALKS IN SPACE-TIME RANDOM ENVIRONMENTS

This paper is published as: Ark, F., Hass, J. B., & Corwin, E. I. (2025, August). Universal Fluctuations in the Tail Probability for d=2 Random Walks in Space-Time Random Environments (No. arXiv:2508.15999). arXiv. doi:10.48550/arXiv.2508.15999. I helped develop much of the numerics while Franscesca Ark did most of the writing and revising.

7.1 Abstract

Many diffusive systems involve correlated random walkers due to a shared environment. Such systems can be modeled as random walks in random environments (RWRE). These models differ from classical diffusion in the behavior of the extremes—the walkers that move the fastest or farthest. In spatial dimension $d = 1$ RWRE models have been well studied numerically and analytically and exhibit universal behavior in the Kardar-Parisi-Zhang universality class. Here, we study discrete lattice RWRE models in $d = 2$. We find that the tail probability exhibits a different universal scaling form, which is nevertheless characterized by the same coefficient, λ_{ext}, as in the $d = 1$ case. We observe a critical scaling regime for fluctuations in the tail probability at positions that scale linearly in time.

7.2 Introduction

The random walk in a random environment (RWRE) model takes into account the shared environment in which particles diffuse, unlike classical diffusion which treats particles as independent and identical [21, 22, 23]. The shared environment is important to the behavior of the extremes: those that travel the fastest or farthest. In many biological and physical systems, such as sperm cells searching for eggs [144, 102], calcium ions traveling across dendritic spinal structures [8], and contagions spreading through a population [145, 17, 146], the meaningful action is accomplished by the first, or first handful, of arriving agent(s). Analytical and numerical results show that RWRE models in dimension $d = 1$ fall into the Kardar-Parisi-Zhang (KPZ) universality class [6, 69, 7, 107, 122, 123, 112, 133, 127, 129] (an analogous link has been conjectured for $d > 1$ [69]), which describes growth processes of random media [1], turbulent liquid crystals [147, 83], and directed polymer [148, 149]. However, diffusion across surfaces and through volumes is physically relevant, and thus it is necessary to understand diffusion in shared environments in $d > 1$.

7.3 RWRE Model Description

We consider random environments in which the probability of moving in each cardinal direction changes at each time and each location, as in a random forcing field. Let $\boldsymbol{n} = \{\hat{x}, \hat{y}, -\hat{x}, -\hat{y}\}$ denote the set of cardinal directions. Let ν be a probability distribution on the space of probability distributions on $\boldsymbol{n}$. We denote $\mathbb{E}_\nu[\bullet]$, $\mathrm{Var}_\nu[\bullet]$ to be the expectation value and variance over all samples of ν. We define the environment $\boldsymbol{\xi} = \{\xi_{\vec{x},t} : \vec{x} \in \mathbb{Z}^2, t \in \mathbb{Z}_{\geq 0}\}$ where $\xi_{\vec{x},t}$ is a probability distribution on $\boldsymbol{n}$, independently sampled according to ν, for each lattice site $(\vec{x}, t)$. We refer to $\xi_{\vec{x},t}$ as the jump distribution of a random walk. Since every jump distribution is only defined on the cardinal directions, $\boldsymbol{n}$, we only consider nearest neighbor random walks. We also only consider environments with no net drift such that $\sum_{\hat{n}\in\boldsymbol{n}} \mathbb{E}_\nu\left[\xi\left(\hat{n}\right)\right]\hat{n} = \vec{0}$, or equivalently, $\mathbb{E}_\nu\left[\xi\left(\hat{n}\right)\right] = 1/4$ for all $\hat{n}$ in $\boldsymbol{n}$. Note, here and below we drop the subscript on $\mathbb{E}_\nu[\xi(\bullet)]$ since all $\xi_{\vec{x},t}$ are independent and identically distributed (i.i.d.) according to ν.

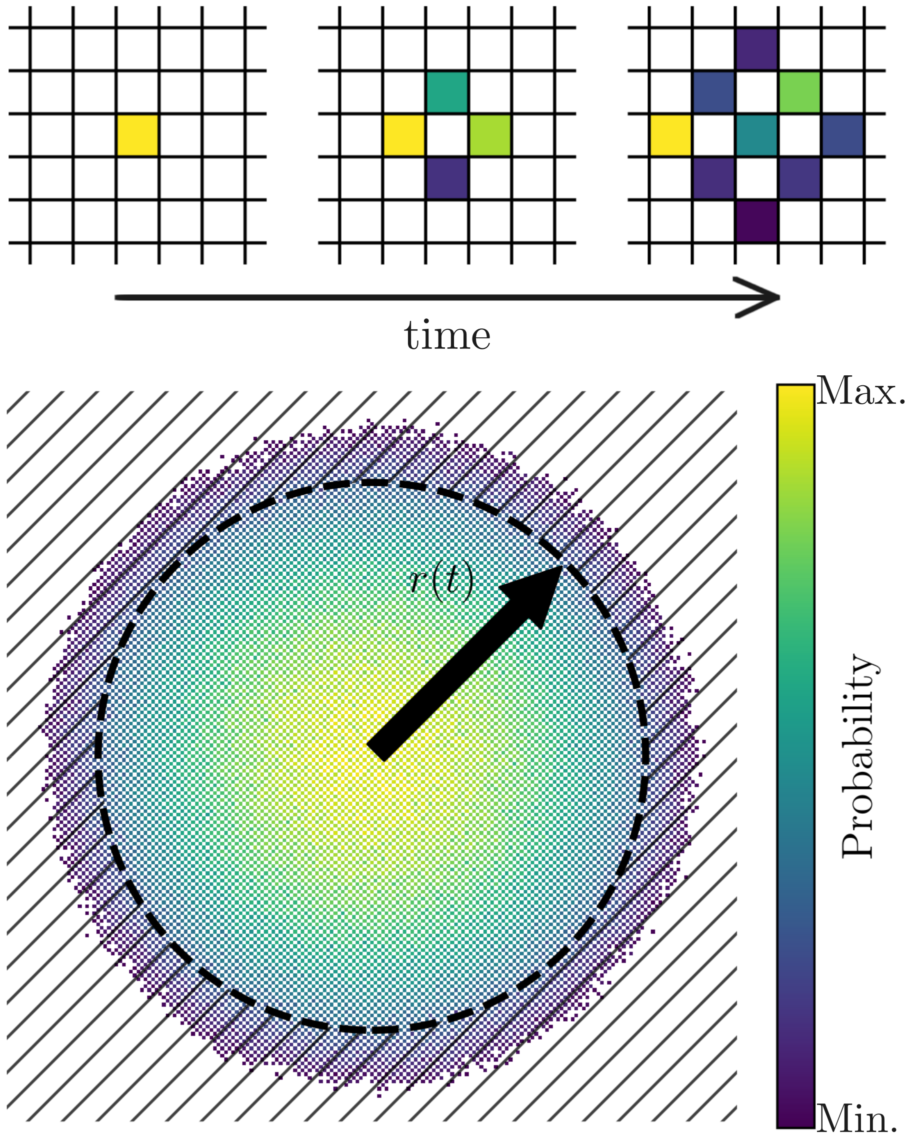

Figure 20. Illustration of the space-time evolution of the probability mass function defined in Eqn. (7.2) and the definition of the tail probability $\mathbb{P}^{\boldsymbol{\xi}}\left(|\vec{S}(t)| \geq r\right)$ for an RWRE in $d = 2$. The color indicates the relative probability. Top: Probability mass function for $t = 0, 1, 2$. Bottom: Probability mass function at time $t = 500$ for a single $\boldsymbol{\xi}$. We sum the probability past a circle of radius r (hatched area) to find the tail probability $\mathbb{P}^{\boldsymbol{\xi}}\left(|\vec{S}(t)| \geq r\right)$.

Let $\vec{S}(t) \in \mathbb{Z}^2$ denote a random walk starting at the origin such that $\vec{S}(0) = \vec{0}$. Let $\mathbb{P}^{\boldsymbol{\xi}}$ denote the probability measure of a random walk in the environment $\boldsymbol{\xi}$, and let $\mathbb{E}^{\boldsymbol{\xi}}[\bullet]$ and $\mathrm{Var}^{\boldsymbol{\xi}}[\bullet]$ be the corresponding expectation value and variance. In the environment $\boldsymbol{\xi}$, the probability of a random walk at $\vec{S}(t) = \vec{x}$ transitioning to $\vec{S}(t+1) = \vec{x} + \hat{n}$ is

$$\mathbb{P}^{\boldsymbol{\xi}}\left(\vec{S}(t+1) = \vec{x} + \hat{n} \mid \vec{S}(t) = \vec{x}\right) = \xi_{\vec{x},t}\left(\hat{n}\right) \tag{7.1}$$

for $\hat{n} \in \boldsymbol{n}$. Then the probability of a random walk being at site $\vec{x}$ at time t, $\mathbb{P}^{\boldsymbol{\xi}}\left(\vec{S}(t) = \vec{x}\right)$, obeys the recursion relation

$$\mathbb{P}^{\boldsymbol{\xi}}\left(\vec{S}(t+1) = \vec{x}\right) = \sum_{\hat{n}\in\boldsymbol{n}} \mathbb{P}^{\boldsymbol{\xi}}\left(\vec{S}(t) = \vec{x} - \hat{n}\right) \xi_{\vec{x}-\hat{n},t}\left(\hat{n}\right) \tag{7.2}$$

with the initial condition $\mathbb{P}^{\boldsymbol{\xi}}\left(\vec{S}(0) = \vec{0}\right) = 1$.

We define

$$\lambda_{\mathrm{ext}} := \frac{1}{2}\frac{D_{\mathrm{ext}}}{D - D_{\mathrm{ext}}} \tag{7.3}$$

where

$$D := \frac{1}{2}\sum_{\hat{n}\in\boldsymbol{n}} \left(\hat{n}\cdot\hat{n}\right)\mathbb{E}_{\nu}\left[\xi\left(\hat{n}\right)\right] \tag{7.4}$$

is the diffusion coefficient of a random walk in the average environment. Since we only consider environments where $\mathbb{E}_{\nu}[\xi(\hat{n})] = 1/4$ for all $\hat{n} \in \boldsymbol{n}$, then $D = 1/2$. We define D_{ext}, the *extreme diffusion coefficient*, as

$$\begin{aligned} D_{\mathrm{ext}} :=& \frac{1}{2}\mathrm{Var}_{\nu}\left[\mathbb{E}^{\boldsymbol{\xi}}\left[\vec{Y}\right]\right] \\ =& \frac{1}{2}\mathbb{E}_{\nu}\left[\left(\mathbb{E}^{\boldsymbol{\xi}}\left[\vec{Y}\right]\right)^2\right] - \frac{1}{2}\mathbb{E}_{\nu}\left[\mathbb{E}^{\boldsymbol{\xi}}\left[\vec{Y}\right]\right]^2 \end{aligned} \tag{7.5}$$

where $\vec{Y}$ is a single step in a random walk, drawn from $\xi_{\vec{x},t}$. Thus we see $\mathbb{E}^{\boldsymbol{\xi}}\left[\vec{Y}\right] = \sum_{\hat{n}\in\boldsymbol{n}} \hat{n}\xi_{\vec{x},t}\left(\hat{n}\right)$. Since we only consider net drift free systems, $\mathbb{E}_{\nu}\left[\mathbb{E}^{\boldsymbol{\xi}}\left[\vec{Y}\right]\right] = \vec{0}$, so we drop the second term in Eqn. (7.5). Thus, D_{ext} simplifies to

$$D_{\mathrm{ext}} = \frac{1}{2}\mathbb{E}_{\nu}\left[\left(\sum_{\hat{n}_1\in\boldsymbol{n}} \hat{n}_1\xi_{\vec{x},t}\left(\hat{n}_1\right)\right)\cdot\left(\sum_{\hat{n}_2\in\boldsymbol{n}} \hat{n}_2\xi_{\vec{x},t}\left(\hat{n}_2\right)\right)\right]. \tag{7.6}$$

Note that we have defined λ_{ext} and D_{ext} as the $d = 2$ extension of their definition in studies of the $d = 1$ model [133]. In the case of $d = 1$, a single step of a random walk is a scalar quantity, therefore $D_{\text{ext}} = \frac{1}{2}\mathbb{E}_\nu\left[\left(\sum_i \xi_{x,t}(i)i\right)^2\right]$. To appropriately generalize this definition to $d = 2$, a single step becomes a vector, and thus we take the dot product to compute the variance.

We now describe the choices of ν that we implement numerically. These distributions include environments in which random walks stick to one another, and environments which are homogeneous, as in the case of classical diffusion. Note that the homogeneous environment which returns classical diffusion is the one where $\xi(\hat{n}) = 1/4$ for all $\hat{n} \in \boldsymbol{n}$, called the *simple symmetric random walk (SSRW)*. These choices probe the universality of $d = 2$ RWRE models.

1. *The Dirichlet distribution*: Let $\xi(\hat{n}) = X_{\hat{n}}/\left(\sum_{\hat{n}} X_{\hat{n}}\right)$ for $\hat{n} \in \boldsymbol{n}$, where $X_{\hat{n}}$ are independent Gamma random variables with shape $\alpha \in \mathbb{R}_{>0}$ and rate $\beta = 1$ such that $X_{\hat{n}} = x$ with probability $x^{\alpha-1}e^{-x}/\Gamma(\alpha)$ where $\Gamma(x)$ is the Gamma function. This distribution is completely determined by the parameter α. As $\alpha \to \infty$, $\xi(\hat{n}) \to 1/4$ for all $\hat{n} \in \boldsymbol{n}$, so the SSRW is obtained. As $\alpha \to 0$, $\xi(\hat{n}) = 1$ for one $\hat{n} \in \boldsymbol{n}$ and $\xi(\hat{n}) = 0$ otherwise. This corresponds to a perfectly sticky environment so that the jump distribution is concentrated in one direction. In this work we choose values of α in steps of size $\sqrt{10}$ ranging from $1/\sqrt{1000}$ to $\sqrt{1000}$.

2. *Log-normal*: Let $\xi(\hat{n}) = X_{\hat{n}}/\left(\sum_{\hat{n}} X_{\hat{n}}\right)$, where $X_{\hat{n}}$ are independent log-normal random variables with location $\mu = 0$ and scale $\sigma = 1$ such that $X_{\hat{n}} = x$ with probability $\left(e^{-(\ln x)^2/2}\right)/\left(x\sqrt{2\pi}\right)$.

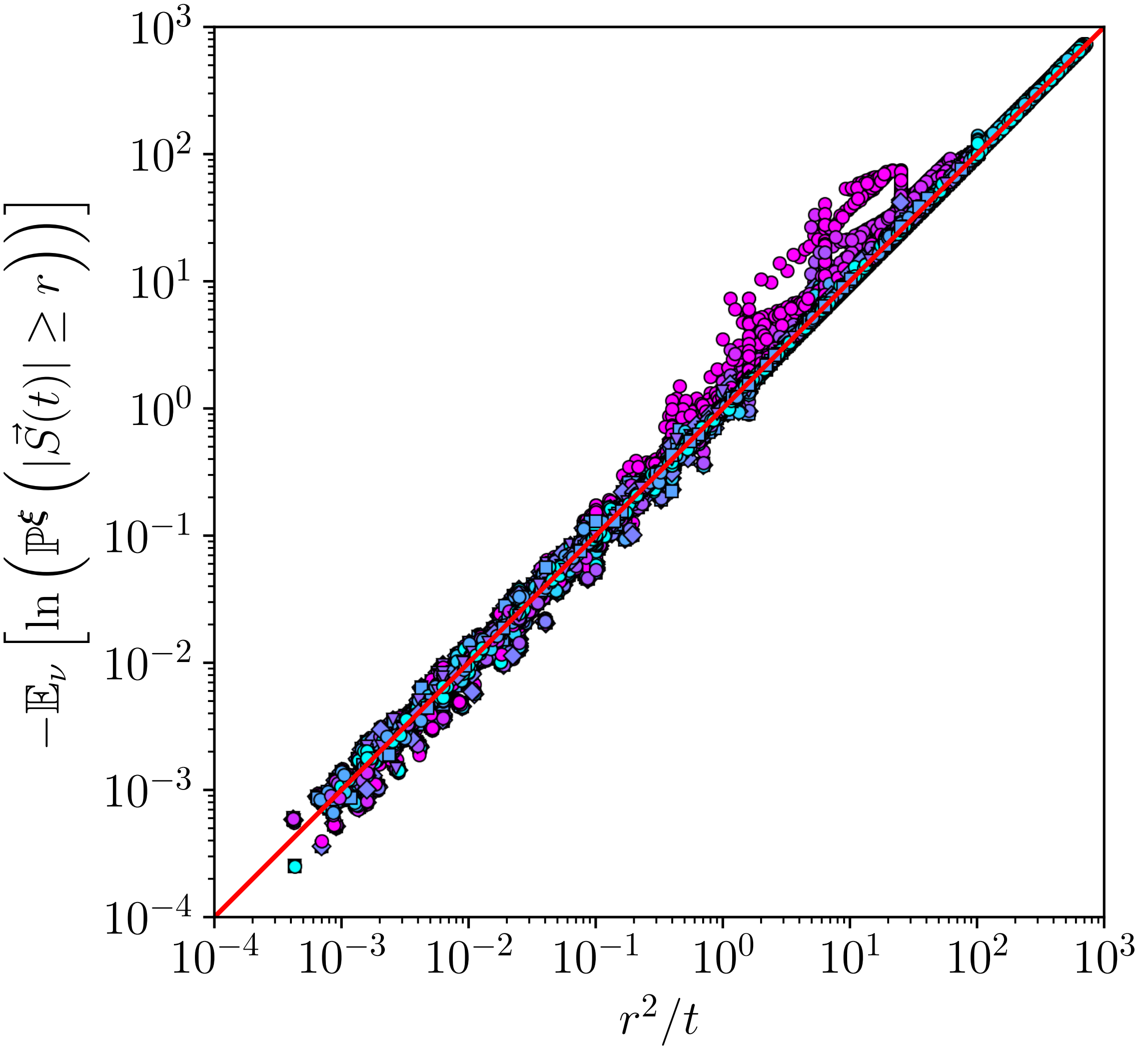

Figure 21. Collapse of the negative mean, with respect to ν, of the natural log of the tail probability to a master curve when plotted against the Gaussian prediction r^2/t. Eqn. (7.7) is plotted as a red line, showing the validity of this prediction.

3. *Random delta*: Let $\vec{X}_1$ and $\vec{X}_2$ be two random vectors uniformly sampled from $\boldsymbol{n}$ without replacement, and set $\xi\left(\vec{X}_1\right) = \xi\left(\vec{X}_2\right) = 1/2$ and $\xi(\hat{n}) = 0$ otherwise.

4. *Corner*: Let X_1 and X_2 be independent uniform random variables on the interval $[0,1]$, and set $\xi\left(\hat{y}\right) = X_1/2$, $\xi\left(\hat{x}\right) = \left(1 - X_1\right)/2$ and similarly, $\xi\left(-\hat{x}\right) = X_2/2$, $\xi\left(-\hat{y}\right) = \left(1 - X_2\right)/2$.

We study the statistics of the tail probability, $\mathbb{P}^{\boldsymbol{\xi}}\left(|\vec{S}(t)| \geq r\right)$ where $|\vec{x}|$ is the L^2 norm of the vector $\vec{x}$. This is the probability that a random walk in a given random environment is past a circle with radius r. A visualization of the definition of the tail probability is shown in Figure 20 (bottom). The tail probability is relevant to the behavior of extreme particles, and its $d = 1$ analogue has been studied extensively for the RWRE model [6, 69, 7, 123, 112, 127]. As in those works, we look at the statistics of $\ln\left(\mathbb{P}^{\boldsymbol{\xi}}\left(|\vec{S}(t)| \geq r\right)\right)$.

7.4 Numerical Methods and Results

To generate pairs of radii and times, we evaluate different functional forms of r. We probe a wide array of pairs of r and t, as described in the end matter.

We numerically evolve the probability mass function of a random walk by direct implementation of Eqn. (7.2) for a $(t + 1) \times (t + 1)$ lattice with origin in the center out to time $t = 10000$. We choose this lattice size to optimize the memory usage of our high performance computing cluster. As this will necessitate probability mass leaving our simulation volume, we use absorbing boundary conditions to collect this probability mass. The effects of the absorbing boundary condition on the tail probability are negligible. We average our data over 500 realizations of $\boldsymbol{\xi}$ for each ν.

As shown in Fig. 21, the mean of the log of the tail probability, $\mathbb{E}_\nu\left[\ln\left(\mathbb{P}^{\boldsymbol{\xi}}\left(|\vec{S}(t)|\geq r\right)\right)\right]$, yields the first order Gaussian behavior as $t\to\infty$ such that [69]

$$\mathbb{E}_\nu\left[\ln\left(\mathbb{P}^{\boldsymbol{\xi}}\left(|\vec{S}(t)|\geq r\right)\right)\right]\approx-\frac{r^2(t)}{t}. \tag{7.7}$$

We expect this Gaussian behavior because the average environment is homogeneous, as in classical diffusion.

In Fig. 22 (top) we plot the scaled variance $\frac{t^2}{r^2(t)\lambda_{\text{ext}}}\text{Var}_\nu\left[\ln\left(\mathbb{P}^{\boldsymbol{\xi}}\left(|\vec{S}(t)|\geq r\right)\right)\right]$ for every r, t, and ν as a function of time, t. We plot the median value of the scaled variance in each of 50 logarithmically spaced bins in time, for each choice of ν, colored by the value of λ_{ext}. We plot the median value of all data in black. The scaling factor $t^2/r^2\lambda_{\text{ext}}$ collapses nearly all of the data onto a single constant as a function of time. Thus, the large deviation regime in which $r\propto t$ will result in a constant-in-time variance of the tail probability. Therefore, the critical scaling regime is the large deviation regime. As discussed below and in the end matter, when $r/t\to 1$, there is non-universal, but easily explained, behavior. This data is excluded from the median calculation.

We find that the data collapses onto

$$\text{Var}_\nu\left[\ln\left(\mathbb{P}^{\boldsymbol{\xi}}\left(|\vec{S}(t)|\geq r\right)\right)\right]=c\lambda_{\text{ext}}\frac{r^2}{t^2} \tag{7.8}$$

for $r<t$, where we empirically determine $c\approx 1.3$. Note that for $d=1$ RWRE models this prefactor is analytically determined [133]. We re-plot our data in Fig. 22 (bottom) onto this universal form, which shows that λ_{ext} captures all relevant information about the environment (i.e. the choice of ν).

The parameter λ_{ext} depends on the stickiness of random walks in the given environment, i.e. how likely two random walks at the same site and same time will

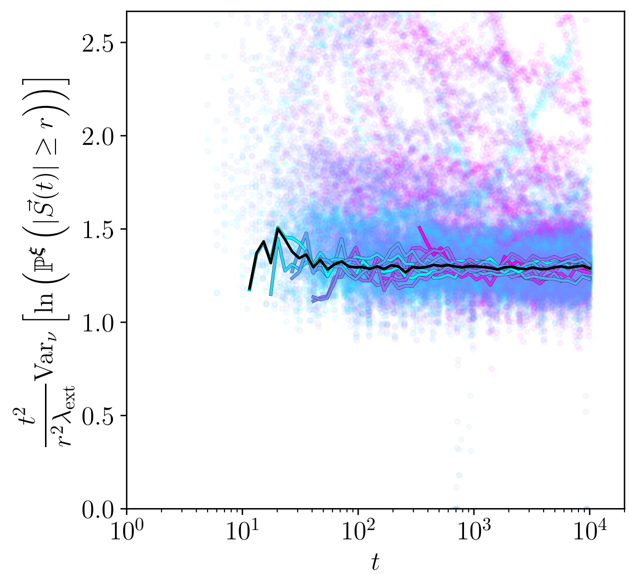

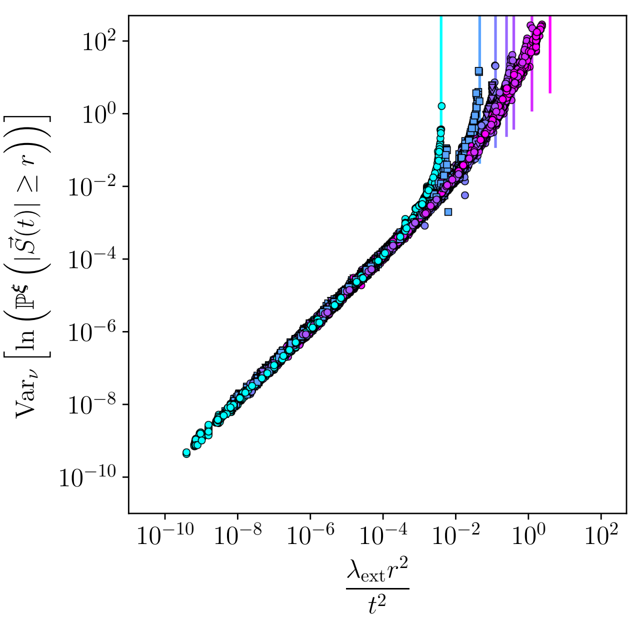

Figure 22. Universal critical behavior of the tail probability in the large deviation regime. Color gradient encodes the value of λ_{ext} from 0.008 (blue) to 8 (pink). Top: Variance of $\ln\left(\mathbb{P}^{\boldsymbol{\xi}}\left(|\vec{S}(t)| \geq r\right)\right)$ as a function of t, normalized by $\lambda_{\text{ext}} r^2(t)/t^2$. The black line plots the median across all ν, calculated as described in the text. The solid colored lines plot the median for each ν. Bottom: Variance of $\ln\left(\mathbb{P}^{\boldsymbol{\xi}}\left(|\vec{S}(t)| \geq r\right)\right)$ as a function of $\lambda_{\text{ext}} r^2(t)/t^2$. Markers indicates specific choices of ν: Dirichlet (circles), random-delta (triangles), and the corner distribution (squares). Vertical lines indicate where $r = t$ for each value of λ_{ext}.

remain together. To illustrate the effect of λ_{ext}, consider the following limits. As $\lambda_{\text{ext}} \to 0$, the jump distribution $\xi_{\vec{x},t}$ approaches classical diffusion where there is no correlation in the movement of particles at the same site $(\vec{x}, t)$ and thus the variance will approach zero. In contrast, as $\lambda_{\text{ext}} \to \infty$, the jump distribution approaches completely sticky behavior, so particles coalesce at the same site $(\vec{x}, t)$ and the variance will approach infinity.

For a given value of λ_{ext}, as r approaches t we see the transition to non-universal behavior. When $r = t$, averaging only occurs over the 4 cardinal direction paths, as opposed to the many possible paths when r is substantially less than t. In the absence of correlated averaging the variance of the tail probability scales linearly with t, as shown in the end matter. When plotted on our master curve, this appears as a deviation to a vertical line at λ_{ext}, as illustrated in Fig. 22 (bottom).

7.5 Conclusion

We have shown in this paper that RWRE models exhibit universal fluctuations of the tail probability in $d = 2$. We find the critical scaling occurs for $r \propto t$, in contrast to the $d = 1$ case for which the critical scaling regime is $r \propto t^{3/4}$. As the large deviation regime is the upper bound on scalings for our model, this means that $d = 2$ RWRE models exhibit universal behavior in *every* scaling. Additionally, the fluctuations of the tail probability decrease in time at every scaling except the critical scaling. Thus, RWRE models in $d = 2$ approach classical behavior at long times in every regime except for the large deviation regime. This results raises the important question of whether or not a critical regime exists in $d > 2$.

A scaling argument in Ref. [69] and unpublished mathematical work by Drillick and Parekh conjecture a critical scaling regime for $d = 2$ RWRE models [143] that differs from the empirically observed large deviation regime. In those works, through a weak disorder one loop RG argument [69] and by studying the tail probability past a line [143], the authors find the critical scaling regime to occur at line positions $\propto t/\sqrt{\ln t}$. This discrepancy is intriguing and will require more work. The fluctuations in the tail probability past a line can be understood as effectively local since they will be dominated by the fluctuations at the point of the line's closest approach to the origin. However, the tail probability past a circle will always be global since every point on the circle is equidistant to the origin and thus the fluctuations are not dominated by any single point. One might expect these two measurements to differ by logarithmic corrections. Further work is necessary to resolve this difference: empirical studies of the fluctuations past a line and analytical studies of the fluctuations past a circle.

The critical scaling regime in $d = 1$ relates to the $(1 + 1)d$ KPZ equation. As we have uncovered the $d = 2$ critical scaling regime, it is natural to ask whether it relates to the $(2 + 1)d$ KPZ equation [149, 150]. Perhaps a detailed examination of the full distribution of the tail probability will be illuminating. Additionally, it would be valuable to extend the exploration of $d = 2$ RWRE models to cover long range jump kernels as well as other measurements such as probability to reach a point and probability to reach a line.

7.6 Acknowledgments

This work was funded by the W.M. Keck Foundation Science and Engineering grant on "Extreme Diffusion." We also thank Axel Saenz Rodriguez, Ivan Corwin, Hindy Drillick and Pierre Le Doussal for discussion. The authors acknowledge Research Advanced Computing Services (RACS) at the University of Oregon for providing computing resources that have contributed to the research results reported within this publication.

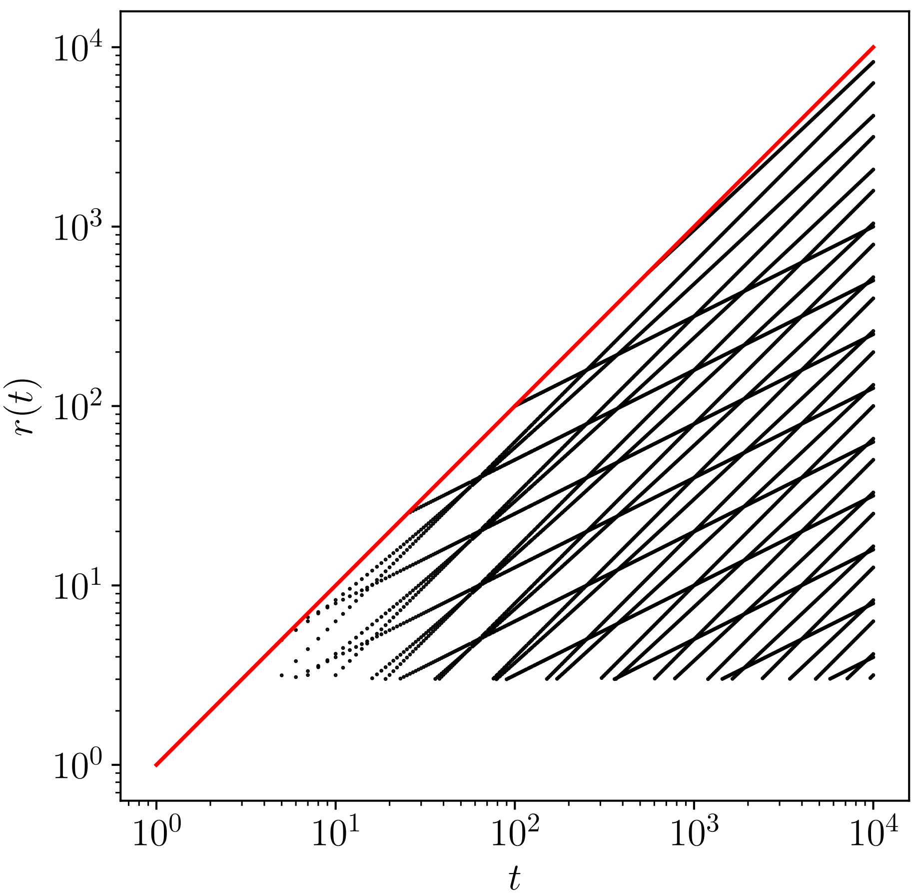

Figure A1. The set of radii, r, versus time, t, at which we measure $\mathbb{P}^{\boldsymbol{\xi}}\left(|\vec{S}(t)| \geq r\right)$. The red line shows $r = t$.

End Matter

7.1 Numerical Methods

At each measurement time t, logarithmically spaced from $t = 1$ to $t = 10000$, we compute the tail probability past a number of different values for r. Fig. A1 plots these pairs (r, t). To generate these pairs we evaluated and $r = vt^{1/2}$, $r = \frac{vt}{\sqrt{\ln t}}$, $r = vt$, where v is varied from 10^{-3} to 10. We exclude pairs of r and t for which $r > t$ (shown as a red line in the figure). Additionally, we only use $r \geq 3$, to exclude short-time lattice effects.

7.2 Non-universal behavior

When $r/t \to 1$ we observe non universal behavior in the fluctuations of the tail probability. This behavior is fundamentally a lattice effect driven by the narrowing of the number of possible paths between the origin and sites past r. When $r = t$ there will only be 4 sites at or past r. Thus, the fluctuations of $\mathbb{P}^{\boldsymbol{\xi}}(|\vec{S}(t)| = t)$ will be well described as the fluctuations of the sum of 4 random and independent paths and so our measured variance should scale linearly with t for large t.

We explicitly compute

$$\mathbb{P}^{\boldsymbol{\xi}}(|\vec{S}(t)| = t) = \sum_{\hat{n}\in\boldsymbol{n}} \mathbb{P}^{\boldsymbol{\xi}}\left(\vec{S}(t) = t\hat{n}\right)$$

as a sum over the 4 cardinal paths.

We consider the probability of reaching site $t\hat{n}$ along a cardinal path,

$$\mathbb{P}^{\boldsymbol{\xi}}(\vec{S}(t) = t\hat{n}) = \prod_{i=1}^{t} \xi_{i\hat{n},i}(\hat{n}), \text{ and}$$
$$\ln\left(\mathbb{P}^{\boldsymbol{\xi}}(\vec{S}(t) = t\hat{n})\right) = \sum_{i=1}^{t} \ln\left(\xi_{i\hat{n},i}(\hat{n})\right).$$

Thus, we find the variance for a single site at the end of the cardinal path to be

$$\begin{aligned}\mathrm{Var}_\nu\left[\ln\left(\mathbb{P}^{\boldsymbol{\xi}}(\vec{S}(t) = t\hat{n})\right)\right] &= \sum_{i=1}^{t} \mathrm{Var}_\nu\left(\ln\left(\xi_{i\hat{n},i}(\hat{n})\right)\right) \\ &= t\mathrm{Var}_\nu\left(\ln\left(\xi_{\vec{x},t}(\hat{n})\right)\right),\end{aligned}$$

where in the first line we used the fact that $\xi_{\vec{x},t}$ are independent at different lattice sites $(\vec{x}, t)$ and in the second line used the property that all $\xi_{\vec{x},t}$ are identically distributed.

To calculate the variance of the tail probability at $r = t$, we need to consider all four cardinal paths to find

$$
\begin{aligned}
&\mathrm{Var}_\nu \left[\ln\left(\mathbb{P}^{\boldsymbol{\xi}}(|\vec{S}(t)| = t)\right)\right] \\
&= \mathrm{Var}_\nu \left[\ln\left(\sum_{\hat{n}\in\boldsymbol{n}} \mathbb{P}^{\boldsymbol{\xi}}\left(\vec{S}(t) = t\hat{n}\right)\right)\right] \\
&\approx \mathrm{Var}_\nu \left[\ln\left(4\mathbb{P}^{\boldsymbol{\xi}}\left(\vec{S}(t) = t\hat{n}\right)\right)\right]
\end{aligned}
$$

using the approximation

$$
\sum_{\hat{n}\in\boldsymbol{n}} \mathbb{P}^{\boldsymbol{\xi}}\left(\vec{S}(t) = t\hat{n}\right) \approx 4\mathbb{P}^{\boldsymbol{\xi}}\left(\vec{S}(t) = t\hat{n}\right)
$$

which we expect to be reasonable in the limit that $t \to \infty$ because the variable $\mathbb{P}^{\boldsymbol{\xi}}\left(\vec{S}(t) = t\hat{n}\right)$ is independent and identically distributed for all $\hat{n} \in \boldsymbol{n}$, except at $t = 0$. Therefore,

$$
\begin{aligned}
&\mathrm{Var}_\nu \left[\ln\left(\mathbb{P}^{\boldsymbol{\xi}}(|\vec{S}(t)| = t)\right)\right] \\
&\approx \mathrm{Var}_\nu \left[\ln(4) + \ln\left(\mathbb{P}^{\boldsymbol{\xi}}\left(\vec{S}(t) = t\hat{n}\right)\right)\right] \\
&= \mathrm{Var}_\nu \left[\ln\left(\mathbb{P}^{\boldsymbol{\xi}}(\vec{S}(t) = t\hat{n})\right)\right] \\
&= t\mathrm{Var}_\nu \left[\ln\left(\xi_{\vec{x},t}(\hat{n})\right)\right]
\end{aligned}
$$

Thus, the variance of the tail probability when $r = t$ scales linearly with time as $t \to \infty$.

CHAPTER VIII

CONCLUSION

This thesis greatly expands on the literature of the Random Walks in Random Environments model for diffusion. I hope this body of work helps contextualize RWRE models in a physical setting and illustrates how the RWRE models can be used to better understand diffusive processes. Chapters II through VI greatly expand upon previous work on 1+1D RWRE models by providing mathematical predictions for the distributions of extreme value statistics for a system of diffusing particles. These predictions are verified using high precision numerics with the hope that experiments could make the same measurements of these extreme value statistics to learn more about the underlying environment. Chapter VII provides results for 2+1D RWRE models which show striking universality similar to results in one dimension.

Many future avenues of research on RWRE models are in higher dimensions. In [69, 143], it was conjectured that the centered and rescaled tail probability for 2+1D RWRE models at positions scaling like $t/\sqrt{\ln(t)}$ should converge to a unique distribution. However, observing this distribution numerically would be quite challenging for the following reasons. For the largest time we are able to simulate numerically, $t = 10000$, $t/\sqrt{\ln(10000)} \approx 3$ which is roughly of order 1. Thus, it is nearly impossible to distinguish the $t/\sqrt{\ln(t)}$ regime from the large deviation regime for positions scaling like t. We would have to go to much larger times to be able to distinguish the $t/\sqrt{\ln(t)}$ scaling from the large deviation regime.

The most interesting question is if RWRE models in 2+1D capture the long time behavior of the 2+1D KPZ equation analogous to results for RWRE models in 1+1D. We think that for large deviations the tail probability maps to the partition function of the 2+1D finite temperature directed polymer in random media (DPRM) model. Only numerical results exist for the 0 temperature, $T = 0$, limit of the 2+1D DPRM model [149, 150], but the results indicate the $T = 0$ DPRM model captures the distribution of the KPZ equation at large times. A future project could be numerically studying if large deviations of the tail probability map onto the finite temperature DPRM model and finding the effective temperature of a given RWRE model.

This mapping is likely sensitive to a number of factors including the following. First, this mapping might be effected by the shape of the area the tail probability is integrated over. We currently only study the probability of being outside a circle, but we should also look at the probability of being past a line. Second, the distribution of the 1+1D KPZ equation is highly sensitive to initial conditions. Thus, it is important to study various initial conditions of RWRE models. Currently, we only consider a delta function initial condition where the probability at the origin is 1 and 0 elsewhere. We should also consider smoother initial conditions like a Gaussian distribution. Lastly, taking the logarithm of the tail probability might affect if RWRE models map to the DPRM model. We think that the tail probability, without taking the logarithm, should map to the DPRM model but it is not clear if the logarithm preserves this mapping.

Since there is evidence that the DPRM model is in the 2+1D universality class, this result would help to expand the 2+1D KPZ universality class to RWRE models. More importantly, it could show that RWRE models are a suitable framework to study the 2+1D KPZ equation which has remained mathematically intractable.

REFERENCES CITED

[1] Mehran Kardar, Giorgio Parisi, and Yi-Cheng Zhang. Dynamic Scaling of Growing Interfaces. *Physical Review Letters*, 56(9):889–892, March 1986.

[2] Robert Brown. XXVII. A brief account of microscopical observations made in the months of June, July and August 1827, on the particles contained in the pollen of plants; and on the general existence of active molecules in organic and inorganic bodies. *The Philosophical Magazine*, 4(21):161–173, September 1828.

[3] Robert Brown. XXIV. Additional remarks on active molecules. *The Philosophical Magazine*, 6(33):161–166, September 1829.

[4] P. H. Kao and R. J. Yang. Virus diffusion in isolation rooms. *Journal of Hospital Infection*, 62(3):338–345, March 2006.

[5] Fischer Black and Myron Scholes. The Pricing of Options and Corporate Liabilities. *Journal of Political Economy*, May 1973.

[6] Guillaume Barraquand and Ivan Corwin. Random-walk in Beta-distributed random environment. *Probability Theory and Related Fields*, 167(3-4):1057–1116, April 2017.

[7] Guillaume Barraquand and Pierre Le Doussal. Moderate deviations for diffusion in time dependent random media. *Journal of Physics A: Mathematical and Theoretical*, 53(21):215002, May 2020.

[8] Kanishka Basnayake, David Mazaud, Alexis Bemelmans, Nathalie Rouach, Eduard Korkotian, and David Holcman. Fast calcium transients in dendritic spines driven by extreme statistics. *PLOS Biology*, 17(6):e2006202, June 2019.

[9] Michael J. Saxton and Ken Jacobson. Single-particle tracking: Applications to membrane dynamics. *Annual Review of Biophysics and Biomolecular Structure*, 26:373–399, 1997.

[10] Philip A. Pinto and Ronald G. Eastman. The Physics of Type Ia Supernova Light Curves. II. Opacity and Diffusion. *The Astrophysical Journal*, 530(2):757–776, February 2000.

[11] Felix Höfling and Thomas Franosch. Anomalous transport in the crowded world of biological cells. *Reports on Progress in Physics*, 76(4), 2013.

[12] Surya K. Ghosh, Andrey G. Cherstvy, and Ralf Metzler. Non-universal tracer diffusion in crowded media of non-inert obstacles. *Physical Chemistry Chemical Physics*, 17(3):1847–1858, January 2015.

[13] Carlo Manzo and Maria F. Garcia-Parajo. A review of progress in single particle tracking: From methods to biophysical insights. *Reports on Progress in Physics*, 78(12), 2015.

[14] Srividya Iyer-Biswas and Anton Zilman. First-Passage Processes in Cellular Biology. In *Advances in Chemical Physics*, chapter NONE, pages 261–306. John Wiley & Sons, Ltd, 2016.

[15] R. Metzler, J.-H. Jeon, and A.G. Cherstvy. Non-Brownian diffusion in lipid membranes: Experiments and simulations. *Biochimica et Biophysica Acta (BBA) - Biomembranes*, 1858(10):2451–2467, October 2016.

[16] Hao Shen, Lawrence J. Tauzin, Rashad Baiyasi, Wenxiao Wang, Nicholas Moringo, Bo Shuang, and Christy F. Landes. Single Particle Tracking: From Theory to Biophysical Applications. *Chemical Reviews*, 117(11):7331–7376, June 2017.

[17] L. Hufnagel, D. Brockmann, and T. Geisel. Forecast and control of epidemics in a globalized world. *Proceedings of the National Academy of Sciences*, 101(42):15124–15129, October 2004.

[18] Warren John Ewens. *Mathematical Population Genetics, I. Theoretical Introduction*, volume 27. 2012.

[19] Ralf Metzler, Gleb Oshanin, and Sidney Redner. *First-Passage Phenomena and Their Applications*. World Scientific Publishing Co., January 2014.

[20] David Waxman. The diffusion equation of random genetic drift–biology's analogue of the Schrödinger equation? *Contemporary Physics*, 58(3):253–261, July 2017.

[21] A. Einstein. Über die von der molekularkinetischen Theorie der Wärme geforderte Bewegung von in ruhenden Flüssigkeiten suspendierten Teilchen. *Annalen der Physik*, 322(8):549–560, 1905.

[22] A. Einstein. Zur Theorie der Brownschen Bewegung. *Annalen der Physik*, 324(2):371–381, January 1906.

[23] A. Einstein. Theoretische Bemerkungen Über die Brownsche Bewegung. *Zeitschrift für Elektrochemie und angewandte physikalische Chemie*, 13(6):41–42, February 1907.

[24] Firas Rassoul-Agha, Timo Seppäläinen, and Atilla Yilmaz. Quenched Free Energy and Large Deviations for Random Walks in Random Potentials. *Communications on Pure and Applied Mathematics*, 66(2):202–244, 2013.

[25] Paul Langevin. Sur La Théorie Du Mouvement Brownien. 146:530–533, 1908.

[26] William Sutherland. The viscosity of gases and molecular force. *Philosophical Magazine Series 5*, 36(223):507–531, 1893.

[27] William Sutherland. LXXV. A dynamical theory of diffusion for non-electrolytes and the molecular mass of albumin. *The London, Edinburgh, and Dublin Philosophical Magazine and Journal of Science*, 9(54):781–785, June 1905.

[28] M. von Smoluchowski. Zur kinetischen Theorie der Brownschen Molekularbewegung und der Suspensionen. *Annalen der Physik*, 326(14):756–780, 1906.

[29] M. Von Smoluchowski. Notiz uiber die Berechnung der Brownschen Molekularbewegung bei der Ehrenhaft-Millikanschen Versuchsanordning. *Phys. Z*, 16:318–321, 1915.

[30] Jean Baptiste Perrin. Le Mouvement Brownien et la Réalité Moleculaire. *Ann. Chimi. Phys.*, 18(8):5–114, 1909.

[31] Jean Perrin. Mouvement brownien et molécules. *JCP*, 8:57–91, 1910.

[32] G. E. Uhlenbeck and L. S. Ornstein. On the Theory of the Brownian Motion. *Physical Review*, 36(5):823–841, September 1930.

[33] Rongxin Huang, Isaac Chavez, Katja M. Taute, Branimir Lukić, Sylvia Jeney, Mark G. Raizen, and Ernst-Ludwig Florin. Direct observation of the full transition from ballistic to diffusive Brownian motion in a liquid. *Nature Physics*, 7(7):576–580, July 2011.

[34] Andrew P. Hammond and Eric I. Corwin. Direct measurement of the ballistic motion of a freely floating colloid in Newtonian and viscoelastic fluids. *Physical Review E*, 96(4):042606, October 2017.

[35] B. Lukić, S. Jeney, C. Tischer, A. J. Kulik, L. Forró, and E.-L. Florin. Direct Observation of Nondiffusive Motion of a Brownian Particle. *Physical Review Letters*, 95(16):160601, October 2005.

[36] Thomas Franosch, Matthias Grimm, Maxim Belushkin, Flavio M. Mor, Giuseppe Foffi, László Forró, and Sylvia Jeney. Resonances arising from hydrodynamic memory in Brownian motion. *Nature*, 478(7367):85–88, October 2011.

[37] Simon Kheifets, Akarsh Simha, Kevin Melin, Tongcang Li, and Mark G. Raizen. Observation of Brownian Motion in Liquids at Short Times: Instantaneous Velocity and Memory Loss. *Science*, 343(6178):1493–1496, March 2014.

[38] Bo Wang, James Kuo, Sung Chul Bae, and Steve Granick. When Brownian diffusion is not Gaussian. *Nature Materials*, 11(6):481–485, May 2012.

[39] Jean-Philippe Bouchaud and Antoine Georges. Anomalous diffusion in disordered media: Statistical mechanisms, models and physical applications. *Physics Reports*, 195(4):127–293, November 1990.

[40] Ralf Metzler. Brownian motion and beyond: First-passage, power spectrum, non-Gaussianity, and anomalous diffusion. *Journal of Statistical Mechanics: Theory and Experiment*, 2019(11):114003–114003, November 2019.

[41] Sriram Ramaswamy. The Mechanics and Statistics of Active Matter. *Annual Review of Condensed Matter Physics*, 1(1):323–345, 2010.

[42] Kiyoshi Kanazawa, Tomohiko G. Sano, Andrea Cairoli, and Adrian Baule. Loopy Lévy flights enhance tracer diffusion in active suspensions. *Nature*, 579(7799):364–367, March 2020.

[43] Ronen Zangi and Laura J. Kaufman. Frequency-dependent Stokes-Einstein relation in supercooled liquids. *Physical Review E*, 75(5):051501, May 2007.

[44] A. A. Chernov. Replication of a multicomponent chain by the "lightning" mechanism. *Biophysics*, 12(2), 1967.

[45] D. E. Temkin. One-dimensional random walks in a two-component chain. *Soviet Math. Docl.*, 13:1172–1176, 1972.

[46] Shlomo Havlin and Daniel Ben-Avraham. Diffusion in disordered media. *Advances in Physics*, 36(6):695–798, January 1987.

[47] Erwin Bolthausen and Alain-Sol Sznitman. *Ten Lectures on Random Media*. Birkhäuser Basel, 2002.

[48] A.-S. Sznitman. Topics in random walks in random environment. Technical Report 92-95003-25-X, International Atomic Energy Agency (IAEA), 2004.

[49] Zeitouni Ofer. Random walks in random environment. In *Lectures on Probability Thorey and Statistics, Lecture Notes*, volume 1837 of *Math*, pages 189–312. Springer, Berlin, 2004.

[50] Barry D. Hughes. *Random Walks and Random Environments: Random Walks*. Clarendon Press, 1995.

[51] H. Kesten, M. V. Kozlov, and F. Spitzer. A limit law for random walk in a random environment. *Compositio Mathematica*, 30(2):145–168, 1975.

[52] Y. Sinai. The Limiting Behavior of a One-Dimensional Random Walk in a Random Medium. *Theory of Probability & Its Applications*, 27(2):256–268, January 1983.

[53] J. P Bouchaud, A Comtet, A Georges, and P Le Doussal. Classical diffusion of a particle in a one-dimensional random force field. *Annals of Physics*, 201(2):285–341, August 1990.

[54] S. F. Burlatsky and John M. Deutch. Transient relaxation of a charged polymer chain subject to an external field in a random tube. *The Journal of Chemical Physics*, 109(6):2572–2578, August 1998.

[55] Pierre Le Doussal, Cécile Monthus, and Daniel S. Fisher. Random walkers in one-dimensional random environments: Exact renormalization group analysis. *Physical Review E*, 59(5):4795–4840, May 1999.

[56] Lewis Fry Richardson and Gilbert Thomas Walker. Atmospheric diffusion shown on a distance-neighbour graph. *Proceedings of the Royal Society of London. Series A, Containing Papers of a Mathematical and Physical Character*, 110(756):709–737, April 1926.

[57] H. G. E. Hentschel and Itamar Procaccia. Relative diffusion in turbulent media: The fractal dimension of clouds. *Physical Review A*, 29(3):1461–1470, March 1984.

[58] J. P. Bouchaud. Diffusion and Localization of Waves in a Time-Varying Random Environment. *Europhysics Letters (EPL)*, 11(6):505–510, March 1990.

[59] M. Chertkov and G. Falkovich. Anomalous Scaling Exponents of a White-Advected Passive Scalar. *Physical Review Letters*, 76(15):2706–2709, April 1996.

[60] Denis Bernard, Krzysztof Gawedzki, and Antti Kupiainen. Anomalous Scaling in the N-Point Functions of Passive Scalar. *Physical Review E*, 54(3):2564–2572, September 1996.

[61] Marie-Caroline Jullien, Jérôme Paret, and Patrick Tabeling. Richardson Pair Dispersion in Two-Dimensional Turbulence. *Physical Review Letters*, 82(14):2872–2875, April 1999.

[62] E. Balkovsky, G. Falkovich, and A. Fouxon. Intermittent Distribution of Inertial Particles in Turbulent Flows. *Physical Review Letters*, 86(13):2790–2793, March 2001.

[63] F. Rassoul-Agha and T. Seppalainen. An almost sure invariance principle for random walks in a space-time random environment. *Probability Theory and Related Fields*, 133(3):299–314, November 2005.

[64] Jean-Dominique Deuschel, Xiaoqin Guo, and Alejandro F. Ramírez. Quenched invariance principle for random walk in time-dependent balanced random environment. *Annales de l'Institut Henri Poincaré, Probabilités et Statistiques*, 54(1):363–384, February 2018.

[65] Marton Balazs, Firas Rassoul-Agha, and Timo Seppalainen. The random average process and random walk in a space-time random environment in one dimension. *Communications in Mathematical Physics*, 266(2):499–545, September 2006.

[66] Ivan Corwin. The kardar–parisi–zhang equation and universality class. *Random Matrices: Theory and Applications*, 01(01):1130001, January 2012.

[67] Jeremy Quastel and Herbert Spohn. The One-Dimensional KPZ Equation and Its Universality Class. *Journal of Statistical Physics*, 160(4):965–984, August 2015.

[68] Craig A. Tracy and Harold Widom. Level-spacing distributions and the Airy kernel. *Physics Letters B*, 305(1):115–118, May 1993.

[69] Pierre Le Doussal and Thimothée Thiery. Diffusion in time-dependent random media and the Kardar-Parisi-Zhang equation. *Physical Review E*, 96(1):010102, July 2017.

[70] Tomohiro Sasamoto and Herbert Spohn. One-Dimensional Kardar-Parisi-Zhang Equation: An Exact Solution and its Universality. *Physical Review Letters*, 104(23):230602, June 2010.

[71] P. Calabrese, P. Le Doussal, and A. Rosso. Free-energy distribution of the directed polymer at high temperature. *EPL (Europhysics Letters)*, 90(2):20002, April 2010.

[72] V. Dotsenko. Bethe ansatz derivation of the Tracy-Widom distribution for one-dimensional directed polymers. *EPL (Europhysics Letters)*, 90(2):20003, April 2010.

[73] Gideon Amir, Ivan Corwin, and Jeremy Quastel. Probability Distribution of the Free Energy of the Continuum Directed Random Polymer in 1+1 dimensions. *Communications on Pure and Applied Mathematics*, 64(4):466–537, April 2011.

[74] Christophe Sabot and Laurent Tournier. Random walks in Dirichlet environment: An overview. *Annales de la Faculté des sciences de Toulouse : Mathématiques*, 26(2):463–509, 2017.

[75] Márton Balázs, Firas Rassoul-Agha, and Timo Seppäläinen. Large deviations and wandering exponent for random walk in a dynamic beta environment. *The Annals of Probability*, 47(4):2186–2229, July 2019.

[76] Guillaume Barraquand and Mark Rychnovsky. Large deviations for sticky Brownian motions. *Electronic Journal of Probability*, 25(none):1–52, January 2020.

[77] Dom Brockington and Jon Warren. The Bethe ansatz for sticky Brownian motions. *Stochastic Processes and their Applications*, 162:1–48, August 2023.

[78] Giancarlos Oviedo, Gonzalo Panizo, and Alejandro F. Ramírez. Second order cubic corrections of large deviations for perturbed random walks. *Electronic Journal of Probability*, 27:1–45, January 2022.

[79] Sergei Korotkikh. Hidden diagonal integrability of q-Hahn vertex model and Beta polymer model. *Probability Theory and Related Fields*, March 2022.

[80] Alexandre Krajenbrink and Pierre Le Doussal. The crossover from the Macroscopic Fluctuation Theory to the Kardar-Parisi-Zhang equation controls the large deviations beyond Einstein's diffusion. *Physical Review E*, 107(1):014137, January 2023.

[81] Tom Alberts, Kostya Khanin, and Jeremy Quastel. Intermediate Disorder Regime for Directed Polymers in Dimension 1+1. *Physical Review Letters*, 105(9):090603, August 2010.

[82] Joachim Krug, Paul Meakin, and Timothy Halpin-Healy. Amplitude universality for driven interfaces and directed polymers in random media. *Physical Review A*, 45(2):638–653, January 1992.

[83] Sylvain Prolhac and Herbert Spohn. The height distribution of the KPZ equation with sharp wedge initial condition: Numerical evaluations. *Physical Review E*, 84(1):011119, July 2011.

[84] Timothy Halpin-Healy and Kazumasa A. Takeuchi. A KPZ Cocktail-Shaken, not Stirred... *Journal of Statistical Physics*, 160(4):794–814, August 2015.

[85] William Feller. Diffusion Processes in Genetics. *Proceedings of the Second Berkeley Symposium on Mathematical Statistics and Probability*, 2:227–247, January 1951.

[86] P. a. P. Moran. Random processes in genetics. *Mathematical Proceedings of the Cambridge Philosophical Society*, 54(1):60–71, January 1958.

[87] W. G. Pollard and R. D. Present. On Gaseous Self-Diffusion in Long Capillary Tubes. *Physical Review*, 73(7):762–774, April 1948.

[88] Sheida Ahmadi and Richard K. Bowles. Diffusion in quasi-one-dimensional channels: A small system n, p, T, transition state theory for hopping times. *The Journal of Chemical Physics*, 146(15):154505, April 2017.

[89] See Supplemental Material.

[90] Michael Prähofer and Herbert Spohn. Universal Distributions for Growth Processes in 1+1 Dimensions and Random Matrices. *Physical Review Letters*, 84(21):4882–4885, May 2000.

[91] Aleksei V. Chechkin, Flavio Seno, Ralf Metzler, and Igor M. Sokolov. Brownian yet Non-Gaussian Diffusion: From Superstatistics to Subordination of Diffusing Diffusivities. *Physical Review X*, 7(2):021002, April 2017.

[92] S. H. Noskowicz and I. Goldhirsch. Average versus Typical Mean First-Passage Time in a Random Random Walk. *Physical Review Letters*, 61(5):500–502, August 1988.

[93] Pierre Le Doussal. First-passage time for random walks in random environments. *Physical Review Letters*, 62(26):3097–3097, June 1989.

[94] Baruch Meerson and S. Redner. Mortality, Redundancy, and Diversity in Stochastic Search. *Physical Review Letters*, 114(19):198101, May 2015.

[95] Z. Schuss, K. Basnayake, and D. Holcman. Redundancy principle and the role of extreme statistics in molecular and cellular biology. *Physics of Life Reviews*, 28:52–79, March 2019.

[96] J. Yang, I. Kupka, Z. Schuss, and D. Holcman. Search for a small egg by spermatozoa in restricted geometries. *Journal of Mathematical Biology*, 73:423–446, 2016.

[97] Renato Germano and Alessandro P. S. de Moura. Traffic of particles in complex networks. *Physical Review E*, 74(3):036117, September 2006.

[98] Shao-Ping Wang and Wen-Jiang Pei. First passage time of multiple Brownian particles on networks with applications. *Physica A: Statistical Mechanics and its Applications*, 387(18):4699–4708, July 2008.

[99] Sidney Redner. *A Guide to First-Passage Processes*. Cambridge University Press, Cambridge, UK ; New York, 1 edition edition, August 2001.

[100] Samantha Linn and Sean D. Lawley. Extreme hitting probabilities for diffusion. *Journal of Physics A: Mathematical and Theoretical*, 55(34):345002, August 2022.

[101] S. Redner and B. Meerson. Redundancy, extreme statistics and geometrical optics of Brownian motion: Comment on "Redundancy principle and the role of extreme statistics in molecular and cellular biology" by Z. Schuss et al. *Physics of Life Reviews*, 28:80–82, March 2019.

[102] Sean D. Lawley. Distribution of extreme first passage times of diffusion. *Journal of Mathematical Biology*, 80(7):2301–2325, June 2020.

[103] Katja Lindenberg, V. Seshadri, K. E. Shuler, and George H. Weiss. Lattice random walks for sets of random walkers. First passage times. *Journal of Statistical Physics*, 23(1):11–25, July 1980.

[104] Jacob B. Madrid and Sean D. Lawley. Competition between slow and fast regimes for extreme first passage times of diffusion. *Journal of Physics A: Mathematical and Theoretical*, 53(33):335002, July 2020.

[105] Denis S. Grebenkov, Ralf Metzler, and Gleb Oshanin. From single-particle stochastic kinetics to macroscopic reaction rates: Fastest first-passage time of N random walkers. *New Journal of Physics*, 22(10):103004, October 2020.

[106] Sean D. Lawley. Universal formula for extreme first passage statistics of diffusion. *Physical Review E*, 101(1):012413, January 2020.

[107] Jacob B. Hass, Aileen N. Carroll-Godfrey, Ivan Corwin, and Eric I. Corwin. Anomalous fluctuations of extremes in many-particle diffusion. *Physical Review E*, 107(2):L022101, February 2023.

[108] Thimothée Thiery and Pierre Le Doussal. Exact solution for a random walk in a time-dependent 1D random environment: The point-to-point Beta polymer. *Journal of Physics A: Mathematical and Theoretical*, 50(4):045001, December 2016.

[109] Ivan Corwin and Yu Gu. Kardar–Parisi–Zhang Equation and Large Deviations for Random Walks in Weak Random Environments. *Journal of Statistical Physics*, 166(1):150–168, January 2017.

[110] Guillaume Barraquand and Mark Rychnovsky. Random Walk on Nonnegative Integers in Beta Distributed Random Environment. *Communications in Mathematical Physics*, 398(2):823–875, March 2023.

[111] Dom Brockington and Jon Warren. At the edge of a cloud of Brownian particles. *arXiv:2208.11952 [math]*, August 2022.

[112] Sayan Das, Hindy Drillick, and Shalin Parekh. Multiplicative SHE limit of random walks in space–time random environments. *Probability Theory and Related Fields*, December 2024.

[113] Alexander K. Hartmann, Alexandre Krajenbrink, and Pierre Le Doussal. Probing the large deviations for the Beta random walk in random medium. *arXiv:2307.15041 [cond-mat]*, July 2023.

[114] Craig A. Tracy and Harold Widom. Level-spacing distributions and the Airy kernel. *Communications in Mathematical Physics*, 159(1):151–174, January 1994.

[115] Konstantin Matetski, Jeremy Quastel, and Daniel Remenik. The KPZ fixed point. *Acta Mathematica*, 227(1):115–203, September 2021.

[116] Sylvain Prolhac. Personal Communication, February 2022.

[117] Lior Zarfaty, Eli Barkai, and David A. Kessler. Accurately approximating extreme value statistics. *Journal of Physics A: Mathematical and Theoretical*, 54(31):315205, July 2021.

[118] Marcelo Hilário, Frank den Hollander, Vladas Sidoravicius, Renato Soares dos Santos, and Augusto Teixeira. Random walk on random walks. *Electronic Journal of Probability*, 20(none):1–35, January 2015.

[119] Takuma Akimoto, Eli Barkai, and Keiji Saito. Universal Fluctuations of Single-Particle Diffusivity in a Quenched Environment. *Physical Review Letters*, 117(18):180602, October 2016.

[120] K. W. Kehr and R. Kutner. Random walk on a random walk. *Physica A: Statistical Mechanics and its Applications*, 110(3):535–549, February 1982.

[121] Ryszard Kutner and Philipp Maass. Lévy flights with quenched noise amplitudes. *Journal of Physics A: Mathematical and General*, 31(11):2603, March 1998.

[122] Jacob B. Hass, Ivan Corwin, and Eric I. Corwin. First-passage time for many-particle diffusion in space-time random environments. *Physical Review E*, 109(5):054101, May 2024.

[123] Shalin Parekh. Invariance principle for the KPZ equation arising in stochastic flows of kernels. January 2024.

[124] Ralf Metzler and Joseph Klafter. The random walk's guide to anomalous diffusion: A fractional dynamics approach. *Physics Reports*, 339(1):1–77, December 2000.

[125] K. Basnayake, Z. Schuss, and D. Holcman. Asymptotic Formulas for Extreme Statistics of Escape Times in 1, 2 and 3-Dimensions. *Journal of Nonlinear Science*, 29(2):461–499, April 2019.

[126] George H. Weiss, Kurt E. Shuler, and Katja Lindenberg. Order statistics for first passage times in diffusion processes. *Journal of Statistical Physics*, 31(2):255–278, May 1983.

[127] Jacob Hass, Hindy Drillick, Ivan Corwin, and Eric Corwin. Universal KPZ Fluctuations for Moderate Deviations of Random Walks in Random Environments, March 2025.

[128] Sayan Das, Hindy Drillick, and Shalin Parekh. KPZ equation limit of sticky Brownian motion. *Journal of Functional Analysis*, 287(10):Paper No. 110609, 90, 2024.

[129] Jacob Hass. Super-Universal Behavior of Outliers Diffusing in a Space-Time Random Environment, May 2025.

[130] Mehran Kardar. Replica Bethe ansatz studies of two-dimensional interfaces with quenched random impurities. *Nuclear Physics B*, 290:582–602, January 1987.

[131] Lorenzo Bertini and Nicoletta Cancrini. The stochastic heat equation: Feynman-Kac formula and intermittence. *Journal of Statistical Physics*, 78(5):1377–1401, March 1995.

[132] J. R. Norris. *Markov Chains*. Cambridge Series in Statistical and Probabilistic Mathematics. Cambridge University Press, Cambridge, 1997.

[133] Jacob B. Hass, Hindy Drillick, Ivan Corwin, and Eric I. Corwin. Extreme Diffusion Measures Statistical Fluctuations of the Environment. *Physical Review Letters*, 133(26):267102, December 2024.

[134] Hsing Liu, Chi-Yo Liao, Jing-Yuan Ko, and Jiann-Shing Lih. Anchoring effect on first passage process in Taiwan financial market. *Physica A: Statistical Mechanics and its Applications*, 477:114–127, July 2017.

[135] Akira Ishimaru. Diffusion of Light in Turbid Material. *Applied Optics*, 28(12):2210–2215, June 1989.

[136] Pierre Le Doussal. Dynamics at the edge for independent diffusing particles. *Physical Review E*, 109(2):024101, February 2024.

[137] T. G. Mason and D. A. Weitz. Optical Measurements of Frequency-Dependent Linear Viscoelastic Moduli of Complex Fluids. *Physical Review Letters*, 74(7):1250–1253, February 1995.

[138] T. G. Mason, H. Gang, and D. A. Weitz. Diffusing-wave-spectroscopy measurements of viscoelasticity of complex fluids. *Journal of the Optical Society of America A*, 14(1):139–149, 1997.

[139] K. L. Chung and W. H. J. Fuchs. On the distribution of values of sums of random variables. *Memoirs of the American Mathematical Society*, 6:12, 1951.

[140] Alexei V. Chechkin, Ralf Metzler, Joseph Klafter, and Vsevolod Yu. Gonchar. Introduction to the Theory of Lévy Flights. In *Anomalous Transport*, chapter 5, pages 129–162. John Wiley & Sons, Ltd, 2008.

[141] I. M. Sokolov and J. Klafter. From diffusion to anomalous diffusion: A century after Einstein's Brownian motion. *Chaos: An Interdisciplinary Journal of Nonlinear Science*, 15(2):026103, June 2005.

[142] The $t^{7/8}$ regime was independently predicted by Pierre Le Doussal.

[143] Hindy Drillick and Shalin Parekh. Random walks in space-time random media in all spatial dimensions: The full subcritical fluctuation regime. *In preparation*, 2025.

[144] Karine Reynaud, Zeev Schuss, Nathalie Rouach, and David Holcman. Why so many sperm cells? *Communicative & Integrative Biology*, 8(3):e1017156, May 2015.

[145] Matt J. Keeling, Mark E. J. Woolhouse, Darren J. Shaw, Louise Matthews, Margo Chase-Topping, Dan T. Haydon, Stephen J. Cornell, Jens Kappey, John Wilesmith, and Bryan T. Grenfell. Dynamics of the 2001 UK Foot and Mouth Epidemic: Stochastic Dispersal in a Heterogeneous Landscape. *Science*, 294(5543):813–817, October 2001.

[146] Flavio Iannelli, Andreas Koher, Dirk Brockmann, Philipp Hövel, and Igor M. Sokolov. Effective distances for epidemics spreading on complex networks. *Physical Review E: Statistical Physics, Plasmas, Fluids, and Related Interdisciplinary Topics*, 95(1):012313, January 2017.

[147] Kazumasa A. Takeuchi and Masaki Sano. Universal Fluctuations of Growing Interfaces: Evidence in Turbulent Liquid Crystals. *Physical Review Letters*, 104(23):230601, June 2010.

[148] Mehran Kardar and Yi-Cheng Zhang. Scaling of Directed Polymers in Random Media. *Physical Review Letters*, 58(20):2087–2090, May 1987.

[149] Timothy Halpin-Healy. (2 + 1)-Dimensional Directed Polymer in a Random Medium: Scaling Phenomena and Universal Distributions. *Physical Review Letters*, 109(17):170602, October 2012.

[150] Timothy Halpin-Healy. Extremal paths, the stochastic heat equation, and the three-dimensional Kardar-Parisi-Zhang universality class. *Physical Review E: Statistical Physics, Plasmas, Fluids, and Related Interdisciplinary Topics*, 88(4):042118, October 2013.